OPTICAL PROPERTIES OF THIN FILMS OF SOME SEMICONDUCTORS

BY

EHSAN ELLAHI KHAWAJA

M.Sc. (PANJAB)

A THESIS

SUBMITTED FOR THE DEGREE OF

DOCTOR OF PHILOSOPHY

IN THE

DEPARTMENT OF PHYSICS

UNIVERSITY OF ADELAIDE

FEBRUARY, 1975

TABLE OF CONTENTS

TABLE OF CONTENTS (cont.)

TABLE OF CONTENTS (cont.)

TABLE OF CONTENTS (cont.)

SUMMARY

The thesis begins with a brief description of band gap, band structure and the electronic transitions in a semiconductor. It is the value of the band gap of a crystal and the occupation of the levels in the bands which tell us whether it is a metal or a semiconductor or an insulator. The best method to determine the band gap and band structure of a semiconductor is a careful study of its optical properties (indices of refraction and absorption).

A critical review of the methods, used to determine the optical constants of materials in bulk form as well as in thin films, is presented in Chapter 1. It is concluded that spectrophotometry at normal incidence is most advantageous.

In Chapter 2 a brief description of the experimental apparatus used for measuring normal incidence reflectance and transmittance (spectrophotometrically) is given.

The method used for determining the optical constants of an absorbing specimen, which does not transmit, is described in detail in Chapter 3. This requires the normal incidence measurements of reflectances firstly from the specimen and secondly from the specimen coated with a transparent layer. The method results in two solutions for the optical constants and therefore an analysis of hypothetical specimen is made in an effort to determine which of the solutions is correct. A straight forward choice can best be made if measurements are taken over a wide spectral range. It is shown how the behaviour of the

calculated solutions under small changes in the thickness of the overlying film enables its thickness to be precisely obtained without recourse to its explicit measurement.

Using the above described method, the optical properties, of amorphous germanium films in the spectral range 700 - 300 nm and of polycrystalline Ge in bulk form in the spectral range 1750 - 300 nm, were studied. These properties together with optical transitions are discussed in Chapter 5.

It is shown in Chapter 3 that in order to achieve a better accuracy in the measured optical constants for a specimen like Ge, a transparent layer of higher refractive index such as ZnS, Ta_2O_5 and ZrO_2 may be used. The optical properties of Ta_2O_5 and ZrO_2 films were thus studied in the spectral range 2000 - 250 nm and described in Chapter 4. It was found that Ta_2O_5 films have an indirect band gap of 4.15 eV. ZrO_2 films were transparent in the spectral range studied.

The optical properties of thin evaporated films of CdS and ZnS have been studied in the spectral range 2000 - 250 nm by measurements of reflectance and transmittance at normal incidence (Chapters 6 and 7). The effects of surface roughness have been taken into account. Analysis of the dependence of absorption on photon energy have shown that the experimental results may be explained by the occurance of direct transitions from 2.42 to 2.82 eV, in the case of CdS, followed by combined direct and indirect transitions beyond 2.82 eV assuming the energy bands to be parabolic, or equally well by assuming only direct transitions between non-parabolic bands, the forms of which may be deduced from the optical absorption curves. The results for ZnS films are similar and may be treated in the same way. It is concluded that these materials both show absorption by direct transitions just beyond

the absorption edge and that at higher energies the form of the absorption curve is probably due to the combined effects of indirect transitions together with direct transitions between non-parabolic bands. It has not been possible, on the basis of these optical measurements alone, to separate these two effects.

DECLARATION

This thesis contains no material which has been accepted for the award of any other degree or diploma in any University and, to the best of the author's knowledge and belief, contains no material previously published or written by another person, except where due reference is made in the text of the thesis.

(E.E. KHAWAJA)

ACKNOWLEDGEMENTS

The author gratefully acknowledges the following people and organisations for their assistance during the course of this work.

Mr. A. Ewart — for his valuable technical assistance.

Mr. J. Ward — for preparation of thin films of Ta_2O_5 and ZrO_2.

Dr. R. Denton, Dr. R. Goodwin and Mr. T.G.K. Murty for many thought provoking discussions.

Mrs. K. Hardie — for typing the thesis.

Mrs. J. Taylor — for drawing the diagrams.

The Radio Research Board of Australia for financing the project.

The University of Adelaide for the award of a University Research Grant.

Finally the author wishes to thank his Supervisor, Dr. S.G. Tomlin, for his guidance and stimulating critical discussions during the course of this work.

CHAPTER 1.

INTRODUCTION

1.1 BAND STRUCTURE AND THE ELECTRONIC TRANSITIONS

An experimental study has been made of the optical properties of different semiconductors (cadmium sulphide, zinc sulphide, germanium) and refractory oxides (tantalum pentoxide, zirconium dioxide) in the form of thin films. Also, the optical properties of polycrystalline germanium in bulk form has been studied.

In crystals the electron energy levels occur in bands of allowed energies separated by forbidden bands. This band structure is the functional dependence of the energy on the electron wavevector and is of fundamental importance in explaining the properties of solids. The value of the band gap, which may be defined as the forbidden energy gap between the highest point of the valence band and the lowest point of the next highest band, usually called the conduction band, is of such vital importance in the theory that even the crudest knowledge of it can tell us a great deal about the properties of the solid. It is just the value of the band gap of a crystal and the occupation of the levels in the bands which tell us whether it is a metal or a semiconductor or an insulator.

The interaction of photons, of energy greater than the band gap, with electrons, generally results in two types of transitions, in which the electrons are transferred from the valence to the conduction band, these are called direct and indirect transitions. When the band structure is such that the lowest point of the conduction band occurs at the same value

of wavevector as the highest point of valence band (this is the case for II - VI compounds like CdS, ZnS etc.), then a direct optical transition of electrons takes place. This is in accordance with the conservation of wavevector. On the other hand when the lowest point of the conduction band occurs at a different value of wavevector to the highest point of the valence band (e.g. silicon, germanium etc.), then an indirect optical transition of electrons takes place. This is accompanied by the absorption or emission of a phonon to ensure conservation of the wavevector.

The band structure may be conveniently divided into four energy regions in accordance with the different transitions of electrons which result due to the absorption of photons.

Consider the first region, the lowest energy region, which is on the lower energy side of the band gap (e.g. in CdS the band gap at room temperature is 2.42 eV). The interaction of a photon, of energy value corresponding to this region, with an electron may result in the transfer of the electron from a filled valence band to an excited state leaving behind a hole. The electron and the hole interact via conlomb forces, whose strength is determined by the crystal structure. This two particle system, the interacting electron and hole constitutes the exciton system. This excited state has a very short life time and the electron returns to the ground state with the emission of a photon, in accordance with the conservation of energy. In this region optical absorption is relatively weak and is very sensitive to crystalline imperfections.

The next higher region starts from the band gap energy E_g. The interaction of photons, of energy corresponding to this region (e.g. in CdS this region is from 2.42 to 2.82 eV), with electrons, results either

in a direct or an indirect transition of electrons from the valence to the conduction band. For example, it is clear from the literature that in the case of germanium and silicon this is an indirect transition, while in the case of II - VI compounds it is a direct transition. For this very reason Ge and Si are known as indirect gap semiconductors and II - VI compounds as direct gap semiconductors. The range of this region is dependent on the type of semiconductor.

The third is the next higher energy region and range of which is dependent on the type of semiconductor. The interaction of photons, of energy corresponding to this region, with electrons, results in two different transitions of electrons, occuring simultaneously, from valence bands to conduction bands. The two transitions can either both be direct or one direct and the other indirect or both indirect, depending upon the semiconducting material, e.g. in CdS and ZnS films this region begins at about 2.82 and 4.1 eV respectively, and for photon energies higher than these, it is observed that the two transitions are one direct and the other indirect. This will be discussed later. The reason why the third region is separated from the second is that it involves more than one transition.

The fourth is the high energy region (e.g. above 5 eV say). The transitions of electrons from valence bands to high energy conduction bands is possible but this will not be considered any further as it is not involved in the experimental work that follows which has been restricted to photon energies in the range of 5 eV.

The experimental work performed allows the study of the first three regions. It may be noted that the second and third regions of a band

structure of a semiconductor described above play the key roles in determining the nature of the conductivity of a semiconductor. This may be of use in the design, of electronic components (e.g. diodes, transistors etc.), photo-detectors, solar cells etc.

There are a large number of different experimental methods used in studying the band gap and the band structure. Various methods discussed by Shigeo Shionoya (1966) are low temperature conductivity measurements, study of emission spectra, magneto absorption, cyclotron resonance, magnetoresistance, interband Faraday effect, photo-emission and optical methods. However, according to C. Kittel (1971)

> "The best values of the band gap are obtained by optical absorption".

A careful study of the optical properties of a material and an analysis of the absorption curves, gives an accurate value of its band gap and also tells us about the optical transitions that occur.

As far as theoretical calculations of band structure of a crystal are concerned there are two schools of thought. One tries to improve first principle methods in order to obtain quantative agreement with experiment; the other makes use of experimental data to which the band structure is fitted. Both of these methods require an accurate study of the optical properties of the semiconducting materials such as CdS, ZnS and Ge.

1.2 OPTICAL PROPERTIES OF A MEDIUM

The significance of the optical properties of a medium can be best understood from the wave equations which are derived using Maxwell's equations.

It can be shown that a monochromatic plane electromagnetic wave of

angular frequency ω travelling in the z-direction in a homogeneons isotropic medium of permittivity ε and permeability μ has the form

$$\vec{E}(z,t) = \vec{E}_0 \exp i\,(\alpha z - \omega t) \exp(-\beta z) \qquad 1.2.1$$

where $\vec{E}$ is the electric field intensity, $\vec{E}_o$ is a constant amplitude and

$$\alpha^2 = \frac{\varepsilon\mu\omega^2 + (\varepsilon^2\mu^2\omega^4 + \mu^2\sigma^2\omega^2)^{\frac{1}{2}}}{2}$$

and

$$\beta^2 = \frac{-\varepsilon\mu\omega^2 + (\varepsilon^2\mu^2\omega^4 + \mu^2\sigma^2\omega^2)^{\frac{1}{2}}}{2}$$

where σ is the conductivity of the medium. It may be noted that MKS units are used.

The complex refractive index N of a medium may be defined as

$$N = \frac{c}{\omega}\gamma \qquad 1.2.2$$

where c is the velocity of light in vacuum and

$$\gamma = \alpha - i\beta \qquad 1.2.3$$

The complex refractive index N can be written in real and imaginary parts as

$$N = n - ik$$

where n is called the refractive index and k, the absorption index. It may be noted here that some authors such as Born and Wolf (1970), Ditchburn (1963) etc. write the complex refractive index N as

$$N = n\,(1 - i\chi)$$

where n is called the refractive index and χ the attenuation index or extiction coefficient. In the present work N = n-ik in accordance with Heavens (1955) will be used and k will be called the absorption index.

These two indices of refraction and absorption constitute the so called optical properties of a medium.

Since $n-ik = (\alpha-i\beta)\ c/\omega$, therefore equation (1.1.1) takes the form

$$\vec{E}(z,t) = \vec{E}_0 \exp i\omega(nz/c-t) \exp(-\omega kz/c) \qquad 1.2.4$$

The above equation represents a plane wave travelling in the z-direction with velocity c/n which is attenuated by $\exp(-\omega kz/c)$. The attenuation of intensity, which is proportional to the square of the attenuation of amplitude is thus given by $\exp(-2\omega kz/c)$. The absorption coefficient K, defined by the relative decrease of the intensity per unit distance in the propagation direction through $I = I_0 \exp(-Kz)$ is then

$$K = 2\omega k/c = 4\pi k/\lambda \qquad 1.2.5$$

where λ is the wavelength in vacuum.

1.3 DETERMINATION OF THE OPTICAL PROPERTIES OF BULK MATERIAL

In the case of a transparent material the optical constant (refractive index) can be determined without difficulty by simply measuring the transmittance of a uniform slab of the material at normal incidence. The polishing of the surface is necessary but not very critical. Also, a transparent material in the form of a prism can be used to determine its refractive index n. This can be determined by measuring the angle of prism A and the angle of minimum deviation Dm, from the relation

$$n = \sin\left(\frac{A+Dm}{2}\right) / \sin A/2$$

In the case of an absorbing material the optical constants are less easily determined, because there are two constants n and k and two different

measurements are needed. Transmittance measurements are not possible because of the absorption.

The possible methods, that can be used in determining the optical constants, of an absorbing bulk material, are discussed below.

1.3.1 REFLECTIVITY MEASUREMENTS AT DIFFERENT ANGLES OF INCIDENCE

It is possible to determine the optical constants of an absorbing bulk material by measuring its reflectivity at different angles of incidence. The accuracy involved in these measurements is not very good and secondly these measurements depend critically on the surface conditions of the specimen. Surface conditions such as surface roughness and possibly different stoichiometry at the surface are quite common.

1.3.2 KRAMERS-KRONIG ANALYSIS OF NORMAL INCIDENCE REFLECTANCE

In the case of absorbing bulk material, normal incidence reflectance is measured over a wide range of wavelengths (or frequency) and the optical constants are determined using Kramers-Kronig analysis. A brief discussion of this method is presented here.

At normal incidence the Fresnel equation for the reflection of radiation from an absorbing medium of complex index of refraction, $N = n-ik$, is

$$r = (n-ik-1) \,/\, (n-ik+1) = |r|e^{i\theta} \qquad 1.3.1$$

where $|r|$ and θ are the amplitude and phase of r. Also $R = |r|^2$ is the reflected intensity (or the measured normal incidence reflectance), such that

$$R = \frac{(n-1)^2 + k^2}{(n+1)^2 + k^2} \qquad 1.3.2$$

and the phase is

$$\theta = \tan^{-1} \left| -2k/(n^2 + k^2 - 1) \right| \qquad 1.3.3$$

The following relation can be easily obtained from the equations 1.3.2 and 1.3.3

$$k = -\left(\frac{1+R}{1-R} \tan \theta\right) n + \tan \theta \qquad 1.3.4$$

According to Jahoda (1957), if $\ln|r|$ is known over the entire frequency spectrum, θ at any single frequency ω_o can be determined from the Kramers-Kronig relation between the real and imaginary parts of the complex function $\ln r = \ln|r| + i\theta$:

$$\theta(\omega_o) = \frac{1}{2\pi} \int_o^\infty \frac{d \ln R(\omega)}{d\omega} \ln \left| \frac{\omega+\omega_o}{\omega-\omega_o} \right| d\omega \qquad 1.3.5$$

In theory, from this value of θ and the known R, the optical constants n and k can be easily determined from the above equations.

This method requires normal incidence reflectivity measurements to be made over a wide spectral range, or to be exact from zero to infinite frequency. In practice this is impossible and measurements are made in a limited frequency range and extrapolation procedures are used in the remaining regions.

According to Seraphin and Bennett (1967)

> "the extrapolation procedures that must then be used cannot be expected to give accurate optical-constant data at a given wavelength unless neighbouring regions where considerable optical activity is present are measured experimentally. For example, the optical constants obtained for absorbing media in the visible region, using a Kramers Kronig analysis, often depend strongly on measurements made in the 500 - 1000Å region of the vacuum ultraviolet."

The uncertainty in the optical constants, determined by this method can be realised from the above comment and the facts, mentioned below:-

(1) It is clear from the literature that in most of the cases where this method is applied, the reflectivity measurements do not extend beyond 12.4 eV (i.e. 100 nm).

(2) The limited accuracy with which the normal incidence reflectivity can be measured in the spectral region beyond 7 eV.

(3) The critical dependence of the reflectivity, on the surface conditions of the specimen, in the vacuum ultra-violet.

The extent of variations, in the optical constants, which result due to the different extrapolation procedures is far too large. For this it is worth mentioning the work of Connel et al (1973). Connel et al have calculated the imaginary part of the dielectric constant $\varepsilon_2=2nk$ for reflectivity data from germanium films for two low energy extrapolations, the first based on the data of Donovan et al (1970) and the second based on the data by Theye (1970), whose films, notably, exhibited similar reflectivity between 2 and 5 eV. It is noted that the difference in two calculated values of ε_2 at 5 eV is as large as 50%.

Apparently this has been the only method applied widely for the determination of the optical constants of an absorbing material. The uncertainty, in the optical constants, which are obtained by this method is fairly large.

1.3.3 VINCENT-GEISSE METHODS

J. Vincent-Geisse (1964) presented a method, for determining the optical constants of an absorbing solid, by means of a thin layer of a dielectric deposited on the solid. The measurements needed in this method are normal incidence reflectances from the bare surface of the solid and

the overlayed thin layer on the solid. The graphical method, for solution for n and k, used in this method, requires that the refractive index of the transparent film be constant in the entire wavelength range. The method was applied in the infrared region where this condition could be met easily, but fails in the visible and ultra-violet regions because it is difficult to find a dielectric, with a constant index of refraction in the last two regions.

J. Vincent-Geisse et al (1967) have proposed another method for the determination of the optical constants of crystals, within the region of strong absorption. This method requires the measurement of three reflectances at normal incidence, first from the surface of the specimen, secondly from a thin transparent layer evaporated on the surface, and thirdly from a second layer of the same material of exactly twice the thickness of the first layer deposited on the specimen. This method has the advantages of normal incidence measurements, which do not depend critically on the surface conditions of the specimen. Also the mathematics involved in determining n and k is reasonably simple. The disadvantages are

(a) It requires three measurements (reflectances) while the method discussed next (Tomlin's, 1972) requires only two measurements (reflectances).

(b) This method requires that the second layer must be twice as thick as the first. This condition may not be achieved easily if two successive evaporations are made on the same specimen. On the other hand, if it is assumed that the method used by J. Vincent-Geisse et al (1967) (wherein the first layer is deposited on one crystal of the specimen and the second layer

on another crystal of the same specimen) results in accurate thicknesses of the two layers, it is still necessary to ensure the preparation of two identical crystal surfaces having the same reflectances. This is probably less difficult for I.R. measurements than for U.V.

It will be shown in Chapter 3 that the optical constants, of a specimen, e.g. Ge, determined by the method of measuring reflectivities of the bare surface of the specimen and of a transparent layer on the specimen, depend critically on the accuracy with which the thickness of the layer can be determined. Also it will be shown that an error as small as 0.7% in the thickness has an appreciable effect on the refractive indices determined.

It should be noted here that in the method discussed next only one specimen and a single layer of a transparent material is desired, and at the same time the advantages of normal incidence measurements, and of the use of simple mathematics are maintained.

1.3.4 TOMLIN'S METHOD

A method of overcoming the uncertainties due to the extrapolations, while retaining the advantages of normal incidence measurements, but valid over a more limited wavelength range, was presented by Tomlin (1972).

This method involves measurements of normal incidence of reflectances from the specimen itself and from an area of the specimen coated with a thin transparent film. This method is applicable when the transmittance of the specimen is very small (almost zero).

If the specimen does not transmit its reflectance is

$$R = \frac{(n_0-n_2)^2+k_2^2}{(n_0+n_2)^2+k_2^2} \qquad 1.3.6$$

where n_0 is the refractive index of air, and n_2-ik_2 is the complex refractive index of the specimen.

The reflectance R_1 from the transparent film of refractive index n_1 deposited on the specimen, is given by the formulae of Tomlin (1968) from which

$$\frac{1+R_1}{1-R_1} = \frac{1}{4n_0n_2n_1^2}\left[(n_0^2+n_1^2)\ (n_1^2+n_2^2+k_2^2)\right.$$

$$\left. + (n_0^2-n_1^2)\ \{(n_1^2-n_2^2-k_2^2)\cos 2\gamma_1 + 2n_1k_2\sin 2\gamma_1\}\right] \qquad 1.3.7$$

where $\gamma_1 = 2\pi n_1 d_1/\lambda$, d_1 is the thickness of the transparent film, λ is the wavelength. If d_1, $n_1(\lambda)$, $R(\lambda)$ and $R_1(\lambda)$ are known then the complex refractive index (n_2-ik_2) for wavelength λ can be determined from the above two equations. The solution of the above equations will be discussed in detail later on, together with modifications necessary to take account of absorption in the overlying film.

In the present work, this method was used in measuring the optical constants of amorphous and polycrystalline germanium.

1.4 ON THE OPTICAL PROPERTIES OF THIN FILMS

Thin films may be prepared by several techniques, e.g. vacuum evaporation, cathode sputtering, chemical deposition, etc.

For thin films of transparent materials, simple transmittance measurements at normal incidence are sufficient to determine the refractive index (Appendix A). But in case of thin films of absorbing materials, the transmittance measurements alone are not sufficient to determine the optical constants n and k of the material. In this case additional measurements

of the intensity or both intensity and phase, of the reflected beam from the film surface, are required. Since these measurements are affected by the surface, in order to get reliable results, care must be taken to avoid contaminations, roughness and irregularities of the specimen surface.

In the literature different values of n and k for the same material have been reported by different people. The possible reasons for this could be:-

(1) CHOICE OF SOLUTIONS

The periodic nature, of the reflectance and transmittance equations for a thin film, which arises due to the multiple interference effect in the film, results in multiple solutions for the optical constants. When the values are well separated (which depends on the wavelength of the incident light, the film thickness and its refractive index), it is in general possible to distinguish the correct solutions. But on the other hand when the values are close together, the correct solutions may not be easily distinguished.

(2) USE OF APPROXIMATE RELATIONS

The mathematical relations, for the optical constants of thin absorbing films, are fairly cumbersome because of the multiple interference effects in the film. It is clear from the literature that various approximations are used.

(3) SURFACE CONDITIONS

(a) It has been shown by electron microscopy that the surfaces of the films have a granular structure, therefore the two

faces of the film are not perfectly parallel or the film is not perfectly flat.

(b) The stoichiometry at the surface may be different from that of the film itself, or the composition may differ, for example an oxide layer may occur on the surface of the film.

(4) FIBRE TEXTURE OF THE FILM

The crystallites of a polycrystalline film deposited at elevated substrate temperatures often have a preferred orientation such that one particular set of crystallographic planes is parallel to the substrate plane in all the crystallites. Such a texture is called fibre texture. The normal of the preferred planes is the axis of fibre texture.

As has been discussed by Rouard and Bousquet (1965) and Heavens (1955), the fibre orientation may be accompanied by optical anisotropy. In a case of oblique incidence measurements, the effect of applying the equations derived for an isotropic film to such a film might well be to yield a complex value for the thickness.

(5) FILM THICKNESS

From the known granular structure of thin films, there is some uncertainty as to the real meaning of 'd' the film thickness which appears in the equations describing the film's optical behaviour. For a detailed study of these points one is referred to Rouard and Bousquet (1965) and Heavens (1955, 1960).

The measurement of the optical constants of a thin absorbing film is not very easy. A brief discussion of various methods of determining the optical constants of a thin film, together with their merits

and demerits, is given in the following section. Extensive reviews on this topic have been given by Heavens (1955, 1960), Rouard and Bousquet (1965) and Abeles (1963).

1.5 METHODS OF DETERMINING THE OPTICAL CONSTANTS OF A THIN ABSORBING FILM

Various methods used in determining the optical constants of a thin absorbing film are briefly described below.

1.5.1 POLARIMETRIC METHODS

These methods involve the measurement of the ratio of the amplitudes of the two components of plane polarized light after reflection at a film and the differential phase change suffered by these components. In most of the cases, plane polarized light with its vibration direction inclined at 45° to the plane of incidence is used. The ellipsometric method comes under this heading.

Since the measurements are taken at non-normal incidence, surface conditions and fibre texture of the film, will have an appreciable effect on the optical constants, thus determined. As Rouard and Bousquet (1965) comment;

> "If we assume that it is possible to work at oblique incidence, in particular at the Brewster angle, and assuming that the films are ideal (that is to say: homogeneous, isotropic and bounded by plane parallel surfaces) then polarimetric methods can be used, see for instance, Forsterling (1937), Essers-Rheindorf (1937), Sommer (1940), Odenbach (1940) and Vasicek (1947, 1949, 1951). Unfortunately most of the results obtained by these authors are inconsistent. In fact in many cases the values obtained for the film thicknesses had an imaginary component of non-negligible magnitude; this is undoubtedly due to the fact that the hypothesis of ideal films was not accurate".

They further say;

"The granular structure of the films as revealed by electron microscopy, the inhomogeneity and the existance of transition layers shown optically by Bousquet (1957) and possible anisotropy make it exceptional for the theoretical conditions on which the polarimetric methods are based to exist. This is the reason for the inconsistent results mentioned above".

1.5.2 SPECTROPHOTOMETRY AT OBLIQUE INCIDENCE

This method involves the measurement of reflectance (R_{11}) from the air side of the film, reflectance (R'_{11}) from the substrate side of the film and transmittance (T_{11}) of the film, all at an oblique incident angle for an incident vibration parallel to the plane of incidence. Three measurements are required in order to determine the unknowns n, k and film thickness d. The method is discussed in detail by Abeles (1963) and has not yet been employed as far as I know.

This method, although appearing very attractive from the theoretical viewpoint, is not much help because measurements taken at oblique incidence will be considerably affected by the fibre texture of the film, which may be accompanied by optical anisotropy. Besides this the surface condition of the film will have an appreciable effect on the results.

1.5.3 COMBINED METHOD

Schoppers method, which is a combination of polarimetric and spectrophotometric (at normal incidence) methods, comes under this heading.

Schoppers method entails measurement of the amplitude and phase of the light reflected from each side of a film and of the light transmitted by the film, all the measurements being at (or as near as is possible to) normal incidence.

This method has the disadvantage that six measurements are required and of these three are measurements of phase change, which are not readily measurable. It may be noted that most of the other methods require four or less than four measurements. The calculations involved in this method are fairly cumbersome and time consuming.

1.5.4 SPECTROPHOTOMETRY AT NORMAL INCIDENCE

There are several variations of this technique, for instance, the methods used by H. Murmann (1933) and Male (1952) require measurements of reflectance at each side of the film and the transmittance of the film. The procedure, involved in determining optical constants in these methods is labourious and time consuming. On the other hand the method, used by Denton et al (1972), involves only two measurements that is reflectance (R) at the air side, and transmittance (T) of a film. This method does not require a separate measurement of the thickness of the film. The procedure, used in determining the optical constants and the film thickness in this method is fairly simple and is less time consuming when compared with other methods such as Murmann (1933), Male (1952), Bennett and Booty (1966). Beside this, it has the following advantages, which are stated briefly and will be discussed later on.

(1) The dispersion curve obtained from the calculations is such that there is no problem in distinguishing the correct solutions from the others which result because of multiple interference effect.

(2) The exact relations are used.

(3) The surface conditions can be allowed for by considering the surface of the film as a separate layer.

(4) According to Heavens (1955)

"For films prepared by evaporation at normal incidence, if a fibre axis develops it is itself normal to the substrate. In measurements made at normal incidence, the light is travelling along the fibre axis direction. This is the one direction along which the effects of optical anisotropy in the film are of no consequence".

(5) It was made clear by Denton et al (1972) that in case of a single film with a smooth surface, there is only one value of film thickness d for which a continuous acceptable dispersion curve can be obtained. In case of a film with a granular surface structure or with an oxide layer on the surface, the relations for a single film do not result in a continuous dispersion curve. In this case, assuming that the surface of the film can be represented by a separate layer, one may use reflectance and transmittance formulae for a double layer and so obtain an acceptable dispersion curve. This curve is obtained when the correct values of the film thickness and the equivalent surface layers are used, and in this method, there is no uncertainty as to the real meaning of the film thickness. Thus the five sources of error in Section 1.4 have been accounted for.

1.6 AIMS OF THE PRESENT PROJECT

The semiconductor, whose optical properties have been most extensively studied, is germanium. The disagreement between the different results published is far too large, which suggests the need of accurate determinations of its optical constants. The aim of the present work is to determine the optical properties of amorphous and polycrystalline germanium by using the accurate method suggested by Tomlin (1972) and discussed earlier. This method of Tomlin's has been applied for the first time as

far as I know.

The optical properties of amorphous germanium films were determined in the spectral range 0.62 to 1.77 eV from the measured normal incidence reflectance and transmittance, and the knowledge of film thickness by the method discussed by Denton et al (1972). These measurements have been extended into the spectral range above 1.77 eV, where the transmittance is very small (less than 1%), using Tomlin's method. Also the optical properties of polycrystalline Ge in the form of a slab, with a carefully polished surface, have been determined in the same way.

It will be shown in Chapter 3 that for a specimen like Ge, the transparent thin film of higher refractive index may be preferred. It was found that thin films, of materials like zirconium dioxide, tantalum pentoxide and zinc sulphide could be used as suitable transparent films. For this reason the optical properties of thin films of ZrO_2 and Ta_2O_5 were determined. ZrO_2 and Ta_2O_5 have high refractive indices and are transparent in the untra-violet down to wavelengths of 250 and 290 nm respectively. Most of the other materials which are transparent in this region e.g. silicon dioxide, sodium chloride, potassium chloride etc. have low refractive indices. Besides this an accurate knowledge of the optical properties of ZrO_2 and Ta_2O_5 is of value in the design of various optical filters, and in the applications as thin film capacitors, where films of higher dielectric constants are required.

The aim of the present work was also to investigate the first three energy regions of the band structure (discussed in Section 1.1) of semiconducting materials such as cadmium sulphide and zinc sulphide as part of a complete study of the II - VI compounds. The best method for such

investigation is the optical absorption method (Kittel, 1971).

It has been shown in the previous section that spectrophotometry at normal incidence is the accurate method for determining the optical constants of a material in the form of thin film. This requires the measurement of reflectance (R) on the air side, and transmittance (T), of a film.

It was made clear by Denton et al (1972) that the use of $(1 \pm R)/T$ relations derived by Tomlin (1968) in place of the separate relations for R and T given by Heavens (1955), is much more convenient and less time consuming. These relations are applicable in case of a single film with a smooth surface. In practice, it is seen that these relations do not always result in a continuous dispersion curve, the reason for this being the surface conditions of the film, or insufficient accuracy in the measurements of R and T where they are very small.

The structures of the films were studied using x-ray powder diffraction method by scraping the films from the substrates, and the film surfaces were investigated by means of electron-microscopy of surface replicas.

It was concluded that the surface conditions must be accounted for in order to obtain an acceptable dispersion curve. Various methods of accounting for the surface conditions were considered and discussed. It was found necessary to treat the surface of the film as a separate layer with different optical constants, from those of the film itself. Hence the simplified relations, for a double layer, derived by Tomlin (1972), were used.

The optical constants, determined by this method, were analyzed to study the band structures of cadmium sulphide, zinc sulphide and tantalum pentoxide and the nature of the optical transitions.

CHAPTER 2.

EXPERIMENTAL APPARATUS

2.1 SPECTROPHOTOMETER

The spectrophotometer, used in the present work, for measuring near normal incidence reflectance (R) and transmittance (T), was a modified form of that due to Strong (Kuhn and Wilson 1950) and was described in detail by Denton (1971). This was built in the Physics Department workshop. The angle of incidence being about 5°, which results in negligible error in the measured R and T. A photograph of the apparatus is shown in Figure 2.1.

The optical system and the measurements of reflectance and transmittance have been described in detail by Denton (1971) and are illustrated in Figures 2.2 and 2.3. Figure 2.2 shows the optical path followed by the light from the monochromator, after being chopped by a mechanical chopper, into the spectrophotometer and then to the detector. While Figure 2.3 shows the procedure adopted in measuring the reflectance and transmittance of the specimen.

2.2 LIGHT SOURCE

A Philips deuterium spectral lamp type 126138 was used in the spectral range from 250 to 500 nm. This lamp was operated on d.c. according to the circuit supplied by the makers. In the spectral range from 450 to 2000 nm light from a 100-Watt quartz iodide lamp, powered by a 12 volt d.c. regulated supply, was used.

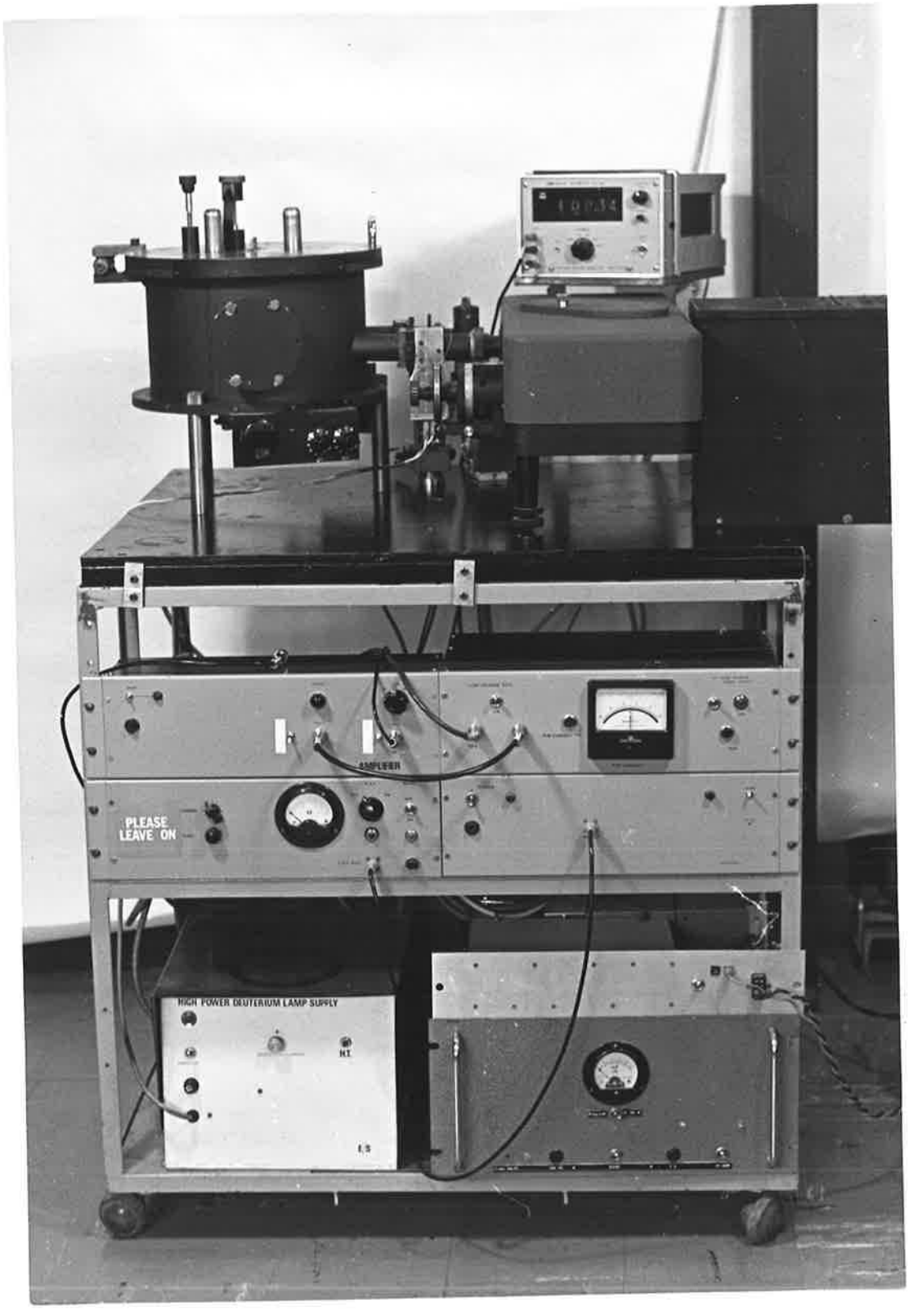

FIGURE 2.1

2.3 MONOCHROMATOR

In the initial stages of the present work the Hilger-Watts prism monochromator of Denton's apparatus was used but was found to be unsatisfactory for the shorter wavelengths (ultra-violet) covered in this work.

Measurements, made using the Hilger-Watts monochromator, showed that the absorption in cadmium sulphide begins at about 520 nm and transmittance goes on decreasing sharply till 390 nm, after which the transmittance starts increasing as lower wavelengths are approached. The transmittance at 390 nm was about 5 to 7% and at 250 nm it was about 50 to 60% for all the films studied, which varied in thickness from 150 to 350 nm. It may be mentioned here that the sharp decrease in the transmittance, in the spectral range 500 - 390 nm, was not the consequence of multiple interference effects in the films, because similar measurements resulted for films of different thicknesses. Also for transmittances of the order of 5 to 7% at about 390 nm, the multiple interference effects would be negligible. The computed absorption index curve showed a peak at 390 nm and after which the absorption index decreases as the shorter wavelengths are approached. The published work on CdS (Moss, 1959) shows that the absorption peak is at about 230 nm.

Then measurements on zinc sulphide films were performed. The results obtained showed that the absorption peak was at 330 nm and after which the absorption index decreases as shorter wavelengths are approached. The published results on ZnS films (Moss, 1959) show the peak to be at about 216 nm.

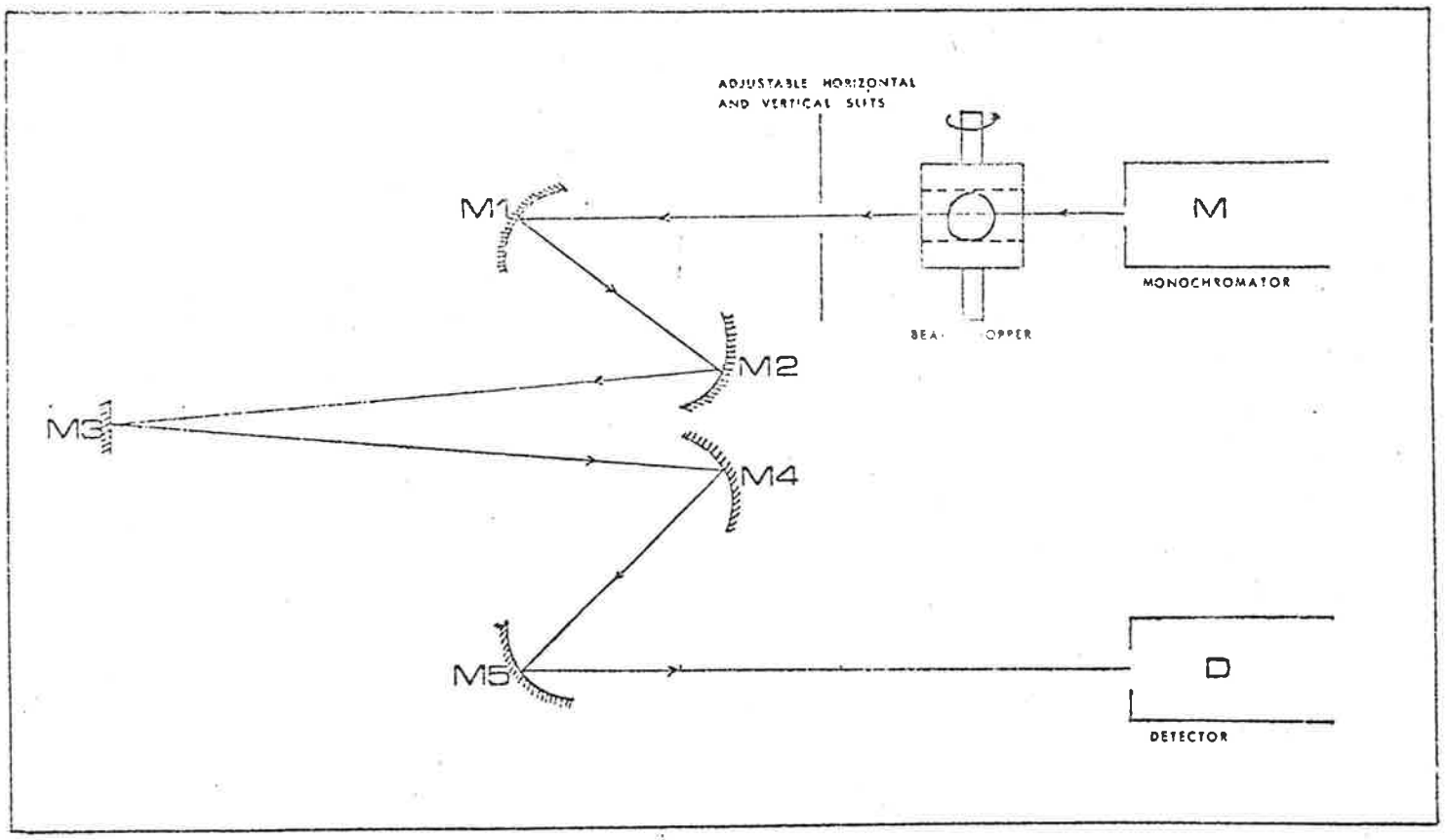

DIAGRAM OF THE OPTICAL SYSTEM

Figure 2.2

In the spectral region, where absorption is high such that the interference maxima and minima disappear, the position of the absorption peak depends on the position of the transmittance minimum. Therefore one suspects that the position of absorption peak as reported by others is unlikely to be much out. This discrepancy was found to be due to a white light background signal present in the ultra-violet output from the monochromator. Furthermore to verify the results, the transmittance of CdS and ZnS films was measured using a Perkin Elmer type 137 spectrometer which ranges from 200 to 750 nm and has an accuracy of about 5%. Measurements of transmittance on this spectrometer showed a minimum at about 235 nm in the case of CdS and at about 220 nm in the case of ZnS, which are in good agreement with the published results (Moss, 1959). Thus it was confirmed that the previous measurements in the ultra-violet were incorrect. It was thought that the errors arose from a background signal due to the scattering of light from the mirrors in the monochromator. The mirrors were cleaned, grounded, repolished and resilvered, but this did not improve the conditions.

Hence it was decided to use a Carl Leiss Mirror-Double-Monochromator with exchangeable prisms. This monochromator was coupled to the existing spectrophotometer via a mechanical chopper. The ultra-violet output from this monochromator had no sign of any background signal. In the spectral region from 450 to 2000 nm flint glass prisms, and in the region from 250 to 450 nm crystal quartz prisms were used. Quartz prisms alone could be used to cover the entire spectral range from 250 to 2000 nm, but the flint prisms were used in the infrared and visible regions because flint glass has better dispersion than quartz in these regions.

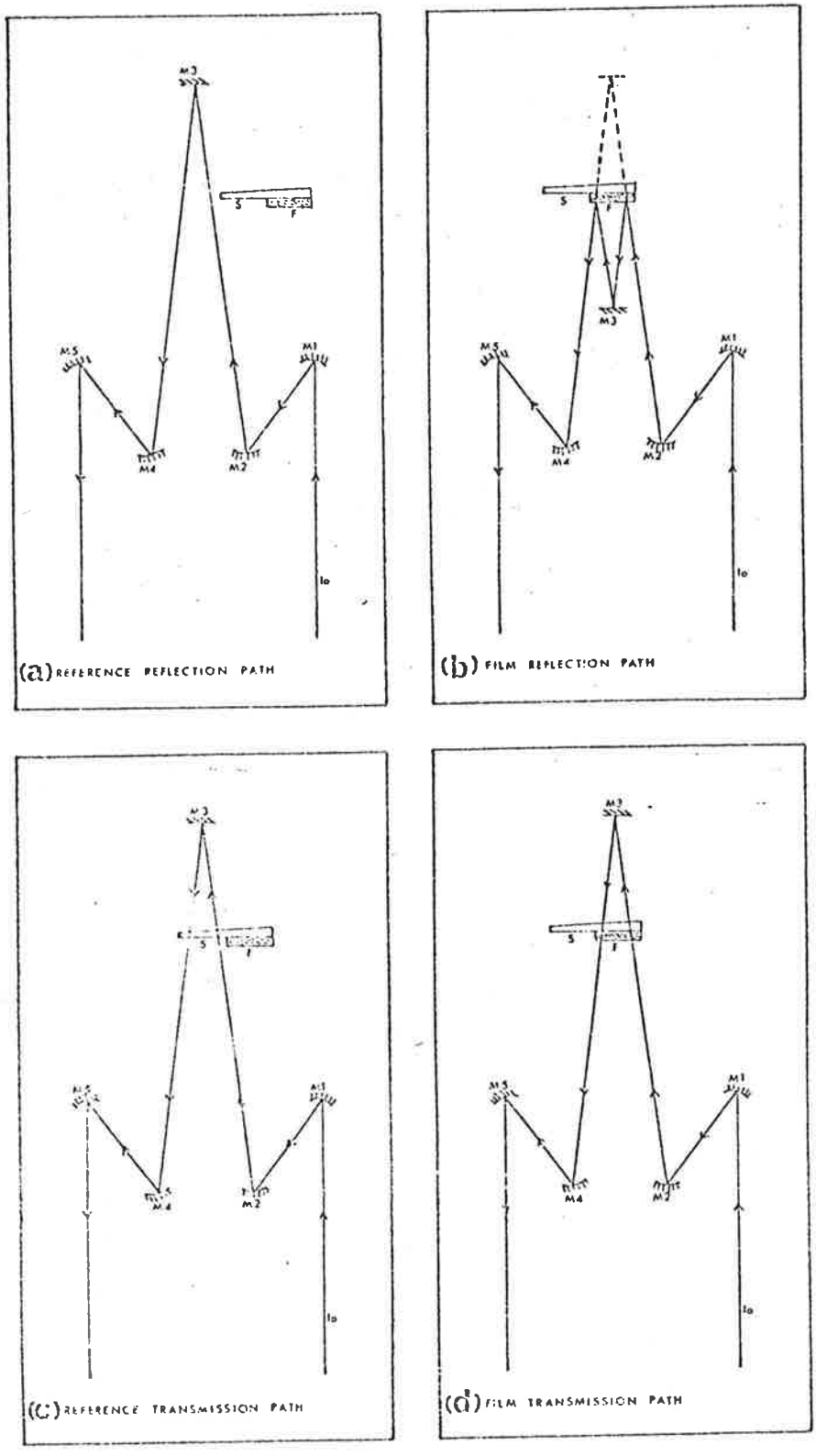
M3
S
F
M5
M1
M4
M2
Io
(a) REFERENCE REFLECTION PATH
(b) FILM REFLECTION PATH
(c) REFERENCE TRANSMISSION PATH
(d) FILM TRANSMISSION PATH

Figure 2.3

These two sets of prisms were calibrated for the output signal wavelength against the drum reading. This was achieved by the help of various spectral lamps, whose emission spectra are accurately known, such as the Philips low pressure Hg (93123), high pressure Hg (93136), He (93098), Na (93122) and Cd (93162) sources. Fig. 2.4 shows the calibration curves.

2.4 LIGHT SENSITIVE DETECTORS

In the present work three different detectors were used to cover the spectral range from 250 to 2000 nm.

In the range from 250 to 500 nm a Philips IP28 photomultiplier was used. From 450 to 1100 nm a UDT - 500 UV silicon diode detector/amplifier combination (enhanced ultra-violet response) was used. And from 900 to 2000 nm a lead sulphide photoconductive cell was used. The lead sulphide cell was maintained at a constant temperature as was discussed by Denton (1971).

As is clear, from the above mentioned ranges, there is some overlap of the spectral range covered by each of the two detectors. The measurements, with two different detectors at a given wavelength, were of great help in detecting film uniformity. At a particular wavelength, the two detectors have different sensitivities which would require input signals, of different intensities, entering the spectrophotometer to enable the measurements to be made. The signal intensities were controlled by the width of the input slits. Therefore for different detectors the slit widths would be different and hence the cross-section of the beam falling on the specimen would be different. If a film was non-uniform the results obtained by the two detectors would be different. This would be noticeable for non-

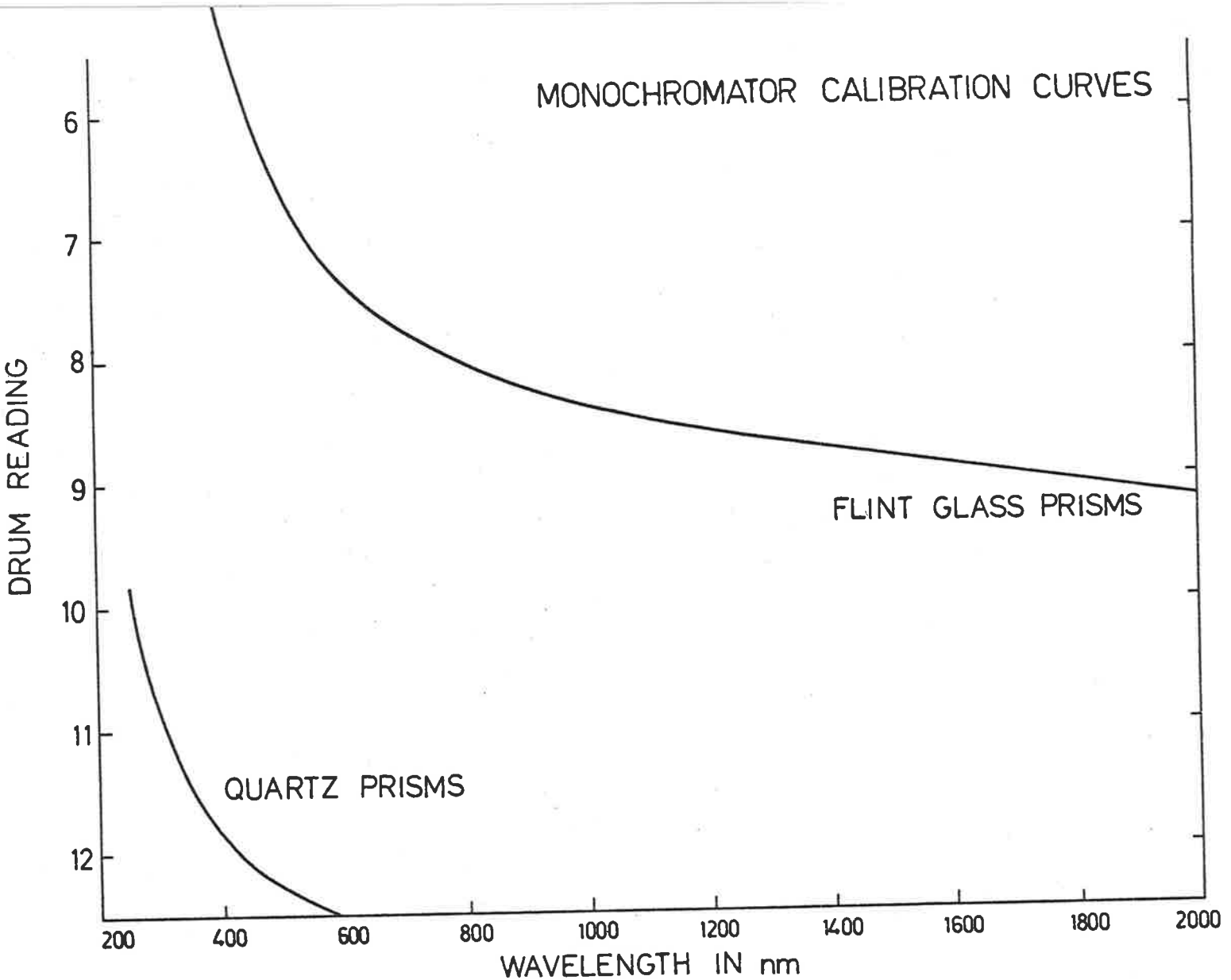
MONOCHROMATOR CALIBRATION CURVES
FLINT GLASS PRISMS
QUARTZ PRISMS
DRUM READING
6
7
8
9
10
11
12
200
400
600
800
1000
1200
1400
1600
1800
2000
WAVELENGTH IN nm

FIGURE 2·4

uniform films which have a large rate of change in R or T with respect to change in film thickness. In case of uniform films, the results obtained by the use of different detectors, in the range where these overlap, were in agreement.

The output from these light sensitive detectors was fed into a high input impedance amplifier with adjustable gains and a digital voltmeter read-out.

2.5 HIGH INPUT IMPEDANCE AMPLIFIER

As the lead sulphide detector has a very high output impedance, a suitable amplifier with very high input impedance (>100 M Ω) was designed. A circuit diagram is shown in Figure 2.5.

The design is somewhat similar to the one used by Denton (1971), except that stable high fixed gains were achieved through the use of the latest MOSFET'S and high speed linear integrated circuits.

The input stage incorporates a dual-gate MOSFET to give high input impedance at unity gain. This stage is built in a shielded box and followed by a double-stage amplifier with switchable stable a.c. gain in x 10, x 100 and x 1000 ranges. A filter resonant at the chopper frequency is placed between this a.c. amplifier and the next stage which is a precision a.c. to d.c. converter, consisting of a rectifier and an integrator. The smoothed d.c. voltage is then displayed on a digital voltmeter. The switchable fixed gains were calibrated and had an accuracy within about 0.1%.

2.6 THE SUBSTRATES

Thin films of the different materials, whose optical properties were

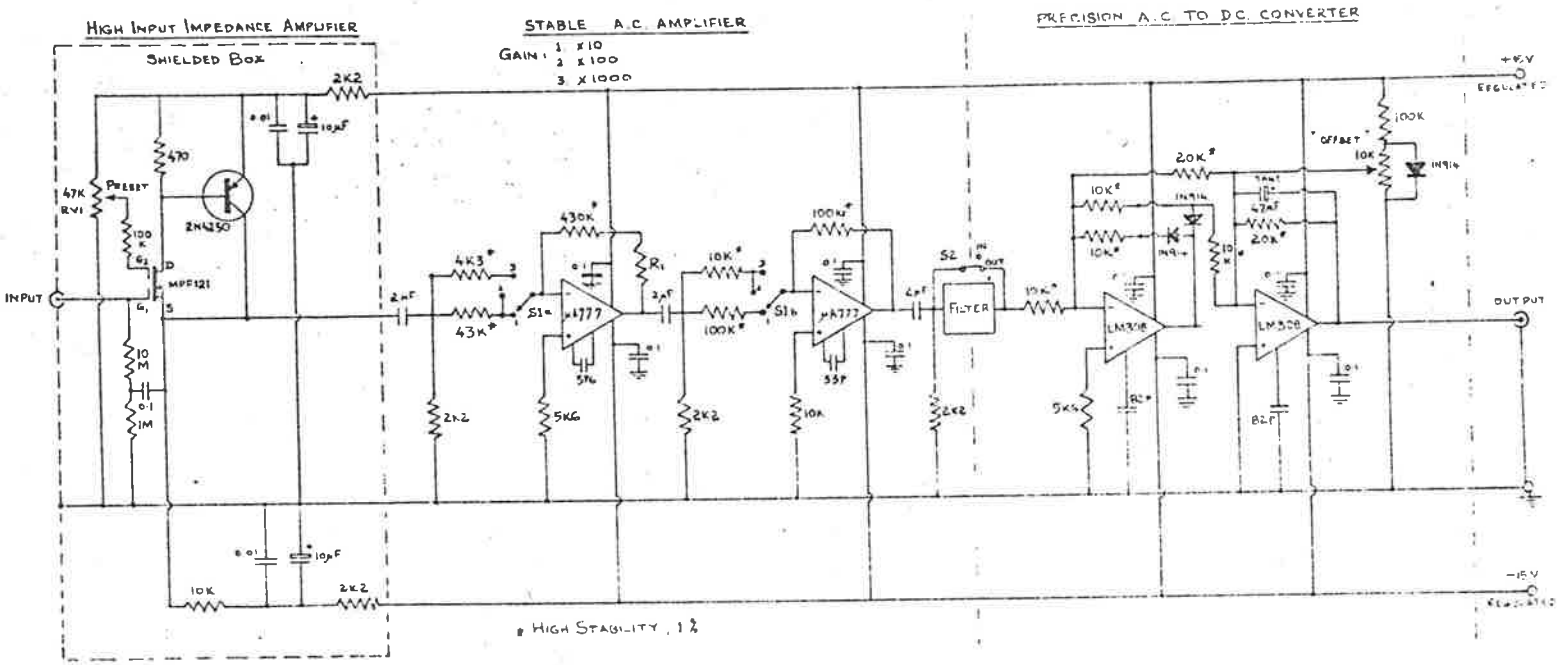
HIGH INPUT IMPEDANCE AMPLIFIER
SHIELDED BOX
STABLE A.C. AMPLIFIER
GAIN: 1 X10
2 X100
3 X1000
PRECISION A.C. TO D.C. CONVERTER
INPUT
OUTPUT
FILTER
OFFSET
+15V
-15V
* HIGH STABILITY, 1%

FIGURE 2.5

studied, were deposited on optically flat quartz wedges. These were prepared to specification by the Scientific and Optical Laboratories of Australia, Adelaide. The angle of each wedge was about 3^{o} between the front and the rear surfaces. Each wedge measured 2" x $1\frac{1}{2}$" and was cut in half to form a thick and thin wedge. The films were deposited on the thicker part and the thin part was left uncoated so that a transmittance reference signal could be measured, as shown in Figure 2.3. Wedges were used instead of flat substrates in order to eliminate the radiation reflected from the rear surface of the substrate, so that the multiple reflections in the substrate did not have to be taken into account.

Careful cleaning of the substrates was essential in order to obtain a uniform film free of pin-holes. The substrates were cleaned in warm chromic acid and then rinsed in double distilled water and dried in a stream of dry air. Afterwards they were wiped with a tissue paper soaked in acetone and again washed in double distilled water and dried in a stream of dry air. Finally they were placed between two electrodes in a vacuum chamber and ion bombarded for about five minutes.

2.7 SUBSTRATE HEATER

Heating the substrate uniformly to high temperature of the order of 400^{o}C in vacuum is a problem. Care must be taken that the vacuum chamber is not overheated, otherwise vacuum seals may deteriorate. After trying various heaters, it was found that the one described below was the most effective. This was based on an idea of a fellow worker in the Physics Department.

A 3" x 3" copper slab of thickness $\frac{1}{2}$" was used as a substrate holder.

The face of this slab to which the substrate was attached, was optically polished, so that the substrate was in a good thermal contact with the holder. In this type of heater, the substrate is heated by conduction and therefore, in order to obtain uniform heating, the polishing of one face of the slab was necessary.

Thin molybdenum wire was wound around a thick mica sheet of dimensions 3" x 3", and this was sandwiched in between two thin mica sheets to provide electrical insulation. The heater assembly was clamped to the unpolished top side of the copper slab with a thin stainless steel sheet. The whole substrate holder/heater assembly was enclosed by a polished stainless steel heat-reflecting shield.

The heater assembly proved to be very effective; high substrate temperatures being achieved with low power input and no over-heating of the vacuum chamber.

The substrate was heated in vacuum for about six hours, before the film was deposited. This was done in order to ensure that the temperature of the substrate was uniform and fully stabilised. The substrate temperature was measured with a chromel-alumel thermocouple, whose junction was in contact with the substrate. The potential difference across the thermocouple was measured using a Cambridge potentiometer type 44228.

CHAPTER 3.

CALCULATION OF THE OPTICAL CONSTANTS OF AN ABSORBING MATERIAL

3.1 INTRODUCTION

A detailed study of Tomlin's method (1972) of determining the optical constants of an absorbing material, by measuring the normal incidence reflectances from the specimen itself, and from an area of the specimen coated with a thin transparent layer, is presented in this chapter.

The application of this method requires that the specimen does not transmit (or that its transmittance is less than say 1%). This requirement is needed because it is assumed that there are no multiple interference effects in the specimen. This situation is met in specimens of the following types:

(a) thin films of highly absorbing material, e.g. germanium films are highly absorbing in the wavelength region below 700 nm. A Ge film of thickness greater than 250 nm has a transmittance less than 1%.

(b) bulk absorbing material of such a thickness that light transmitted through it, is less than 1%.

The optical properties of films in the spectral range where they have transmittance higher than 1% can be determined by measuring their normal incidence reflectance and transmittance, as was discussed in Chapter 1. Hence using these two methods, the measurements of optical constants can be extended over a wide spectral range.

Two different methods (i.e. graphical and computer) are described for solving the equations from which the optical constants n and k are obtained. A program has been written for a digital computer and is shown to be more convenient than the graphical method of solution. In calculations of the optical constants, multiple solutions occur, and the solutions for the refractive index are markedly affected by small changes in the overlying film thickness. The behaviour of the solutions under such changes is discussed, and the results of this investigation show that the choice of the correct solutions depends critically on film thickness, and use can be made of this in determining the optical film thickness in much the same way as described for semi-transparent films by Denton et al (1972).

It is shown that with some modifications this method could be applied in case where the overlying film is semi-transparent.

3.2 TOMLIN'S METHOD

The method, suggested by Tomlin (1972) for determining the optical constants of an absorbing material, is described below.

Films which are highly absorbing in some part of the spectral range may transmit so little light that only reflectance can be measured. A possibility is to consider the reflectances from the specimen itself, and from an area of the specimen coated with a thin transparent film. If the specimen does not transmit its reflectance is

$$R = \{(n_2-n_0)^2 + k_2^2\} / \{(n_2+n_0)^2 + k_2^2\} \qquad 3.2.1$$

where n_0 is the refractive index of air and n_2-ik_2 is the complex refractive index of the specimen.

The reflectance R_1 from the transparent film of refractive index n_1 deposited on the speciman, which may be regarded as a substrate, since it does not transmit, is given by the formulae of Tomlin (1968) from which

$$\frac{1+R_1}{1-R_1} = \frac{1}{4n_o n_1^2 n_2}\left[(n_o^2+n_1^2)\ (n_1^2+n_2^2+k_2^2)\right.$$
$$\left. + (n_o^2-n_1^2)\ \{(n_1^2-n_2^2-k_2^2)\cos 2\gamma_1 + 2n_1 k_2 \sin 2\gamma_1\}\right] \qquad 3.2.2$$

where $\gamma_1 = 2\pi n_1 d_1/\lambda$; d_1 is the thickness of the transparent film; λ is the wavelength.

Equation 3.2.1 can be written as

$$\left[n_2 - n_o\,\frac{1+R}{1-R}\right]^2 + k_2^2 = 4n_o^2 R/(1-R)^2 \qquad 3.2.3$$

which is a circle in the n_2/k_2 plane with centre $n_o(1+R)/(1-R)$, 0 and radius $2n_o\sqrt{R}/(1-R)$.

From equations 3.2.2 and 3.2.3

$$k_2 = \frac{n_1^2+n_o^2}{2n_1}\tan\gamma_1 + \frac{2n_o}{n_1(n_1^2-n_o^2)}\ \frac{1}{\sin 2\gamma_1}\left[\frac{1+R}{1-R}\,(n_1^2\cos^2\gamma_1\right.$$
$$\left. + n_o^2\sin^2\gamma_1) - n_1^2\,\frac{1+R}{1-R_1}\right]\ n_2 \qquad 3.2.4$$

which is a straight line in the n_2, k_2 plane, and the equations may be solved graphically or by computer.

If $\gamma_1 = (p+\frac{1}{2})\pi$ then from equation 3.2.4, by multiplying through by $\sin 2\gamma_1$ before putting $\gamma_1 = (p+\frac{1}{2})\pi$, the following relation can be obtained

$$n_2 = (n_1^4-n_o^4)\ /\ 2n_o\left(n_1^2\,\frac{1+R_1}{1-R_1} - n_o^2\,\frac{1+R}{1-R}\right) \qquad 3.2.5$$

3.3 SOLUTION OF EQUATIONS FOR n_2 and k_2

A graphical and a computer method, of solution of equations 3.2.1 and 3.2.2 for n_2 and k_2, are discussed below.

3.3.1 GRAPHICAL METHOD

If R and R_1 are measured and assuming that thickness d_1 and refractive index n_1 of the overlying transparent film are known, then equations 3.2.3 and 3.2.4 can be solved graphically for n_2 and k_2 as follows.

A circle in the n_2/k_2 plane with centre $n_o(1+R)/(1-R)$, 0 and radius $2n_o\sqrt{R}/(1-R)$ can be drawn. A straight line for the same values of R, R_1, d_1 and n_1 can be drawn, in the same plane, using equation 3.2.4. The intersection of the straight line with the circle results in two possible solutions for n_2 and k_2. The choice of correct solutions may be a problem, especially at wavelengths where the two intersecting points lie close together, this depends on the thickness and refractive index of the overlying transparent film. Tomlin (1972) has suggested that the choice of the correct solution might depend upon continuing the dispersion curve found for the less absorbing part of the wavelength range (from reflectance and transmittance measurements), or upon making measurements with two different thicknesses of the overlying thin film. It may be commented here that a reasonable continuation can be obtained by the use of slightly incorrect thickness but this will not result in a continuous dispersion curve in the other parts of the spectral region covered. This is because the optical constants depend critically on the accuracy with which the thickness of the layer can be determined, e.g. in the case of

germanium a continuous dispersion curve could not be obtained if the error in the thickness was as small as 0.7%. This will be discussed later on in this chapter. Even if the measurements are made with two different thicknesses of the overlying thin film, the problem of accurate determination of thicknesses is still there. On the other hand the computer method of solution, which is discussed below, is less labourious and the choice of correct solutions is no problem, besides which this method has an advantage that it does not require a separate accurate measurement of film thickness.

3.3.2 COMPUTER METHOD

It is clear from the equations 3.2.1 and 3.2.2 that relations giving explicit values of n_2 and k_2 cannot be obtained.

Equation 3.2.1 can be written

$$k_2^2 = 2n_2 \frac{1+R}{1-R} - (n_2^2+1) \qquad 3.3.1$$

or

$$k_2 = \pm \{2n_2 \frac{1+R}{1-R} - (n_2^2+1)\}^{\frac{1}{2}} \qquad 3.3.2$$

As k_2 cannot be imaginary therefore $2n_2 \frac{1+R}{1-R} > (n_2^2+1)$

It follows from the above that for a given value of n_2 and R, k_2 has two values, which are equal in magnitudes but differ in signs. Though it is known that the positive k_2 is the only acceptable value (as absorption cannot be negative), the negative k_2 value had to be considered to obtain all possible solutions.

Equation 3.2.2 may be written in functional form

$$F(n_2,k_2) = \frac{1}{4n_0n_1^2n_2}\left[(n_0^2+n_1^2)(n_1^2+n_2^2+k_2^2) + (n_0^2-n_1^2)\{(n_1^2-n_2^2-k_2^2)\cos 2\gamma_1+2n_1k_2\sin 2\gamma_1\}\right] - \frac{1+R_1}{1-R_1} = 0 \qquad 3.3.3$$

If R and R_1 at a wavelength λ are measured and the film thickness is known, then the solutions to the equations 3.3.2 and 3.3.3 for n_2 and k_2 may be determined as follows:

Firstly, the positive value of k_2 is calculated from equation 3.3.2, by setting n_2 to a lower limit (i.e. $n_2 = \frac{1-\sqrt{R}}{1+\sqrt{R}}$) for the measured value of R. This ensures that only positive values of k_2^2 will result, i.e. real values of k_2. The set value of n_2 and calculated value of k_2 are substituted in the equation 3.3.3. If $F(n_2, k_2) = 0$, then this (n_2, k_2) satisfies both equations 3.3.2 and 3.3.3 and hence constitutes a solution.

If $F(n_2, k_2) \neq 0$, these values of n_2, k_2 and $F(n_2, k_2)$ are stored in the computer. An increment is added to n_2 (say 0.05), and the process repeated. The sign of the new value of $F(n_2, k_2)$ is compared with that of the stored value, and if it is the same the stored values of n_2, k_2 and $F(n_2, k_2)$ are rejected and the new values stored. A further increment is added to n_2 and the procedure continued until a change of sign occurs between corresponding values of $F(n_2, k_2)$, which then implies that a solution exists between these two values of n_2. This can be seen from Figure 3.1 where $F(n_2, k_2)$ is plotted as a function of n_2 for $n_1 = 2$, $k_2 = 2$, $\frac{1+R_1}{1-R_1} = 1.5$ and $\gamma_1 = 1.333\pi$.

Let $n_2^{(a)}$ and $n_2^{(b)}$ be the values of n_2 corresponding to the values

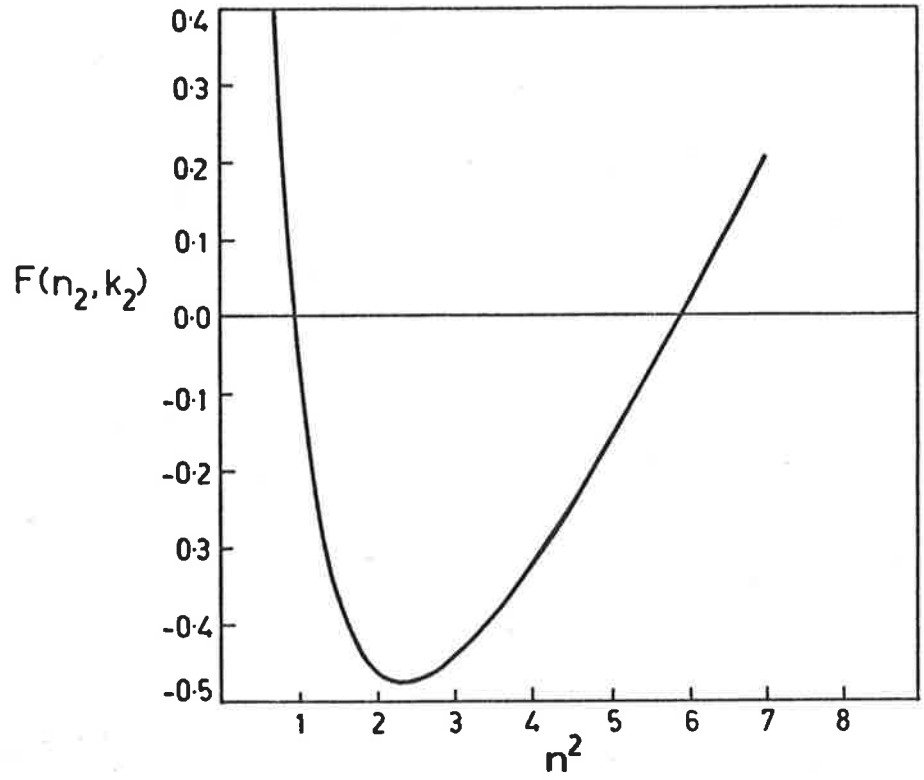

FIGURE 3·1

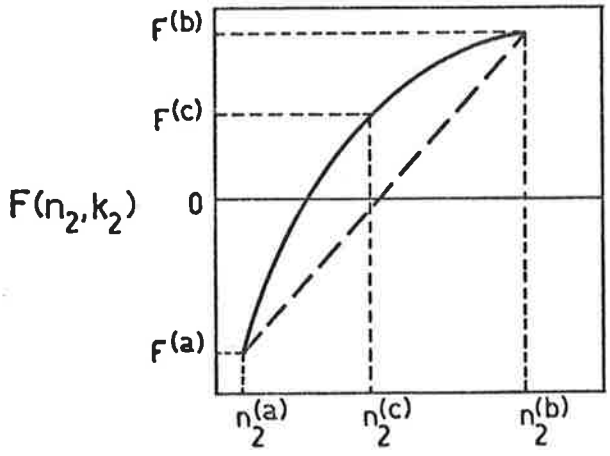

FIGURE 3·2

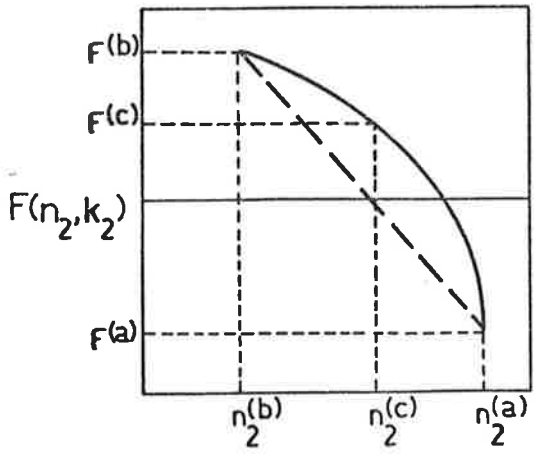

FIGURE 3·3

of $F(n_2, k_2)$ between which there occured a change of sign. Let $F^{(a)} = F(n_2^{(a)}, k_2)$ and $F^{(b)} = F(n_2^{(b)}, k_2)$. There are two cases to consider corresponding to $F^{(a)}$ being positive or negative. Consider the case where $F^{(a)}$ is negative. An approximation to n_2 can be found by linear interpolation between $n_2^{(a)}$ and $n_2^{(b)}$.

From Figures 3.2 and 3.3, an approximate solution is $n_2^{(c)}$ where, from similar triangles,

$$n_2^{(c)} = n_2^{(b)} - \frac{\{n_2^{(b)} - n_2^{(a)}\} F^{(b)}}{F^{(b)} - F^{(a)}} \qquad 3.3.4$$

k_2 is calculated as before for this new value of n_2, and the corresponding $F^{(c)} = F(n_2^{(c)}, k_2)$ calculated. If $F^{(c)} < 0$ then $F^{(a)}$ and $n_2^{(a)}$ are replaced by $F^{(c)}$ and $n_2^{(c)}$ and equation 3.3.4 again applied. If $F^{(c)} > 0$, then $F^{(b)}$ and $n_2^{(b)}$ are replaced by $F^{(c)}$ and $n_2^{(c)}$ and equation 3.3.4 again applied. By continuing this process until some preset limit is reached (e.g. $|F^{(c)}| < 0.001$), the values $n_2^{(c)}$ and corresponding k_2 are good approximations to the correct solutions.

For the case where $F^{(a)}$ is initially positive, the procedure and equations are identical to the above if $(n_2^{(a)}, F^{(a)})$ and $(n_2^{(b)}, F^{(b)})$ are interchanged. Thus n_2 and k_2 can be found to any required degree of accuracy by imposing appropriate limits.

Although for a given n_2, there is only one positive k_2 which satisfies equation 3.3.2, there exists another set of n_2 and k_2 which satisfy both equations 3.3.2 and 3.3.3. Consequently, further increments must be added to n_2 (until $\{2n_2 \frac{(1+R)}{(1-R)} - (n_2^2+1)\}$ is negative) to determine the other possible solution. It is clear from Figure 3.5 (which presents

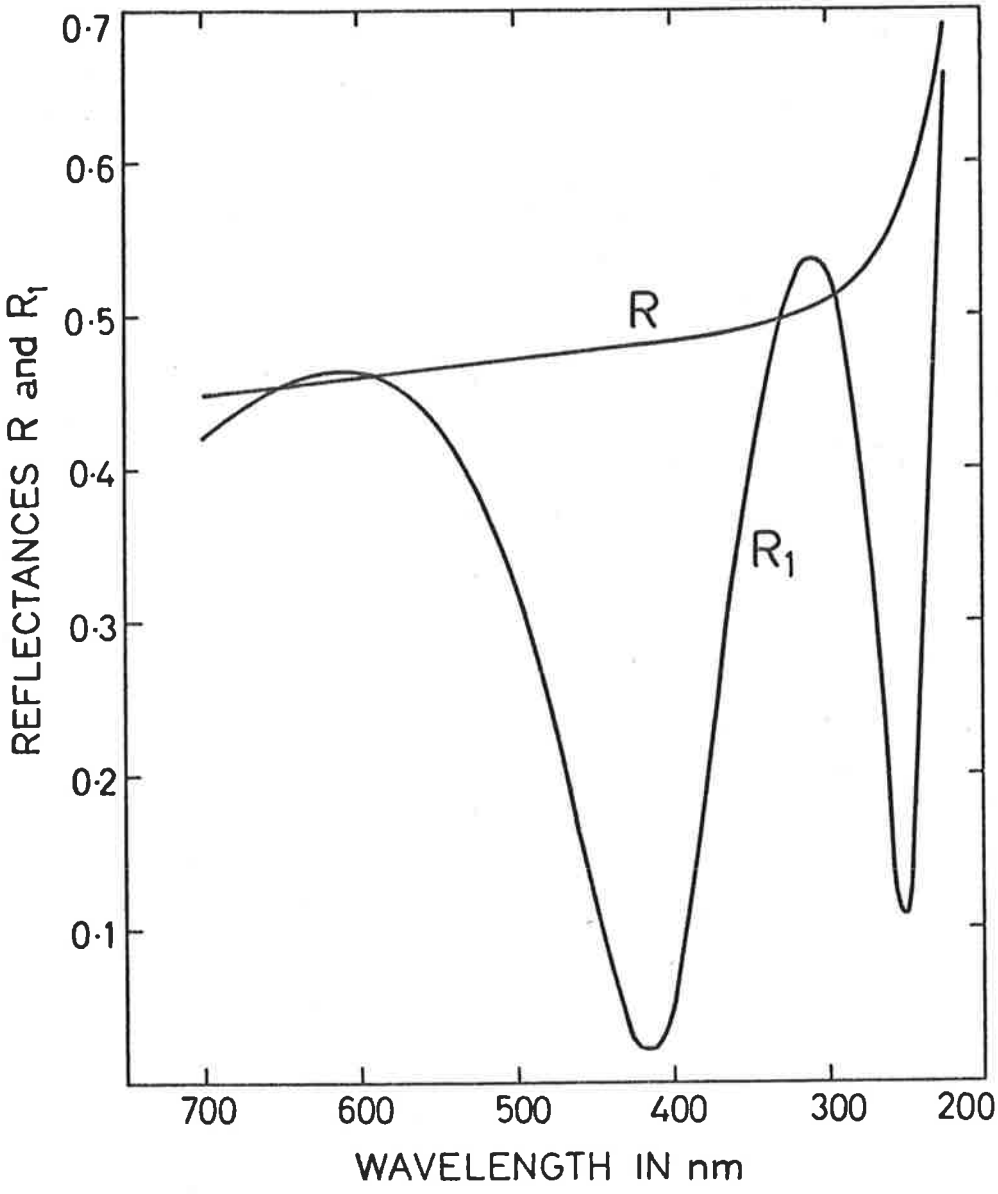
0·7
0·6
0·5
0·4
0·3
0·2
0·1
REFLECTANCES R and R1
R
R1
700
600
500
400
300
200
WAVELENGTH IN nm

FIGURE 3·4

the graphical solutions, discussed in the Section 3.4) that at certain wavelengths the other solution corresponds to negative k_2-values. Therefore, in order to determine all possible solutions, the procedure described above was repeated for negative k_2 values, obtained from the equation 3.3.2. It is necessary to find the multiple solutions in order to obtain the correct dispersion curve by making use of a closure criterion similar to that discussed by Denton et al (1972) for semi-transparent films on transparent substrates.

3.4 THE SOLUTIONS OBTAINED BY THE GRAPHICAL AND THE COMPUTER METHODS FOR A HYPOTHETICAL SPECIMEN

To illustrate the nature of the solutions of equations 3.2.1 and 3.2.2, a hypothetical specimen of complex refractive index n_2-ik_2, which does not transmit, was considered, so that for wavelengths less than 700 nm

$$n_2 = 5.1 - 0.2/\lambda^2 \qquad 3.4.1$$

$$k_2 = 4.1 - 4\lambda \qquad 3.4.2$$

where wavelength λ is in μm. (These values correspond roughly to amorphous germanium). Assume that a portion of the specimen was coated with a transparent layer of refractive index $n_1 = 2.1$ and thickness $d_1 = 140$ nm.

For the values of n_1, n_2, k_2 and d_1 mentioned above, the reflectances R and R_1 were calculated, in the spectral range from 280 to 700 nm at an interval of 1 nm, using equations 3.2.1 and 3.2.2. Figure 3.4 shows the plot of the calculated R and R_1 versus wavelength for such a system.

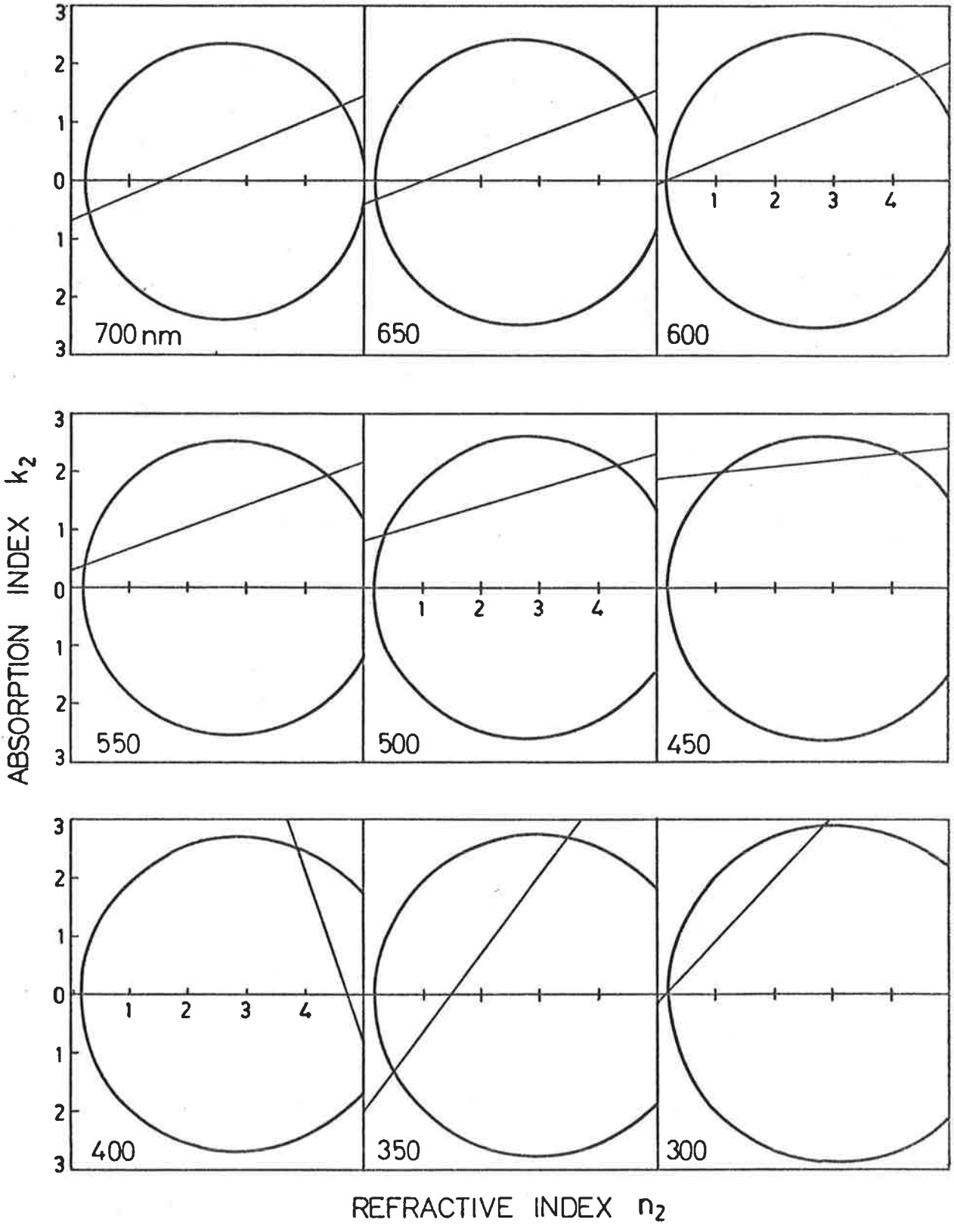
700 nm
650
600
550
500
450
400
350
300
ABSORPTION INDEX k_2
REFRACTIVE INDEX n_2

FIGURE 3·5

From the values of R and R_1, shown in Figure 3.4, which are used as data and d_1 = 140 nm, the calculations of n_2 and k_2 were performed by the graphical and computer methods, in the manner discussed in Section 3.3. The graphical solutions for n_2 and k_2 are shown in Figure 3.5 for the wavelengths indicated. Figure 3.6 is the plot of n_2 versus wavelength obtained by the computer method.

It is clear from Figure 3.6 that the correct solutions result in a smooth continuous curve, while the unwanted solutions lie on another continuous curve with repeated maxima and minima which eliminates any doubts about the choice of solutions.

3.5 EFFECTS OF ERRORS IN FILM THICKNESS

Using the same reflectances R and R_1 (Figure 3.4) as data, n_2 and k_2 were calculated by the computer method, assuming an overlying film thickness of 141 nm instead of the correct value of 140 nm. The dispersion curve shown in Figure 3.7 was obtained. And if d_1 = 139 nm, instead of the correct value of 140 nm, was used in the calculations, the n_2-curve shown in Figure 3.8 was obtained.

It is clear from Figures 3.7 and 3.8 that a continuous dispersion curve cannot be obtained even if the error in film thickness was as small as 0.7%. Thus a direct experimental measurement of film thickness will not be adequate for obtaining reliable values of refractive index over the whole wavelength range. The curves corresponding to overestimates (Figure 3.7) or underestimates (Figure 3.8) of thickness are easily distinguishable by their different forms.

In the present work an approximate knowledge of film thickness,

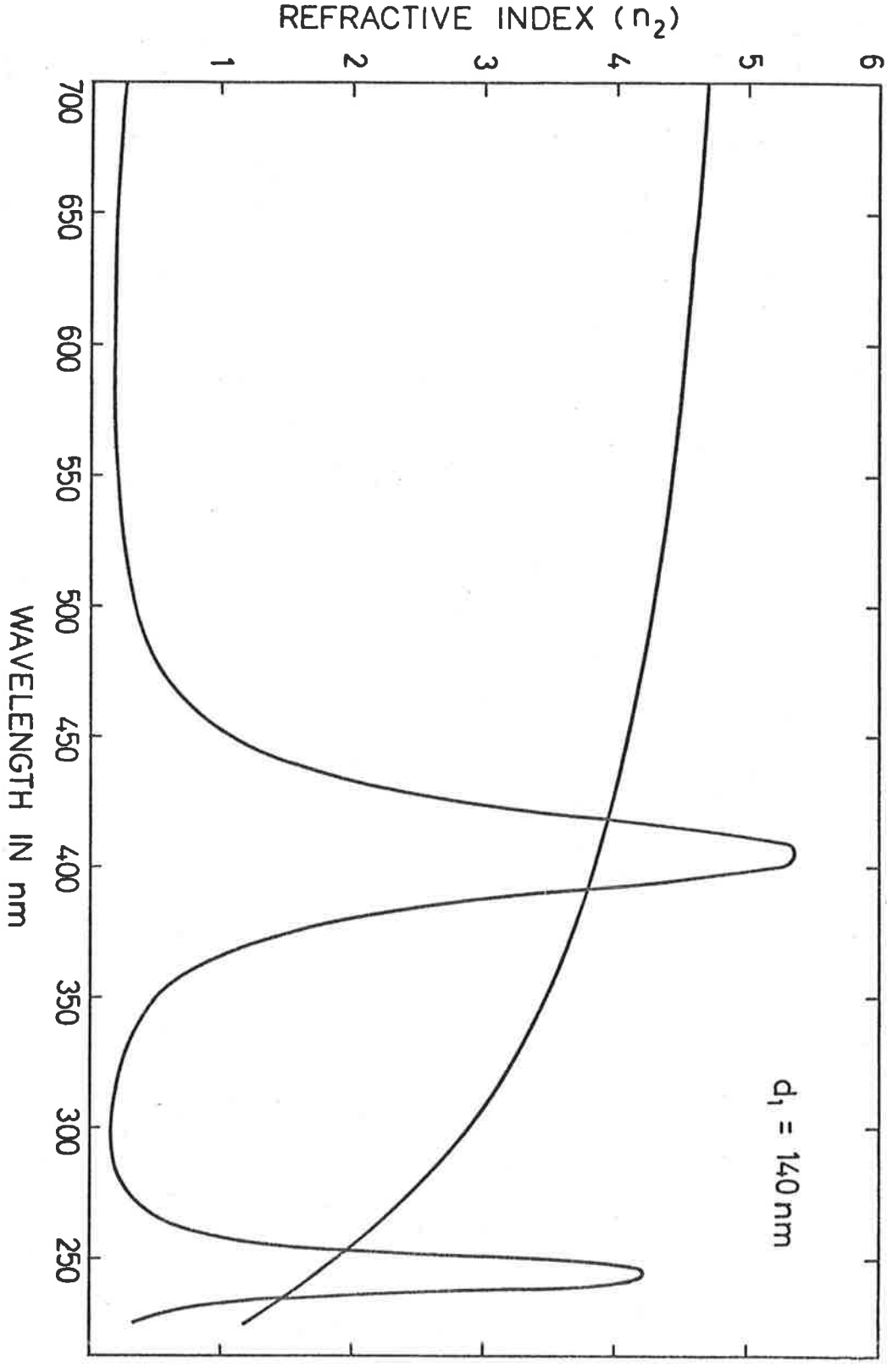
REFRACTIVE INDEX (n_2)
1
2
3
4
5
6
700
650
600
550
500
450
400
350
300
250
WAVELENGTH IN nm
d_1 = 140 nm

FIGURE 3·6

which could be obtained in the manner discussed in the next Section, was used to compute a preliminary result. The dispersion curve thus obtained made it clear whether the thickness was underestimated or overestimated. The thickness could be then adjusted until a continuous dispersion curve resulted. By adopting this criterion the correct optical constants could be obtained together with an accurate value of the thickness of the overlying transparent layer. It may be mentioned here, that the experimental measurements were made at a wavelength interval of 5 nm, therefore some of the details seen in Figures 3.6, 3.7 and 3.8 are lost. Nevertheless a dispersion curve obtained from experimental results clearly indicated whether the used thickness of the overlying layer was over or underestimated.

3.6 APPROXIMATE FILM THICKNESS

An approximate knowledge of the film thickness (d_1) was required in the solution of equations 3.3.2 and 3.3.3 for n_2 and k_2, as was discussed above. This was achieved as follows:

The transparent layer was deposited simultaneously on the specimen and on a clean quartz wedge. The optical properties and thickness (D1) of this transparent film on the quartz substrate were determined by measuring the normal incidence reflectance and transmittance from it. This will be discussed in Chapter 4. A rough estimate of the thickness d_1 of the transparent layer on the specimen may be taken to be equal to D1. This is termed a rough estimate because sticking coefficients may be different for different substrates. After some experience it was found that a reasonable guess of the thickness d_1 could be made by

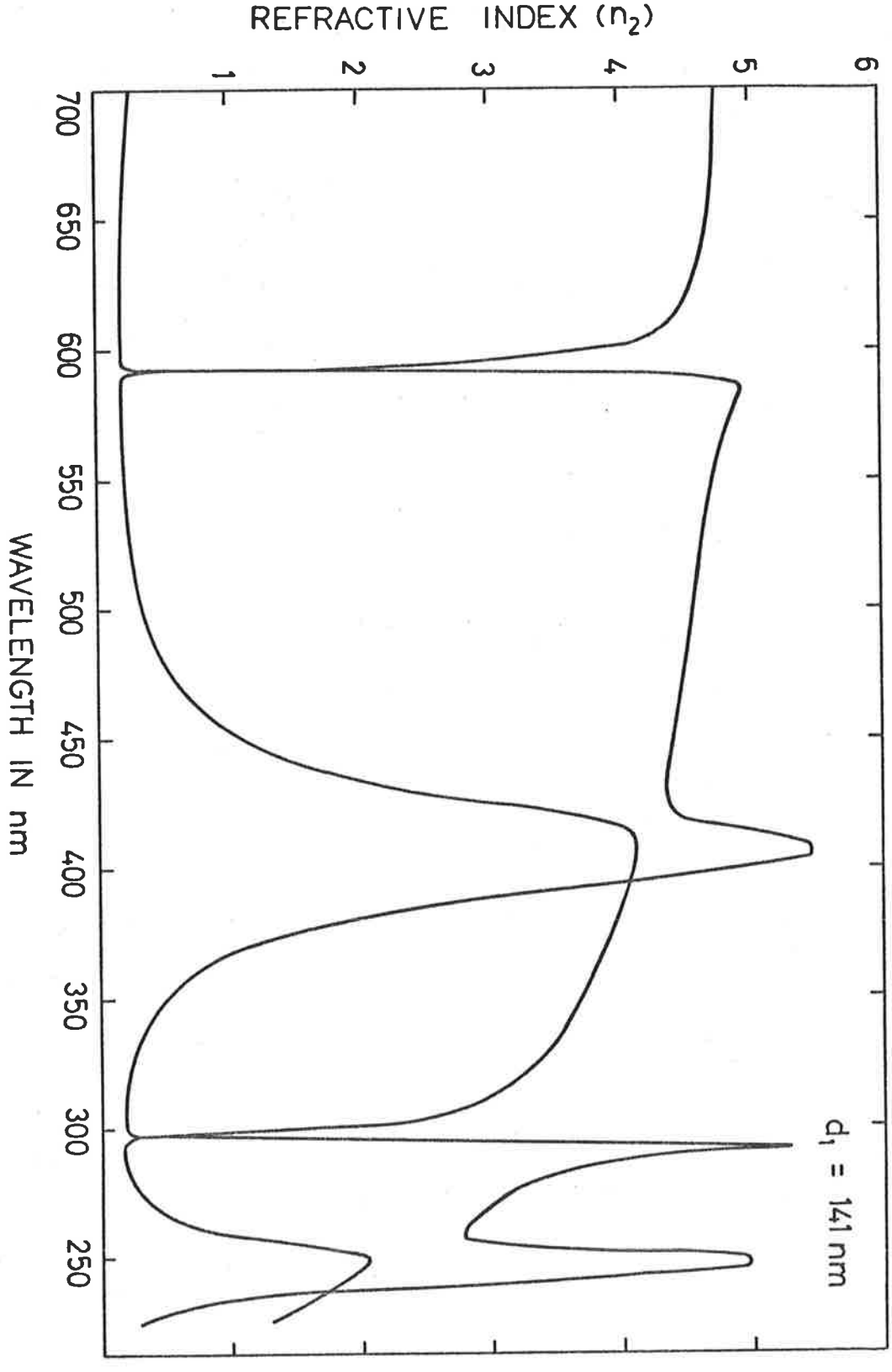
REFRACTIVE INDEX (n_2)
1
2
3
4
5
6
700
650
600
550
500
450
400
350
300
250
WAVELENGTH IN nm
d_1 = 141 nm

FIGURE 3·7

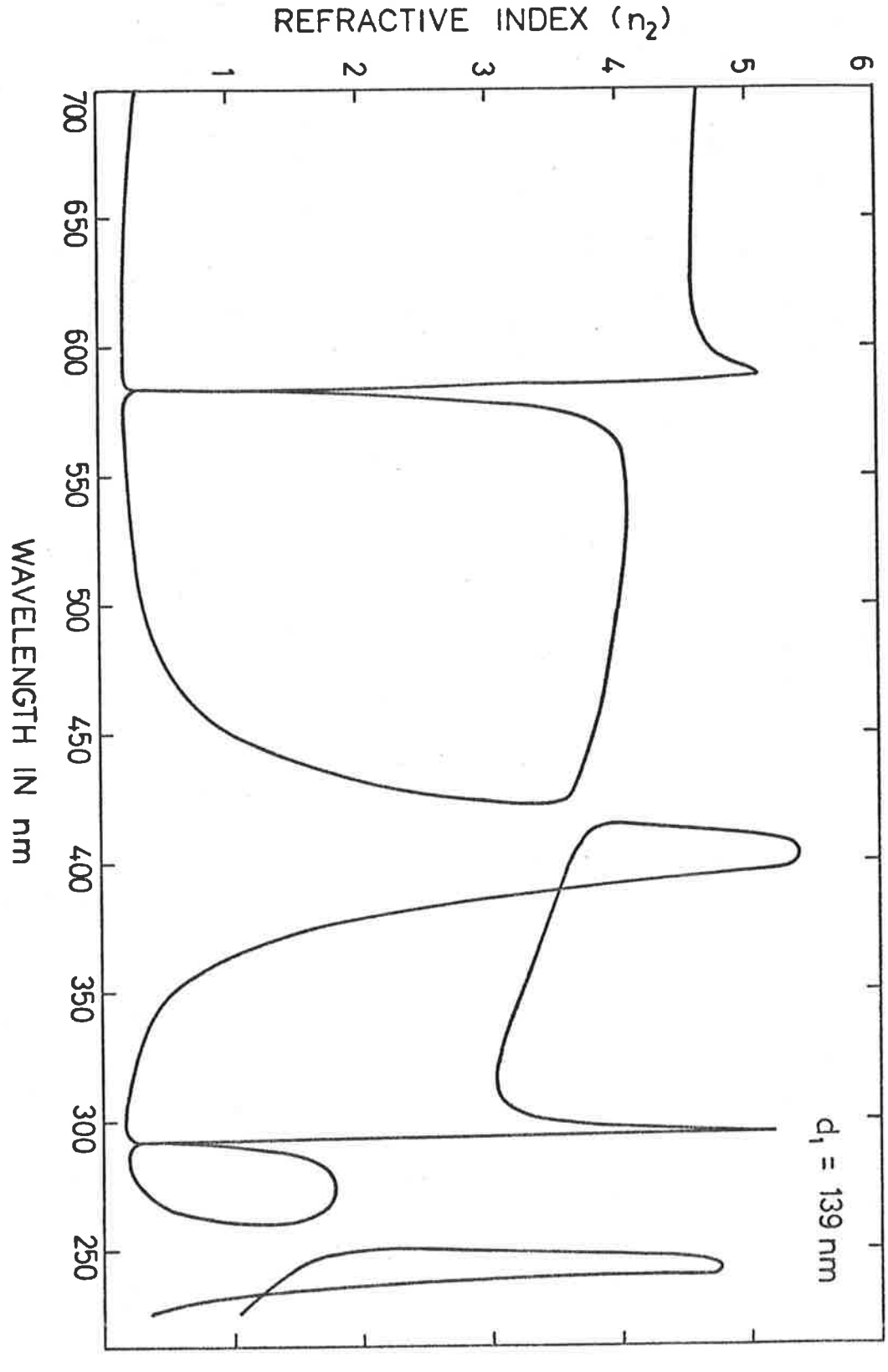
REFRACTIVE INDEX (n_2)
1
2
3
4
5
6
WAVELENGTH IN nm
700
650
600
550
500
450
400
350
300
250
d_1 = 139 nm

FIGURE 3·8

observing the change in colour of the light reflected from the specimen at the time when the transparent film was being deposited on it.

Alternatively, a reasonably good approximation to d_1 was obtained utilizing the following conditions, which could be deduced easily from equation 3.2.2.

CONDITION I

$R_1 = R$ when

$\gamma_1 = p\pi - \tan^{-1}\{|2n_1k_2/n_1^2-n_2^2-k_2^2|\}$

where p is an integer

CONDITION II

R_1 has a maximum, when

$\gamma_1 = p\pi - \frac{1}{2}\tan^{-1}\{|2n_1k_2/n_1^2-n_2^2-k_2^2|\}$

CONDITION III

$R_1 = R$, when

$\gamma_1 = p\pi$

In Figure 3.9, R_1 is plotted as a function of γ_1 for $n_1 = 2$, $n_2 = 4$ and $k_2 = 2$. Also is shown a straight line corresponding to a constant $R = 0.448$. For the above mentioned values of n_1, n_2 and k_2, $|2n_1k_2/n_1^2-n_2^2-k_2^2| = 0.15\pi$ radians. Hence the first condition is satisfied at $\gamma_1 = 0.85\pi$ and the second at $\gamma_1 = 0.925$ and the third at $\gamma_1 = \pi$ as can be seen from Figure 3.9.

It is the Condition III, which is important in determining the approximate d_1-value as it does not involve the unknown optical constants of the specimen. It follows from the above discussion that if $R_1 = R$ at γ_1, which lies on the lower wavelength side of the R_1

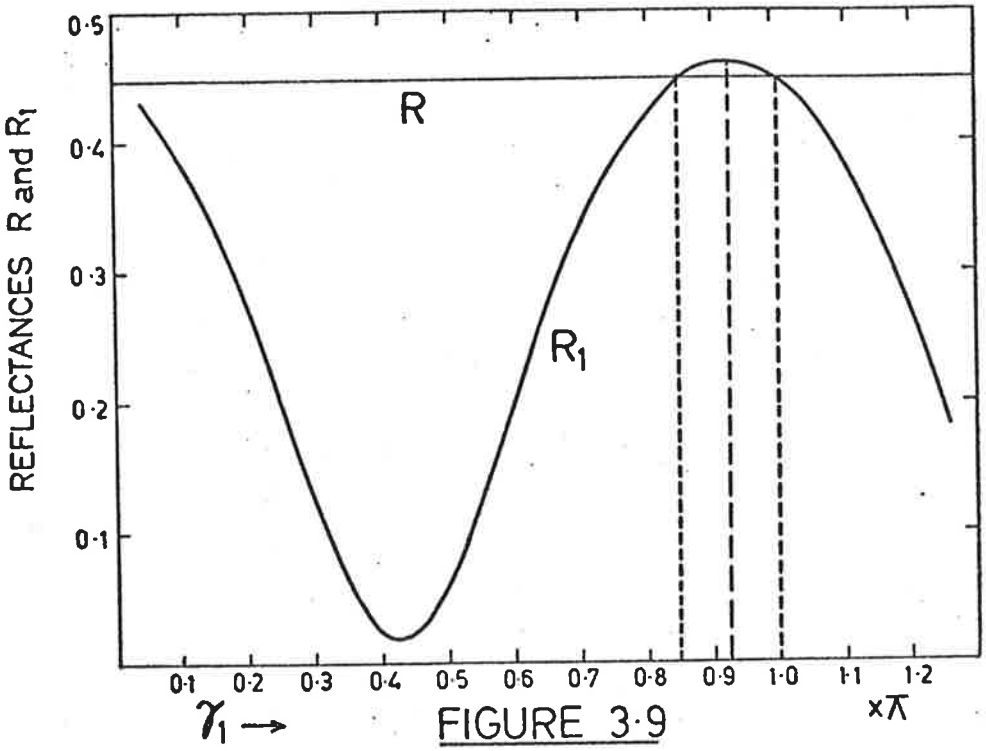

FIGURE 3·9

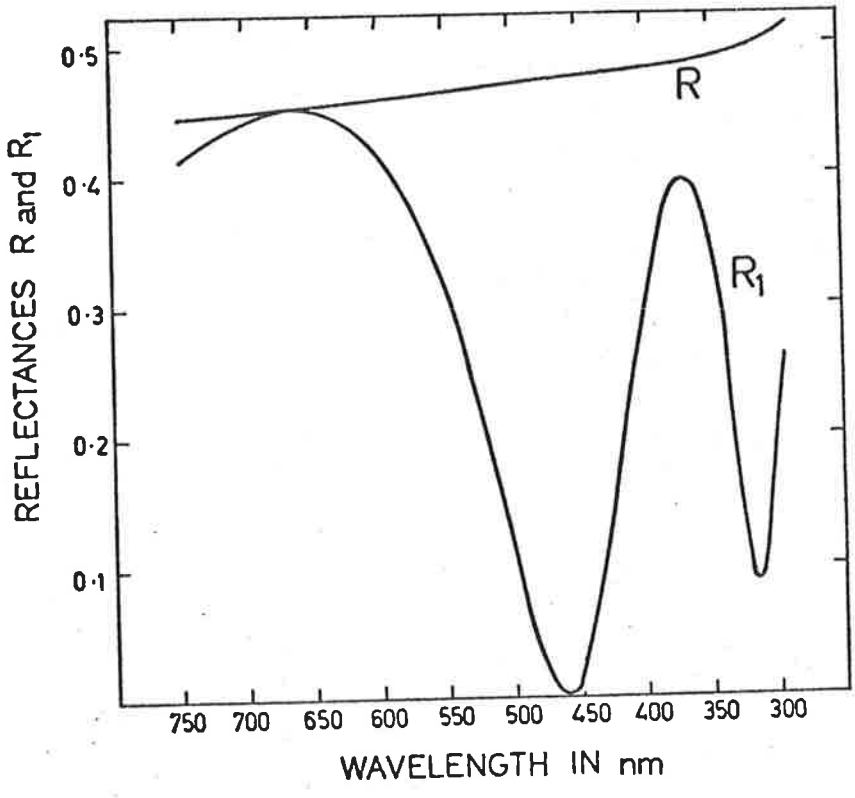

FIGURE 3·10

maxima, then $\gamma_1 = p\pi$ (Condition III). It may be mentioned here that the order p did not create any problem, because as was stated above, a rough estimate of thickness was already known from the appearance of the film.

3.7 CALCULATION OF THE ERROR IN THE SOLUTION

The maximum possible error in n_2 and k_2 at each wavelength was calculated as follows:

Writing R and $\frac{1+R}{1-R_1}$ in the functional form as

$$R = F(n_2, k_2) \qquad 3.7.1$$

$$\frac{1+R_1}{1-R_1} = G(n_2, k_2, n_1, d_1) \qquad 3.7.2$$

Taking total derivatives

$$dF = \frac{\partial F}{\partial n_2} dn_2 + \frac{\partial F}{\partial k_2} dk_2 \qquad 3.7.3$$

$$dG = \frac{\partial G}{\partial n_2} dn_2 + \frac{\partial G}{\partial k_2} dk_2 + \frac{\partial G}{\partial n_1} dn_1 + \frac{\partial G}{\partial d_1} dd_1 \qquad 3.7.4$$

From equations 3.7.3 and 3.7.4

$$dk_2 = \frac{1}{J}\left[dG \frac{\partial F}{\partial n_2} - dF \frac{\partial G}{\partial n_2} - \frac{\partial F}{\partial n_2} \cdot \frac{\partial G}{\partial d_1} \cdot dd_1 - \frac{\partial F}{\partial n_2} \cdot \frac{\partial G}{\partial n_1} dn_1\right] \qquad 3.7.5$$

$$dn_2 = \frac{1}{J}\left[dF \cdot \frac{\partial G}{\partial k_2} - dG \frac{\partial F}{\partial k_2} + \frac{\partial F}{\partial k_2} \cdot \frac{\partial G}{\partial d_1} dd_1 + \frac{\partial F}{\partial k_2} \cdot \frac{\partial G}{\partial n_1} dn_1\right] \qquad 3.7.6$$

where

$$J = \frac{\partial G}{\partial k_2} \cdot \frac{\partial F}{\partial n_2} - \frac{\partial G}{\partial n_2} \cdot \frac{\partial F}{\partial k_2} \qquad 3.7.7$$

Although explicit expressions for n_2 and k_2 cannot be found, they may be written in the functional form

$$n_2 = n_2\ (F,\ G,\ d_1,\ n_1) \qquad 3.7.8$$

$$k_2 = k_2\ (F,\ G,\ d_1,\ n_1) \qquad 3.7.9$$

Similarly

$$dn_2 = \frac{\partial n_2}{\partial F}\,dF + \frac{\partial n_2}{\partial G}\,dG + \frac{\partial n_2}{\partial d_1}\,dd_1 + \frac{\partial n_2}{\partial n_1}\,dn_1 \qquad 3.7.10$$

$$dk_2 = \frac{\partial k_2}{\partial F}\,dF + \frac{\partial k_2}{\partial G}\,dG + \frac{\partial k_2}{\partial d_1}\,dd_1 + \frac{\partial k_2}{\partial n_1}\,dn_1 \qquad 3.7.11$$

$$\frac{\partial n_2}{\partial F} = \frac{1}{J}\,\frac{\partial G}{\partial k_2} \qquad 3.7.12$$

$$\frac{\partial n_2}{\partial G} = -\frac{1}{J}\,\frac{\partial F}{\partial k_2} \qquad 3.7.13$$

$$\frac{\partial n_2}{\partial d_1} = \frac{1}{J}\,\frac{\partial F}{\partial k_2}\cdot\frac{\partial G}{\partial d_1} \qquad 3.7.14$$

$$\frac{\partial n_2}{\partial n_1} = \frac{1}{J}\,\frac{\partial F}{\partial k_2}\cdot\frac{\partial G}{\partial n_1} \qquad 3.7.15$$

$$\frac{\partial k_2}{\partial F} = \frac{1}{J}\,\frac{\partial F}{\partial n_2} \qquad 3.7.16$$

$$\frac{\partial k_2}{\partial G} = -\frac{1}{J}\,\frac{\partial G}{\partial n_2} \qquad 3.7.17$$

$$\frac{\partial k_2}{\partial d_1} = -\frac{1}{J}\,\frac{\partial F}{\partial n_2}\cdot\frac{\partial G}{\partial d_1} \qquad 3.7.18$$

$$\frac{\partial k_2}{\partial n_1} = -\frac{1}{J}\,\frac{\partial F}{\partial n_2}\cdot\frac{\partial G}{\partial n_1} \qquad 3.7.19$$

Hence an estimate of the maximum error in n_2 and k_2 is given by

$$\Delta n_2 = \left|\frac{\partial n_2}{\partial F}\cdot\Delta F\right| + \left|\frac{\partial n_2}{\partial G}\cdot\Delta G\right| + \left|\frac{\partial n_2}{\partial d_1}\,\Delta d_1\right| + \left|\frac{\partial n_2}{\partial n_1}\,\Delta n_1\right| \qquad 3.7.20$$

$$\Delta k_2 = \left|\frac{\partial k_2}{\partial F}\cdot\Delta F\right| + \left|\frac{\partial k_2}{\partial G}\cdot\Delta G\right| + \left|\frac{\partial k_2}{\partial d_1}\,\Delta d_1\right| + \left|\frac{\partial k_2}{\partial n_1}\,\Delta n_1\right| \qquad 3.7.21$$

where the partial derivatives of n_2 and k_2 are given by equations 3.7.12 to 3.7.19; ΔF and ΔG are found from the experimental errors in R and R_1, Δd_1

is the estimate of the error in the film thickness, and Δn_1 is the error in n_1. The partial derivatives of F and G are given in Appendix B. These first order formulae are valid provided J is not too small. The random errors in R and R_1 were estimated to be 0.002 and that in n_1 to be 0.005.

It will be seen that there are regions where the computed errors in n_2 and k_2 are large. These correspond to a wavelength range in the neighbourhood of $\gamma_1 = p\pi$ (where p is an integar). This fact follows from the discussion in the following section.

3.8 A COMMENT ON ERRORS IN THE SOLUTIONS AND THE CHOICE OF INDEX OF REFRACTION OF THE OVERLYING TRANSPARENT FILM

The transparent films, of materials such as ZnS($n \simeq 2.3$), Ta_2O_5($n \simeq 2.1$) and ZrO_2($n \simeq 2.0$) are preferred to other transparent materials, such as Nacl, KCl, MgF, SiO_2, Al_2O_3etc., which have refractive indices lower than 1.5, for reasons discussed below.

The accuracy with which n_2 and k_2 can be found depends upon the accuracy of n_1, d_1, $\frac{1+R}{1-R}$ and $\frac{1+R_1}{1-R_1}$. In the present work, n_1 the refractive index of the transparent layer was determined with accuracy better than 1% as will be discussed in Chapter 4 (Ta_2O_5 and ZrO_2). The thickness d_1, which was determined by the method of obtaining a continuous dispersion curve has already been discussed. Hence the contribution of n_1 and d_1 to the errors in n_2 and k_2 was very little. The main sources of errors in n_2 and k_2 were the errors in the measured reflectances R and R_1. In the present experiment the random errors in R or R_1 did not exceed $\pm$ 0.002. From the graphical method of solution, it is clear that the error of 0.002 in R, will have little effect on the centre and radius of the circle (in the case of Ge where

$R > 0.375$). Therefore the errors in n_2 and k_2 will be mainly due to the errors in the straight line (given by equation 3.2.4) intersecting the circle. Once again since the intercept of this line along the k_2-axis is independent of R and R_1 therefore the slope of this line will be the main contributor to the errors in n_2 and k_2.

The slope of the line is (equation 3.2.4)

$$S = \frac{2}{n_1(n_1^2-n_0^2)} \cdot \frac{1}{\sin 2\gamma_1} \left[\frac{1+R}{1-R} (n_1^2\cos^2\gamma_1 + n_0^2\sin^2\gamma_1) - \frac{1+R_1}{1-R_1} n_1^2 \right] \qquad 3.8.1$$

The maximum error in the slope due to errors in $\frac{1+R}{1-R}$ and $\frac{1+R_1}{1-R_1}$ is given by

$$\Delta S = \left| \frac{2}{n_1(n_1^2-n_0^2)} \cdot \frac{1}{\sin 2\gamma_1} \right| \left[\left| n_1^2\cos^2\gamma_1 + n_0^2\sin^2\gamma_1 \right| \Delta\left(\frac{1+R}{1-R}\right) + n_1^2 \, \Delta\left(\frac{1+R_1}{1-R_1}\right) \right] \qquad 3.8.2$$

where $\Delta\left(\frac{1+R}{1-R}\right) = \frac{2\Delta R}{(1-R)^2}$

$$\Delta\left(\frac{1+R_1}{1-R_1}\right) = \frac{2\Delta R_1}{(1-R_1)^2}$$

and $\Delta R = \Delta R_1 = 0.002$

It follows from numerical solutions of the above equations (shown in Appendix C) that for a given specimen at a given γ_1, the relative error in slope is dependent on the value of n_1. The larger the value of n_1 the smaller is the relative error and vice versa.

3.9 EFFECTS OF ERRORS IN R AND R_1 ON THE CALCULATED OPTICAL CONSTANTS AND FILM THICKNESS

In the present work the thickness of the overlying film was determined by the criterion of obtaining a continuous dispersion curve (already discussed in Section 3.5). To check the accuracy with which this thickness can be determined, by this method, it was necessary to determine the sensitivity of the continuity of the dispersion curve to errors in R and R_1.

This was achieved by the use of the hypothetical case discussed in Section 3.4. The calculated reflectances R from the hypothetical specimen and R_1 from the transparent film on the specimen (Figure 3.4), were altered in the four following ways:

(1) $R - 0.002$ $\qquad$ $R_1 - 0.002$

(2) $R + 0.002$ $\qquad$ $R_1 + 0.002$

(3) $R - 0.002$ $\qquad$ $R_1 + 0.002$

(4) $R + 0.002$ $\qquad$ $R_1 - 0.002$

For cases (1) and (2) proper continuity of the dispersion curves was obtained for the overlying film thickness = 140 nm, which means that these alterations in R and R_1 did not affect the calculated film thickness. Also the optical constants (n_2, k_2) thus calculated were practically unaffected.

In cases (3) and (4) proper continuity of the dispersion curves, except for a small region at about $\gamma_1 = p\pi$, was obtained for d_1 = 139.5 nm and 140.5 nm respectively. This would be expected because the solutions near $\gamma_1 = p\pi$ depend critically on the errors in R and R_1 as follows from

Section 3.8. In these two cases the observed deviation in the calculated optical constants from the actual values was about 2%.

It follows from the above discussion that if errors in R and R_1 do not exceed 0.002 then the thickness of the overlying film can be determined with considerable precision.

3.10 MODIFICATION OF TOMLIN'S METHOD (WHEN OVERLYING FILM IS SEMI-TRANSPARENT)

The condition, that the overlying film should be transparent (Tomlin's Method) usually limits the wavelength range over which the measurements can be made. For example it is observed that ZnS films are transparent in the I.R. and visible regions but are semi-absorbing in U.V. (At a wavelength of 300 nm, the transmittance of 120 nm thick film was about 16%). The use of such an overlying layer would restrict the measurements to be made to the I.R. and visible regions. It was found that this method of Tomlin's, with some modifications, could be applied easily in a case where the overlying film is semi-transparent.

If a semi-transparent film of complex refractive index n_1-ik_1 is deposited on a specimen of complex refractive index n_2-ik_2 (which does not transmit) then equation 3.2.2 needs to be modified while equation 3.2.1 still holds (as it is independent of the overlying film). The reflectance R_1 from the semi-transparent film of thickness d_1 on an absorbing specimen, at a wavelength λ, is given by the formula for an absorbing film on an absorbing substrate (Heavens, 1955) as

$$R_1 = \frac{(g_1^2+h_1^2)e^{2\alpha_1}+(g_2^2+h_2^2)e^{-2\alpha_1}+A\cos 2\gamma_1+B\sin 2\gamma_1}{e^{2\alpha_1}+(g_1^2+h_1^2)(g_2^2+h_2^2)e^{-2\alpha_1}+C\cos 2\gamma_1+D\sin 2\gamma_1} \qquad 3.10.1$$

where

$$A = 2(g_1g_2 + h_1h_2) \qquad B = 2(g_1h_2 - g_2h_1)$$

$$C = 2(g_1g_2 - h_1h_2) \qquad D = 2(g_1h_2 + g_2h_1)$$

$$g_1 = \frac{n_o^2-n_1^2-k_1^2}{(n_o+n_1)^2+k_1^2} \qquad h_1 = \frac{2n_ok_1}{(n_o+n_1)^2+k_1^2}$$

$$g_2 = \frac{n_1^2-n_2^2+k_1^2-k_2^2}{(n_1+n_2)^2+(k_1+k_2)^2} \qquad h_2 = \frac{2(n_1k_2-n_2k_1)}{(n_1+n_2)^2+(k_1+k_2)^2}$$

$$\alpha_1 = \frac{2\pi k_1 d_1}{\lambda} \qquad \text{and} \qquad \gamma_1 = \frac{2\pi n_1 d_1}{\lambda}$$

and n_o is index of refraction of air. (Notations are the same as used by Heavens).

From the measured R and R_1 and the knowledge of n_1, k_1 and d_1, equations 3.2.1 and 3.10.1 could be solved for n_2 and k_2 in a manner similar to one discussed for transparent films in Section 3.3.2.

3.10.1 THE SOLUTIONS OBTAINED FOR A HYPOTHETICAL SPECIMEN WHEN A SEMI-TRANSPARENT FILM IS USED

To illustrate the nature of the solutions of equations 3.2.1 and 3.10.1, the hypothetical specimen of complex refractive index n_2-ik_2, described in Section 3.4 was considered. Assuming that a portion of the specimen was coated with a semi-transparent layer of thickness d_1 = 140 nm and complex refractive index n_1-ik_1, so that for wavelengths less than 750 nm

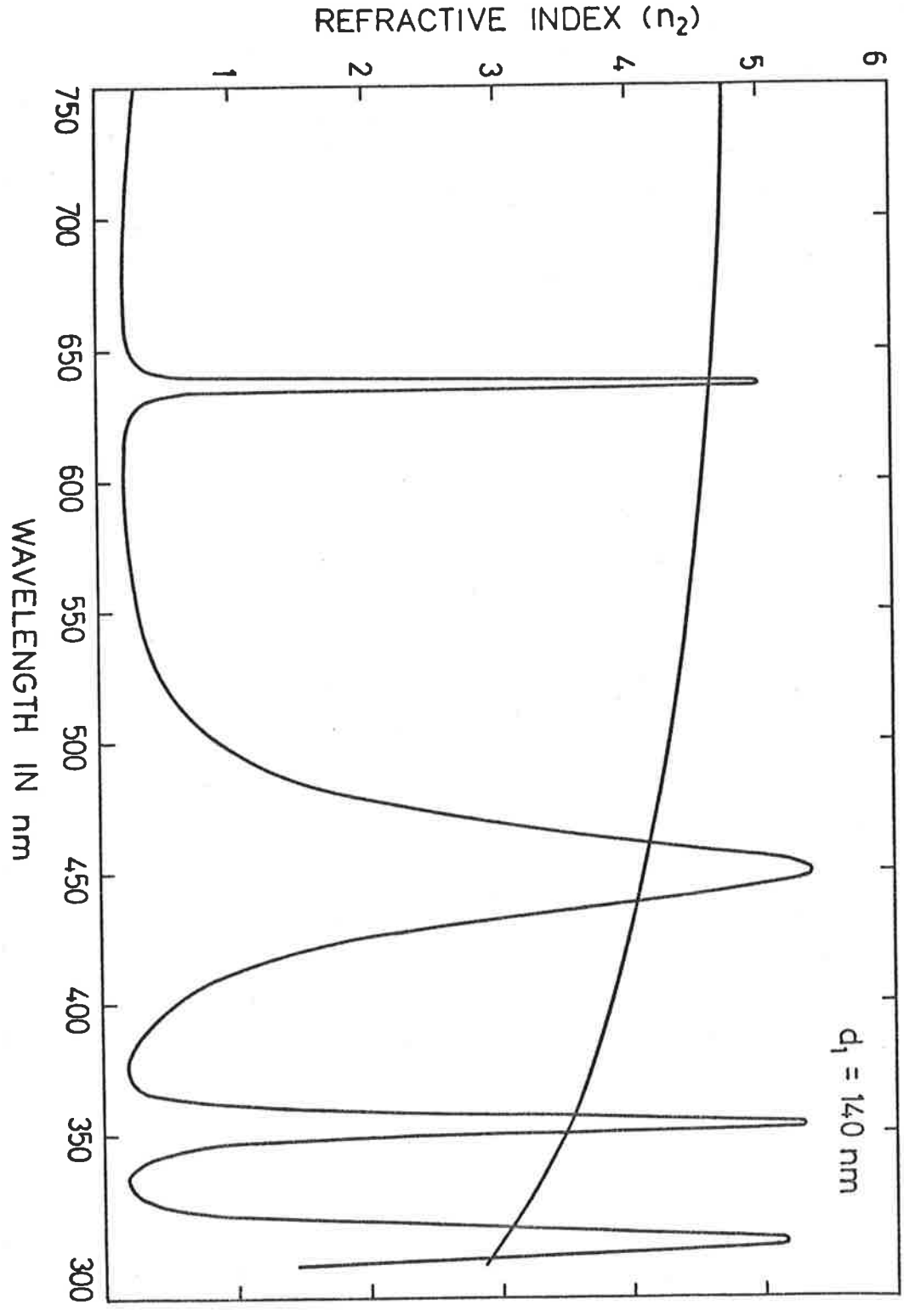
REFRACTIVE INDEX (n_2)
1
2
3
4
5
6
WAVELENGTH IN nm
750
700
650
600
550
500
450
400
350
300
d_1 = 140 nm

FIGURE 3·11

$$n_1 = 2.25 + 0.004/\lambda^4 \qquad 3.10.2$$

$$k_1 = 0.0015/\lambda^4 \qquad 3.10.3$$

where λ is the wavelength in μm.

(These values correspond roughly to those of ZnS films).

For the values of n_1, k_1, n_2, k_2 and d_1 mentioned above, the reflectances R and R_1 were calculated, in the spectral range from 300 to 750 nm at an interval of 1 nm, using equations 3.2.1 and 3.10.1. Figure 3.10 shows the plot of the calculated R and R_1 versus wavelengths for such a system.

From the values of R and R_1, shown in Figures 3.10, which are used as data and d_1 = 140 nm, the calculations of n_2 and k_2 were performed, using the procedure outlined in Section 3.10. Figure 3.11 shows the dispersion curve thus obtained. It is clear from the figure that the correct solutions result in a continuous curve and the unwanted solutions form another continuous curve with repeated maxima and minima. This behaviour of the dispersion curve (or solutions) is similar to that in the case of a transparent overlying layer (Section 3.4).

3.10.2 EFFECT OF ERRORS IN THICKNESS OF THE SEMI-TRANSPARENT OVERLYING FILM

Using the reflectances R and R_1, shown in Figure 3.10, as data, n_2 and k_2 were calculated by the method, mentioned in Section 3.10, assuming an overlying film of thickness 141 nm instead of the correct value of 140 nm. The dispersion curve shown in Figure 3.12 was obtained. If d_1 = 139 nm, instead of the correct value of 140 nm, was used in calculations, then a dispersion curve shown in Figure 3.13 was obtained. Once again,

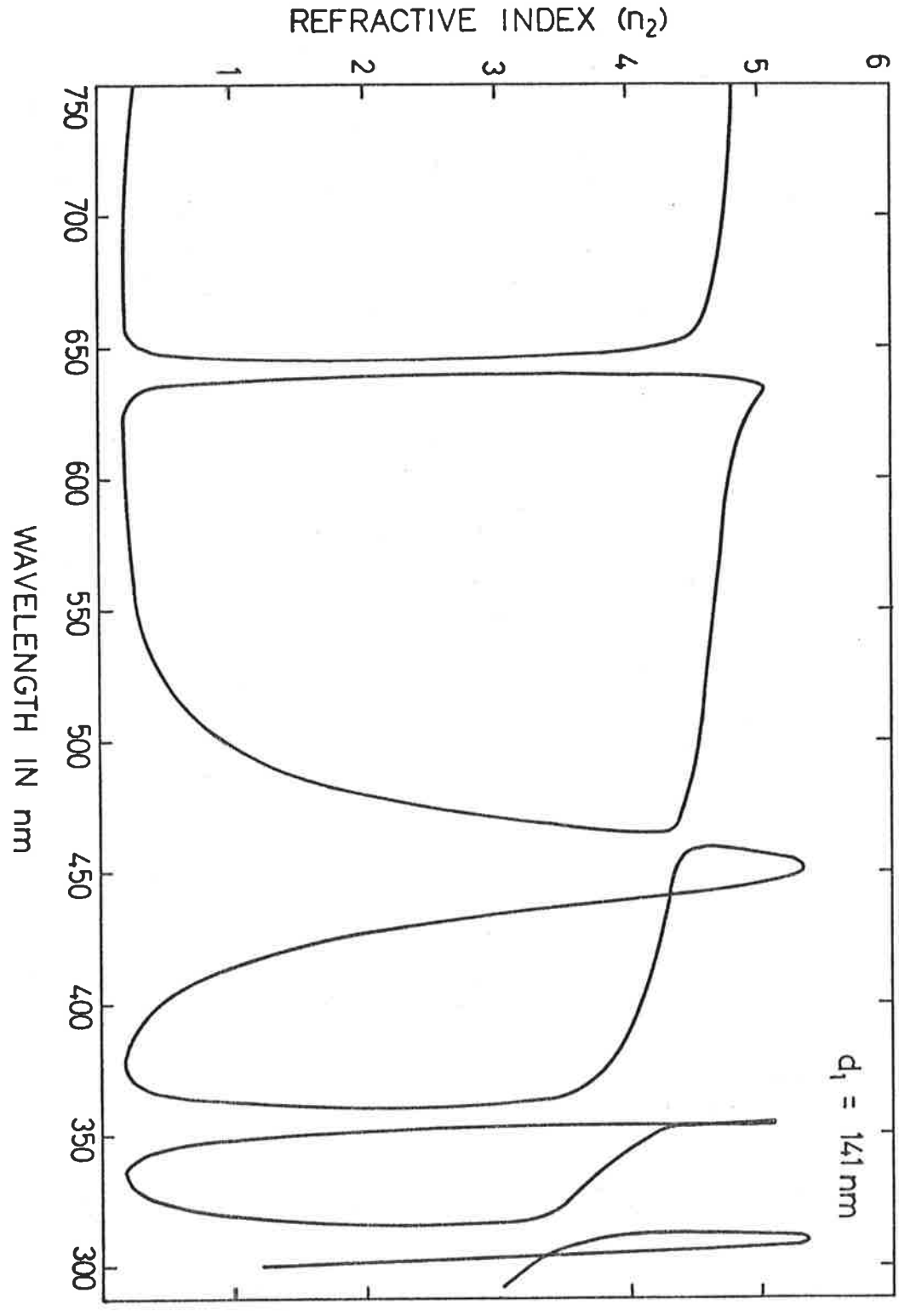
REFRACTIVE INDEX (n_2)
1
2
3
4
5
6
750
700
650
600
550
500
450
400
350
300
WAVELENGTH IN nm
d_1 = 141 nm

FIGURE 3·12

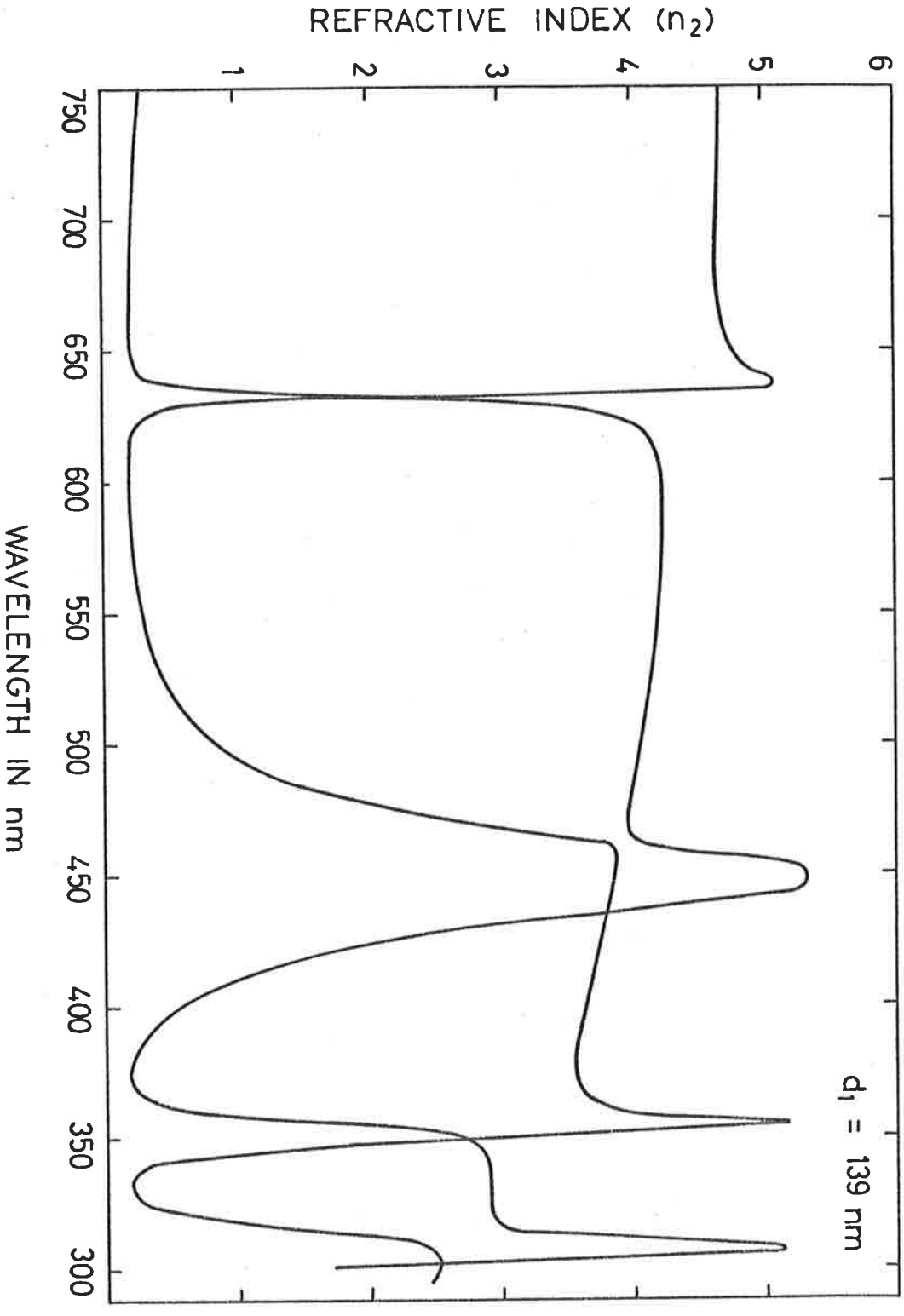
REFRACTIVE INDEX (n_2)
1
2
3
4
5
6
750
700
650
600
550
500
450
400
350
300
WAVELENGTH IN nm
d_1 = 139 nm

FIGURE 3·13

as was observed in the case of a transparent overlying film (Figures 3.7 and 3.8), it is clear, from Figures 3.12 and 3.13, that a continuous dispersion curve could not be obtained unless the error in film thickness was less than 0.7%.

Initially an approximate value of thickness (Section 3.6) of the overlying film was needed to compute the results. Then the correct optical constants could be obtained together with an accurate value of the thickness by using the criterion discussed in Section 3.5.

3.11 OVERLYING FILM WITH ROUGH SURFACE

It is clear from the literature, e.g. Heavens (1955), Rouard and Bousquet (1965) and Daude et al (1972), that films of different materials often have rough surfaces. Besides which there is a possibility of different stoichiometry at the surfaces (surface may not be of the same nature as the film itself). In such cases continuous dispersion curves may not be obtained. While studying the optical properties of Ge films, with ZnS layer deposited on them, it was found that a continuous dispersion curve could not be obtained from measured R and R_1, using the method discussed in Section 3.10. It was concluded that the measured R_1 was not that appropriate to a perfectly plane parallel uniform thin film such as is assumed for the derivation of the formula used. In such a case it was found that the surface of the film must be treated as a separate uniform layer with optical constants different from those of the film itself, and thus obtain a continuous dispersion curve. This will be discussed in detail later on. Hence a system of two layers on an absorbing specimen is considered in the next section.

3.12 SYSTEM OF TWO SEMI-TRANSPARENT LAYERS ON AN ABSORBING SPECIMEN

Since the specimen does not transmit (Section 3.2) such a system may be regarded as consisting of two absorbing layers on an absorbing substrate. Figure 3.14 shows such a system, where n_o is the refractive index of air, n_1-ik_1 is the complex refractive index of the first layer of thickness d_1, n_2-ik_2 is the complex refractive index of the second layer of thickness d_2 and n_3-ik_3 is the complex refractive index of the substrate (specimen) from Heavens (1955).

$$g_1 = \frac{n_o^2-n_1^2-k_1^2}{(n_o+n_1)^2+k_1^2} \qquad h_1 = \frac{2n_ok_1}{(n_o+n_1)^2+k_1^2}$$

$$g_2 = \frac{n_1^2-n_2^2+k_1^2-k_2^2}{(n_1+n_2)^2+(k_1+k_2)^2} \qquad h_2 = \frac{2(n_1k_2-n_2k_1)}{(n_1+n_2)^2+(k_1+k_2)^2}$$

$$g_3 = \frac{n_2^2-n_3^2+k_2^2-k_3^2}{(n_2+n_3)^2+(k_2+k_3)^2} \qquad h_3 = \frac{2(n_2k_3-n_3k_2)}{(n_2+n_3)^2+(k_2+k_3)^2}$$

$$p_2 = e^{\alpha_1}\cos\gamma_1 \qquad q_2 = e^{\alpha_1}\sin\gamma_1$$

$$t_2 = e^{-\alpha_1}(g_2\cos\gamma_1+h_2\sin\gamma_1)$$

$$u_2 = e^{-\alpha_1}(h_2\cos\gamma_1-g_2\sin\gamma_1)$$

$$\alpha_1 = 2\pi k_1d_1/\lambda \qquad \alpha_2 = 2\pi k_2d_2/\lambda$$

$$\gamma_1 = 2\pi n_1d_1/\lambda \qquad \gamma_2 = 2\pi n_2d_2/\lambda$$

$$p_{12} = p_2+g_1t_2-h_1u_2 \qquad q_{12} = q_2+h_1t_2+g_1u_2$$

$$t_{12} = t_2+g_1p_2-h_1q_2 \qquad u_{12} = u_2+h_1p_2+g_1q_2$$

$$p_3 = e^{\alpha_2}\cos\gamma_2 \qquad q_3 = e^{\alpha_2}\sin\gamma_2$$

$$t_3 = e^{-\alpha_2}(g_3\cos\gamma_2+h_3\sin\gamma_2)$$

$$u_3 = e^{-\alpha_2}(h_3\cos\gamma_2-g_3\sin\gamma_2)$$

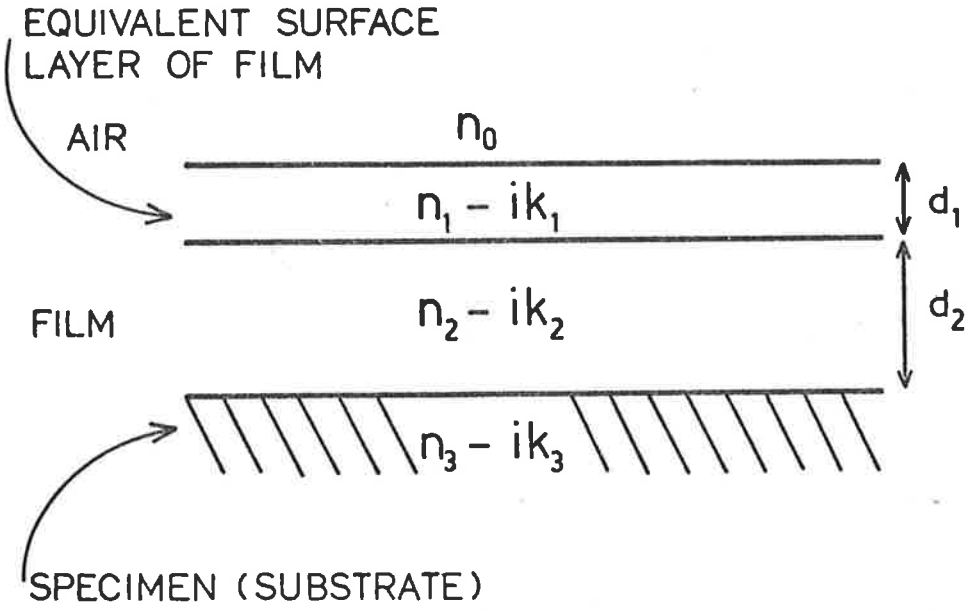
EQUIVALENT SURFACE
LAYER OF FILM
AIR
n_0
$n_1 - ik_1$
d_1
FILM
$n_2 - ik_2$
d_2
$n_3 - ik_3$
SPECIMEN (SUBSTRATE)

FIGURE 3·14

$$r_2 = e^{\alpha_1}(g_2\cos\gamma_1 - h_2\sin\gamma_1)$$

$$s_2 = e^{\alpha_1}(h_2\cos\gamma_1 + g_2\sin\gamma_1)$$

$$v_2 = e^{-\alpha_1}\cos\gamma_1 \qquad w_2 = e^{-\alpha_1}\sin\gamma_1$$

$$r_{12} = r_2 + g_1 v_2 - h_1 w_2 \qquad s_{12} = s_2 + h_1 v_2 + g_1 w_2$$

$$v_{12} = v_2 + g_1 r_2 - h_1 s_2 \qquad w_{12} = w_2 + h_1 r_2 + g_1 s_2$$

$$p_{13} = p_{12}p_3 - q_{12}q_3 + r_{12}t_3 - s_{12}u_3$$

$$q_{13} = q_{12}p_3 + p_{12}q_3 + s_{12}t_3 + r_{12}u_3$$

$$t_{13} = t_{12}p_3 - u_{12}q_3 + v_{12}t_3 - w_{12}u_3$$

$$u_{13} = u_{12}p_3 + t_{12}q_3 + w_{12}t_3 + v_{12}u_3$$

hen the reflectance (R_2) of the double layer system, at a wavelength λ, is given by

$$R_2 = \frac{t_{13}^2 + u_{13}^2}{p_{13}^2 + q_{13}^2}$$

3.13 THE NATURE OF SOLUTIONS IN CASE OF A DOUBLE LAYER ON AN ABSORBING SUBSTANCE

If reflectances R from the specimen and R_2 from the double layer system (already described), are measured and assuming that n_1, k_1, d_1, n_2, k_2, and d_2 are known then equations 3.2.1 and 3.12.1 can be solved for n_3 and k_3 in a manner similar to one discussed in Section 3.3.2.

To illustrate the nature of solutions in such a case, a hypothetical system was considered so that for wavelengths less than 750 nm

$$n_1 = 1.7$$

$$k_1 = 0.0005/\lambda^4$$

$$n_2 = 2.5 + 0.004/\lambda^4$$

$$k_2 = 0.0015/\lambda^4$$

d_1 = 10 nm

d_2 = 140 nm

where λ is wavelength in μm.

The specimen considered here was the same as described in Section 3.4.

For the values stated above, R and R_2 were calculated, in the spectral range 750 - 300 nm, at an interval of 1 nm, from equations 3.2.1 and 3.12.1. Using these calculated values of R and R_2 as data and same values of n_1, k_1, d_1, n_2, k_2 and d_2, the optical constants of the specimen (n_3, k_3) were calculated by the method outlined above. Figure 3.15 shows the plot of n_3 versus wavelength. It is clear from the figure that solutions in a double layer system behave in a similar manner to those for a single layer on the specimen.

3.14 SYSTEM OF TWO TRANSPARENT LAYERS ON AN ABSORBING SPECIMEN

In Sections 3.12 and 3.13, the overlying film, on the absorbing specimen, was semi-transparent and had a rough surface. In a case when the overlying film, on the specimen, is transparent and has a rough surface (e.g. ZrO_2 films, Chapter 4), then equation 3.12.1 for R_2 can be used by putting $k_1 = k_2 = 0$. This is once again based on the assumption that the rough surface of the film may be treated as a separate uniform layer with a refractive index different from that of the film itself. Alternatively the following simplified relation, which was obtained from the formulae given by Tomlin (1972a) could be used.

$$\frac{1+R_2}{1-R_2} = \frac{(n_0^2+n_1^2)F_1 + (n_0^2-n_1^2)F_2}{16n_0n_1^2n_2^2n_3} \qquad 3.14.1$$

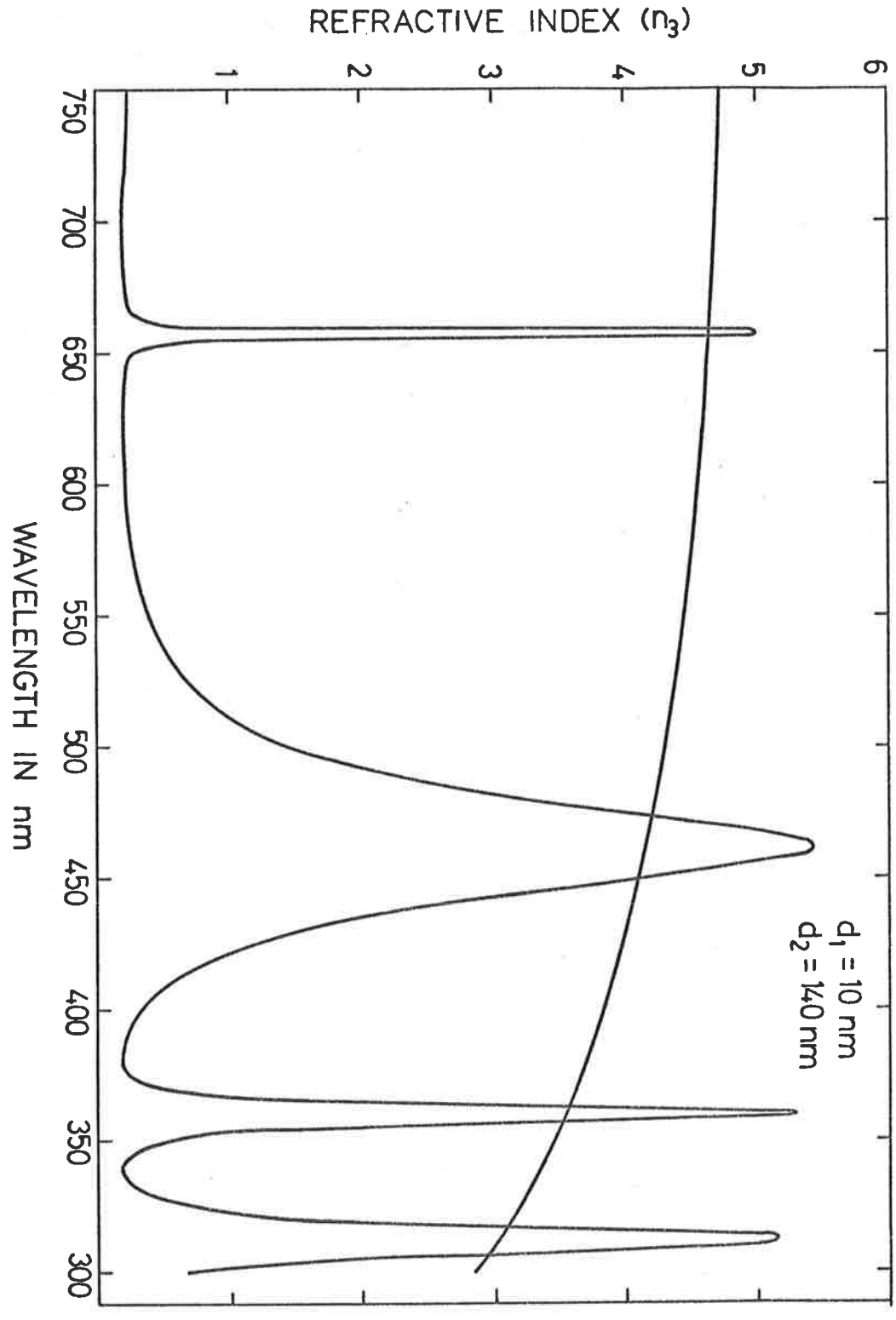
REFRACTIVE INDEX (n_3)
1
2
3
4
5
6
WAVELENGTH IN nm
750
700
650
600
550
500
450
400
350
300
d_1 = 10 nm
d_2 = 140 nm

FIGURE 3·15

where

$$F_1 = 2\{(n_1^2+n_2^2)(n_2^2+n_3^2+k_3^2) + (n_1^2-n_2^2)B\}$$

$$F_2 = (n_1+n_2)^2\{(n_2^2-n_3^2-k_3^2)\cos 2(\gamma_2+\gamma_1)+2n_2k_3\sin 2(\gamma_2+\gamma_1)\}$$
$$+ (n_1-n_2)^2\{(n_2^2-n_3^2-k_3^2)\cos 2(\gamma_2-\gamma_1)+2n_2k_3\sin 2(\gamma_2-\gamma_1)\}$$
$$+ 2(n_1^2-n_2^2)(n_2^2+n_3^2+k_3^2)\cos 2\gamma_1$$

and $$B = (n_2^2-n_3^2-k_3^2)\cos 2\gamma_2 + 2n_2k_3\sin 2\gamma_2$$

Notations used are the same as used in Section 3.12.

If d_1, d_2, n_1 and n_2 are known and R and R_2 are measured then equations 3.2.1 and 3.14.1 can be solved for n_3 and k_3 by the method outlined in Section 3.3.2. In such a case it was found that the nature of the solutions for n_3 was similar to that shown in Figure 3.6.

The procedure adopted for determining the thicknesses d_1 and d_2 was only slightly different from the one outlined by Denton et al (1972) and will be treated in Chapter 5.

3.15 APPLICATION OF TOMLIN'S METHOD IN A REGION OF LOW ABSORPTION NEAR THE ABSORPTION EDGE OF A SEMICONDUCTOR

Tomlin's method (Section 3.2) in principle can be applied, in the case of a semiconductor in bulk form (thick enough to prevent any light passing through it), in a region of low absorption near its absorption edge. It is found that, unless the reflectivities R and R_1 are measured very accurately, the method fails in determining reliable absorption in this region of low absorption. This could be understood from the example of a solution considered below:

Consider a specimen with $n_2 = 4.0$ and $k_2 = 0.05$ and $n_1 = 2.0$ and $\gamma_1 = \pi/4$. In Figure 3.16 the intersection of the solid line with the

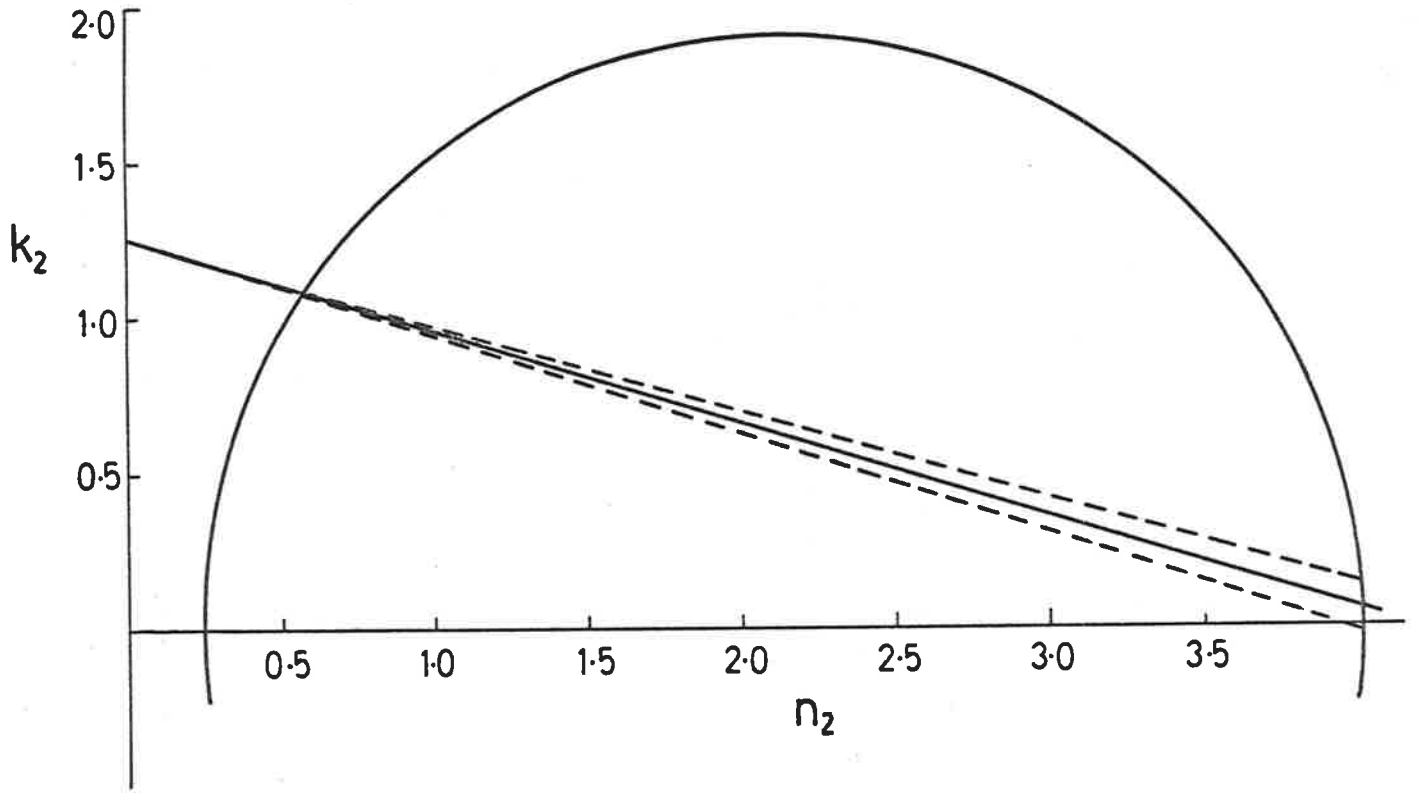

FIGURE 3·16

circle shows the solution for such a system. The dotted lines in the same figure represent the errors, in the slope of the line, calculated by the method outlined in Section 3.8. It may be mentioned that besides the errors in the slope due to R and R_1, considered here, there would be some errors due to errors in n_1 and d_1, and there would be some errors in the intercept of this line on the k_2-axis (due to errors in n_1 and d_1), also there would be errors in the position of the centre and the radius of the circle (due to errors in R and R_1), but these would be comparitively small. The error in the slope of the line is a function of γ_1 (Section 3.8 and Appendix C). In the example above, $\gamma_1 = \pi/4$ was chosen because the errors in the slope are relatively small for such a value of γ_1. Thus the uncertainty in the absorption value, in the low absorbing region, resulting from errors in R and R_1 can be realised from Figure 3.16.

On the other hand the refractive index (n_2), in this region can be determined with a reasonable accuracy (Figure 3.16). Alternatively, n_2 can be determined near the absorption edge, with almost the same accuracy, from the following simple relation, which results from equation 3.2.1 when absorption is neglected.

$$n = \frac{1+\sqrt{R}}{1-\sqrt{R}} \qquad 3.15.1$$

CHAPTER 4.

OPTICAL PROPERTIES OF TANTALUM PENTOXIDE AND ZIRCONIUM DIOXIDE

4.1 INTRODUCTION

The optical constants of amorphous germanium films in the spectral range from 0.5 to 1.77 eV, were studied by Denton et al (1972). The method used by Denton to determine these constants from the measured normal incidence reflectance and transmittance, fails when the transmittance is too small for accurate measurement. For this reason Denton limited his measurements to 1.77 eV.

It was decided to extend the measurements on Ge films in the higher energy region, using Tomlin's method, discussed in the previous chapter. Also optical constants of polycrystalline Ge in the form of a slab were determined using the same method. The application of this method required that an area of the specimen be coated with a suitable thin transparent film. From the discussion of Section 3.8 it is advantageous to use a film of refractive index as high as possible. It was found that thin films of materials like tantalum pentoxide, zirconium dioxide and zinc sulphide could be used as the required transparent film.

Due to the discrepancies in the results, quoted in the literature, for the optical constants of the Ta_2O_5 and ZrO_2, as mentioned below, it was decided to study these constants.

Young (1961) discusses the refractive indices for anodic films of Ta_2O_5, obtained by different workers. Young reported a refractive index

of 2.2 at a wavelength of 600 nm, while Vermilyea (1953) and Charlesby et al (1955) report values larger than 2.4 at the same wavelength. Burgiel et al (1968) studied the refractive indices of sputtered films of Ta_2O_5 and found that these were about 10% smaller than corresponding results for anodic films of the same material obtained by Young. Westwood et al (1974) discusses the effects of sputtering pressure on the refractive indices of Ta_2O_5 films. They observed a variation in the refractive index value from about 2.1 to 2.2 at a wavelength of 488 nm for different sputtering pressures. According to them thermally prepared films of Ta_2O_5 have a refractive index of about 2.28 at the same wavelength.

Tauber et al (1971) studying the properties of chemical vapour deposited zirconium dioxide films quote a refractive index value of 2.1 ± 0.1 for a wavelength of 546 nm. Wilkens (1964), studying infrared interference of anodic and thermal zirconium oxide obtained a value for the index of refraction of 2.00 ± 0.05 in the wavelength region 1000 - 7000 nm. Single crystal results show indices of refraction of 2.13, 2.19 and 2.20 for the a_o, b_o and c_o axes respectively (Handbook of Chemistry and Physics, 1968 - 1969).

The optical properties of thin films of Ta_2O_5 and ZrO_2 were studied in the spectral range from 250 to 2000 nm. These materials have high refractive indices and are transparent in the ultra-violet down to wavelengths of 300 nm (Ta_2O_5) and 250 nm (ZrO_2). Most of the other materials which are transparent in this region e.g. silicon dioxide, sodium chloride, potassium chloride etc. have low indices of refraction.

The absorption curves, for Ta_2O_5 thus obtained, were analysed to determine the band gap value and the nature of the electronic transitions involved. Besides which an accurate knowledge, of the optical properties of Ta_2O_5 and ZrO_2, is of value in the design of various optical filters, and in the construction of thin film capacitors, where films of higher dielectric constant are required.

4.2 METHOD OF PREPARATION OF TANTALUM PENTOXIDE FILMS

Tantalum pentoxide films were deposited on clean quartz wedges. These films were prepared at W.R.E. Laboratories, Salisbury, South Australia, by the method of sputtering. The plant used was an MRC type 8620 sputtering module; comprising an 18" diameter glass vacuum chamber, 10" high, a 6" diameter diffusion pump and 600 litre/min rotary pump. The size of Ta_2O_5 target was 6" diameter and anode/cathode potential difference was 1.2 kV and anode to cathode distance was 9.2 cm. The chamber atmosphere consisted of 90% argon and 10% oxygen. The deposited films were uniform and had optical properties which were independent of their thickness. The rate of evaporation was about 5 to 7 nm per minute.

4.3 METHOD OF DETERMINING THE OPTICAL CONSTANTS

The optical properties, of Ta_2O_5 films, were determined by measuring the normal incidence reflectance (R) and transmittance (T), in the spectral range from 250 to 2000 nm. These were obtained, using the following exact relations, for a single film on a substrate derived by Tomlin (1968).

$$\frac{1+R}{T} = \frac{1}{4n_o n_2 (n_1^2+k_1^2)} \left[(n_o^2+n_1^2+k_1^2) \{ (n_1^2+n_2^2+k_1^2) \cosh 2\alpha_1 + 2n_1 n_2 \sinh 2\alpha_1 \} + (n_o^2-n_1^2-k_1^2) \{ (n_1^2-n_2^2+k_1^2) \cos 2\gamma_1 - 2n_2 k_1 \sin 2\gamma_1 \} \right] \quad 4.3.1$$

$$\frac{1-R}{T} = \frac{1}{2n_2 (n_1^2+k_1^2)} \left[n_1 \{ (n_1^2+n_2^2+k_1^2) \sinh 2\alpha_1 + 2n_1 n_2 \cosh 2\alpha_1 \} + k_1 \{ (n_1^2-n_2^2+k_1^2) \sin 2\gamma_1 + 2n_2 k_1 \cos 2\gamma_1 \} \right] \quad 4.3.2$$

where $n_1 - ik_1$ is the complex refractive index of the film of thickness d_1, resting on the substrate of refractive index n_2 at a wavelength λ and

$$\alpha_1 = 2\pi k_1 d_1 / \lambda \qquad \text{and} \qquad \gamma_1 = 2\pi n_1 d_1 / \lambda$$

The procedure adopted in solving these relations for n_1 and k_1 was the same as used by Denton et al (1972). For a start an approximate film thickness was needed which could be obtained from the reflectance or transmittance curve (Figure 4.1), using the following relation

$$d = \frac{\lambda_1 \lambda_2}{4n_1 (\lambda_1 - \lambda_2)} \quad 4.3.3$$

where λ_1 and λ_2 are the wavelengths of consecutive turning points in the non-absorbing region, and n_1 is the long-wavelength refractive index. Then this value of thickness was adjusted in an attempt to obtain a closed dispersion curve.

It was shown by Denton et al (1972) that calculations are much simplified by using expression for $(1 \pm R)/T$ rather than those for R and T, and that the correct choice from the multiple solutions can be

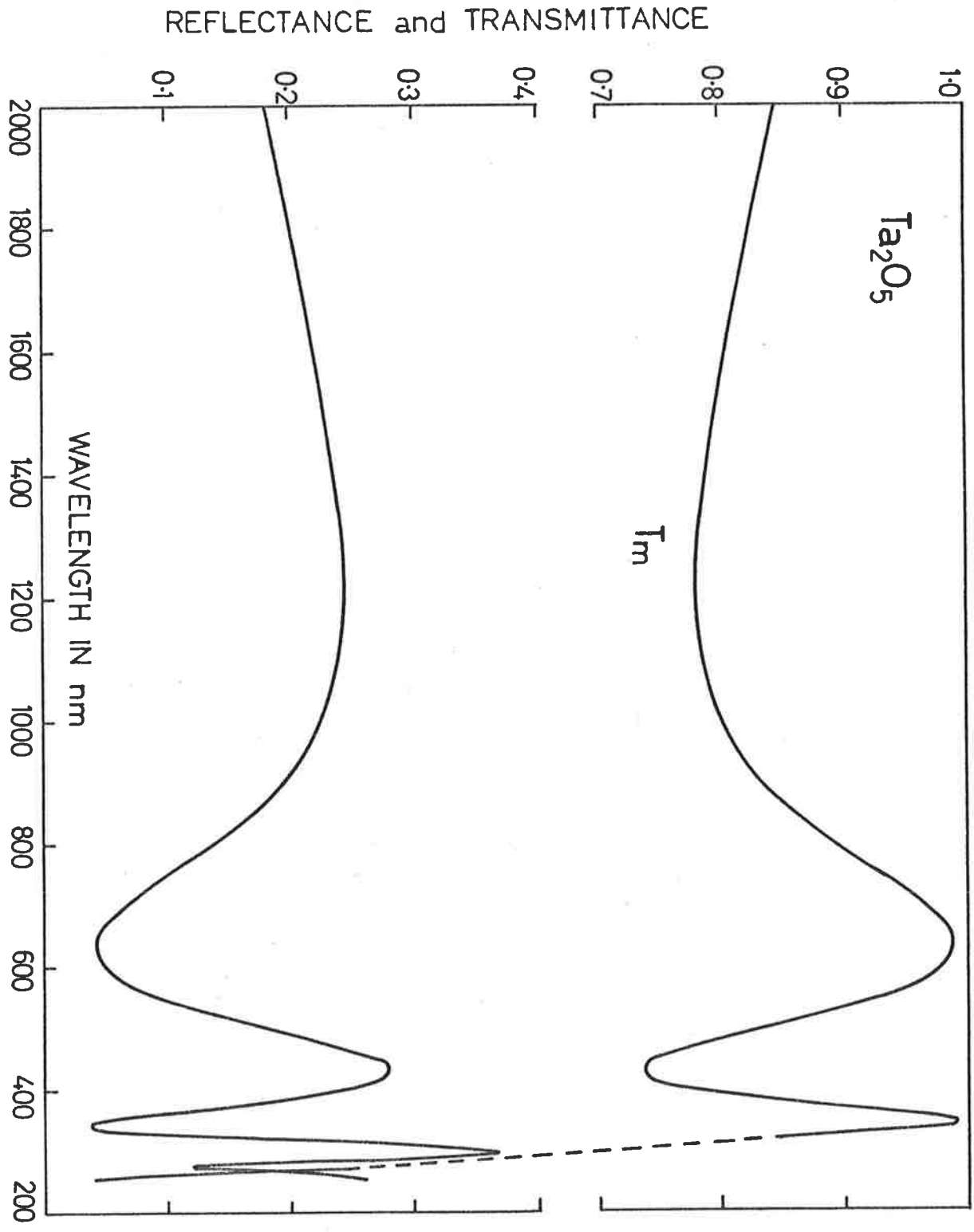
REFLECTANCE and TRANSMITTANCE
0·1
0·2
0·3
0·4
0·7
0·8
0·9
1·0
2000
1800
1600
1400
1200
1000
800
600
400
200
WAVELENGTH IN nm
Ta_2O_5
T_m

FIGURE 4·1

made unambiguously, together with an accurate determination of film thickness provided measurements are made over a sufficiently wide range of wavelengths.

4.4 RESULTS FOR Ta_2O_5 FILMS

The thin films, of tantalum pentoxide, studied varied in thickness from 60 to 150 nm. Figure 4.1 is an example of the reflectance (R) and transmittance (T_m) curves for a Ta_2O_5 film of 147 nm. It should be noted that transmittance (T) used in the equations 4.3.1 and 4.3.2 is the transmittance into the substrate. The measured transmittance (T_m) is $T_m = T/Ts$, where Ts is the transmittance across the back face of the substrate and is $4n_0n_2/(n_0+n_2)^2$, where n_0 and n_2 are the indices of refraction of air and the substrate respectively.

From these measured R and Tm (Figure 4.1) the dispersion and the absorption curves shown in Figures 4.2.a and 4.2.b were obtained, using the method discussed in the previous section. These are typical of the results for four different films of Ta_2O_5 of different thicknesses. Figure 4.2.a shows multiple solutions and proper closure of the curve. Where the error bars are large they probably grossly overestimate the error for reasons discussed by Denton et al (1972).

4.4.1 REFRACTIVE INDEX (Ta_2O_5)

The results, obtained for the films of Ta_2O_5 of different thicknesses, all show proper closure of the loops and continuity of dispersion curves (Figure 4.2.a). In Figure 4.3, the curve marked (b) is the average

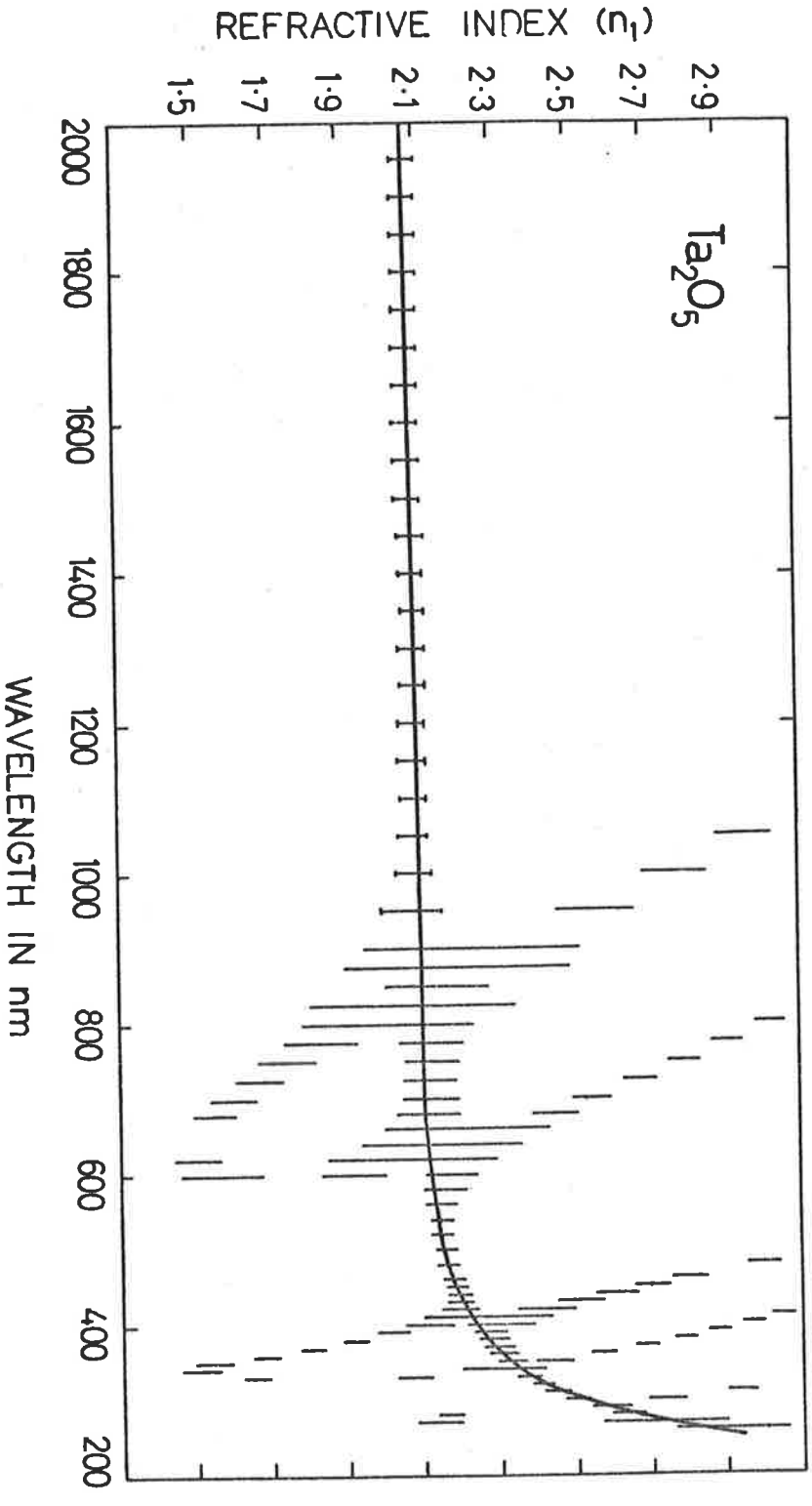
REFRACTIVE INDEX (ε_1)
1·5
1·7
1·9
2·1
2·3
2·5
2·7
2·9
Ta_2O_5
WAVELENGTH IN nm
2000
1800
1600
1400
1200
1000
800
600
400
200

FIGURE 4·2a

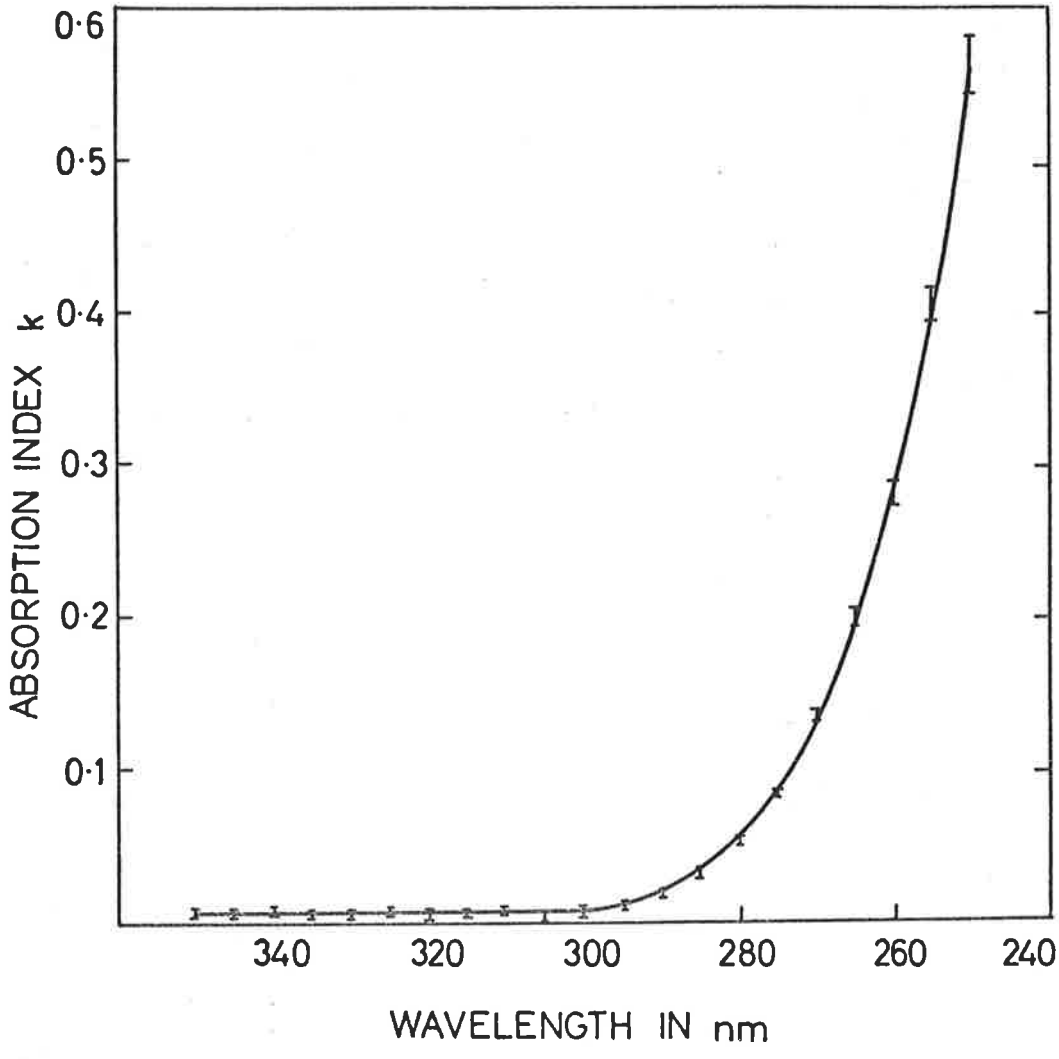
0·6
0·5
0·4
0·3
0·2
0·1
ABSORPTION INDEX k
340
320
300
280
260
240
WAVELENGTH IN nm

FIGURE 4·2b

dispersion curve from the four different Ta_2O_5 films. The vertical bars show the ranges within which the individual curves fell. The results for different films were reasonably reproducable as is clear from Figure 4.3.

In Figure 4.3 are also shown the dispersion curves marked (a) and (c), obtained by Young (1961) and Burgiel et al (1968), respectively. Young's results were obtained from anodic films of Ta_2O_5 while those of Burgiel et al were from sputtered films of Ta_2O_5. It is clear from these curves that anodic films have higher refractive indices than sputtered films.

4.4.2 ABSORPTION AND OPTICAL TRANSITIONS

In Figure 4.3 is also shown the average values of absorption index (represented by the vertical bars) obtained from the four different Ta_2O_5 films. The vertical bars show the ranges within with the individual absorption indices fell. The continuous curve passing through these bars, show how well a theoretical curve, based upon certain assumptions discussed below, fits the experimental results.

In the spectral region 2000 ~ 300 nm the values of absorption index were about 0.001 to 0.003. Since an error of 0.002 in the measured reflectance and transmittance is sufficient to produce an error of this amount, it may be concluded that the films were virtually transparent in this wavelength range. Numerical values of n and k at different wavelengths for Ta_2O_5 films are listed in Appendix D.

The theory of absorption processes in crystalline materials is treated in detail by a number of authors (e.g. Smith 1961). It is shown

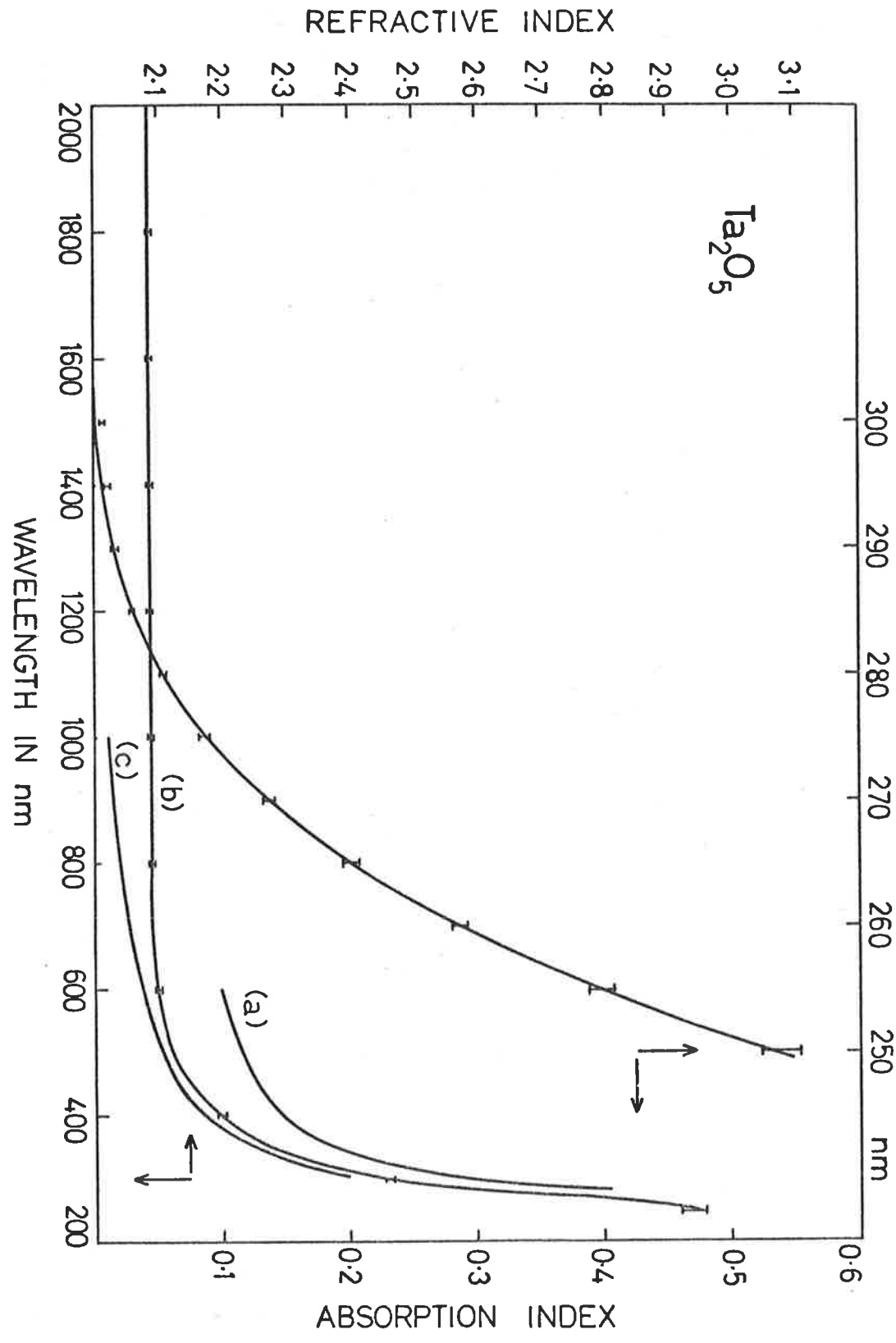
REFRACTIVE INDEX
2·1
2·2
2·3
2·4
2·5
2·6
2·7
2·8
2·9
3·0
3·1
Ta_2O_5
2000
1800
1600
1400
1200
1000
800
600
400
200
WAVELENGTH IN nm
300
290
280
270
260
250
nm
(a)
(b)
(c)
0·1
0·2
0·3
0·4
0·5
0·6
ABSORPTION INDEX

FIGURE 4·3

that for the interaction of a photon with an electron, resulting in a direct transition of the electron from the valence to the conduction band, the absorption follows the relation

$$(EnK)^2 = c_1(E-Eg) \qquad 4.4.1$$

where E is the photon energy, Eg is the band gap, $K = 4\pi k/\lambda$, and n and k are the indices of refraction and absorption respectively at wavelength λ corresponding to energy E. And c_1 is a constant.

For the interaction of a photon and a phonon with an electron, resulting in an indirect (or phonon assisted) transition, the absorption follows the relation

$$(EnK)^{\frac{1}{2}} = c_2\ (E-Eg') \qquad 4.4.2$$

where Eg' is the band gap and c_2 is a constant. In the above relation the very small phonon energy is neglected.

Equation 4.4.2 may be written as

$$(E^2nk)^{\frac{1}{2}} = c_3\ (E-Eg') \qquad 4.4.3$$

since $K = 4\pi k/\lambda$ and $E = \frac{1239.6}{\lambda(nm)}$

Figure 4.4 shows a plot of $(E^2nk)^{\frac{1}{2}}$ against E for a tantalum pentoxide film. The absorption follows the law for indirect transitions (with a band gap of 4.15 eV) up to an energy of about 4.57 eV at which point another absorption process begins to operate. If the absorption index due to the first transition is k_1 then the line (a) in Figure 4.4 is the plot of $(E^2nk_1)^{\frac{1}{2}}$ (i.e. $k = k_1$) and if the absorption index due to the

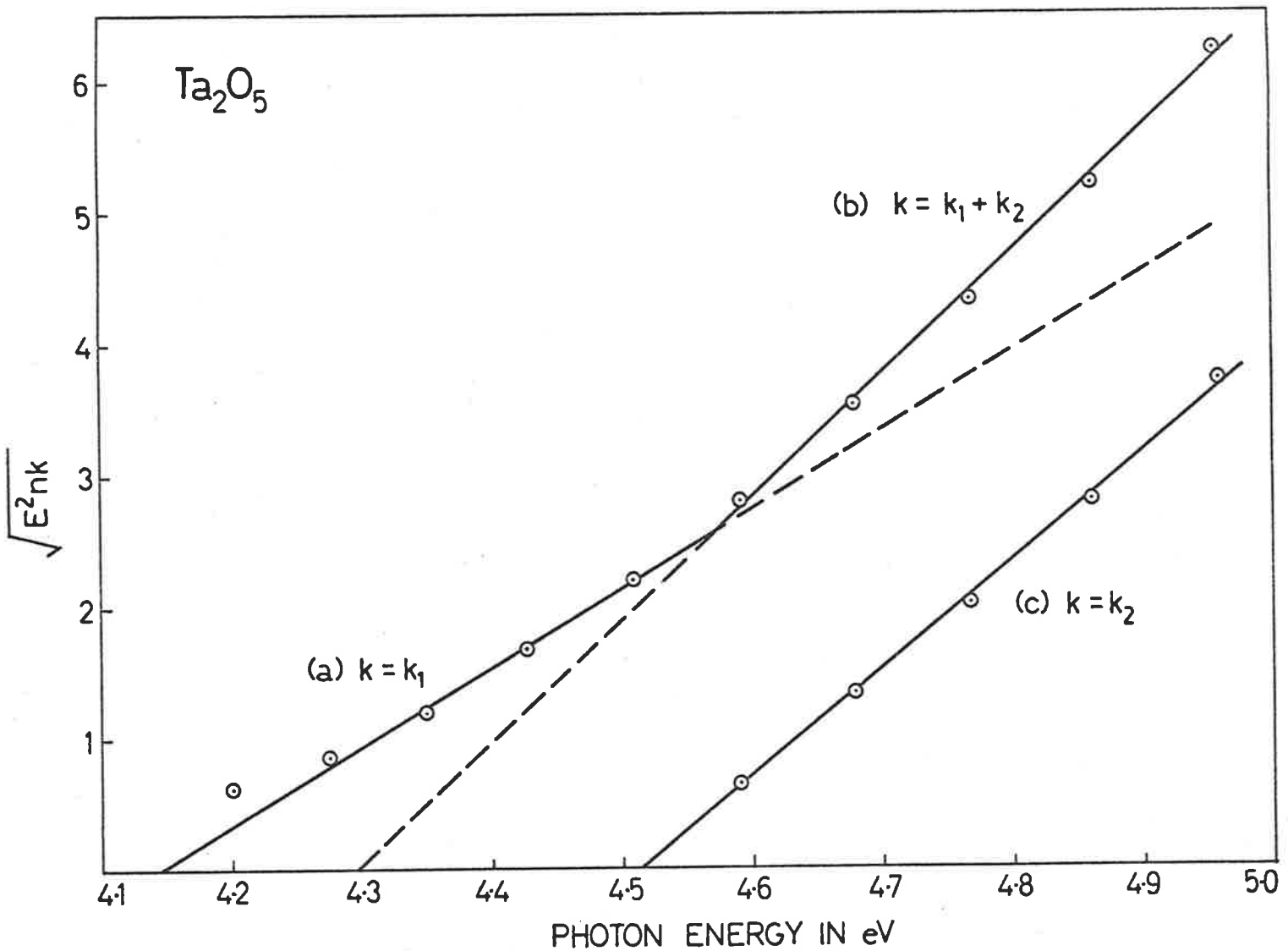
Ta_2O_5
(a) $k = k_1$
(b) $k = k_1 + k_2$
(c) $k = k_2$
$\sqrt{E^2_{nk}}$
PHOTON ENERGY IN eV
1
2
3
4
5
6
4·1
4·2
4·3
4·4
4·5
4·6
4·7
4·8
4·9
5·0

FIGURE 4·4

second transition is k_2, then the line (b) is the plot of $\{E^2n(k_1+k_2)\}^{\frac{1}{2}}$ (i.e. $k = k_1+k_2$). k_2 may be found by extrapolating the straight line (a) and substrating the resulting values of k_1 from the total absorption index k. Thus the straight line (c) is the plot of $(Enk_2)^{\frac{1}{2}}$ against E. It is clear from Figure 4.4 that the total absorption index k for Ta_2O_5 films follows the relations

$$k = k_1 = \frac{c_3^2}{E^2n}(E-Eg)^2 \quad \text{for } 4.15 < E < 4.51 \text{ eV} \qquad 4.4.4$$

and

$$k = k_1+k_2 = \frac{1}{E^2n}\{c_3^2(E-Eg)^2 + c_4^2(E-Eg_1)^2\} \quad \text{for } E > 4.51 \text{ eV} \qquad 4.4.5$$

where

$Eg = 4.15$ eV $\qquad Eg_1 = 4.51$ eV

$c_3 = 6.2$ $\qquad c_4 = 8.2$

The continuous absorption curve shown in Figure 4.3 represents the absorption index calculated from the above theoretical formulae for the values of Eg, Eg_1, c_3 and c_4 stated. The agreement between these theoretical curve and the experimental vertical bars shown in Figure 4.3 is remarkably good.

Westwood et al (1974) have reported that sputtered and anodic films of Ta_2O_5 are amorphous. John Ward of W.R.E., Laboratories, Salisbury, South Australia, has mentioned, in a private communication, that an x-ray study of sputtered Ta_2O_5 films, has revealed that these films are amorphous. Also electron microscopic study of the surfaces has shown that Ta_2O_5 of thicknesses as large as 600 nm have smooth surfaces.

4.5 RESEMBLANCE OF ELECTRONIC TRANSITIONS IN AMORPHOUS Ta_2O_5 FILMS WITH THOSE IN AMORPHOUS GERMANIUM FILMS

The plots, of $(E^2nk)^{\frac{1}{2}}$ against E for Ta_2O_5 films (Fig. 4.4) resemble to the corresponding plots for amorphous germanium films obtained by Tauc et al (1964) and Denton and Tomlin (1972). The plots for amorphous Ge films, shown by them, appear to consist of two straight lines as does that for Ta_2O_5 films (Fig. 4.4).

Tauc et al (1964) have suggested that in the case of amorphous materials it might be expected that if the energy band structure is substantially unaltered then the indirect transitions will occur as for the crystalline material. But on the other hand the formula for direct transitions will not hold because this results from a selection rule which depends upon the periodic crystal structure. When this rule is relaxed and all direct transitions which conserve energy are considered, instead of only those allowed in the perfect lattice, then the relation is of the same form as equation 4.4.3. The experimental results from amorphous Ge films were explained successfully on the basis of these assumptions (Tauc et al; Denton and Tomlin).

It follows from the above discussion that the expressions, relating the absorption (k) to the photon energy (E), in the cases of a direct and an indirect transition of electrons, from the valence bands to the conduction bands, in amorphous materials, are of the same form. It is not possible to differentiate between the two processes in the method adopted here for the Ta_2O_5 films. The two transitions, with onsets of 4.15 eV and 4.51 eV may, therefore, both be indirect or both direct or

the first indirect and the second direct or the first direct and the second indirect. One might think of differentiating the processes by considering the strengths of the absorptions involved in different processes. Generally, absorption in a direct transition is expected to be much larger than that in an indirect transition unless the electron state density (in the valance and conduction bands) strongly favours the latter. In the absence of any definite informations on this point it is only from the resemblance of the $(E^2nk_1)^{\frac{1}{2}}$ versus E plots of amorphous, Ge and Ta_2O_5 that it may be said that these two materials may possibly have similar band structure. I have not come across any published work on theoretically calculated band structure for crystalline Ta_2O_5.

It may be noted that the interpretation, for the onset of the second transition, followed in Figure 4.4, was different from that of the same for Ge results given by Tauc et al (1964) and Denton and Tomlin (1972a). This will be treated in detail later on in the chapter on Ge.

4.6 METHOD OF PREPARATION OF ZIRCONIUM DIOXIDE FILMS

Zirconium dioxide films were deposited in vacuum on clean quartz wedges at W.R.E. Laboratories, Salisbury, South Australia. The vacuum system consisted of an 18" diameter glass bell jar pumped by a 9" diameter diffusion pump which was backed by a rotary pump. Pure ZrO_2 was heated in a ring type electron gun. The accelerating voltage for the electron beam was 5 kV (200 - 300 mA) and the filament current was 30 A. During deposition the pressure in the chamber was 10^{-5} torr. The source to substrate distance was 10.6" and the substrate was rotated while deposition

took place. The rate of evaporation was about 20 nm per minute.

4.7 DERIVATION OF THE OPTICAL CONSTANTS FOR ZrO_2 FILMS (SINGLE FILM ON A SUBSTRATE METHOD)

The normal incidence reflectance and transmittance, of the ZrO_2 films prepared by the above method, were measured in the spectral range from 250 to 2000 nm. Figure 4.5 is an example of the measured reflectance (R) and transmittance (Tm) curves for a ZrO_2 film of about 220 nm thickness.

At first the optical constants were calculated from measured R and T, using the formulae for $(1 \pm R)/T$ for a single film on a substrate. And the procedure adopted, was the same as mentioned in Section 4.3. Figure 4.6 shows the result of such a calculation based on the data of Figure 4.5 and is typical of the results for seven different films of ZrO_2 of different thicknesses. It shows that no choice of thickness was possible for which closure of the dispersion curve over the whole range of wavelengths could be achieved. In the light of the discussion of Denton et al (1972) it shows that the chosen thickness (d_1 = 220 nm) was too large for closure at (A) and (B) (Figure 4.6) and just correct for proper closure at (C) and too small for closure at (D). No variation of film thickness improved this situation.

As will be discussed later, a similar situation was observed for films of cadmium and zinc sulphides. It was concluded that the measured values of R and T were not those appropriate to a perfectly plane parallel uniform thin film such as is assumed for the derivation of the formulae used. This conclusion was supported, by the observed, rough surfaces of the ZrO_2 films, as is discussed below.

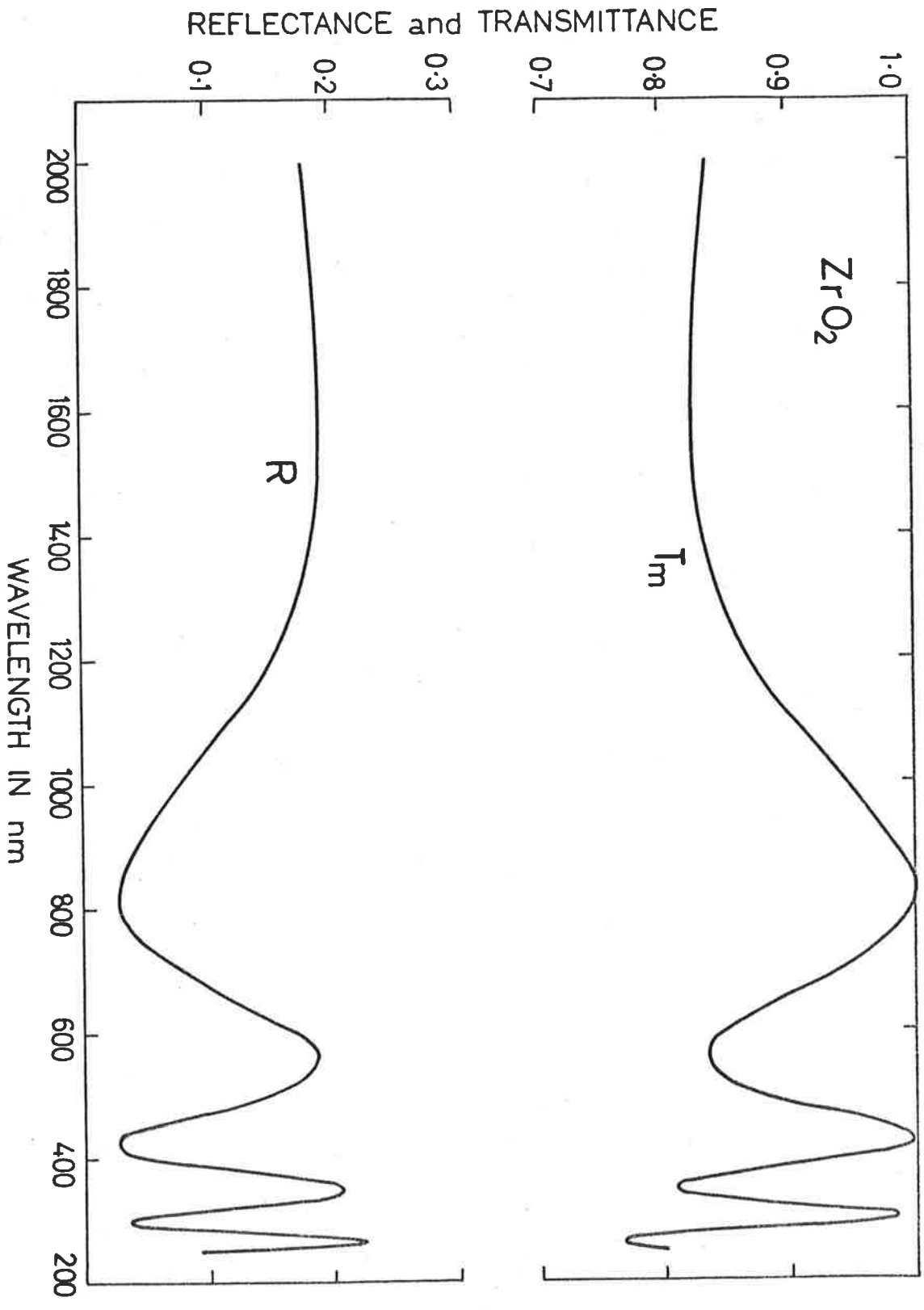
REFLECTANCE and TRANSMITTANCE
0·1
0·2
0·3
0·7
0·8
0·9
1·0
2000
1800
1600
1400
1200
1000
800
600
400
200
WAVELENGTH IN nm
R
T_m
ZrO_2

FIGURE 4·5

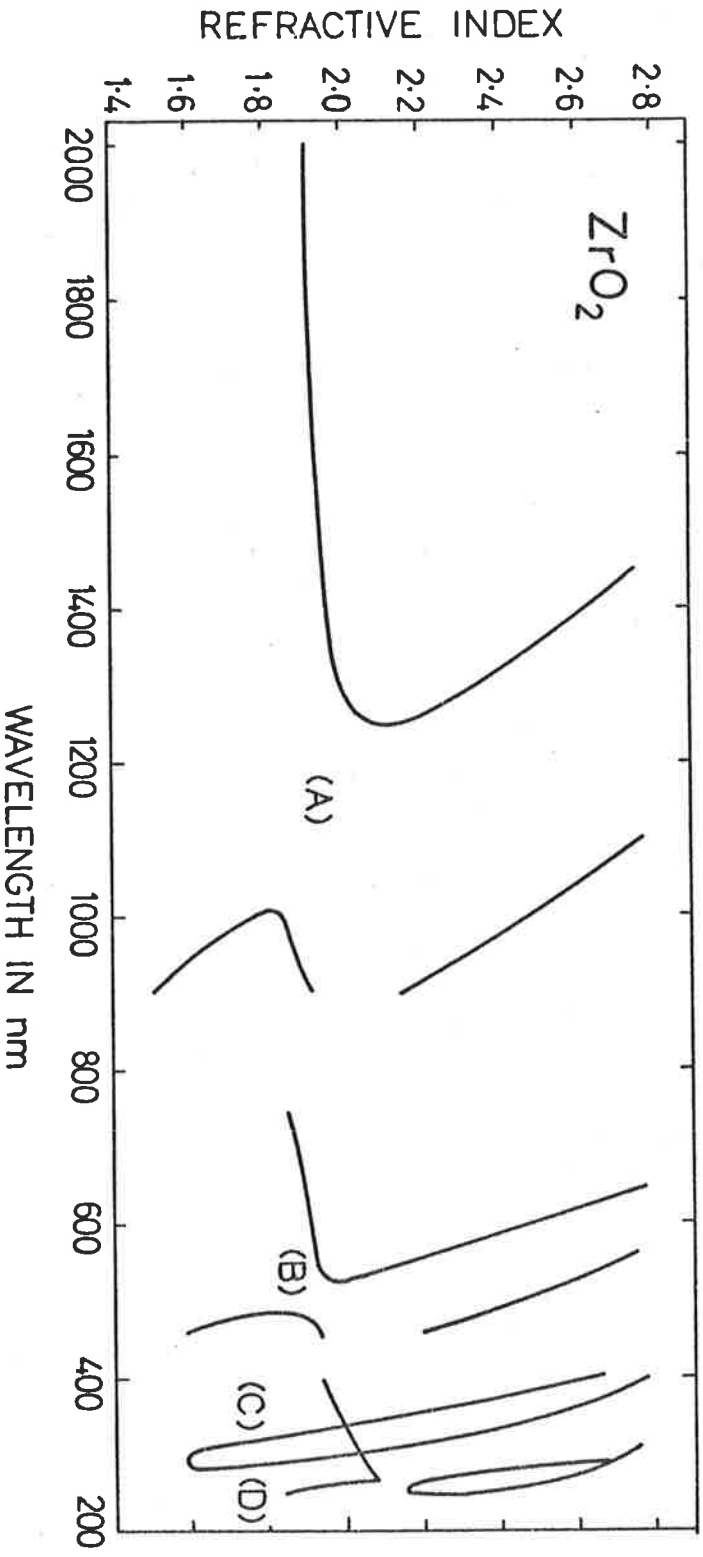
REFRACTIVE INDEX
2·8
2·6
2·4
2·2
2·0
1·8
1·6
1·4
ZrO_2
(A)
(B)
(C)
(D)
2000
1800
1600
1400
1200
1000
800
600
400
200
WAVELENGTH IN nm

FIGURE 4·6

4.8 SURFACE TOPOGRAPHY OF THE ZrO_2 FILMS

Surface replicas of ZrO_2 films deposited on quartz wedges were prepared and studied with the aid of an electron microscope. Carbon replicas of ZrO_2 films surfaces were obtained by evaporating thin films of carbon onto ZrO_2 films and then floating off the carbon films on sulphuric acid, which disolves ZrO_2. These carbon replicas were collected on grids and then Pd shadowed. Figure 4.7 is the electron micrograph of the surface replica of a ZrO_2 film and is typical of the results for different films of ZrO_2, studied. The surfaces are indeed rough (i.e. have a pebbly appearance) with a roughness dimension of about 12 to 16 nm.

4.9 DERIVATION OF THE OPTICAL CONSTANTS OF ZrO_2 FILMS BY THE METHOD OF A DOUBLE FILM ON THE SUBSTRATE

From the above discussion it follows that surface roughness must be accounted for in order to obtain a continuous dispersion curve. Two different methods for allowing for this roughness effect are considered later in the chapter, on the optical properties of cadmium sulphide films. It will be shown that the method, which allows the replacement of the rough surface layer of a film by an equivalent smooth surface layer, resting on an ideal film of the evaporated material, is the better of the two discussed. It is then necessary to use the formulae for $(1\pm R_2)/T_2$ for a double layer on a substrate (Tomlin 1972a) for the calculation of the optical constants of the film. It should be noted that T_2 is the transmittance into the substrate, and R_2 is the reflectance from the upper surface of the double film. When the first layer and substrate are transparent the formulae become

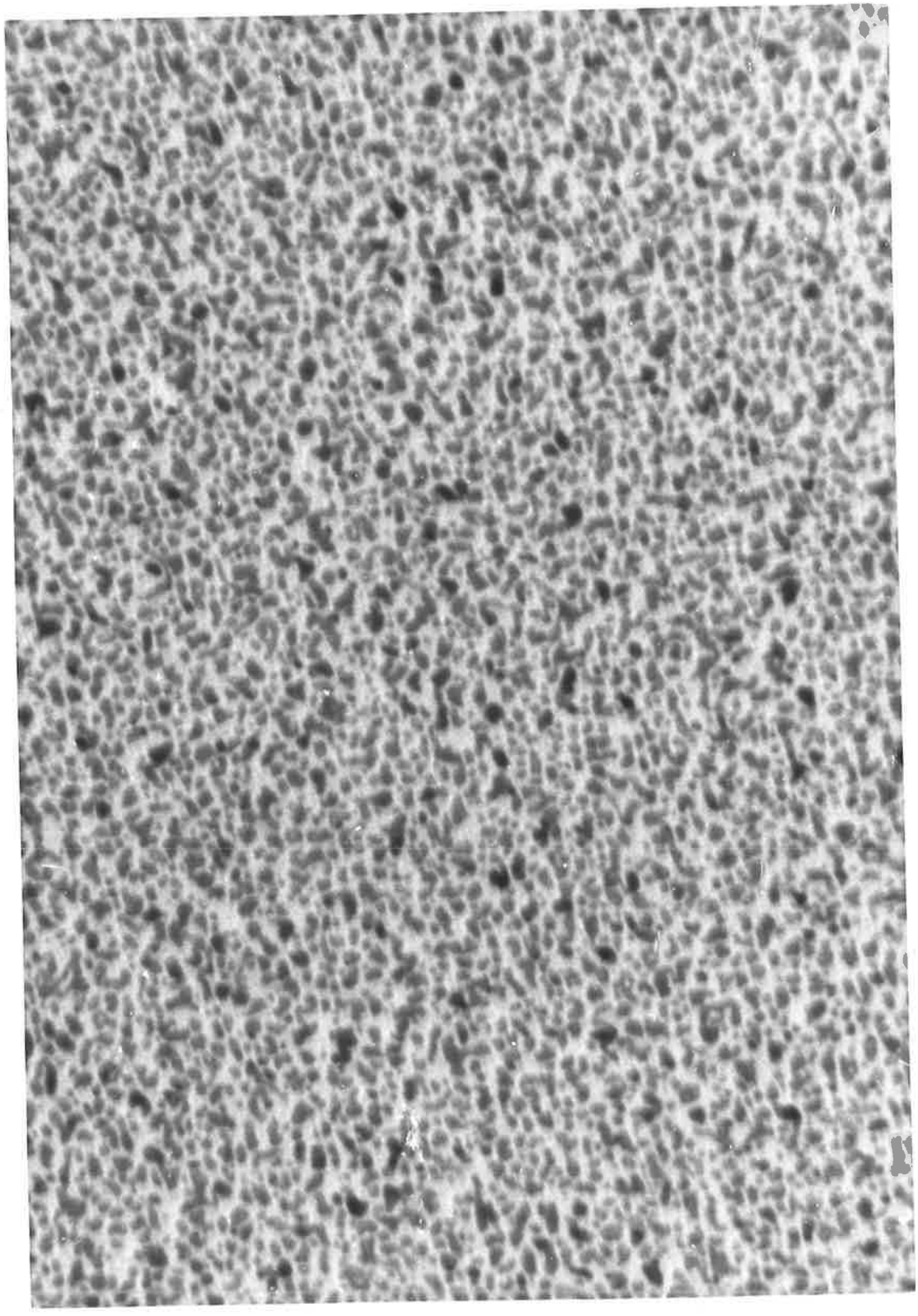

FIGURE 4.7 (ZrO_2 Surface Replica) 2×10^5

$$\frac{1+R_2}{T_2} = \frac{1}{16\ n_0 n_3 n_1^2 (n_2^2+k_2^2)} \{(n_0^2+n_1^2)F_1 + (n_0^2-n_1^2)F_2\} \qquad 4.9.1$$

$$\frac{1-R_2}{T_2} = \frac{n_1\ G_1}{8\ n_3 n_1^2 (n_2^2+k_2^2)} \qquad 4.9.2$$

where $F_1 = 2(n_1^2+n_2^2+k_2^2)\ \{(n_2^2+n_3^2+k_2^2)\cosh 2\alpha_2 + 2n_2 n_3 \sinh 2\alpha_2\}$

$+ 2(n_1^2-n_2^2-k_2^2)\ \{(n_2^2-n_3^2+k_2^2)\cos 2\gamma_2 - 2n_3 k_2 \sin 2\gamma_2\}$

$F_2 = \{(n_1+n_2)^2+k_2^2\}\ \{(n_2^2-n_3^2+k_2^2)\cos 2(\gamma_1+\gamma_2) - 2n_3 k_2 \sin 2(\gamma_1+\gamma_2)\}$

$+ \{(n_1-n_2)^2+k_2^2\}\ \{(n_2^2-n_3^2+k_2^2)\cos 2(\gamma_1-\gamma_2) + 2n_3 k_2 \sin 2(\gamma_1-\gamma_2)\}$

$+ 2(n_1^2-n_2^2-k_2^2)\cos 2\gamma_1\ \{(n_2^2+n_3^2+k_2^2)\cosh 2\alpha_2 + 2n_2 n_3 \sinh 2\alpha_2$

$+ 4n_1 k_2 \sin 2\gamma_1\ \{(n_2^2+n_3^2+k_2^2)\sinh 2\alpha_2 + 2n_2 n_3 \cosh 2\alpha_2\}$

$G_1 = 4n_1 \left[n_2\ \{(n_2^2+n_3^2+k_2^2)\sinh 2\alpha_2 + 2n_2 n_3 \cosh 2\alpha_2\} \right.$

$\left. + k_2\ \{(n_2^2-n_3^2+k_2^2)\sin 2\gamma_2 + 2n_3 k_2 \cos 2\gamma_2\} \right]$

and $\alpha_2 = 2\pi k_2 d_2/\lambda \qquad \gamma_1 = 2\pi n_1 d_1/\lambda$

and $\gamma_2 = 2\pi n_2 d_2/\lambda$

n_0 is the refractive index of air

n_1 is the refractive index of the first layer (equivalent surface roughness layer) of thickness d_1

$n_2 - ik_2$ is the complex refractive index of the second layer (specimen film) of thickness d_2

n_3 is the refractive index of the substrate

λ is the wavelength of the light

Since ZrO_2 films show very little absorption in the spectral region covered, therefore the absorption, in the very thin (about 15 nm) first layer, which is the equivalent surface layer, is neglected. A constant value of $n_1 = 1.7$ was used in the entire spectral range. In practice it is found that for a thin surface layer the value of n_1 is not critical and change in this value only modifies the thickness of the surface layer for which closure of the dispersion curve occurs, without appreciable effect on the calculated values of n_2 and k_2 for the film itself. However an accurate result for the thickness of the surface layer can be found only if n_1 is known accurately.

It may be mentioned here that Bousquet (1957) accounted for his results from calcium fluoride films by considering transition layers (or surface layers) of thicknesses of about 10% of the thicknesses of the films themselves.

The method adopted for solving equations 4.9.1 and 4.9.2 for n_2 and k_2 was the same as used by Denton et al (1972).

4.10 RESULTS FOR ZrO_2 FILMS

All of the optical results discussed here for ZrO_2 films were obtained by the double layer method outlined above. Figure 4.8 is the dispersion curve obtained, from the data shown in Figure 4.5, for the surface layer thickness $d_1 = 15$ nm and the film thickness $d_2 = 205$ nm. This shows multiple solutions and proper closure of the curve. Where the error bars are large they probably grossly overestimate the error for reasons discussed by Denton et al (1972).

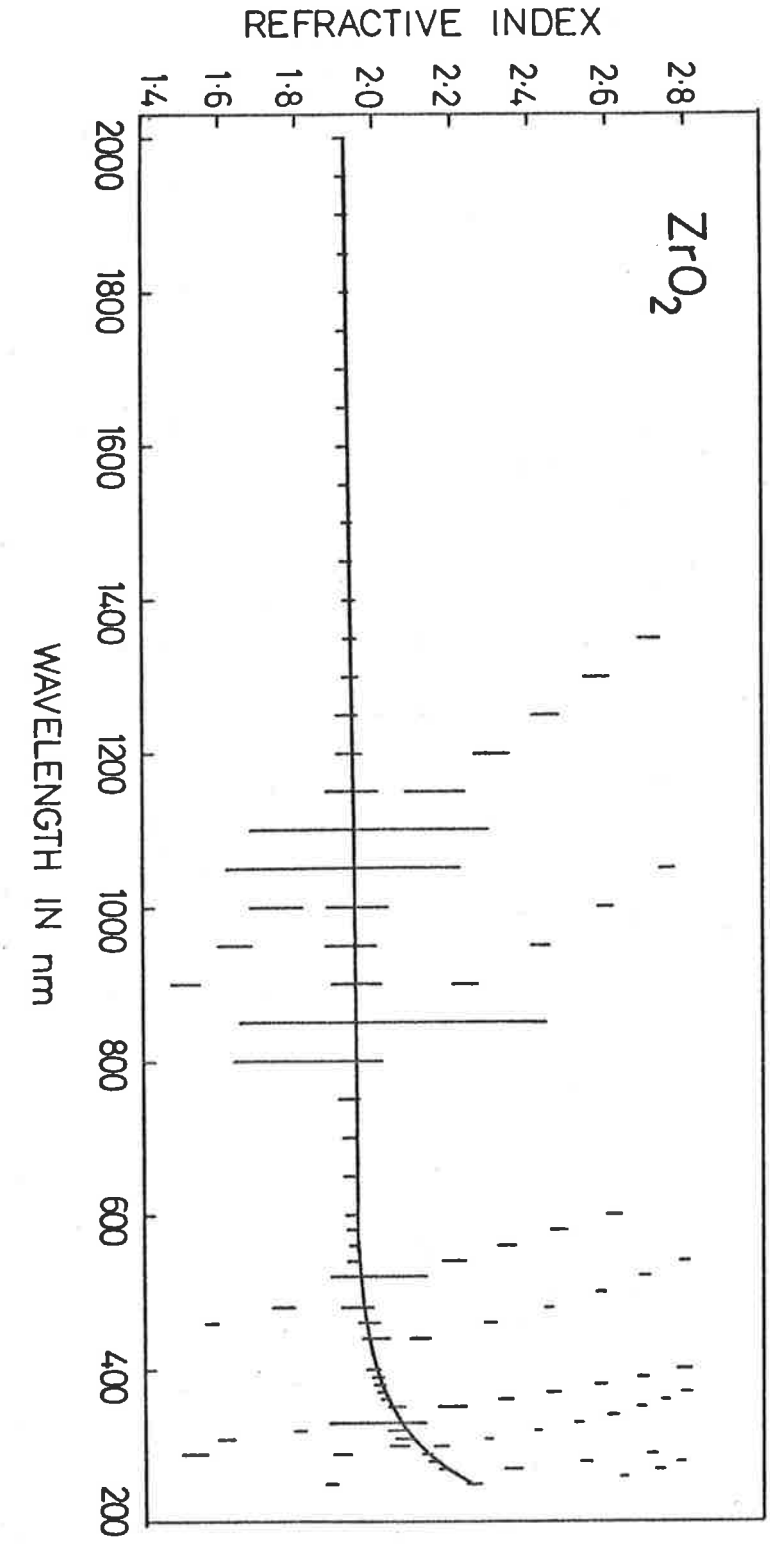
REFRACTIVE INDEX
1·4
1·6
1·8
2·0
2·2
2·4
2·6
2·8
ZrO_2
WAVELENGTH IN nm
2000
1800
1600
1400
1200
1000
800
600
400
200

FIGURE 4·8

Figure 4.9 shows the averaged dispersion curve from five different ZrO_2 films (of different thicknesses) with the vertical bars indicating the limits within which the individual curve lay. The results are in a very good agreement with those of Liddel's (1974), which were obtained from films of ZrO_2, also prepared by electron bombardment evaporation. The numerical values of n and k for ZrO_2 at different wavelengths are given in Appendix E. The calculations resulted in absorption indices of about 0.003 to 0.005 in the region 2000 - 255 nm. Which, once again for the reasons given in Section 4.4.2, may be attributed to errors in measured R and T. At a wavelength of 250 nm, the absorption index was 0.010. Since this was at the lower limit of the measurements made nothing can be said about the absorption processes in ZrO_2 films.

4.11 ON THE SURFACES OF THIN FILMS

The nature, of the surfaces of different films, was observed to depend on the structure of the films. For example amorphous films of Ta_2O_5 have smooth surfaces as was revealed by the study of optical constants and electron microscopy. Similar studies have shown that amorphous films of Ge have smooth surfaces (Dention, 1971) and polycrystalline films of Ge have rough surfaces (Dention, 1971 and Tauc et al, 1964). Similar studies have also revealed that polycrystalline films of ZrO_2, ZnS and CdS have rough surfaces (present work).

These results are consistent with those reported by Grigorovici (1973). It is reported by Grigorovici that, amorphous films of carbon, selenium, chalcogenide, silicon and germanium are known to be very smooth and homogeneous, and polycrystalline films have a much rougher surface

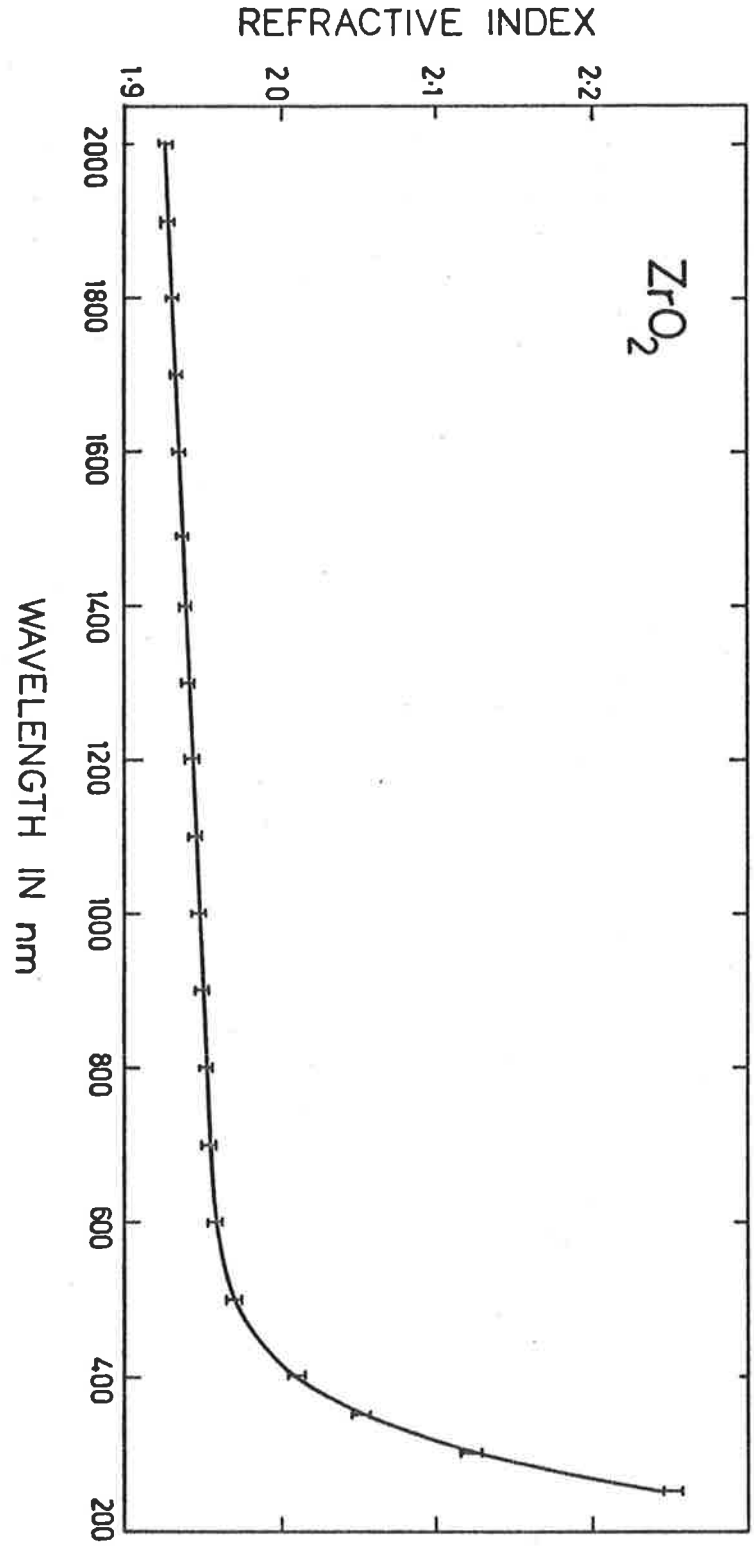
REFRACTIVE INDEX
1·9
2·0
2·1
2·2
ZrO_2
WAVELENGTH IN nm
2000
1800
1600
1400
1200
1000
800
600
400
200

FIGURE 4·9

and scatter therefore short wavelength light much more than amorphous films.

However there is not sufficient evidence to justify a generalization that amorphous films always have smooth surfaces and polycrystalline films rough surfaces.

CHAPTER 5

OPTICAL PROPERTIES OF AMORPHOUS AND POLYCRYSTALLINE GERMANIUM

5.1 INTRODUCTION

The optical constants of amorphous germanium films, have been determined in the wavelength range 2000-700 nm from the measured reflectance and transmittance at normal incidence (Dental et al, 1972). These results will be discussed further together with the results of new measurements in the spectral range 700-300 nm, where the films are highly absorbing (films of thickness > 250 nm, had transmittance less than 1%). The constants in this range were determined using Tomlin's method and the modified Tomlin's method (described in Chapter 3).

Tomlin's method is being applied for the first time as far as I know. In order to find a suitable material to be used as an overlying layer on the specimen, dielectrics such as Ta_2O_5, ZnS and ZrO_2 were tried. It was concluded that Ta_2O_5 was the most suitable of the three. Sputtered films of Ta_2O_5 were amorphous, uniform, and had smooth surfaces and were transparent down to 300 nm. On the other hand films of ZnS and ZrO_2 had rough surfaces and were polycrystalline.

The optical constants of polycrystalline Ge in a bulk form were also studied in the spectral range 1750-300 nm, using Tomlin's method. The overlying layer of Ta_2O_5 was used in this case. Near the absorption edge, reliable data on the absorption could not be obtained, though refractive indices were determined with reasonable accuracy (Section 3.15).

5.2 PREPARATION OF Ge FILMS

Ge films were deposited on clean quartz substrates by evaporation in a vacuum of the order of 10^{-5} torr. Pure Ge lumps, supplied by New Metals and Chemicals Ltd., England, were placed in a tungstun conical basket. An electromagnetically operated shutter was positioned above the source to enable the Ge to be outgassed prior to evaporation onto the substrate. The rate of evaporation was about 20 to 40 nm per minute, which was controlled by varying the current flowing through the conical basket.

5.3 OPTICAL PROPERTIES OF Ge FILMS IN THE WAVELENGTH RANGE 2000-700 nm

In the laboratory here, the optical properties of Ge films, in the spectral range 2000-700 nm, were studied by Denton et al (1972). Figure 5.1 shows the plots of indices of refraction and absorption against the wavelength obtained. Denton (1971) reports that the films of Ge deposited on room temperature substrates and subsequently annealed at 350^{o}C for several hours exhibited optical constants similar to those of films which were not annealed.

In the present work, the optical properties of Ge films deposited on room temperature substrates and subsequently annealed at 180^{o}C for about six hours, were studied in the spectral range, mentioned above. The method applied was similar to the one used by Denton. While studying the optical properties of Ge films in the range 700-300 nm (using Tomlin's method), it was found that ZnS films deposited on room temperature Ge/quartz substrate systems (Ge film deposited on quartz substrate), were

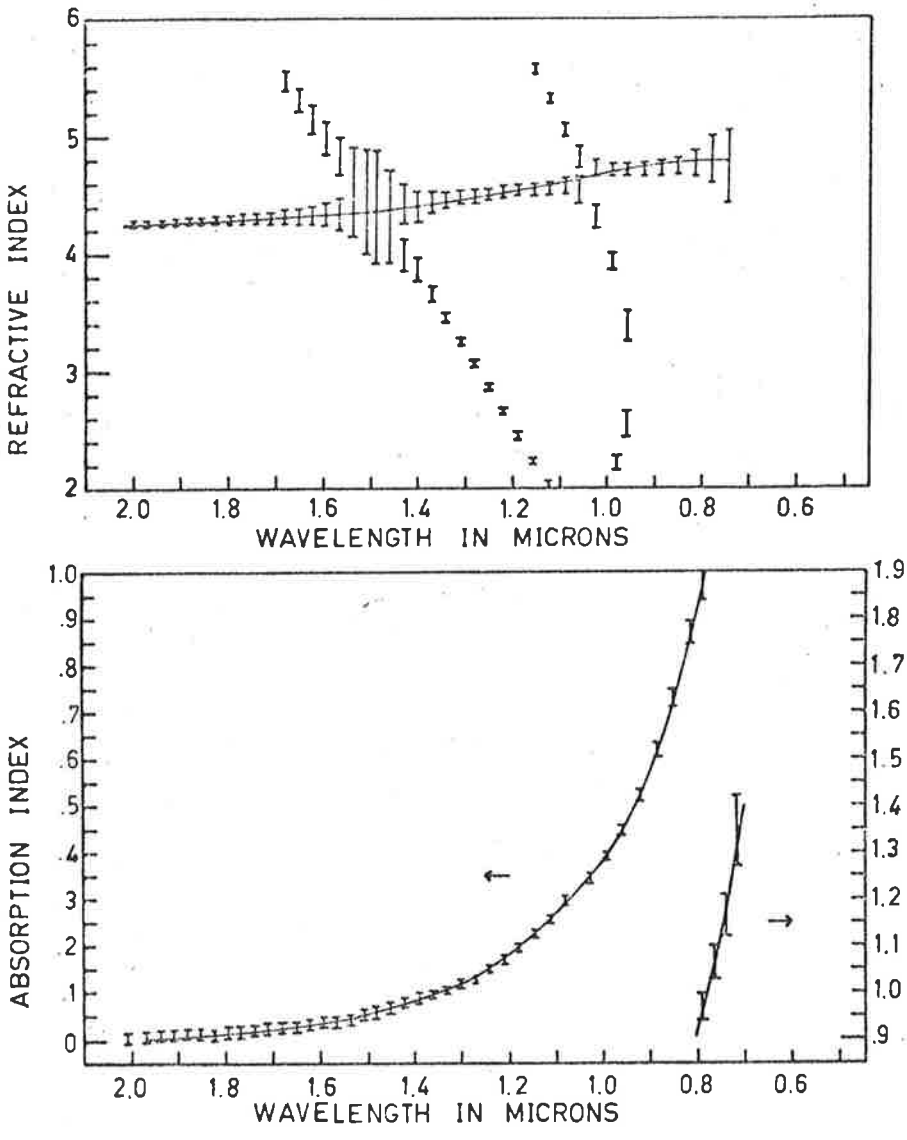

from Denton et al (1972)

FIGURE 5·1

non-uniform. On the other hand ZnS films deposited on Ge/quartz substrate system, maintained at higher temperatures (e.g. 180°C), were uniform. Thus the study of optical properties of Ge films deposited on room temperature substrates and subsequently annealed at 180°C, was made in the region 2000 - 700 nm. The results thus obtained from one of the annealed films, of thickness of about 288 nm, is shown in Figure 5.2. The results, obtained from these annealed films of different thicknesses (100 - 300 nm) were similar to those obtained by Denton, discussed above.

Hence it may be concluded that films of Ge deposited on room temperature substrates and subsequently annealed at 180°C or 350°C for several hours have optical constants in the spectral range 2000 - 700 nm of films which are not significantly different from those of unannealed films.

5.4 STRUCTURE AND SURFACES OF Ge FILMS

In the present work the Ge films studied were deposited on room temperature quartz substrates, and subsequently annealed at 180°C for about six hours, or at 350°C for about half an hour. The films were annealed in vacuum of the order of 10^{-5} torr.

The measured normal incidence reflectivities of such films and of polycrystalline Ge in bulk form are shown in Figure 5.3 (Section 5.5.1). It is seen that the fine structure, in the reflectivity data from polycrystalline Ge, is missing in the similar data from these films. From this it may be concluded that these films were amorphous. This conclusion is supported by other workers, e.g. Tauc et al (1964), Donovan

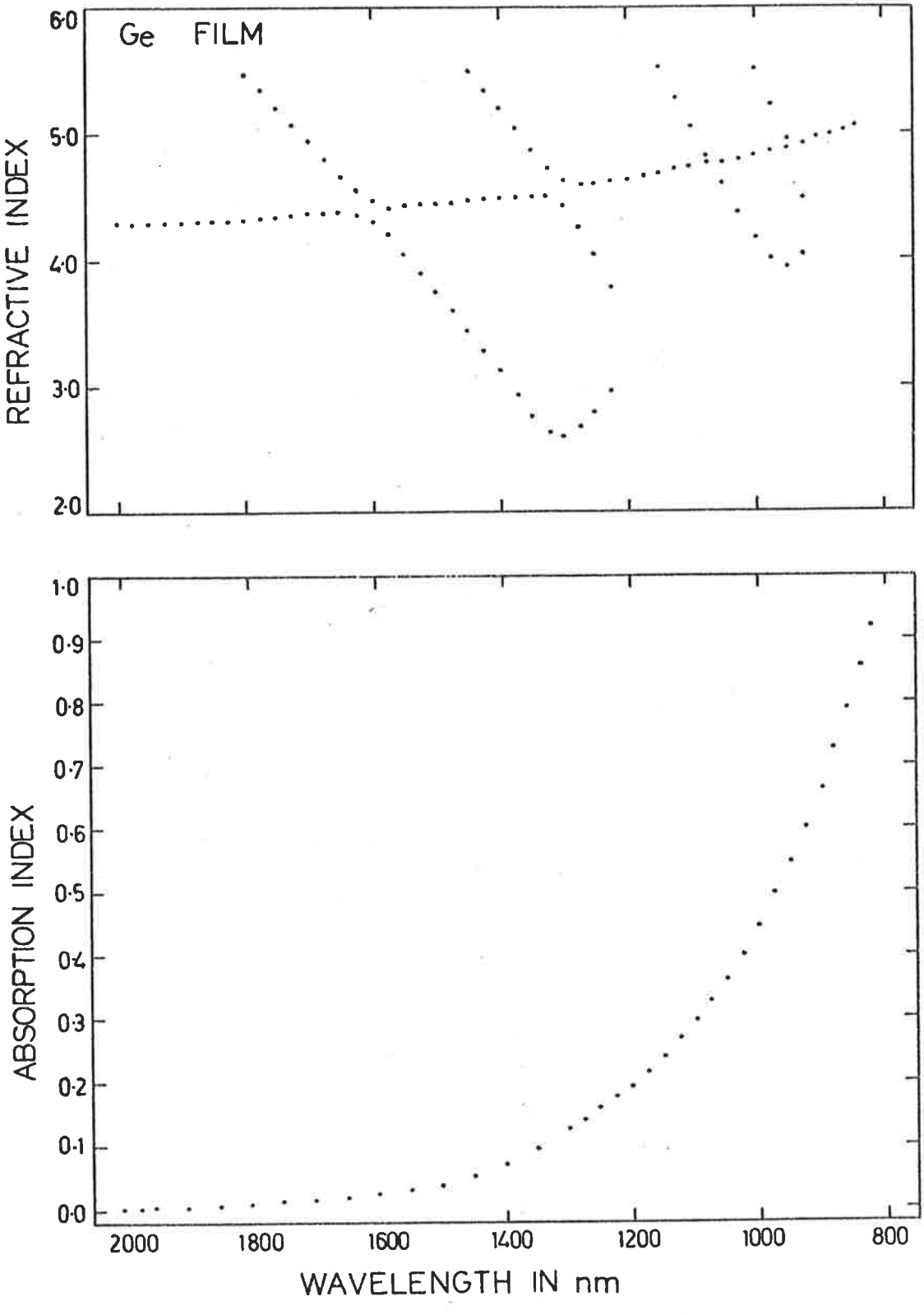
Ge FILM
REFRACTIVE INDEX
6·0
5·0
4·0
3·0
2·0
ABSORPTION INDEX
1·0
0·9
0·8
0·7
0·6
0·5
0·4
0·3
0·2
0·1
0·0
2000
1800
1600
1400
1200
1000
800
WAVELENGTH IN nm

FIGURE 5·2

and Ashley (1964), Theye (1971) and Paul et al (1973), who report that Ge films deposited on room temperature substrates are amorphous. According to Theye a film deposited at room temperature and taken through successive annealing cycles at increasing temperatures remains amorphous until the annealing temperature is 400^{o}C. This was revealed by the study of electron diffraction patterns and also electron transmission micrographs obtained from Ge films.

Our study of optical constants and examination of surface replica by E.M. have shown that these films of Ge had smooth surfaces and were uniform. The observed roughness of the order of 0.5 to 1.0 nm, could be the result of the surface conditions of the substrates used. Thus it may be concluded that these Ge films were amorphous, uniform and had smooth surfaces.

5.5 STUDY OF OPTICAL PROPERTIES OF Ge FILMS IN THE WAVELENGTH RANGE 700 - 300 nm BY THE USE OF TOMLIN'S METHOD

The optical properties of Ge films were determined from the measured reflectances R and R_1 (Chapter 3) in the spectral range 700 - 300 nm, using Tomlin's method (with and without modifications, discussed in Chapter 3). The overlying film of either Ta_2O_5 or ZnS or ZrO_2 was used. The procedure adopted in doing so is outlined below.

5.5.1 REFLECTIVTIES OF ANNEALED AND UNANNEALED Ge FILMS

The Ge films were deposited simultaneously on two quartz substrates in vacuum. The films were of thicknesses greater than 250 nm, such that the transmittance of these for the wavelengths below 700 nm was less than

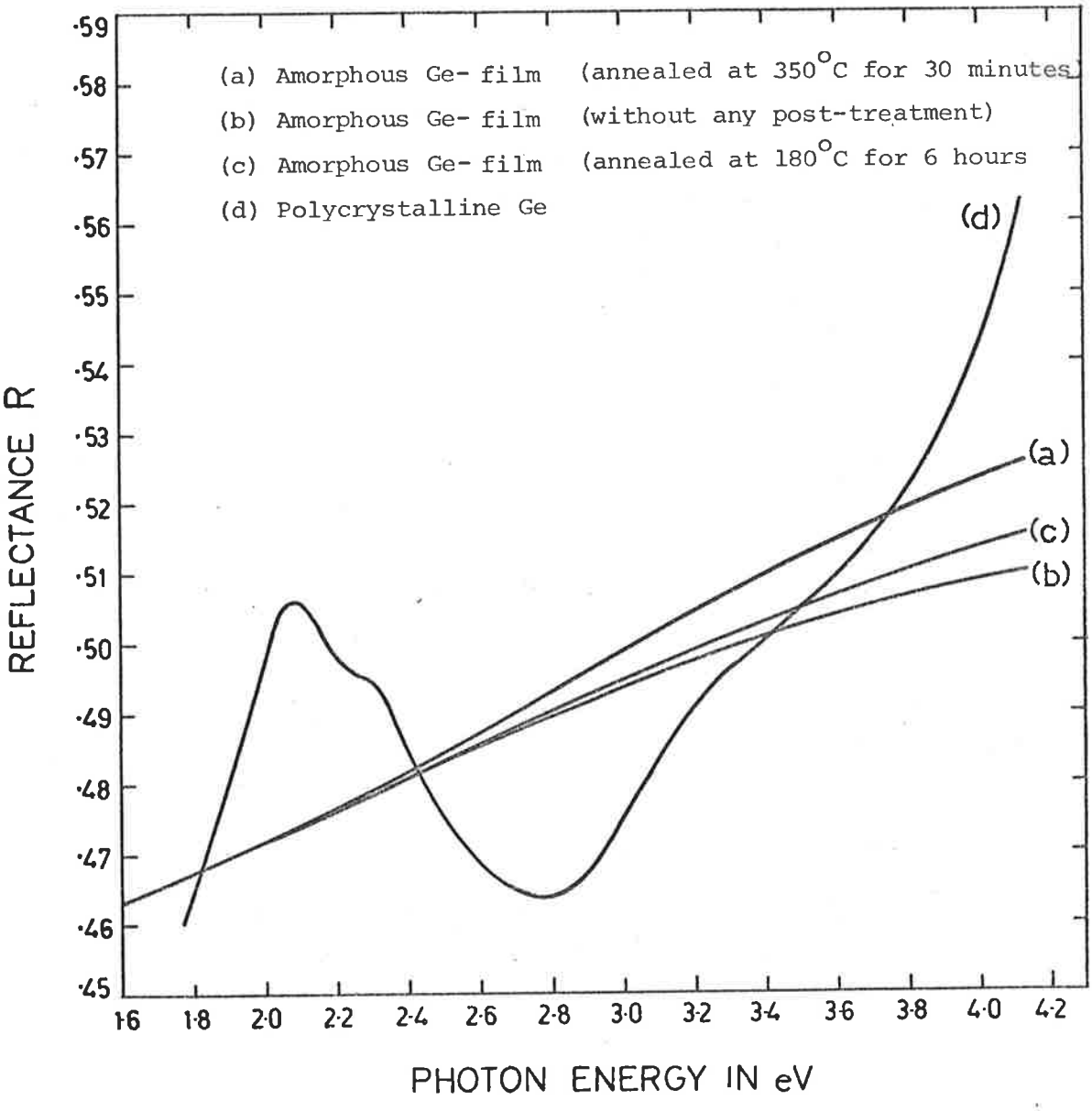
(a) Amorphous Ge- film (annealed at 350°C for 30 minutes)
(b) Amorphous Ge- film (without any post-treatment)
(c) Amorphous Ge- film (annealed at 180°C for 6 hours
(d) Polycrystalline Ge
(d)
(a)
(c)
(b)
REFLECTANCE R
·59
·58
·57
·56
·55
·54
·53
·52
·51
·50
·49
·48
·47
·46
·45
1·6
1·8
2·0
2·2
2·4
2·6
2·8
3·0
3·2
3·4
3·6
3·8
4·0
4·2
PHOTON ENERGY IN eV

FIGURE 5·3

1%. These two films were then exposed to the atmosphere. The first of them was used to measure the reflectance (R) of Ge, and on the second film a dielectric layer was put and the resulting reflectance R_1 was measured (Chapter 3).

During deposition of Ta_2O_5 (see Chapter 4) over the second Ge film, the temperature of the Ge film arose to about 350°C. The duration of the deposition was about 20 - 40 minutes. In order to ensure similar properties of the two Ge films, the first Ge film was annealed in vacuum for about 30 minutes. Then the reflectivities of the annealed Ge film (R) and of Ta_2O_5 over Ge (R_1) were measured. A continuous curve marked (a) in Figure 5.3 shows the values of the reflectances averaged for five films which had been prepared in the same way, plotted against photon energy. The observed variation in R from film to film was less than 0.005.

When ZrO_2 was deposited over the second Ge film, the temperature of the Ge film did not show any appreciable rise. Therefore the first Ge film was not treated any further. The reflectivity (R) of such Ge films is presented by the curve marked (b) shown in Figure 5.3.

To obtain visibly uniform films of ZnS over Ge, the ZnS was deposited in vacuum on Ge-quartz substrates, which were heated to a temperature of 180°C for about 6 hours in vacuum (to ensure uniform heating). This required annealing of the uncoated Ge films in vacuum for the same temperature and time, to ensure that the two Ge films had similar properties. The curve marked (c) in Figure 5.3 shows the measured reflectivity (R) of such films.

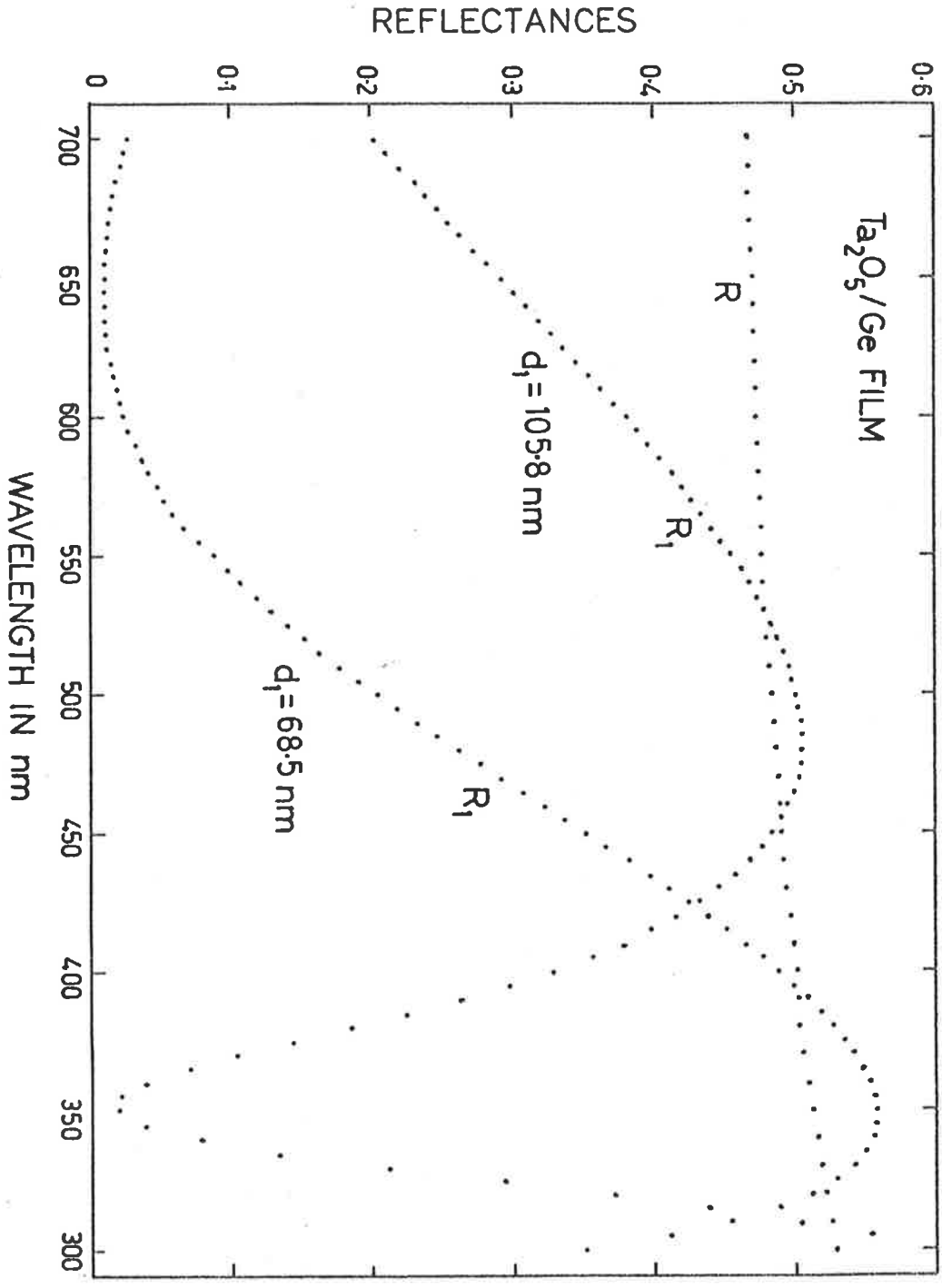
REFLECTANCES
0
0·1
0·2
0·3
0·4
0·5
0·6
700
650
600
550
500
450
400
350
300
WAVELENGTH IN nm
Ta_2O_5/Ge FILM
R
R_1
d_1= 105·8 nm
R_1
d_1= 68·5 nm

FIGURE 5·4

5.5.2 OPTICAL CONSTANTS OF AMORPHOUS Ge FILMS (WHEN OVERLYING LAYER WAS OF Ta_2O_5)

The measured normal incidence reflectances, R from a Ge film and R_1 from a Ta_2O_5 film of thickness of 105.8 nm on the Ge film, are shown in Figure 5.4. The measurements were made in the spectral range 700 - 300 nm at an interval of 5 nm.

From the above values of R and R_1, the optical constants (n_2 and k_2) of Ge films were derived by the method described in Section 3.3.2. The values of the refractive index (n_1) of Ta_2O_5 films at different wavelengths, are listed in Appendix D. n_2 and k_2 were calculated initially for an approximate value of the thickness d_1 of the Ta_2O_5 film (Section 3.6) which was then adjusted in an attempt to obtain a continuous dispersion curve (Section 3.5). Figures 5.5.a and 5.5.b show the result of such a calculation. The dispersion curve shows a proper continuity (Section 3.4). The error bars shown, were calculated by the method outlined in Section 3.7. In the vicinity of $\gamma_1 = p\pi$, they are very large. The uncertainty in this region can be avoided by applying an overlying film of different thickness which shifts the spectral position of the point where $\gamma_1 = p\pi$. For example, in Figure 5.4 is also shown the measured R_1 from a Ta_2O_5 film, of thickness 68.5 nm on Ge and the corresponding dispersion curve, obtained from these results, is shown in Figure 5.6. Thus the spectral shift of the position of the point ($\gamma_1 = p\pi$) can be seen from Figures 5.5.a and 5.6. The points shown by (x) in Figure 5.5.a represents solutions obtained from another Ta_2O_5-Ge-substrate system, where Ta_2O_5 film was 68.5 nm thick (Figures 5.4 and 5.6).

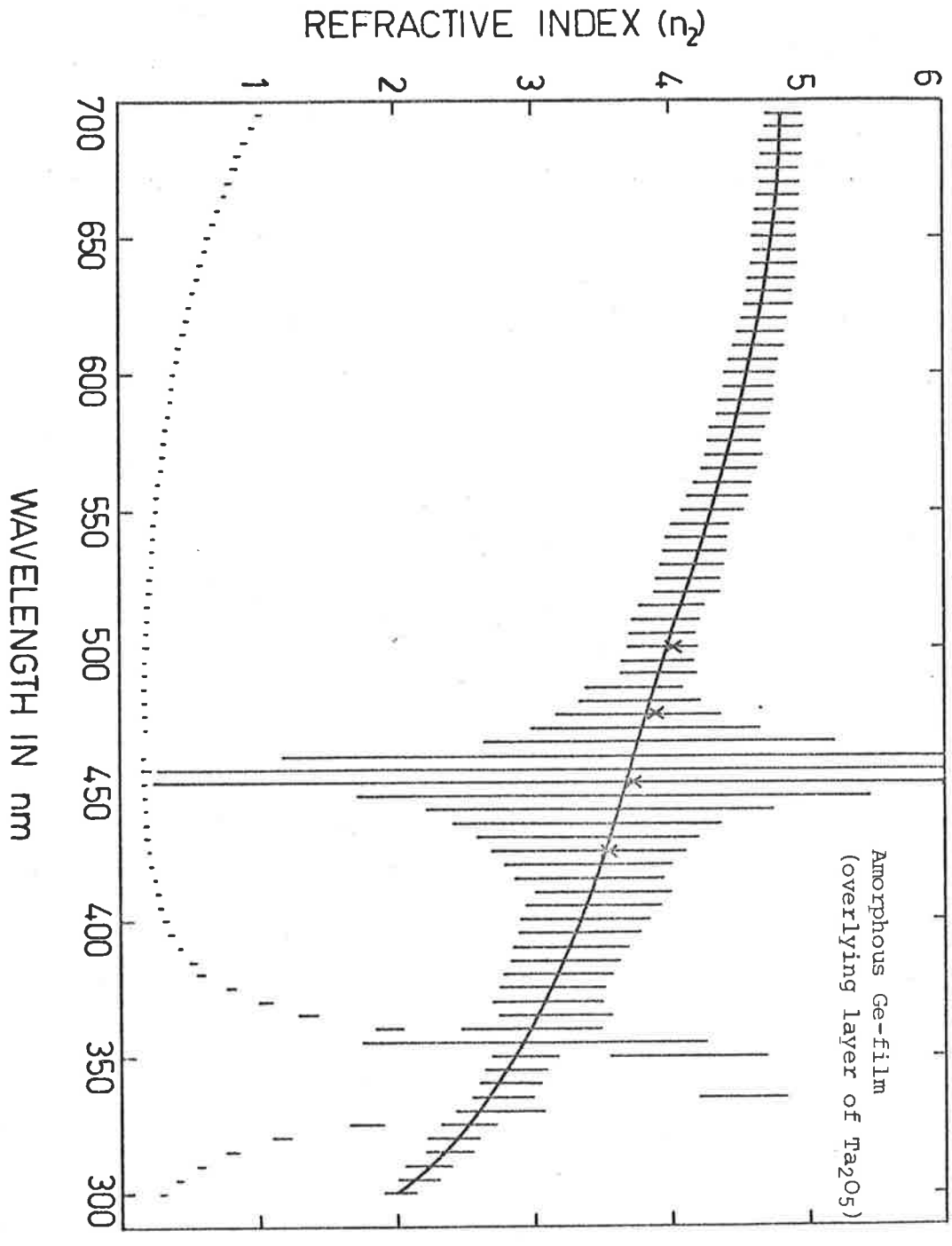
REFRACTIVE INDEX (n_2)
1
2
3
4
5
6
WAVELENGTH IN nm
700
650
600
550
500
450
400
350
300
Amorphous Ge-film
(overlying layer of Ta_2O_5)

FIGURE 5·5a

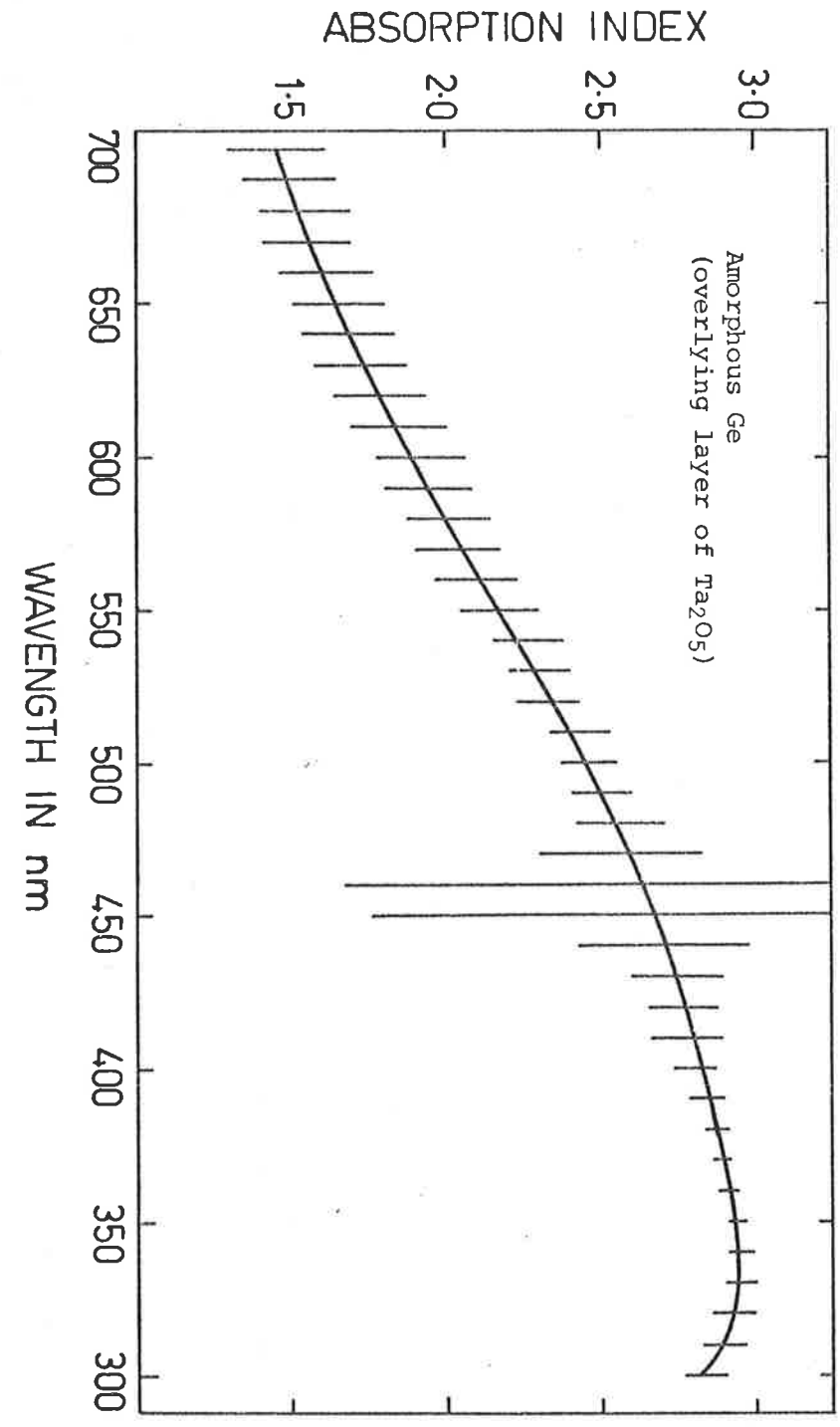
ABSORPTION INDEX
1·5
2·0
2·5
3·0
700
650
600
550
500
450
400
350
300
WAVENGTH IN nm
Amorphous Ge
(overlying layer of Ta_2O_5)

FIGURE 5·5b

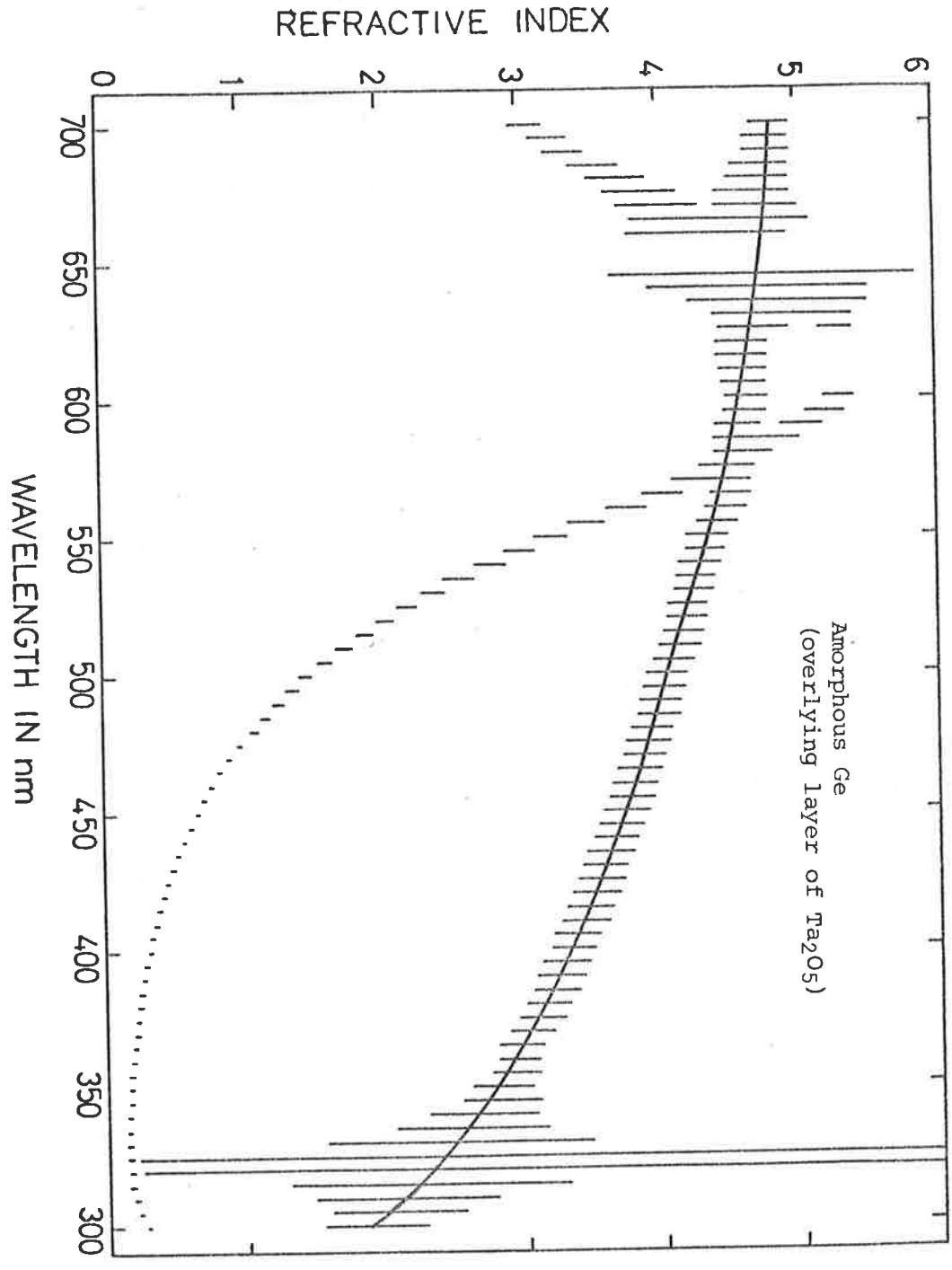
REFRACTIVE INDEX
0
1
2
3
4
5
6
WAVELENGTH IN nm
700
650
600
550
500
450
400
350
300
Amorphous Ge
(overlying layer of Ta2O5)

FIGURE 5·6

5.5.3 THE THICKNESS OF AN OVERLYING FILM DETERMINED FROM R AND R_1 DATA

The quoted thickness of 105.8 nm (Figure 5.4) of the overlying film of Ta_2O_5, was determined by the method, discussed in Section 3.5, in which an attempt was made to obtain a proper continuous dispersion curve.

The thickness d_1 can also be found from the condition (Section 3.6) that $R = R_1$ when

$$\gamma_1 = \frac{2\pi n_1 d_1}{\lambda} = p\pi$$

It is seen from Figure 5.4 that $R = R_1$ for $\lambda = 455$ nm. Knowing $p = 1$ (Section 3.6) and $n_1 = 2.146$ (Appendix D), a thickness equal to 106 nm was calculated from the above equation. Thus it can be seen that the values of film thickness, determined by two different methods, are in very good agreement. From the other plot of R_1, shown in Figure 5.4, the values of thickness (68.5 nm), determined by the two methods were almost the same. This is only applicable when the surfaces, of the specimen and the overlying film, are smooth (as was the case in the examples above). A case where the overlying film had rough surface will be considered later.

5.5.4 OPTICAL PROPERTIES OF AMORPHOUS Ge FILMS USING OVERLYING LAYER OF ZnS

The measured normal incidence reflectances, R from a Ge film and R_1 (curve marked 'a') from a ZnS film, of thickness of about 126 nm on the Ge film, are shown in Figure 5.7. At first the optical constants of Ge (n_2 and k_2) were calculated from the above R and R_1 data, using the formulae for R and R_1 for a single film on a specimen (Section 3.10). Beginning with an approximate thickness of ZnS film obtained by the method discussed in Section 3.6, this was then adjusted in an attempt to

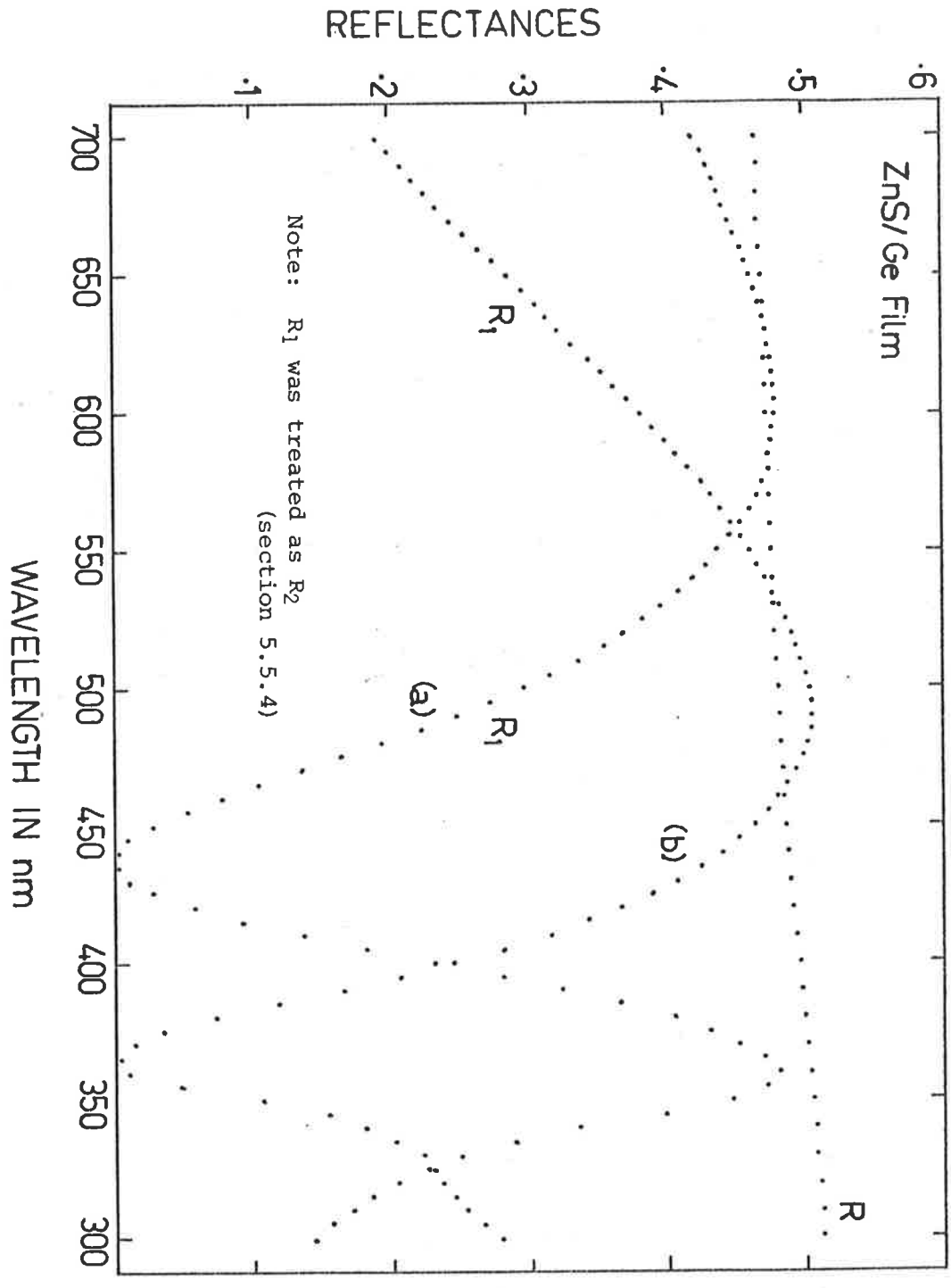
REFLECTANCES
.1
.2
.3
.4
.5
.6
ZnS/Ge Film
R
R1
R1
(a)
(b)
Note: R1 was treated as R2
(section 5.5.4)
700
650
600
550
500
450
400
350
300
WAVELENGTH IN nm

FIGURE 5·7

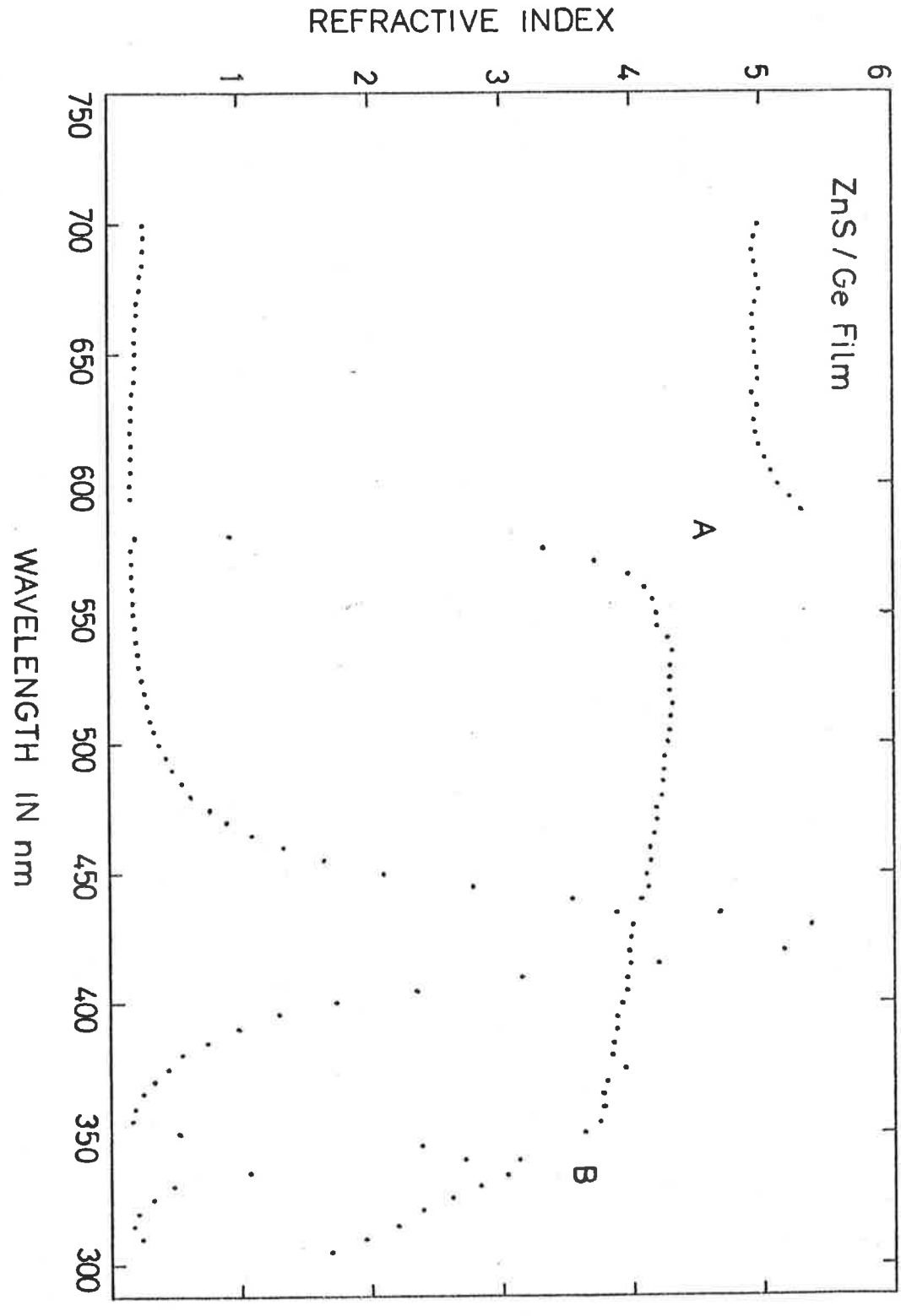
REFRACTIVE INDEX
1
2
3
4
5
6
ZnS / Ge Film
A
B
WAVELENGTH IN nm
750
700
650
600
550
500
450
400
350
300

FIGURE 5·8

obtain a continuous dispersion curve (Section 3.10.2). For the optical constants (n_1, k_1) of ZnS films see Chapter 6. Figure 5.8 shows the result of such calculations based on the data R and R_1, mentioned above, and is typical of the results for some eight different systems of ZnS/Ge, in which the ZnS films varied in thickness from 80 to 150 nm. It shows that no choice of thickness of overlying film (ZnS) was possible for which the proper continuity of the dispersion curve over the whole range of wavelengths could be achieved. In the light of the discussion of Section 3.10.2 it shows that the chosen thickness was small for closure at A (Figure 5.8) and large for closure at B. No variation of film thickness improved this situation.

It was concluded that the measured values of R_1 were not those appropriate to a perfectly plane parallel uniform film such as is assumed for the derivation of the formula for R_1. This was to be expected from the study of the optical constants of ZnS films on amorphous quartz substrates as described in Chapter 6, where it will be shown that the ZnS films had rough surfaces.

In accordance with the discussion, which follows in Chapter 6, the present case of a rough ZnS film on Ge was treated as a smooth equivalent surface layer (with optical constants n_1 and k_1) on a smooth ZnS film (n_2, k_2) which rested on Ge (n_3, k_3). Then the measured reflectance becomes R_2, the reflectance from a double layer on a substrate, and use of the method outlined in Sections 3.12 and 3.13 could be made in order to determine n_3 and k_3. Thus the results shown in Figures 5.9.a and 5.9.b were obtained from the data shown in Figure 5.7 for d_1 = 8 nm and

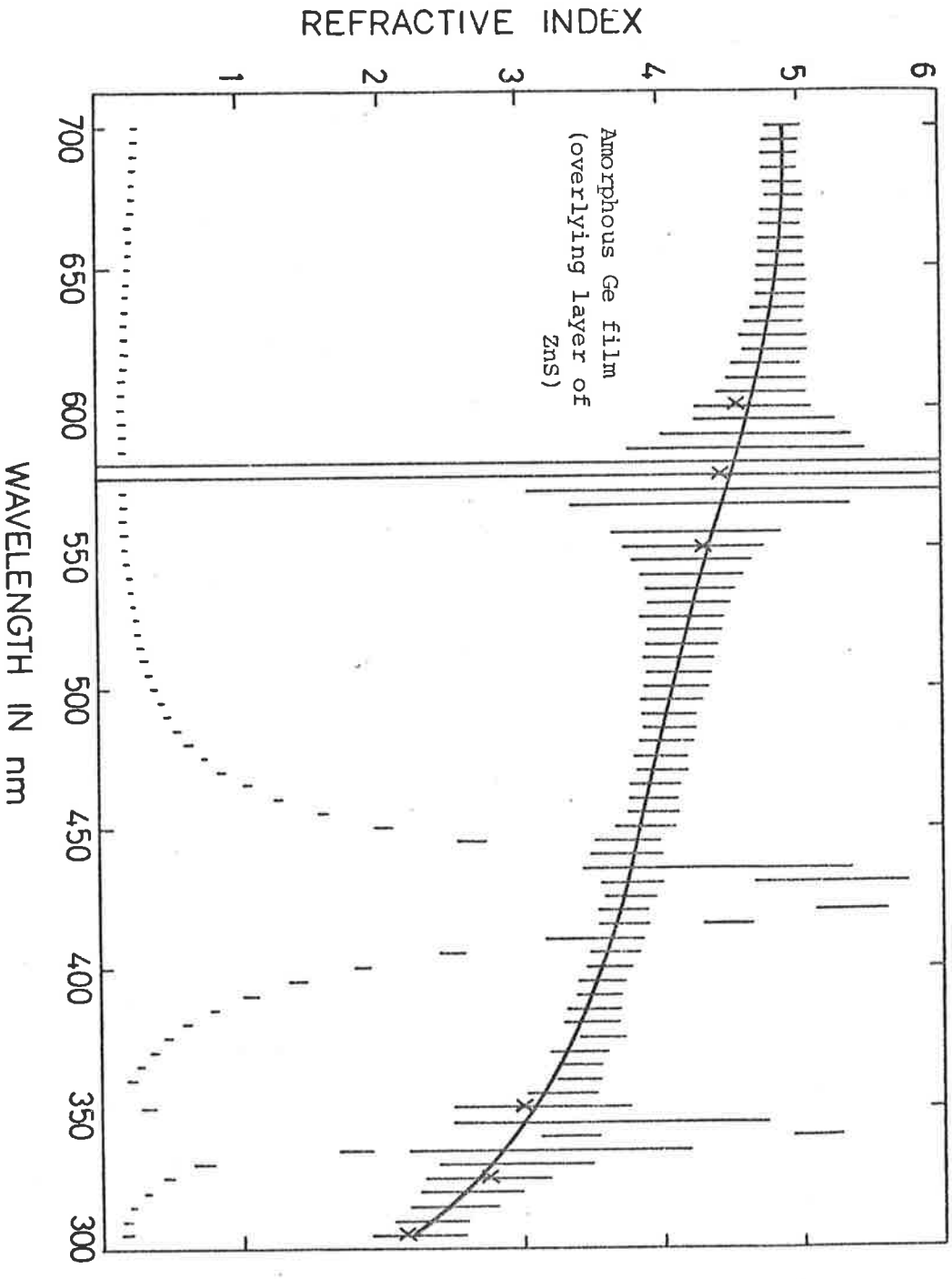
REFRACTIVE INDEX
1
2
3
4
5
6
Amorphous Ge film
(overlying layer of
ZnS)
700
650
600
550
500
450
400
350
300
WAVELENGTH IN nm

FIGURE 5·9a

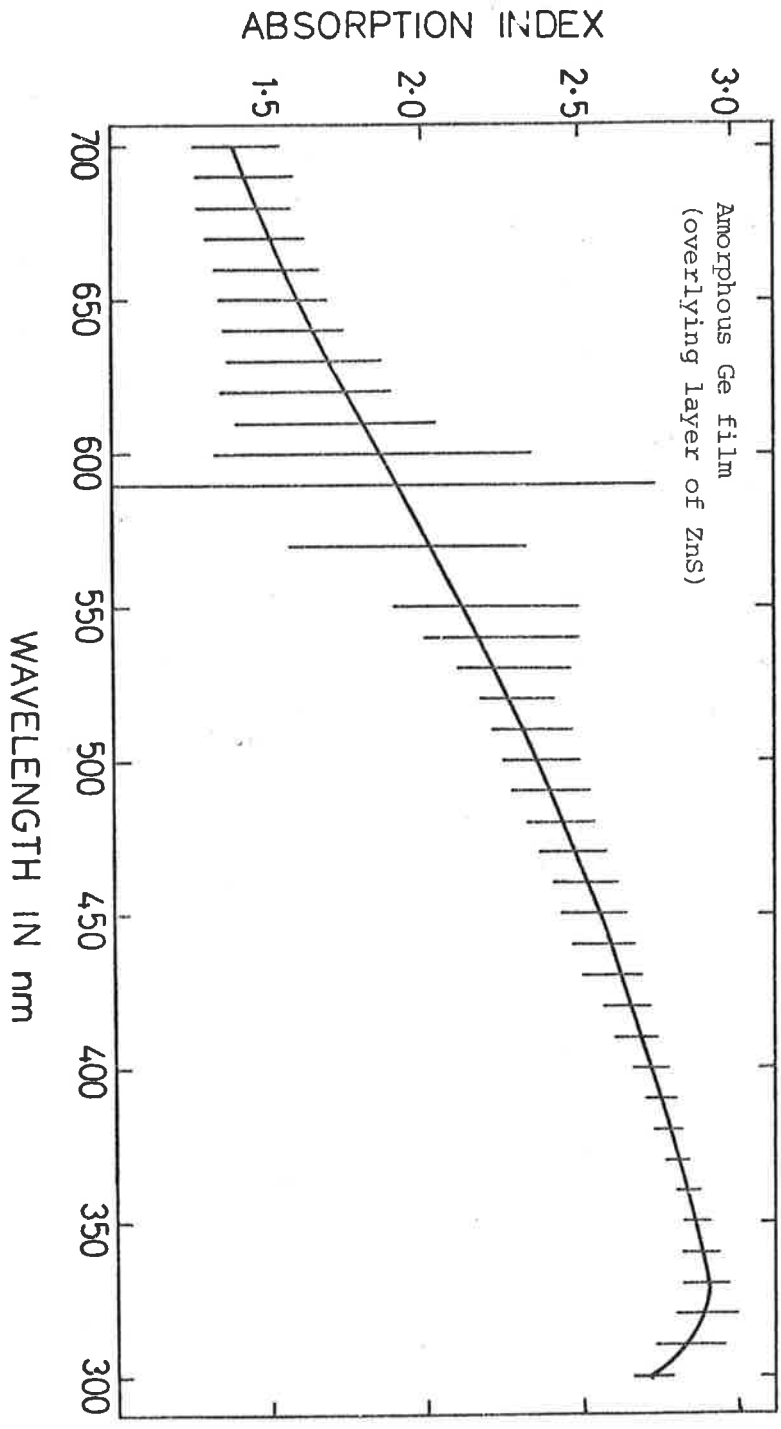
ABSORPTION INDEX
1·5
2·0
2·5
3·0
Amorphous Ge film
(overlying layer of ZnS)
700
650
600
550
500
450
400
350
300
WAVELENGTH IN nm

FIGURE 5·9b

d_2 = 122.8 nm. The procedure adopted in determining d_1 and d_2 is outlined in the following section. It may be mentioned that the structure and surface conditions of ZnS films on amorphous Ge may be expected to be the same as those of ZnS films on amorphous quartz. On this assumption the optical constants used for ZnS films (n_2, k_2) and their equivalent surface layers (n_1, k_1) were those from Chapter 6.

Also in Figure 5.7 is shown a reflectivity (R_1) curve (b), obtained from another ZnS/Ge system. The corresponding dispersion curve obtained from this data is shown in Figure 5.10. The dispersion curve was obtained for d_1 = 6 nm and d_2 = 94 nm. It may be seen that the use of ZnS films of different thicknesses shifts the point $\gamma_1 = p\pi$ (corresponding to large errors) to different spectral positions. Use of this was made in order to determine reliable optical constants of Ge films. The points (x) shown in Figure 5.9.a represent the solutions obtained from Figure 5.10.

5.5.5 DETERMINATION OF THICKNESSES d_1 AND d_2 IN A DOUBLE LAYER SYSTEM

The thicknesses d_1 and d_2 of the two layers on a substrate were determined by a method, described below, which is slightly different from one that was used by Denton et al (1972).

In the case of a transparent double layer on an absorbing substrate (Section 3.14), when the first layer is very thin so that $2\gamma_1 = 4\pi n_1 d_1/\lambda$ is a small angle, then $\sin 2\gamma_1 \simeq 2\gamma_1$ and $\cos 2\gamma_1 \simeq 1$. For such a condition, the following relation can be obtained from equation 3.14.1.

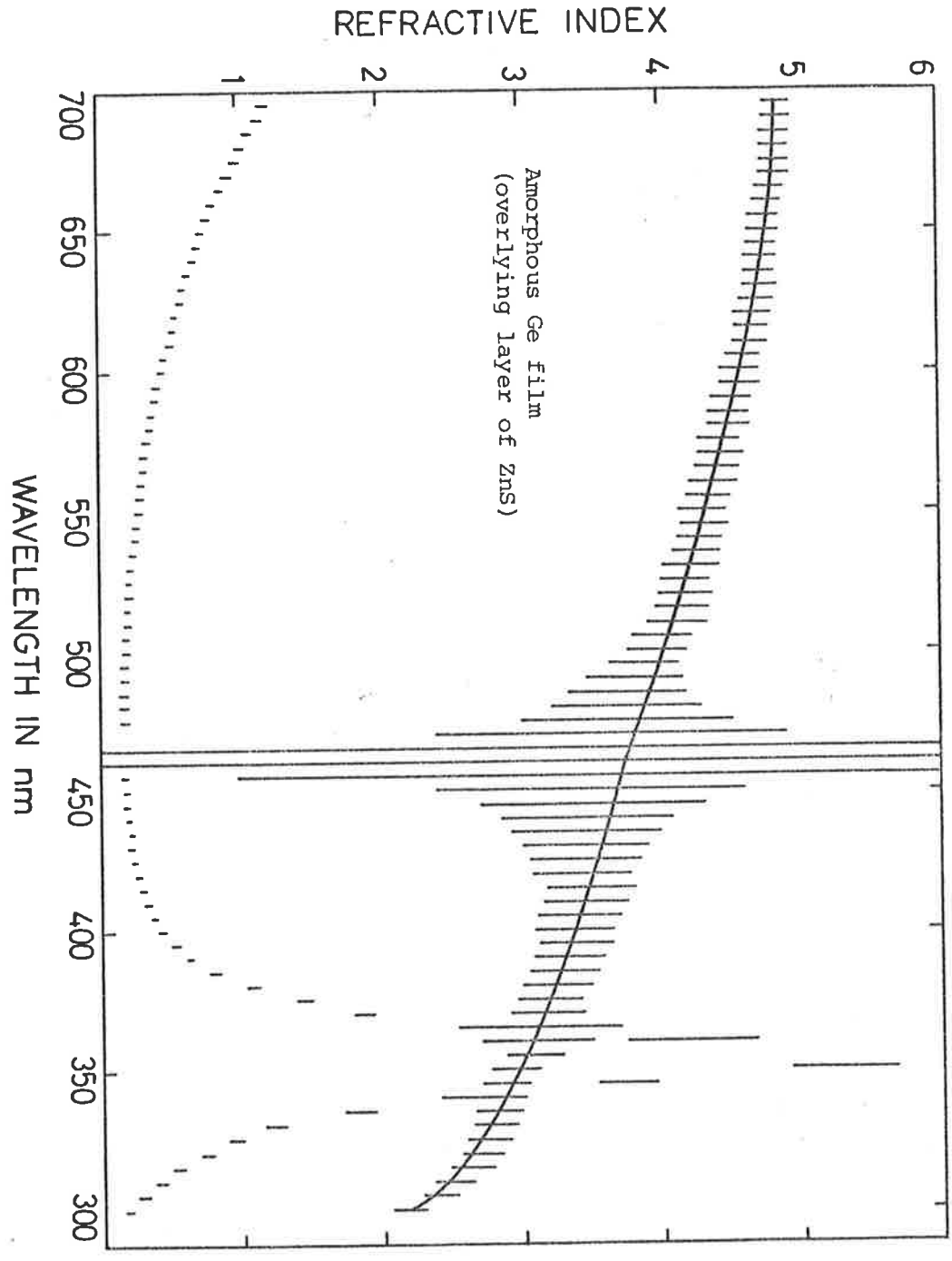
REFRACTIVE INDEX
1
2
3
4
5
6
Amorphous Ge film
(overlying layer of ZnS)
WAVELENGTH IN nm
700
650
600
550
500
450
400
350
300

FIGURE 5·10

$$\frac{1+R_2}{1-R_2} = \frac{1}{4n_0n_2^2n_3}\{(n_0^2+n_2^2)(n_2^2+n_3^2+k_3^2)$$

$$+ (n_0^2-n_2^2)B - \frac{4\pi d_1}{\lambda}(n_0^2-n_1^2)n_2D\} \qquad 5.5.1$$

where

$$B = (n_2^2-n_3^2-k_3^2)\cos 2\gamma_2 + 2n_2k_3 \sin 2\gamma_2$$

and

$$D = (n_2^2-n_3^2-k_3^2)\sin 2\gamma_2 - 2n_2k_3 \sin 2\gamma_2$$

For $d_1 = 0$, the above formula becomes that for a single film of refractive index n_2 on a substrate of complex refractive index n_3-ik_3 (Section 3.2).

Consider a double layer, and also a single layer of the second material the thickness of which has been increased by a small amount d_o, as shown in Figure 5.11. For the first case $\frac{1+R_2}{1-R_2}$ is given by equation 5.5.1 and for the second case $\frac{1+R_1}{1-R_1}$ is given by (Section 3.2).

$$\frac{1+R_1}{1-R_1} = \frac{1}{4n_0n_2^2n_3}\left[(n_0^2+n_2^2)(n_2^2+n_3^2+k_3^2)\right.$$

$$\left. + (n_0^2-n_2^2)\{(n_2^2-n_3^2-k_3^2)\cos 2(\gamma_2+\gamma_0)+2n_2k_3\sin 2(\gamma_2+\gamma_0)\}\right] \qquad 5.5.2$$

Here $\gamma_0 = \frac{2\pi n_2 d_0}{\lambda}$ and if this is small enough equation 5.5.2 may be written as

$$\frac{1+R_1}{1-R_1} = \frac{1}{4n_0n_2^2n_3}\{(n_0^2+n_2^2)(n_2^2+n_3^2+k_3^2)$$

$$+ (n_0^2-n_2^2)B - \frac{4\pi d_0}{\lambda}(n_0^2-n_2^2)n_2D\} \qquad 5.5.3$$

The two systems will be equivalent if $\frac{1+R_2}{1-R_2} = \frac{1+R_1}{1-R_1}$ for all λ, which will be the case if

$$d_o = \frac{n_1^2-n_o^2}{n_2^2-n_o^2}\, d_1 \qquad 5.5.4$$

The above treatment is similar to the one given by Tomlin (1972a) except that $\frac{1+R_1}{1-R_1}$ is used in place of Tomlin's $\frac{1+R_1}{T_1}$.

The condition found for a single film on an absorbing substrate that $R = R_1$ when $\gamma_1 = p\pi$, can now be replaced for a double layer film, provided the films are non-absorbing and the first layer is very thin, by the condition $R = R_2$ when

$$\gamma_2 + \gamma_o = p\pi \qquad 5.5.5$$

when R is the reflectance from the substrate given by

$$R = \frac{(n_3-1)^2 + k_3^2}{(n_3+1)^2 + k_3^2}$$

Hence the equivalent single film thickness ($d = d_o+d_2$) of the double layer can be determined. Using this as an initial value for d_2 in the two-layer equations, d_1 was increased from zero, and d_2 correspondingly diminished to keep d constant, until completion of the dispersion curve could be achieved. With some experience completion of the dispersion curve could be obtained in about five or six steps.

For example in Figure 5.7 (ZnS/Ge) $R_2 = R$ for a wavelength of 580 nm (curve (a)) giving d = 126 nm. The continuous dispersion curve (Figure 5.9.a) was obtained from the above results for $d_1 = 8$ nm and $d_2 = 122.8$ nm. For the used $n_o = 1$, $n_1 = 1.613$ and $n_2 = 2.30$ and $d_1 = 8$ nm, d_o was calculated from equation 5.5.4 to be 3 nm. Thus $d = d_2 + d_o = 125.8$ nm was close to 126 nm.

It may be noted that ZnS films were transparent for $\lambda = 580$ nm. Also for $d_1 = 8$ nm, $2\gamma_1$ was small (= 0.279 radians) so that the above conditions hold.

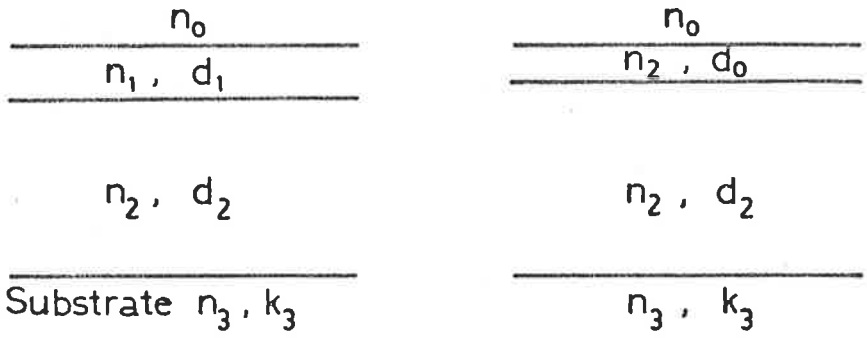

FIGURE 5·11

A double layer on a substrate, and a possible equivalent single layer on the substrate.

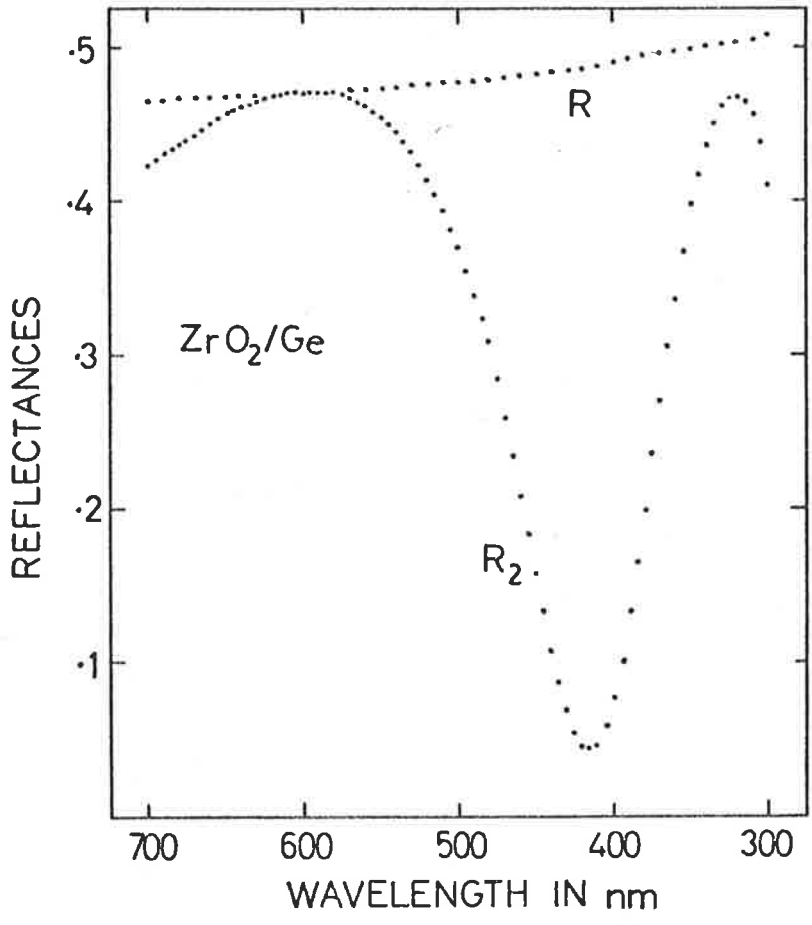

FIGURE 5·12

5.5.6 THE OPTICAL PROPERTIES OF AMORPHOUS Ge FILMS USING AN OVERLYING LAYER OF ZrO_2

When ZrO_2 was used as an overlying layer on the amorphous Ge film, a continuous dispersion curve could not be obtained by the use of the relation for the reflectance R_1 (Section 3.10), from a single film on the Ge substrate. As in the case of the overlying film of ZnS (Section 5.5.4), it was necessary to use the procedure outlined in Sections 5.5.4 and 5.5.5. In this way continuous dispersion and absorption curves for Ge films were obtained. The optical constants n_2 and n_1 used for the ZrO_2 film, and its equivalent surface roughness layer, were those from Chapter 4.

Three different ZrO_2/Ge systems, wherein ZrO_2 films varied in thicknesses from 120-160 nm, were studied. In case of two of these systems, proper continuous dispersion and absorption curves were obtained, as was the case for the ZnS/Ge systems. For the third system, whose reflectivity data (R and R_2) are shown in Figure 5.12, a continuous dispersion curve could not be obtained. This was to be attributed to absorption in the ZrO_2 film because near the wavelength λ = 320 nm, where $\gamma = p\pi$, R must be equal to R_2, if the film is transparent, but the curves do not intersect. Similar behaviour, for a ZnS/Ge system, can be seen in Figure 5.7 where R_2 (curve 'a') is smaller than R for λ = 360 nm, corresponding to the point where $\gamma = p\pi$. This is because ZnS is absorbing at this wavelength, as will be shown in Chapter 6.

The observed absorption in this particular film of ZrO_2 was not the property of pure ZrO_2 films, as these were transparent in this spectral region (Chapter 4). This may have been due to different stoichiometry of this film and could have resulted from a dissociation of ZrO_2 material

at the time of evaporation.

5.6 OPTICAL CONSTANTS OF AMORPHOUS Ge FILMS

Figure 5.13 shows the optical constants n and k of the Ge films, thus determined, in the spectral range 2000-300 nm. These are the averaged dispersion and absorption curves from a number of Ge films, with the vertical bars indicating the limits within which the individual curves lay. In the spectral range 600 to 300 nm, the refractive index, of the Ge films deposited at room temperature, was higher than that of those annealed at 180^{o}C, which in turn was higher than that of those annealed at 350^{o}C. The absorption index followed the opposite. All these values fell within the limit of the bars shown in Figure 5.13.

The real part of the dielectric constant $\varepsilon_1 = n^2-k^2$ and its imaginary part $\varepsilon_2 = 2nk$ are plotted in Figures 5.17 and 5.18 respectively. These plots are based on the results shown in Figure 5.13 and will be discussed later.

5.7 PREVIOUS WORK ON THE OPTICAL PROPERTIES OF Ge FILMS

The optical properties of Ge films have been studied by a large number of workers, e.g. O'Bryan (1936), Brattain and Briggs (1949), Lukes (1960), Grant and Paul (1964), Tauc et al (1964, 1969), Wales et al (1967), Clark (1967), Theye (1970, 1971), Donovan et al (1970), Bauer and Galeemer (1972) and Connell et al (1973). There is a large variation in the optical constants, published in the above references.

The general shapes of the dispersion, absorption, $\varepsilon_1 = n^2-k^2$ and $\varepsilon_2 = 2nk$ curves, in the present work, are in agreement with the

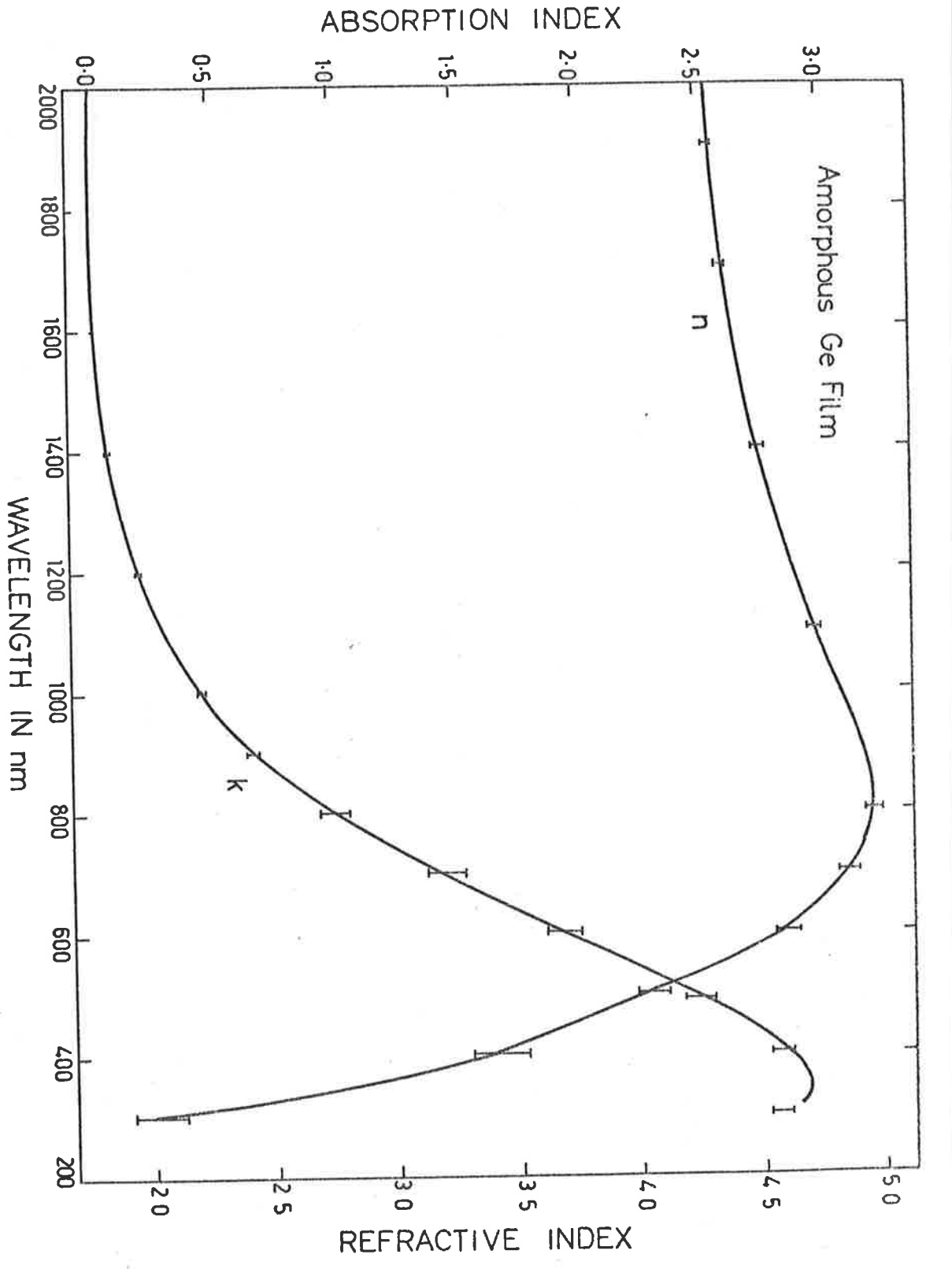
ABSORPTION INDEX
0·0
0·5
1·0
1·5
2·0
2·5
3·0
Amorphous Ge Film
n
k
WAVELENGTH IN nm
2000
1800
1600
1400
1200
1000
800
600
400
200
REFRACTIVE INDEX
2·0
2·5
3·0
3·5
4·0
4·5
5·0

FIGURE 5·13

corresponding results of Tauc et al, Donovan et al and Connel et al.

The indices of refraction and absorption, given by Brattain and Briggs, are in reasonable agreement with those of the present work, in the spectral range 2000-600 nm, but at shorter wavelengths, although the absorption is in agreement, their refractive index is lower than that shown in Figure 5.13.

The results, of Donovan et al, in the spectral range 2000-700 nm, determined from the measured normal incidence reflectance and transmittance, are in a good agreement with those shown in Figure 5.13. For wavelengths smaller than 700 nm the two results are not in good agreement. This may be due to the fact that they used Kramers-Kronig analysis of their reflectivity data to determine n and k for wavelengths less than 700 nm, and the optical constants determined by this method are dependent on the choice of the two extrapolations involved (Section 1.3.2).

The results (n, k, ε_1 and ε_2) of the present work are in reasonable agreement, in the whole wavelength region covered, with those of Connell et al (1973). It may be mentioned that the results of Connell et al were determined from 0.05 to 4.5 eV by a combination of reflectance, transmittance and ellipsometric measurements.

5.8 DETERMINATION OF THE OPTICAL CONSTANTS OF POLYCRYSTALLINE Ge IN BULK FORM

5.8.1 PREPARATION OF SAMPLE

Two flat pieces, each of dimensions 2.5 x 3.75 cm and of thickness 2 mm, were cut by a diamond saw from a piece of high purity polycrystalline germanium. The polycrystalline Ge sample was supplied by Rofin Ltd.,

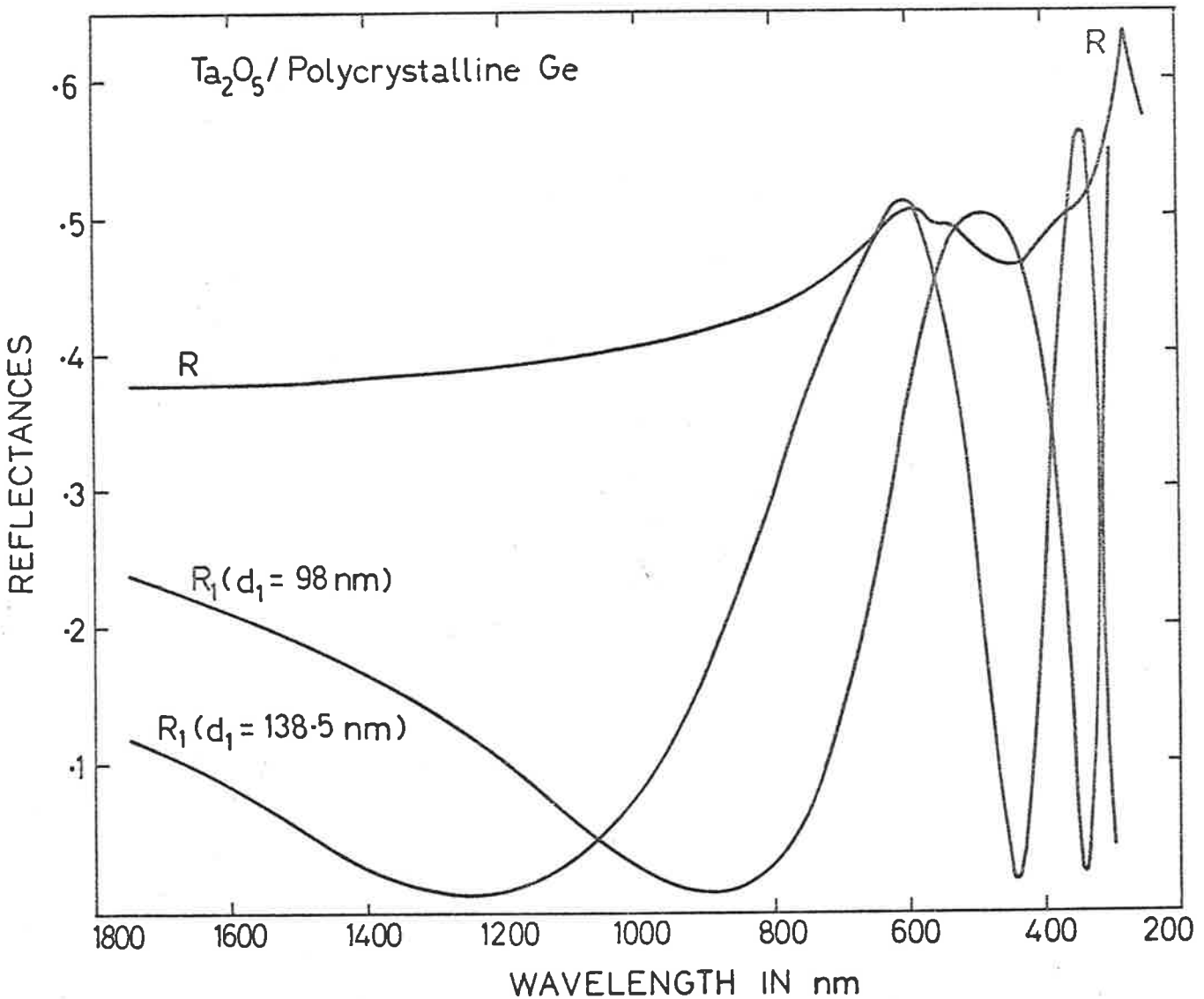
Ta_2O_5/ Polycrystalline Ge
R
R
R_1 (d_1 = 98 nm)
R_1 (d_1 = 138·5 nm)
REFLECTANCES
·6
·5
·4
·3
·2
·1
1800
1600
1400
1200
1000
800
600
400
200
WAVELENGTH IN nm

FIGURE 5·14

England. The faces of these flat pieces were ground with successively finer grades of diamond abrasive, and then optically polished with aluminium oxide polishing powder on a beeswap lap. Thus four polished surfaces were obtained.

5.8.2 MEASUREMENTS

The optical constants of such Ge specimens were determined using Tomlin's method (Section 3.2). The required measurements were carried out as follows:

The normal incidence reflectance (R), from the optically polished faces, was measured in the spectral range 1750-250 nm. Figures 5.3 and 5.14 show the averaged reflectance for the four surfaces as a function of wavelength. The variation in R from face to face was less than 0.004. Then each of the four faces was coated with a thin layer of Ta_2O_5 (these layers varied in thicknesses from 100 to 270 nm). The reflectance (R_1) from these Ta_2O_5 films on Ge was measured in the spectral range 1750-300 nm. For example plots of R_1, obtained for the Ta_2O_5 films of thickness 98 and 138.5 nm, are shown in Figure 5.14. The long wavelength limit of measurements was chosen so that the transmittance of Ge specimen was less than 1%, to eliminate any effects of multiple reflections in it. The lower limit of 300 nm was so chosen because for wavelengths below this Ta_2O_5 was absorbing. Ta_2O_5 was preferred to ZrO_2 (which is transparent down to 255 nm) because Ta_2O_5 films were smooth, uniform and showed consistent optical constants.

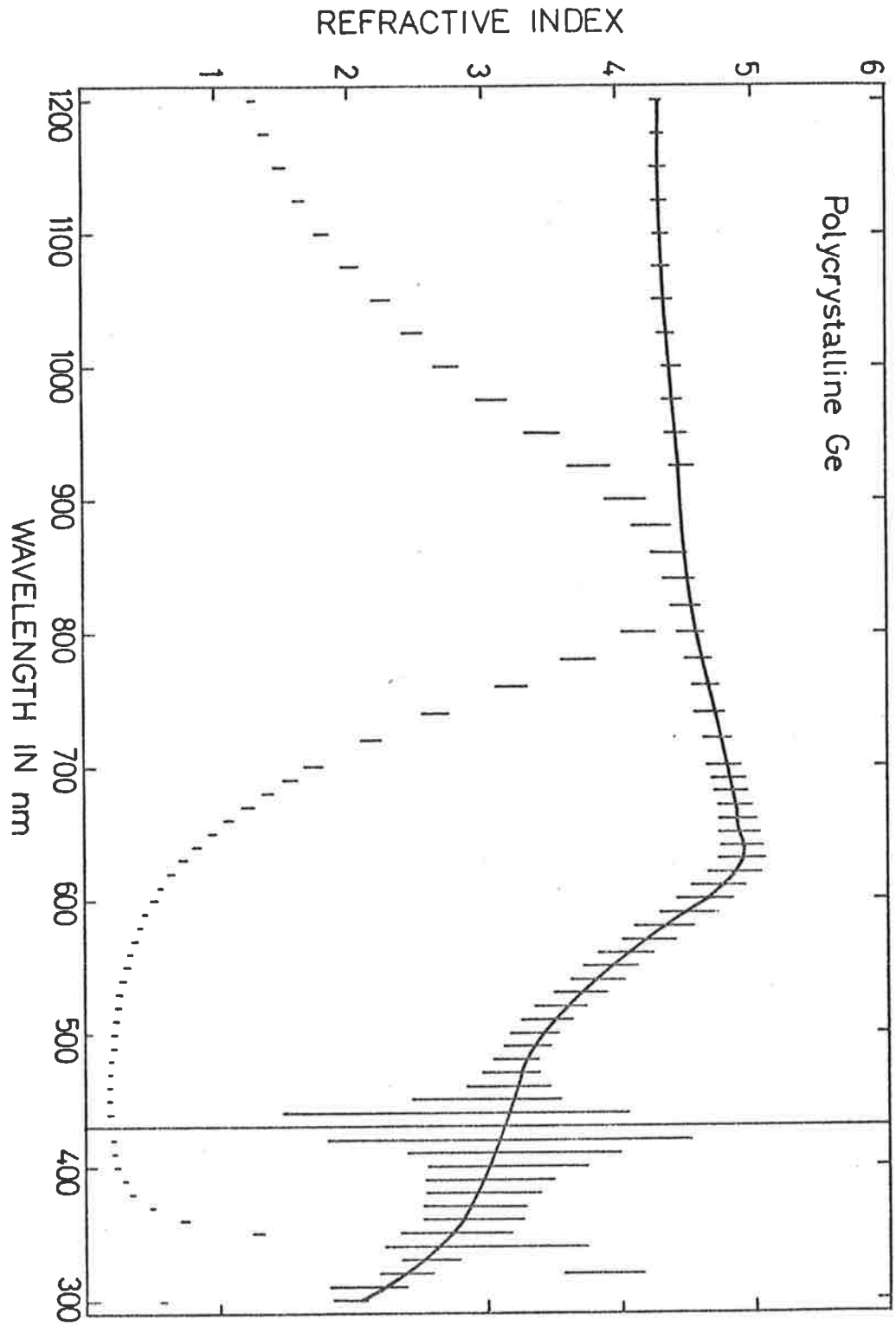
REFRACTIVE INDEX
1
2
3
4
5
6
WAVELENGTH IN nm
1200
1100
1000
900
800
700
600
500
400
300
Polycrystalline Ge

FIGURE 5·15a

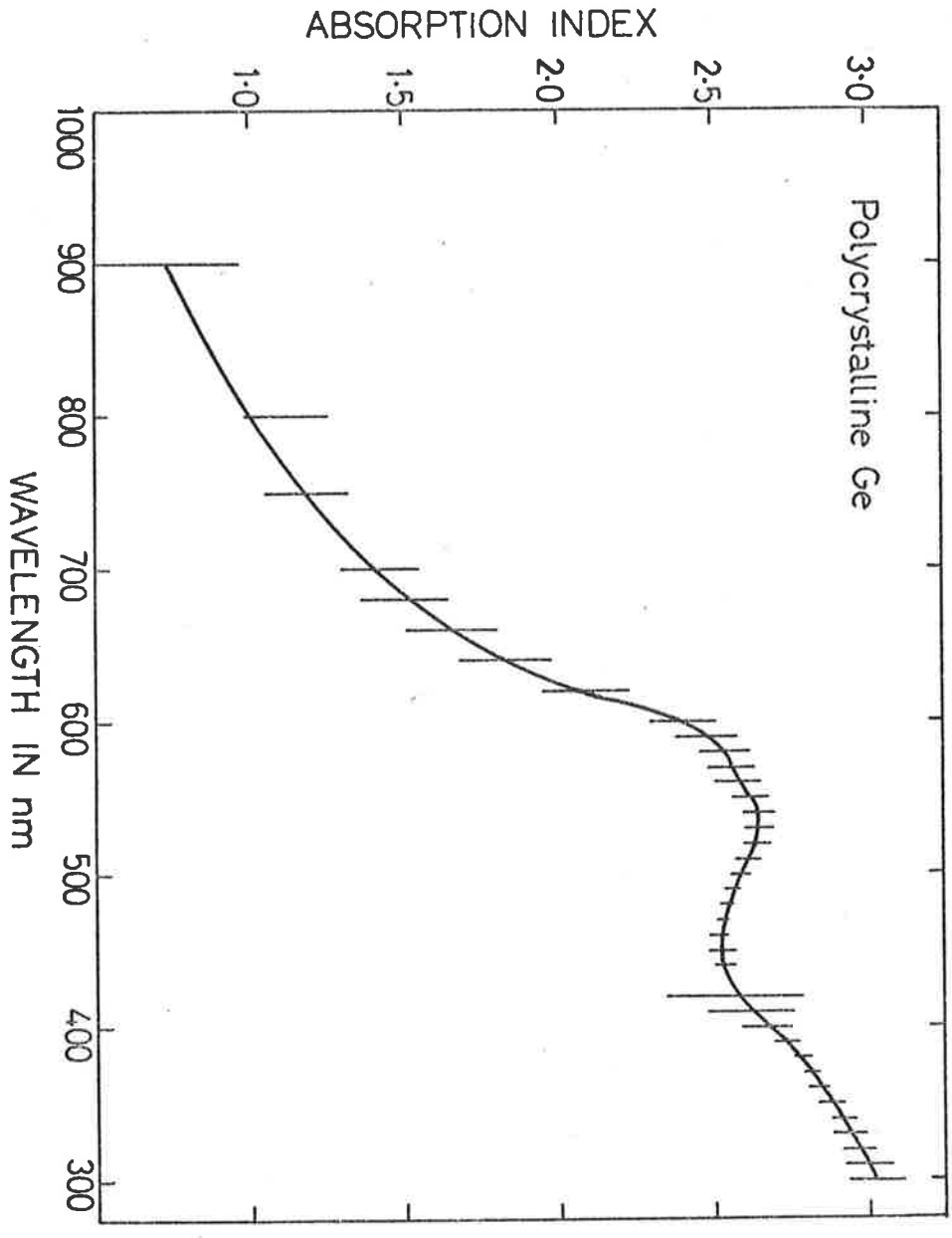
ABSORPTION INDEX
1·0
1·5
2·0
2·5
3·0
Polycrystalline Ge
1000
900
800
700
600
500
400
300
WAVELENGTH IN nm

FIGURE 5·15b

5.8.3 METHOD

From the measured reflectances (R) and (R_1), the optical constants (n_2 and k_2) of the polycrystalline Ge specimen were calculated from the relations given in Section 3.2. Continuous dispersion and absorption curves together with the thickness of the overlying layers were obtained by adopting the procedure outlined in Section 3.5. As an example figures 5.15.a and 5.15.b show the dispersion and absorption curves for Ge, obtained using a Ta_2O_5 film of thickness 98 nm (for R and R_1 data shown in Figure 5.14). Any reliable data on absorption, in the spectral range 1750-900 nm, could not be obtained by this method for the reason discussed in Section 3.15.

5.8.4 OPTICAL CONSTANTS OF POLYCRYSTALLINE Ge

Figure 5.16 shows the optical constants n and k of the polycrystalline Ge, thus determined, in the spectral range 1750-300 nm. These are the averaged dispersion and absorption curves from the four results, with the vertical bars indicating the limits within which the individual curves lay. The real part of the dielectric constant $\varepsilon_1 = n^2-k^2$ and its imaginary part $\varepsilon_2 = 2nk$ are plotted in Figures 5.17 and 5.18 respectively. These plots are based on the results shown in Figure 5.16.

5.9 PREVIOUS WORK ON CRYSTALLINE Ge

Avery and Clegg (1953) have determined the optical constants from a natural crystal face found on a Ge single crystal by analysing the reflectance of poarized radiation from the specimen.

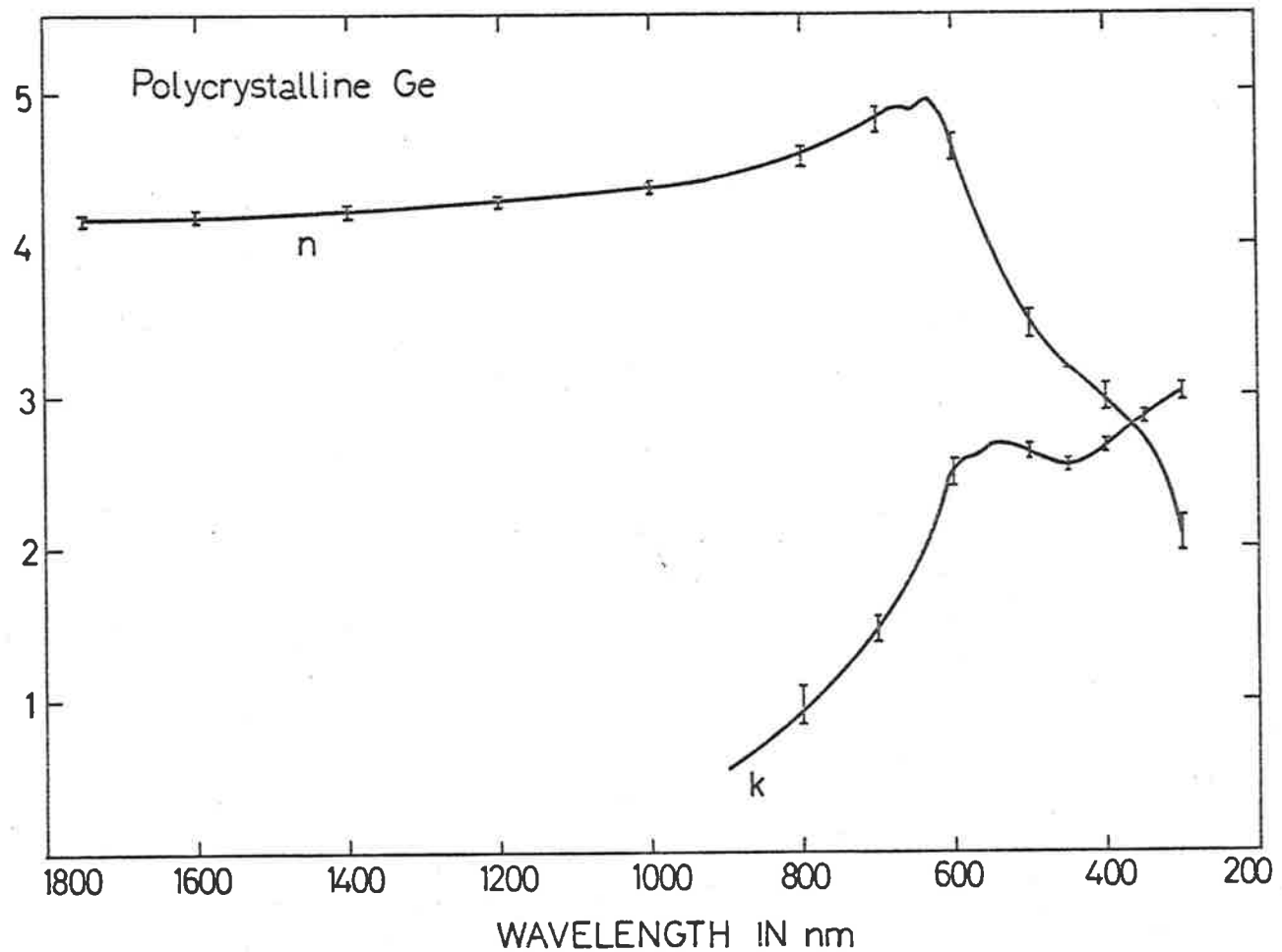
Polycrystalline Ge
n
k
5
4
3
2
1
1800
1600
1400
1200
1000
800
600
400
200
WAVELENGTH IN nm

FIGURE 5·16

Dash and Newman (1955) obtained the absorption coefficient of Ge single crystals from the transmission measurements in the energy region from 0.6 to 2.0 eV. Macfarlane et al (1957) have determined absorption in the range from 0.6 to 0.86 eV, also from transmission measurements.

Archer (1958) from the ellipticity of reflected polarized light and Potter (1966) from measurements based on the pseudo-Brewster angle technique, have determined the optical constants of single crystals of Ge in the spectral regions 1.77 - 3.44 eV and 0.5 - 3 eV, respectively.

The most frequently quoted work on the optical properties of crystalline Ge is that of Philipp and Taft (1959). They determined these constants by using Kramers-Kronig analysis of the measured normal incidence reflectance in the spectral range from 0.6 to 11 eV. For comparison with the present work, their results are shown in Figure 5.19.

5.10 DISCUSSION OF CRYSTALLINE Ge

The reflectivity data from polycrystalline Ge, in the present work, were obtained in the energy range from 0.7 to 5.0 eV. But the optical constants were not calculated beyond 4.13 eV because in the higher energy region the overlying layer of Ta_2O_5 becomes absorbing. In this range the measured reflectivities are practically the same as those given by Philipp and Taft (Figure 5.19), although the peak in the reflectivity data, which occurs at 4.44 eV, is about 5% less for the polycrystalline material. Since the two reflectivities in the remaining region (0.7 to 4.2 eV) are in good agreement this loss cannot be attributed to surface roughness of the specimen, but is probably due to the specimens not having been etched after polishing, as was done by Philipp and Taft.

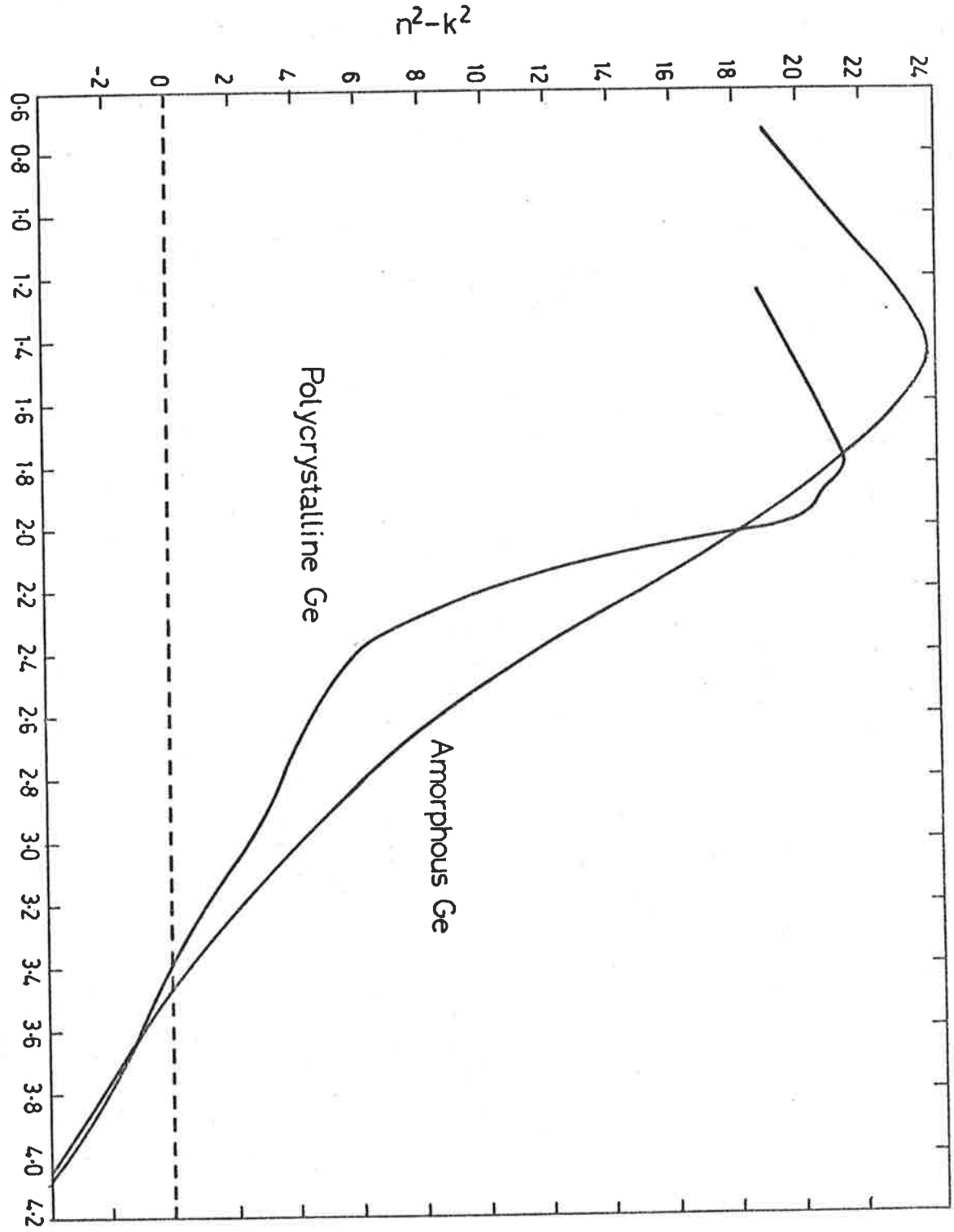
n^2-k^2
-2
0
2
4
6
8
10
12
14
16
18
20
22
24
0·6 0·8 1·0 1·2 1·4 1·6 1·8 2·0 2·2 2·4 2·6 2·8 3·0 3·2 3·4 3·6 3·8 4·0 4·2
PHOTON ENERGY IN eV
Polycrystalline Ge
Amorphous Ge

FIGURE 5 17

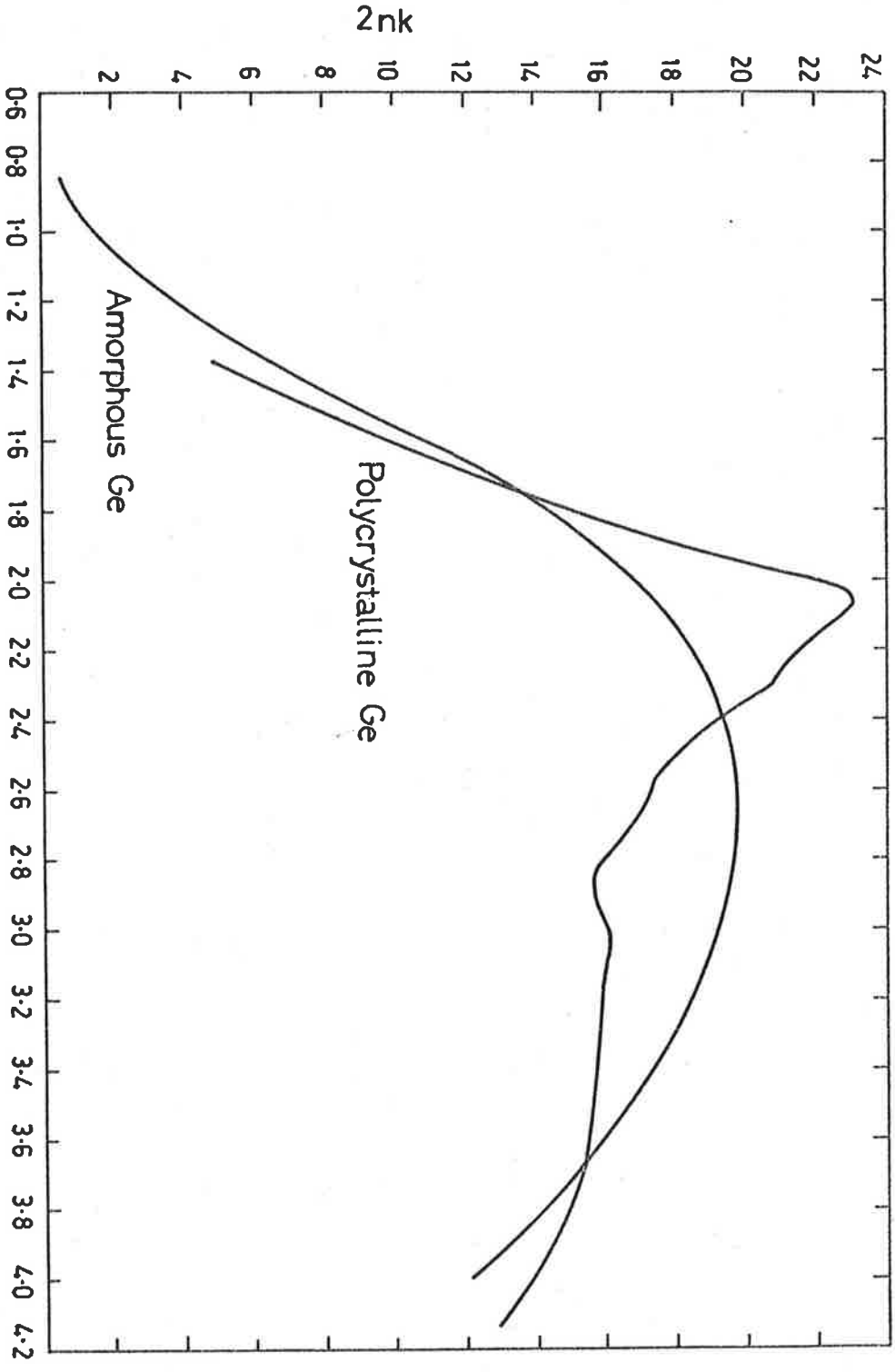
2nk
2
4
6
8
10
12
14
16
18
20
22
24
0·6
0·8
1·0
1·2
1·4
1·6
1·8
2·0
2·2
2·4
2·6
2·8
3·0
3·2
3·4
3·6
3·8
4·0
4·2
Amorphous Ge
Polycrystalline Ge
PHOTON ENERGY IN eV

FIGURE 5·18

According to them this does effect the height of the peak.

Though the two reflectivities (Figures 5.3 and 5.19) agree very well, yet the optical constants, determined from them, by our method and by Kramers-Kronig analysis, do not agree. The two absorption curves have similar structure but the magnitudes are different. The absorption determined in the present work is higher than that shown in Figure 5.19. For energies above 2.5 eV the refractive indices of the present work are lower than those of Figure 5.19. Figure 5.20, shows the plots of the imaginary part of the dielectric constant, $\varepsilon_2 = 2nk$, versus photon energy E, which is from Herman et al (1967). The continuous curve is based on the experimental results of Philipp and Taft. It is clear from Figures 5.18 and 5.20 that in the energy range from 1.8 to 3.0 eV, the present results are in better agreement with the theoretical ones than those of Philipp and Taft. But for energies above 3 eV the present results show a large deviation from the results shown in Figure 5.20, even where the reflectances agree well with those of Philipp and Taft.

Possible reasons for the differences in the two results, are discussed below:

(a) The optical constants, used for the overlying films of Ta_2O_5 were those of Chapter 4, for an amorphous film. It may be thought that there is a possibility that Ta_2O_5 films may not be amorphous when deposited on polycrystalline Ge substrates, and these may have different optical properties. No attempt was made to check the structure of such films. In the case of Ge the difference in refractive index of amorphous and crystalline material (in the

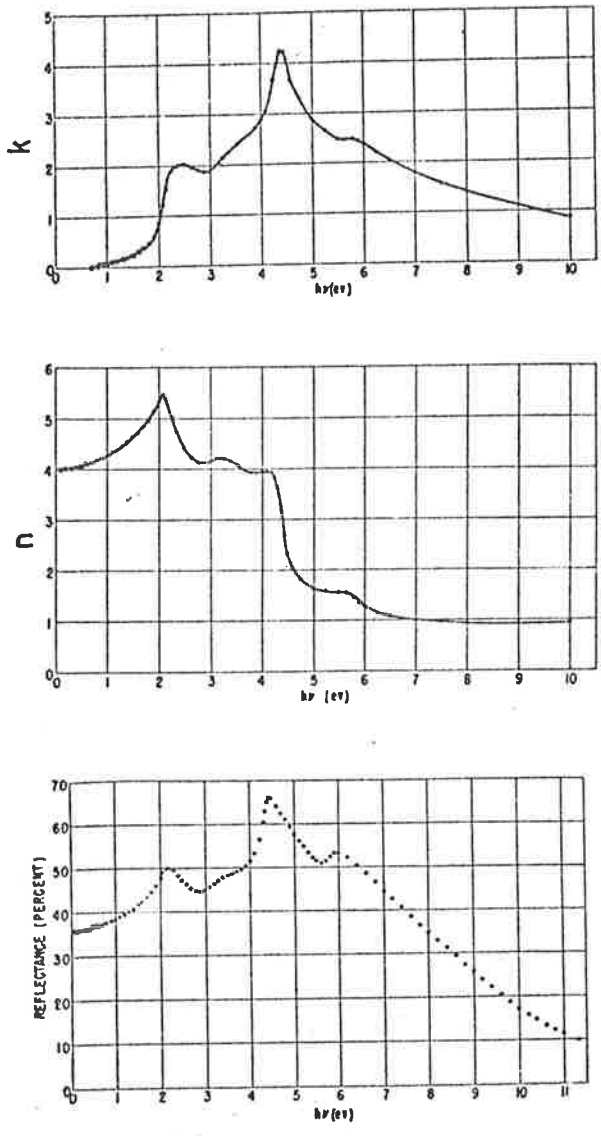

FIGURE 5.19 from Philipp and Taft (1959)

region where these are transparent) is about 5% and numerical solutions show that such small variations of refractive index (of Ta_2O_5 film) do not prevent closure of dispersion curves provided the thickness d_1 is adjusted to keep n_1d_1 constant. The effect of change of 5% in n_1, either way, did not result in uncertainties of more than 5% in the optical constants of the specimen, which are well within the limits of the bars shown in Figure 5.16. Hence this effect cannot be the cause of the differences between the two results.

(b) There may have been a layer of some type on the Ge specimens e.g. polishing usually produces a surface structure (Bielby layer) in which the normal crystal structure of the material is considerably disordered. The presence of a thin film remaining after polishing, or formed in some other way (e.g. oxidation) will also alter the measured values (R). Since the two reflectivties, in the region concerned, are almost the same, so one would expect similar surface conditions of the specimens used.

(c) The main reason for the difference in the two results is most likely due to the uncertainties in the use of Kramers-Kronig analysis of the reflectivity data. According to Philipp and Taft the inaccuracy in the measured reflectance above 7 eV may be considerable. This inaccuracy, plus the two rather uncertain extrapolations of reflectivity data on the lower and higher energy sides, may result in errors in the optical constants derived by Philipp and Taft. This is because the optical constants, determined at any particular wavelength, by the use of Kramers-Kronig analysis

are dependent on the reflectivity values over the entire energy range (from zero to infinity). The disadvantages, of the use of Kramers-Kronig analysis, to determine the optical constants, were discussed in detail in Section 1.3.2.

5.11 ABSORPTION PROCESSES AND ELECTRONIC TRANSITIONS IN AMORPHOUS Ge

There have been conflicting results, on the band edge value of amorphous germanium, reported in the literature. Adler and Moss (1973) have summarised these results of different workers and say that "the disparity in optical absorption edge remains the largest unresolved problem in amorphous Ge". An attempt is made here to explain the electronic transitions near the band gap of amorphous Ge, and to relate these to those observed in crystalline Ge.

5.11.1 PUBLISHED WORK

Results, in the energy range 0.6 - 1.6 eV, from Tauc et al (1964) and Denton and Tomlin (1972) show that, in amorphous Ge films, the plot of $(EnK)^{\frac{1}{2}}$ or $E(nk)^{\frac{1}{2}}$ versus E constitutes two straight lines (Figure 5.21, from Denton and Tomlin). Where n-ik is the complex refractive index and K the absorption coefficient, of Ge films, for photon energy E. The open circles in Figure 5.21 represent the experimental points obtained by Denton and Tomlin, while the solid dots correspond to the theoretical work, carried out in the present work, as will follow from the discussion below. According to Tauc et al, the absorption corresponding to the line marked 'a' (Figure 5.21) is due to indirect transitions of electrons from valence to conduction band $[\Gamma_{8+}\ (\Gamma_{25'}) \rightarrow L_{1c}]$ with an onset at 0.72 eV

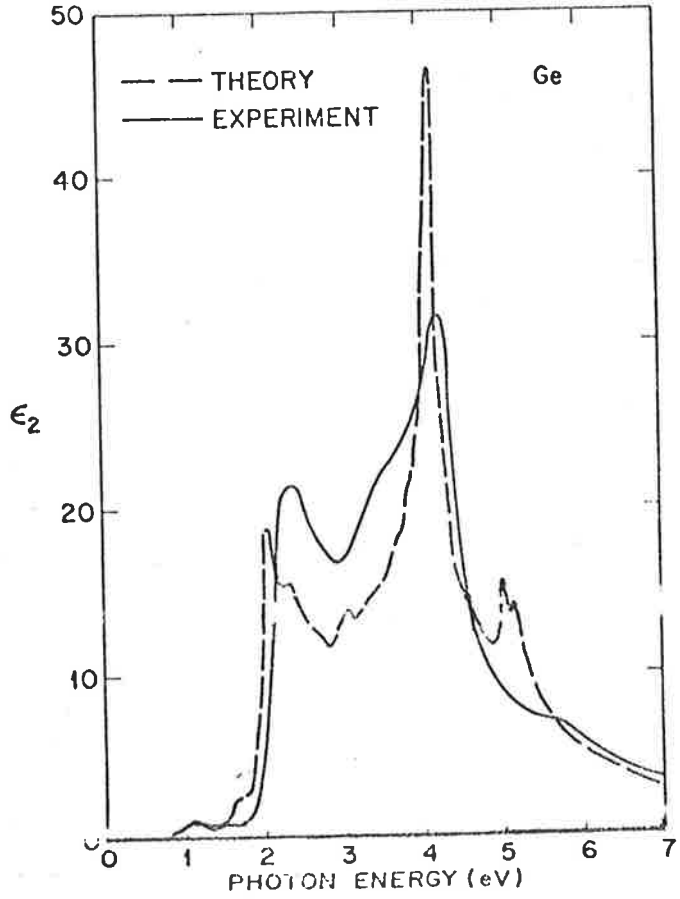

FIGURE 5.20 (from Herman et al, 1967)

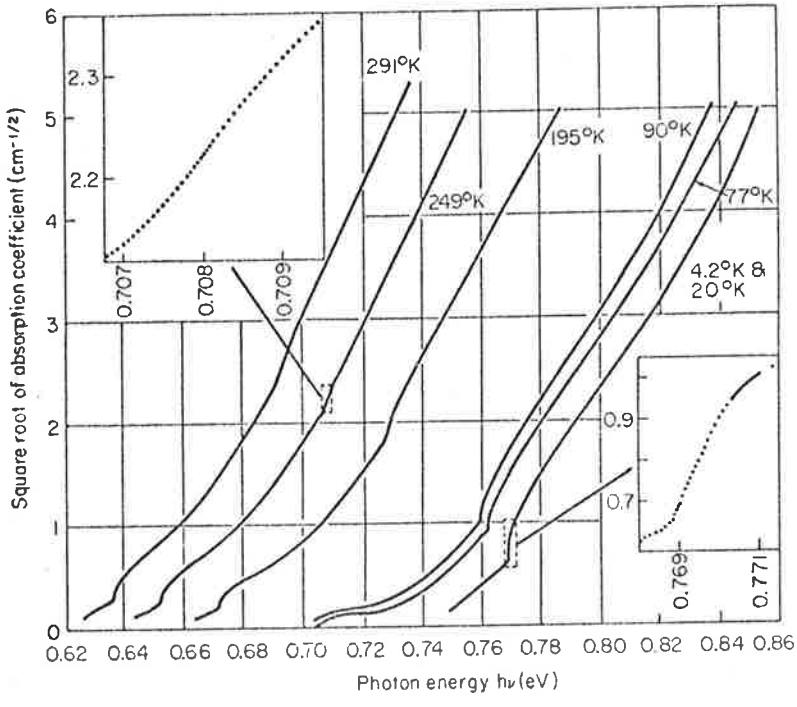

Fig. 5.22 The absorption-edge spectrum of Ge at various temperatures. [From G. G. MacFarlane, T. P. McLean, J. E. Quarrington, and V. Roberts, *Phys. Rev.* 108, 1377 (1957).]

(0.71 eV, Figure 5.21). Tauc et al state that for the electronic transitions in an amorphous material, only energy but not the k-vector is conserved. This results in apparent indirect (or non-direct) transitions of electrons instead of the corresponding direct transitions observed in the crystalline form of the same material. This view is supported by the photemission results (Donovan and Spicer, 1968) and is also explained theoretically (Herman and Van Dyke, 1968). On this assumption Tauc et al interpret the absorption, corresponding to the line marked 'b' (Figure 5.21), to be due to a direct transition $[\Gamma_{8+}(\Gamma_{25}') \rightarrow \Gamma_{7-}(\Gamma_2')]$, with an onset of 0.89 eV (or 0.86 eV, Figure 5.21). The onset of the second transition in both cases was obtained from the intercept of the line marked (b) on the E-axis. The value, of absorption edge thus obtained is 0.71 or 0.72 eV, which is much higher than that reported for crystalline Ge (0.66 eV, Maclean, 1960). However, this treatment of the data is now believed to be erroneous, as will be shown.

5.11.2 PRESENT INTERPRETATION

On reanalyzing the data for amorphous Ge by the procedure described in Section 4.4.2, a satisfactory interpretation can be given.

In the photon energy range from 0.72 to 1.02 eV the relation for indirect transitions holds:

$$(EnK)^{\frac{1}{2}} = C_1(E-Eg)$$

Beyond 1.02 eV a second transition of a similar kind appears and in this region

$$(EnK)^{\frac{1}{2}} = \{C_1^2(E-Eg)^2 + C_2^2(E-Eg_1)^2\}^{\frac{1}{2}}$$

where c_1, c_2, Eg and Eg_1 are constants.

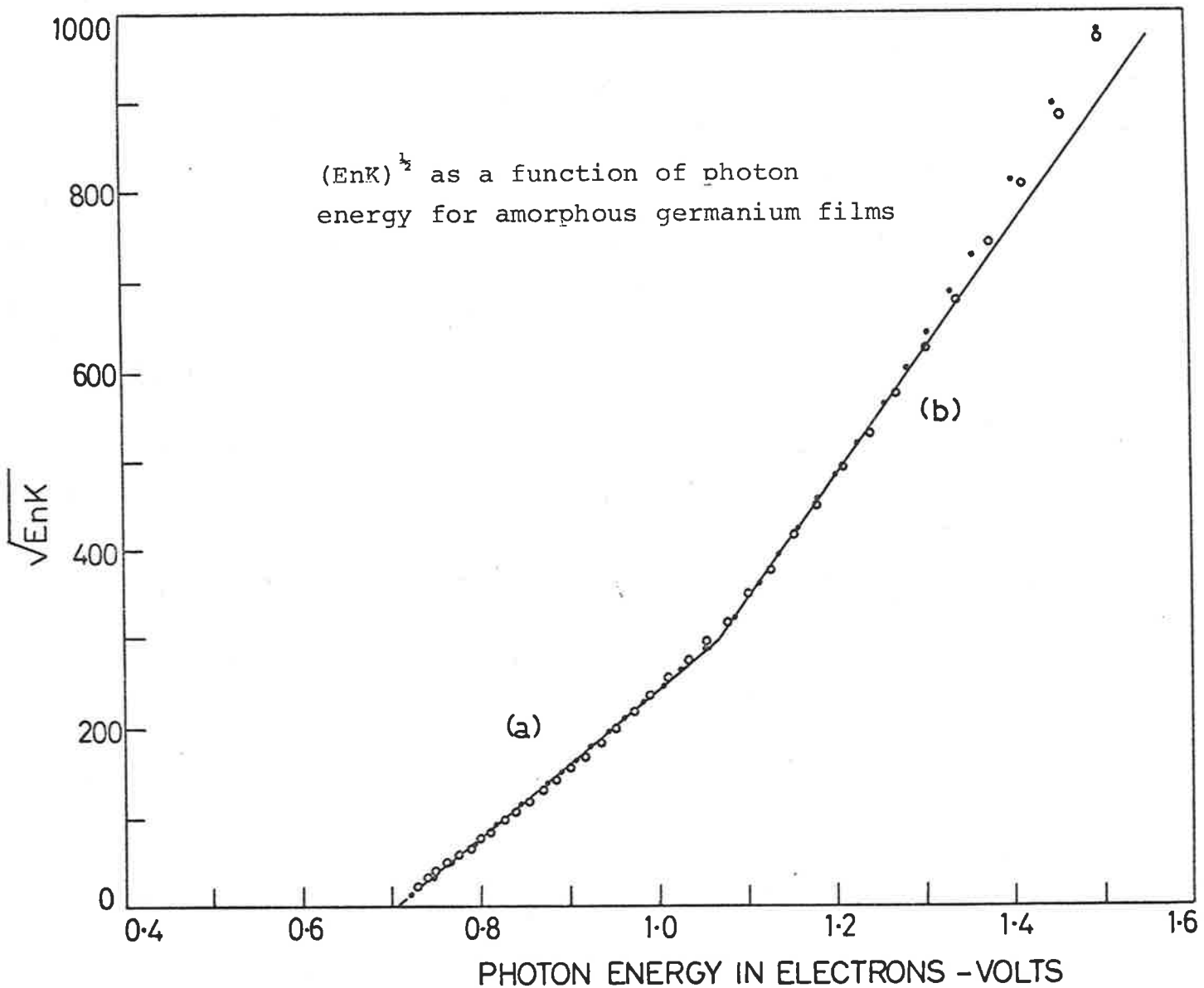
1000
800
600
400
200
0
$\sqrt{EnK}$
$(EnK)^{\frac{1}{2}}$ as a function of photon energy for amorphous germanium films
(a)
(b)
0·4
0·6
0·8
1·0
1·2
1·4
1·6
PHOTON ENERGY IN ELECTRONS - VOLTS

FIGURE 5·21

On carrying out the graphical procedure of Section 4.4.2 the following constants were found:-

$Eg = 0.72$ eV $\qquad C_1 = 883 \ eV^{-\frac{1}{2}} \ cm^{-\frac{1}{2}}$

$Eg_1 = 1.02$ eV $\qquad C_2 = 1550 \ eV^{-\frac{1}{2}} \ cm^{-\frac{1}{2}}$

In Figure 5.21 the solid dots show how well the above formulae fit the experimental results, using these constants.

For an indirect gap semiconductor, such as Ge, the low absorption near the band gap can be best determined by transmission measurements made on a bulk form of the semiconductor, such as those of Macfarlane et al (1957). Figure 5.22, taken from Macfarlane et al, show the absorption results for crystalline Ge, in the low absorption region, near the edge. In this region, a precise measurement of absorption cannot be obtained by the method used in the present work because an error of 0.001 in reflectance and transmittance, results in an error of about 0.001 to 0.002 in k (i.e. 60 to 120 cm^{-1} in K). This accounts for the failure to detect the true indirect band gap by the present methods, and there is no inconsistency in its being less than the cut off at 0.72 eV.

If it is assumed that the band structure of amorphous Ge near k = 0 is not much different from that of the crystalline material, but that the relationship between EnK and E-Eg for a direct transition is modified, as argued by Tauc et al (1964), so as to take the form

$$(EnK)^{\frac{1}{2}} \propto E-Eg$$

then the edges at 0.72 and 1.02 eV may be explained as follows.

In the expectation that the band gap for the amorphous material might be less than in the crystal it seems reasonable to ascribe the observed gaps of 0.72 eV and 1.02 eV to two direct transitions separated by the

valence band splitting. That is, the edge at 0.72 eV may be attributed to the corresponding direct transition $\Gamma_{8+}(\Gamma_{25}') \rightarrow \Gamma_{7-}(\Gamma_2')$ in crystalline Ge (the value of which is 0.8 eV, Maclean, 1960 and Cardona, 1967). And the edge at 1.02 eV to the direct transition $\Gamma_{7+}(\Gamma_{25}') \rightarrow \Gamma_{7-}(\Gamma_2')$ in crystalline Ge (which is 1.1 eV, Cardona, 1967).

Since a shift of the edges by about 0.08 eV, towards lower energy, is observed in amorphous Ge, therefore it may be concluded that the band edge in amorphous Ge is close to 0.58 eV (i.e. about 0.08 eV smaller than 0.66 eV, observed in crystalline Ge, Maclean, 1960). The notations used, for different transitions, are those from Cardona (1967).

In the above calculations, the absorption, due to the indirect transition ($\Gamma \rightarrow L$) with edge of 0.58 eV, have been ignored. The absorption involved (Figure 5.22) in such a transition is negligible in comparison with the experimental results, as is clear from Figure 5.1.

5.11.3 CONCLUSIONS

The following conclusions may be drawn from the above results:-

(1) The conclusion, drawn by Tauc et al (1964), Donovan and Spicer (1968) and Herman and Van Dyke (1968) that only apparent indirect (or non-direct) transitions of electrons occur in amorphous materials instead of the direct transitions in crystals, is confirmed by the above results.

(2) In amorphous Ge, the band edges shift to the lower energy by about 0.08 eV, when compared to crystalline Ge. The resulting value of band edge of 0.58 eV for amorphous Ge is confirmed by Donovan et al (1970).

(3) The valence band spin-orbit splitting at Γ in amorphous Ge is 0.30 eV, which is in agreement with that for crystalline Ge, determined experimentally (0.30 eV) and theoretically (0.29 eV), Cardona, 1967. Cardona's work is based on the absorption, measured by Hobden (1962), of crystalline films of Ge. Hobden observed an abrupt change in slope at an energy 0.3 eV above the direct edge. Which was interpreted as evidence for the spin-orbit splitting of the valence band in crystalline Ge. Donovan et al (1970), commenting on this, say that there was no evidence for an abrupt change in slope at energies above the absorption edge in their results (absorption), which were on amorphous Ge films. It may be commented here that in amorphous semiconductors the absorption follows the law $\{Enk \alpha (E-Eg)^2\}$ for indirect (or non-direct) transitions, therefore one would not expect an abrupt change in slope, similar to the one observed by Hobden in case of crystalline Ge, where the absorption followed the law $\{EnK = (E-Eg)^{\frac{1}{2}}\}$ for direct transition.

CHAPTER 6

DETERMINATION OF THE OPTICAL CONSTANTS OF CADMIUM SULPHIDE AND ZINC SULPHIDE FILMS

6.1 INTRODUCTION

The optical properties of thin evaporated films of cadmium sulphide (in the spectral range 2000-300 nm) and zinc sulphide (in the spectral range 2000-250 nm), were studied. The optical constants (n and k), of these films, were determined from measurements of reflectance and transmittance at normal incidence, using the method devised by Denton et al (1972). This is part of a systematic investigation of the optical properties of the II - VI compounds attempting to eliminate discrepancies apparent in reported results by using a method which avoids the use of approximate formulae relating reflectance R and transmittance T to n and k, the refractive and absorption indices respectively.

It was found that the surfaces of these films were rough. The surface roughness was found to be dependent on film thickness and on the temperature of the substrates, on which they were deposited. It is shown that the optical properties could not be interpreted satisfactorily without accounting for the surface roughness. Different methods of accounting for the surface roughness were considered. It was concluded that a method, in which the surface of the film was treated as a separate uniform layer, on the film, with optical constants different from the

film itself, gave satisfactory results. The optical constants of the surface layers were determined, using Schopper's method (1951). Thus a film of CdS (or ZnS) on a substrate was treated as a double film on the substrate (i.e. a very thin surface roughness layer, of the order of 6-15 nm, on a uniform film of CdS or ZnS, which rested on the substrate). Formulae for $\frac{1 \pm R_2}{T_2}$ for such a system, by Tomlin (1972a), were used to obtain acceptable dispersion and absorption curves for CdS and ZnS films.

6.2 PREPARATION OF CdS AND ZnS FILMS

The same method was used for the preparation of films of CdS and ZnS. They were prepared on quartz wedges (Chapter 2) by the method of evaporation in vacuum. Pure powdered CdS (or ZnS) was evaporated from an alumina crucible, heated by a current passing through a tungstun wire surrounding it, at pressures of the order of 10^{-5} torr. The evaporation rate was controlled by varying the current flowing through the tungstun basket. An electromagnetically operated shutter was positioned above the source to enable the powder to be outgassed prior to evaporation onto the substrate.

The prepared films varied in thicknesses from 40 to 350 nm. These were deposited on substrates maintained at different temperatures, from room temperature to 180^{o}C. The rate of formation of the films varied from 20 to 60 nm per minute.

6.3 MEASUREMENTS

The reflectance and transmittance of such films, at near normal incidence, were measured in air using the reflectometer described in

For CdS films the measurements were made in the spectral range 2000-700 nm at an interval of 25 nm and in the range 700-300 nm at an interval of 10 nm.

For ZnS films the measurements were made in the spectral range 2000-600 nm at an interval of 25 nm, in the range 600-400 nm at an interval of 10 nm and in the range 400-250 nm at an interval of 5 nm.

It may be mentioned that the measured transmittance $T_m = T/T_s$, where T is the transmittance of the film into the substrate and T_s is the transmittance across the back face of the substrate and is $4n_on_2/(n_o+n_2)^2$ where n_o and n_2 are the indices of refraction of air and the substrate, respectively. In the expressions, relating the optical constants of a film and a substrate to the reflectance and transmittance, given by Heavens (1955) and Tomlin (1968), the transmittance used is T, which is readily obtained from the measured transmittance.

6.4 RESULTS : USING THE FORMULAE FOR A SINGLE FILM ON A SUBSTRATE

The measured reflectance (R) and transmittance (T_m), of a CdS film, which was deposited on a substrate, maintained at 140°C, is shown in Figure 6.1. At first the optical constants of the film were calculated from R and T_m data shown in Figure 6.1, using the method for a single film on a substrate, starting with an approximate film thickness, and then adjusting this value in an attempt to obtain a continuous dispersion curve. This method was described in detail by Denton et al (1972). An approximate knowledge of the film thickness (d_1) was obtained from the R or T_m curves by the use of the following relation

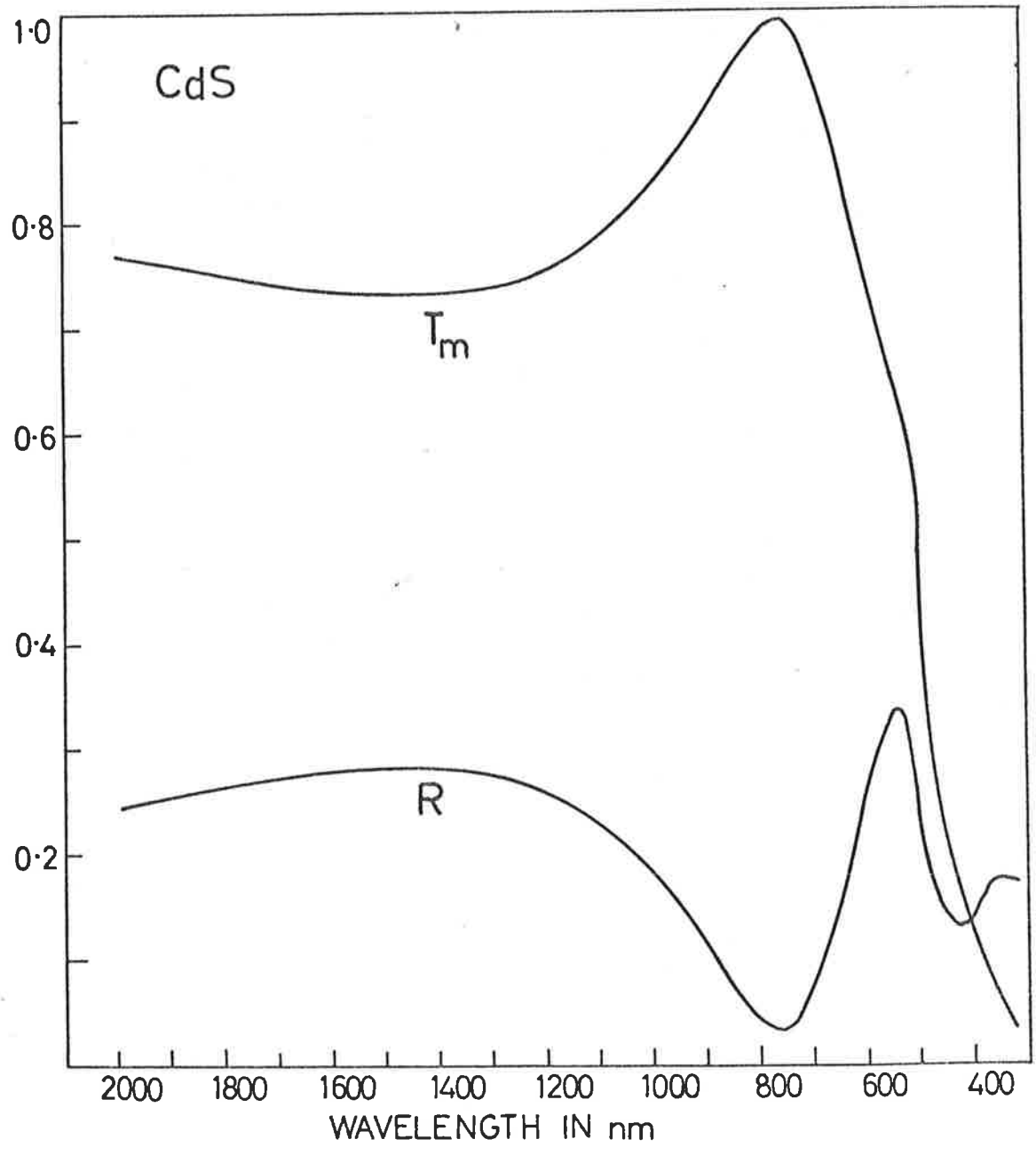
1·0
0·8
0·6
0·4
0·2
CdS
T_m
R
2000
1800
1600
1400
1200
1000
800
600
400
WAVELENGTH IN nm

FIGURE 6·1

$$d_1 = \frac{\lambda_1\lambda_2}{4n_1(\lambda_1-\lambda_2)}$$

where n_1 is the long wavelength refractive index of the film and λ_1 and λ_2 are the turning points of reflectance or transmittance curves in the non-absorbing region.

Figure 6.2 shows the result of such a calculation based on the data shown in Figure 6.1. In accordance with the discussion of Denton et al (1972), the loop marked (A) in Figure 6.2, shows that the estimated thickness of the film was too large, while the loop marked (B) shows that this thickness was too small. Change of the film thickness either way in the calculations improved the continuity of the dispersion curve near one of the loops while the continuity of the dispersion curve near the other loop deteriorated. Thus it was clear that a proper continuity of the dispersion curve, in the whole wavelength region, could not be obtained for any choice of the thickness of the film, in the calculations, when the formulae for a single film on a substrate, were used.

A similar behaviour was observed for all the CdS and ZnS films, studied, irrespective of the film thicknesses, rate of evaporations and the substrate temperatures at which the films were deposited.

The reason for such a behaviour of the dispersion curves was clear when surfaces of these films were studied. The surfaces were found to be rough as will be discussed in the next section. It was concluded that the measured values of R and T_m were not those appropriate to a perfectly plane parallel uniform film such as is assumed for the derivation of the formulae used. This view was supported by comparing the reflectance curves in the U.V. region, where the films were strongly absorbing so that multiple reflections were ineffective, with corresponding results

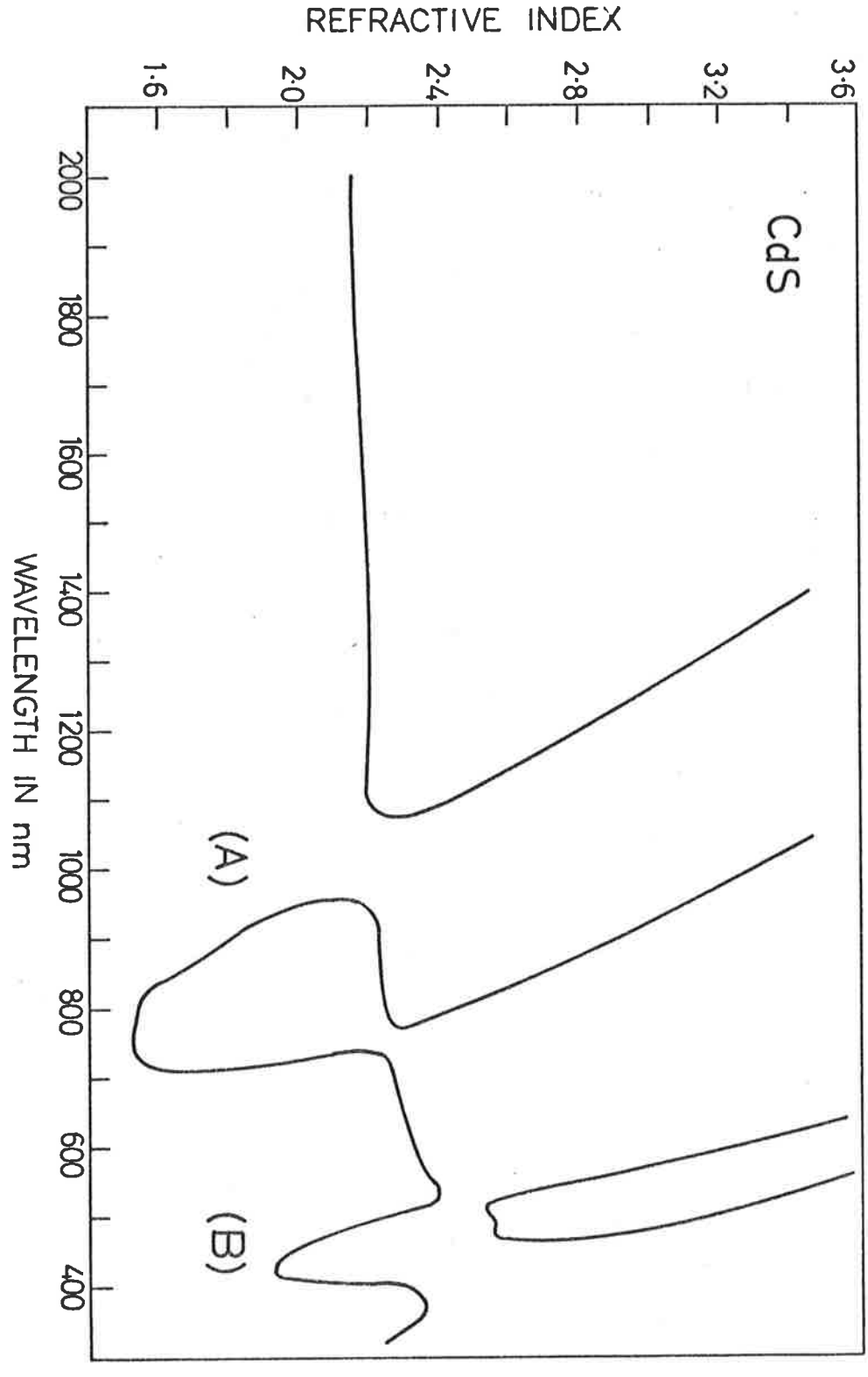
REFRACTIVE INDEX
1·6
2·0
2·4
2·8
3·2
3·6
CdS
(A)
(B)
2000
1800
1600
1400
1200
1000
800
600
400
WAVELENGTH IN nm

FIGURE 6·2

for single crystals (Cardona and Harbeke, 1965). The reflectance of a 150 nm film of CdS (or ZnS), for example, was about 10 to 20% less in the U.V. region than for the, presumably, smooth crystalline surfaces. This effect could be attributed to surface roughness of the films, as is discussed in the following section.

6.5 SURFACE TOPOGRAPHY OF CdS AND ZnS FILMS

Surface replicas of the films were studied under an electron microscope. These replicas were obtained by a method similar to that discussed in Section 4.8. A typical micrograph obtained from a replica of CdS film, is shown in Figure 6.3. The surface looks rough, i.e. it has a pebbly nature. Micrographs, obtained of CdS films by Simov (1973) and Shallcross (1967) show similar structure. Coogan (1957) reports the possibility of voids present on surfaces of films of ZnS.

It was observed that the surface roughness had very little effect on the optical constants of films in the I.R., and in the visible regions, except in those cases where the films were absorbing in those regions. But it has an appreciable influence on the reflectivity in the U.V. region. This is also reported by Tauc et al (1964) and Daude et al (1972). Bujatti and Marcelja (1972), while studying the absorption edge of CdS films took into account corrections for the reflection losses at the surfaces.

6.6 DIFFERENT METHODS OF ACCOUNTING FOR SURFACE ROUGHNESS

Various methods accounting for surface roughness are discussed below:

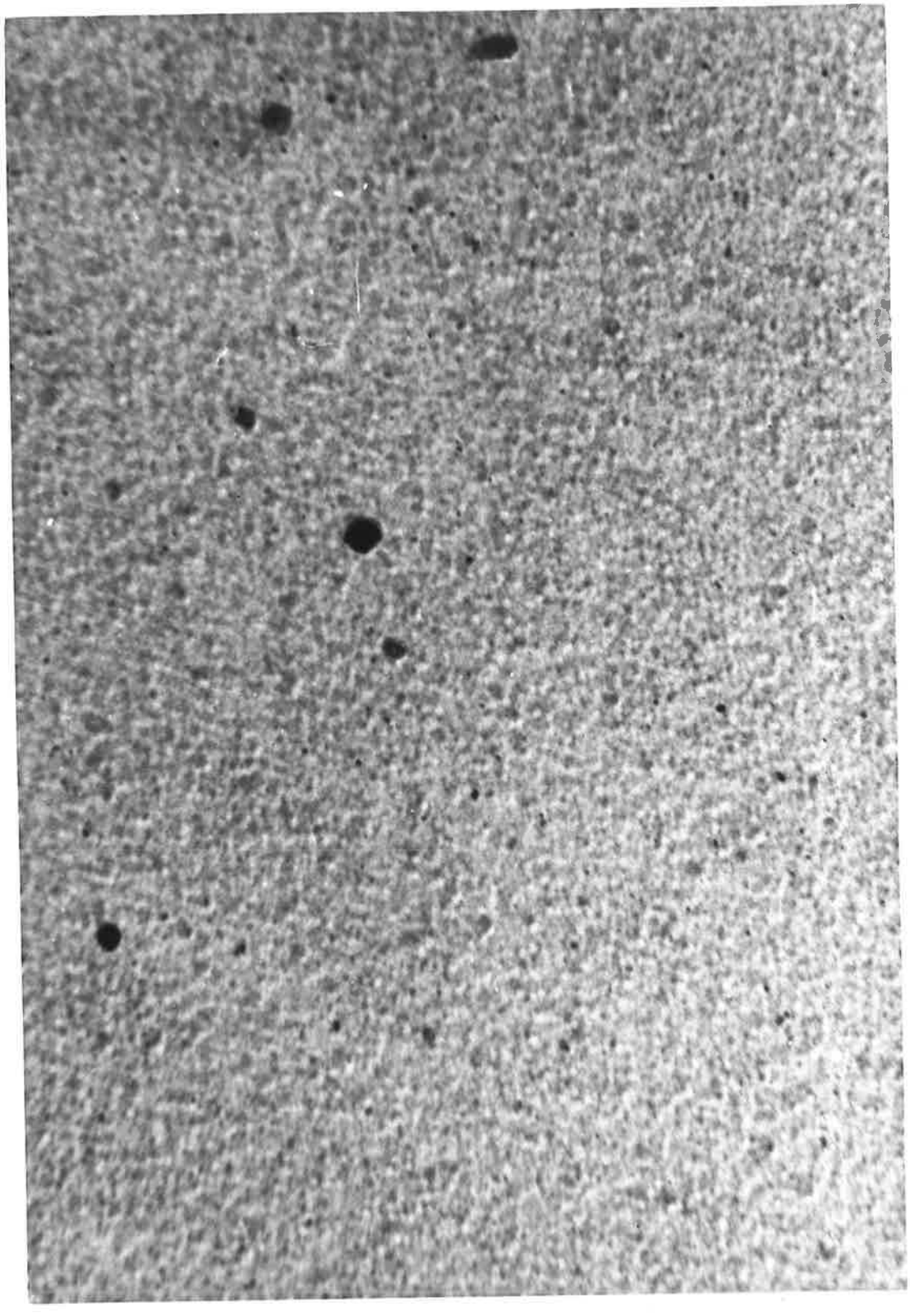

FIGURE 6.3 CdS SURFACE REPLICA $x(1.28 \times 10^5)$

6.6.1 REFLECTION CORRECTION BY DAVIES METHOD

Bennett and Porteus (1961), Bennett (1963) and Daude et al (1972) have successfully applied Davies (1954) method to account for losses in normal incidence reflectance from films with rough surfaces. Their films had high reflectance and absorptance and no multiple interference took place in them. It is different with the present films of CdS and ZnS. For films of thicknesses from 40 to 350 nm, the transmittance in the I.R. and visible regions was not small, so multiple interference effects were appreciable. This complicates the reflection corrections. On the other hand in the U.V. region, below 400 nm for CdS, and below 290 nm for ZnS, for films thicker than 150 nm, the transmittance was small enough for multiple reflection effects to be negligible. Then the method of correction using Davies formula could be applied approximately.

According to Davies (1954) the relative reflectance loss (for normal incidence radiation) is

$$\frac{R_o - R}{R_o} = 1 - e^{-\left(\frac{4\pi\sigma}{\lambda}\right)^2} \qquad 6.6.1$$

where R_o is the reflectance of a perfectly smooth surface, R is the reflectance of a rough surface of the same material at the wavelength λ. σ is the root mean square roughness.

From equation 6.6.1 the reflectivity loss is

$$\Delta R = R_o - R = R_o \left\{1 - e^{-\left(\frac{4\pi\sigma}{\lambda}\right)}\right\} \qquad 6.6.2$$

This loss in reflectance was calculated for a value of σ obtained in the method discussed in Section 6.6.3, and the values of R_o taken from the bulk CdS (or ZnS) reflectivity measured by Cardona and Harbeke (1965).

It was found possible, using the corrected reflectance in U.V. and the measured transmittance, in the single film formulae (Denton et al, 1972), to obtain a continuous dispersion curve by eliminating the gaps at both A and B in Figure 6.2. Thus it was concluded that the use of Davies's formula, with the parameter σ estimated from electron micrographs of surface replicas (or more effectively from the method, discussed in Section 6.6.3) provides a suitable means of correcting the observed reflectances of rough films in the region of strong absorption.

However the method is not entirely satisfactory for the present work because of the limitations to the strongly absorbing region of the spectrum.

Since $\frac{4\pi\sigma}{\lambda} < 1$ for the values of λ (2000-250 nm) and the order of roughness (15 nm), involved in the present work, therefore equation 6.6.1 could be approximated to

$$\frac{R_o - R}{R_o} \simeq \left(\frac{4\pi\sigma}{\lambda}\right)^2 - \frac{1}{2!}\left(\frac{4\pi\sigma}{\lambda}\right)^4 + \frac{1}{3!}\left(\frac{4\pi\sigma}{\lambda}\right)^6 \qquad 6.6.3$$

It is clear that the first term in the above equation is dominent. This will be used in the next method discussed.

6.6.2 REFLECTION CORRECTION BY TAUC et al

Tauc et al (1964) have proposed that the relative reflection loss is inversely proportional to the fourth power of the wavelength i.e.

$$\frac{R_o - R}{R_o} \propto \frac{1}{\lambda^4} \qquad 6.6.4$$

Once again this correction is limited to the U.V. region for the reasons discussed in the last section. The results obtained by this method were not in agreement with those derived using the methods of Sections 6.6.1

and 6.6.3. This is clear when relation 6.6.4 is compared with equation 6.6.3.

6.6.3 DOUBLE LAYER ON A SUBSTRATE METHOD

To account satisfactorily for results on films of CaF_2 (Bousquet, 1957) and on Ge films (Denton et al, 1972) the surfaces of the films were treated as separate uniform layers with refractive indices different from the film themselves. Bousquet calls these surface layers transition layers and, as is discussed in detail by Rouard and Bousquet (1965), they may be due to surface roughness. Bousquet as well as Denton et al used constant values of refractive indices of the surface layers, which were smaller than those of the film themselves and larger than those of the substrates. The films of CaF_2 studied by Bousquet were transparent with transition layers of thicknesses as much as 10% of the values of the thicknesses of the films themselves. With the amorphous films of Ge, studied by Denton et al (1972), the surface layers were found to be very thin (= 0.6 nm). Therefore the method of taking the surface layers to be transparent with constant indices of refraction in cases of CaF_2 and Ge films was reasonable. But in the present cases of CdS and ZnS films the surface roughnesses, observed by electron microscopy were of the order of about 14 nm, and in these cases it was necessary to allow for absorption in the surface layers. This required the determination of the complex refractive index n_1-ik_1 of the surface layer, which was obtained by the use of Schopper's theory (Schopper, 1951 and Heavens, 1955) as is discussed below.

In the simple case, Schopper's theory deals with the optical constants of a discontinuous layer represented by an assembly of ellipsoidal particles of the same size and axial ratio. According to Schopper (1951) if $N = n+ik$ is the complex refractive index of the bulk material, and N_1 is that of the ideal equivalent film by which the particulate layer may be replaced

$$\gamma(N_1^2-1) = \frac{N^2-1}{(N^2-1)f+1} \qquad 6.6.5$$

where γ is the ratio of the average film thickness to that deduced from the mass per unit area of the particulate film and the bulk density; f is a function of the axial ratio of the ellipsoids known as David's function (Heavens, 1955).

From the above equation, the following relations giving explicit values of n_1 and k_1 can be easily derived.

$$n_1 = \frac{1}{\sqrt{2}} \{X + (X^2+4y^2)^{\frac{1}{2}}\}^{\frac{1}{2}} \qquad 6.6.6$$

$$k_1 = y/n_1 \qquad 6.6.7$$

where

$$X = 1 + \frac{1}{\gamma} \frac{\{A(Af+1) + 4n^2k^2f\}}{(Af+1)^2 + (2nkf)^2}$$

$$y = \frac{1}{\gamma} \frac{nk}{(Af+1)^2 + (2nkf)^2}$$

$$A = n^2-k^2-1$$

It is not possible to measure f and γ but these can be estimated from the electron micrographs of the replicas. In order to determine n_1 and k_1 from the formulae above, n, k, γ and f must be known. The procedure adopted in determining n and k is outlined below.

The values of n for the wavelength region 2000-520 nm for CdS, and 2000-400 nm for ZnS, in which the films are transparent, were those from crystals (Roskovcova and Pastrnak, 1967, Czyak et al, 1957 and Czyak et

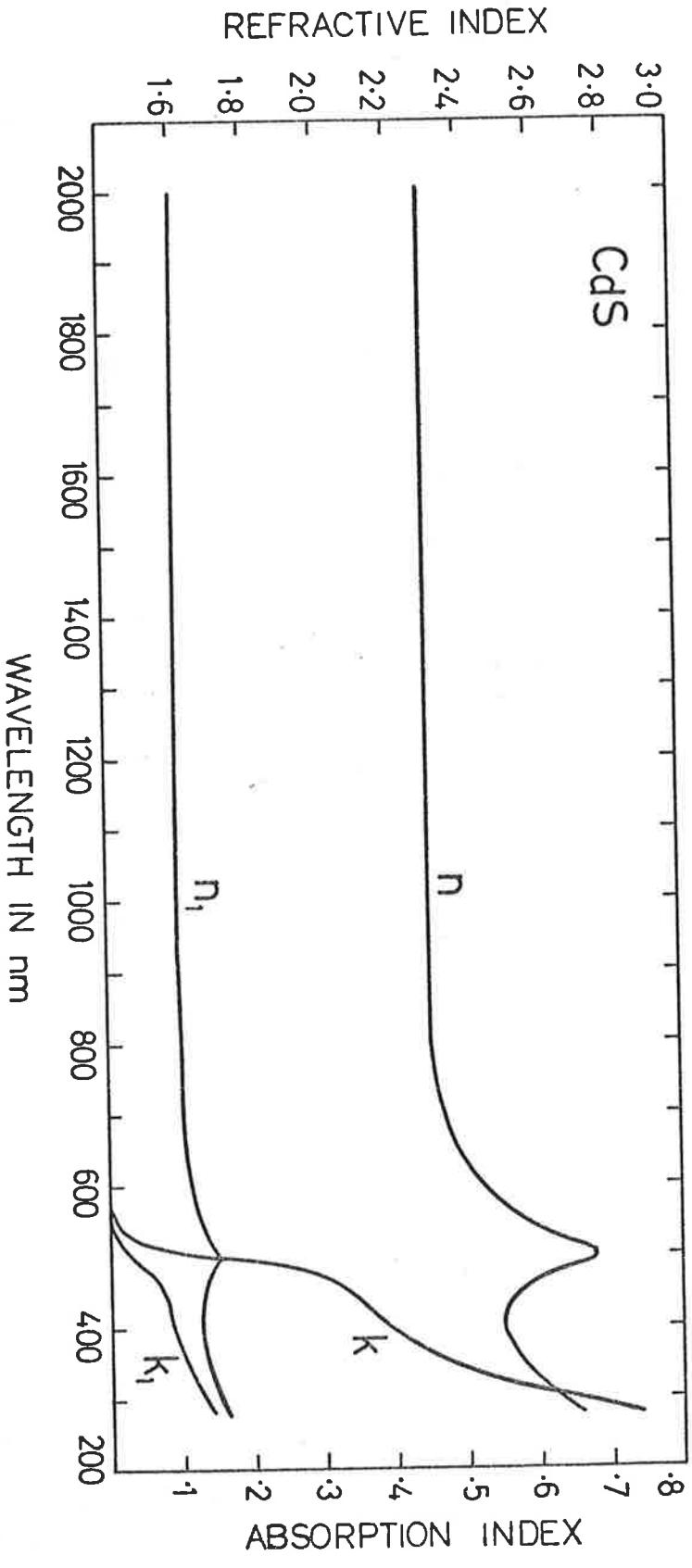
REFRACTIVE INDEX
1·6
1·8
2·0
2·2
2·4
2·6
2·8
3·0
CdS
n
n1
k
k1
2000
1800
1600
1400
1200
1000
800
600
400
200
WAVELENGTH IN nm
·1
·2
·3
·4
·5
·6
·7
·8
ABSORPTION INDEX

FIGURE 6·4

al, 1959). In the absorbing region the values of absorption index k were calculated from the experimental thin film data using the single film formulae since it is known that the absorption curve is not very dependent upon precise closure of the dispersion curves. These approximate values of k were then used together with experimental results for reflectance from a bulk specimen (Cardona and Harbeke, 1965) to find n, in the absorbing region, from the formula

$$R = \frac{(n-1)^2 + k^2}{(n+1)^2 + k^2}$$

The error in n is considerably less than that in k as is clear from plots of n against R, for different k, shown by Coogan (1957).

Thus n and k were determined in the wavelength ranges, 2000-300 nm for CdS and 2000-250 nm for ZnS, and are shown in Figure 6.4 and Figure 6.5, respectively.

Alternatively n and k may be estimated with what appears to be sufficient accuracy by treating the film as a single layer and completing the dispersion curve by eye where it does not close properly. This will give a fairly good estimate of n and the values of k are known to be relatively independent of the precise closure of the dispersion curve.

The David's function f was estimated from the electron micrographs, such as that shown in Figure 6.3. For the estimated axial ratio of ellipsoids, from the micrographs, f was about 0.2 (Heavens, 1955). γ cannot be determined experimentally. However $\gamma = 1.5$ was chosen so that the values of n_1 and k_1 (Figures 6.4 and 6.5) thus calculated from equation 6.6.5, when used in the double layer method resulted in similar thicknesses for the equivalent surface roughness layers of the films,

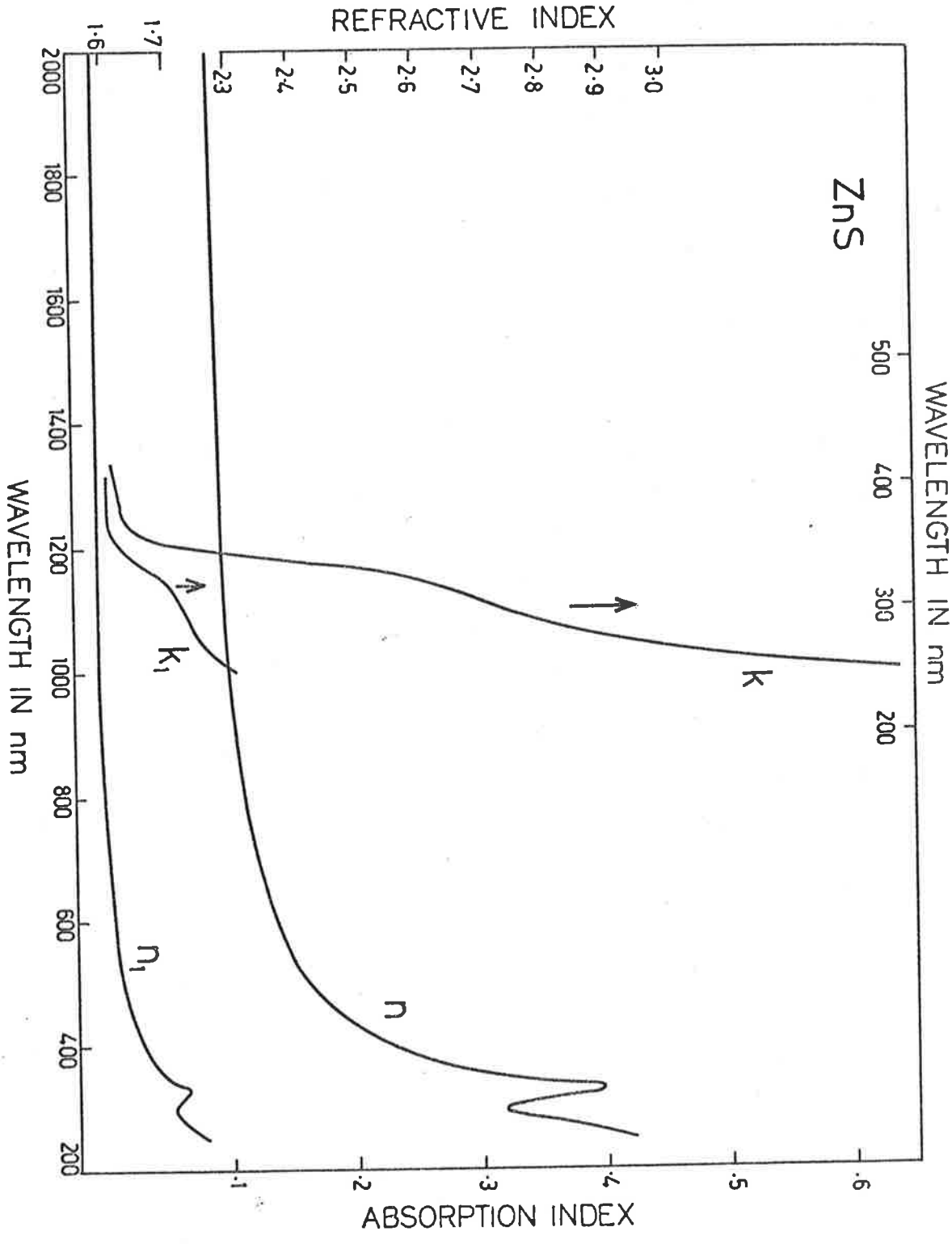
REFRACTIVE INDEX
2·3
2·4
2·5
2·6
2·7
2·8
2·9
3·0
ZnS
WAVELENGTH IN nm
500
400
300
200
k
k1
n
n1
1·6
1·7
2000
1800
1600
1400
1200
1000
800
600
400
200
WAVELENGTH IN nm
·1
·2
·3
·4
·5
·6
ABSORPTION INDEX

FIGURE 6·5

as those obtained by the use of the method of Davies (i.e. σ - values, Section 6.6.1). It may be mentioned that Heavens (1955) uses q in place of $1/\Upsilon$ (= 0.66 in present work) and says that in practice, values of q observed are generally greater than 0.5, e.g. for gold films q = 0.6 - 0.7. A change of 10% in the above value of Υ resulted in a change of about 4% in n and k.

However, in practice it is found that for a thin surface layer the values of n_1 and k_1 are not critical and changes in these values only modify the thickness of the surface layer for which closure occurs, without appreciable affect on the calculated values of n_2 and k_2 for the film itself. However, an accurate result for the thickness of the surface layer can be found only if n_1 and k_1 are known accurately.

6.7 EQUATIONS FOR A DOUBLE LAYER ON A SUBSTRATE

If R_2 is the reflectance from the upper surface of a double film on a transparent substrate and T_2 is the transmittance into the substrate, both at normal incidence, then the following formulae for a non-absorbing substrate could be obtained from those derived by Tomlin (1972a).

$$\frac{1+R_2}{T_2} = \frac{1}{16n_0n_3(n_1^2+k_1^2)(n_2^2+k_2^2)} \{(n_0^2+n_1^2+k_1^2)F_1+(n_0^2-n_1^2-k_1^2)F_2\} \qquad 6.7.1$$

$$\frac{1-R_2}{T_2} = \frac{1}{8n_3(n_1^2+k_1^2)(n_2^2+k_2^2)} (n_1G_1 + k_1G_2) \qquad 6.7.2$$

where $F_1 = \{(n_1+n_2)^2+(k_1+k_2)^2\}\{(n_2^2+n_3^2+k_2^2)\cosh 2(\alpha_2+\alpha_1)$

$+2n_2n_3 \sinh 2(\alpha_2+\alpha_1)\}$

$+\{(n_1-n_2)^2+(k_1-k_2)^2\}\{(n_2^2+n_3^2+k_2^2)\cosh 2(\alpha_2-\alpha_1)$

$+2n_2n_3 \sinh 2(\alpha_2-\alpha_1)\}$

$+2(n_1^2-n_2^2+k_1^2-k_2^2)B\cosh 2\alpha_1+4(n_1k_2-n_2k_1)D\sinh 2\alpha_1$

$$F_2 = \{(n_1+n_2)^2+(k_1+k_2)^2\}\{(n_2^2-n_3^2+k_2^2)\cos 2(\gamma_2+\gamma_1)$$
$$-2n_3k_2\sin 2(\gamma_2+\gamma_1)\}$$
$$+\{(n_1-n_2)^2+(k_1-k_2)^2\}\{(n_2^2-n_3^2+k_2^2)\cos 2(\gamma_2-\gamma_1)$$
$$-2n_3k_2\sin 2(\gamma_2-\gamma_1)\}$$
$$+2(n_1^2-n_2^2+k_1^2-k_2^2)A\cos 2\gamma_1+4(n_1k_2-n_2k_1)C\sin 2\gamma_1$$

$$G_1 = \{(n_1+n_2)^2+(k_1+k_2)^2\}\{(n_2^2+n_3^2+k_2^2)\sinh 2(\alpha_2+\alpha_1)$$
$$+2n_2n_3\cosh 2(\alpha_2+\alpha_1)\}$$
$$-\{(n_1-n_2)^2+k_1-k_2)^2\}\{(n_2^2+n_3^2+k_2^2)\sinh 2(\alpha_2-\alpha_1)$$
$$+2n_2n_3\cosh 2(\alpha_2-\alpha_1)\}$$
$$+2(n_1^2-n_2^2+k_1^2-k_2^2)B\sinh 2\alpha_1+4(n_1k_2-n_2k_1)D\cosh 2\alpha_1$$

$$G_2 = \{(n_1+n_2)^2+(k_1+k_2)^2\}\{(n_2^2-n_3^2+k_2^2)\sin 2(\gamma_2+\gamma_1)$$
$$+2n_3k_2\cos 2(\gamma_2+\gamma_1)\}$$
$$-\{(n_1-n_2)^2+(k_1-k_2)^2\}\{(n_2^2-n_3^2+k_2^2)\sin 2(\gamma_2-\gamma_1)$$
$$+2n_3k_2\cos 2(\gamma_2-\gamma_1)\}$$
$$+2(n_1^2-n_2^2+k_1^2-k_2^2)A\sin 2\gamma_1 - 4(n_1k_2-n_2k_1)C\cos 2\gamma_1$$

$$A = (n_2^2+n_3^2+k_2^2)\cosh 2\alpha_2 + 2n_2n_3\sinh 2\alpha_2$$

$$B = (n_2^2-n_3^2+k_2^2)\cos 2\gamma_2 - 2n_3k_2\sin 2\gamma_2$$

$$C = (n_2^2+n_3^2+k_2^2)\sinh 2\alpha_2 + 2n_2n_3\cosh 2\alpha_2$$

$$D = (n_2^2-n_3^2+k_2^2)\sin 2\gamma_2 + 2n_3k_2\cos 2\gamma_2$$

$$\alpha_1 = \frac{2\pi k_1 d_1}{\lambda} \qquad \alpha_2 = \frac{2\pi k_2 d_2}{\lambda}$$

$$\gamma_1 = \frac{2\pi n_1 d_1}{\lambda} \qquad \gamma_2 = \frac{2\pi n_2 d_2}{\lambda}$$

n_1-ik_1 is the complex refractive index of the first layer of thickness d_1 which is equivalent rough surface layer.

n_2-ik_2 is the complex refractive index of the second layer (which was a CdS or ZnS film) of thickness d_2.

λ is the wavelength of light.

The measured reflectance and transmittance of CdS and ZnS films were treated as R_2 and T_2 respectively, i.e. from double films. Thus from known values of n_1, k_1, R_2 and T_2, the solutions, of the above equations for n_2 and k_2, and the thicknesses d_1 and d_2, were obtained by the procedure discussed in detail by Denton et al (1972). In this way, i.e. using the Schopper formula to estimate the constants for the surface layer and then solving the double layer equations, it has been found possible to obtain satisfactory closure of dispersion curves and consequently unambiguous values for the optical constants of the films, and in particular accurate determinations of absorption curves.

6.8 EXPERIMENTAL RESULTS

6.8.1 CADMIUM SULPHIDE

Some fifty different films of CdS deposited at different rates, at different substrate temperatures and of different thicknesses, were studied in the present work. It was found that the optical properties of these films were independent of film thicknesses (60-350 nm) and rate of depositions (20 to 60 nm per minute), but were dependent on substrate temperatures. In respect to the substrates temperatures at which they were deposited, these may be divided into three groups:

type I those deposited on substrates at 25°C
type II those deposited on substrates at 140°C
type III those deposited on substrates at 180°C

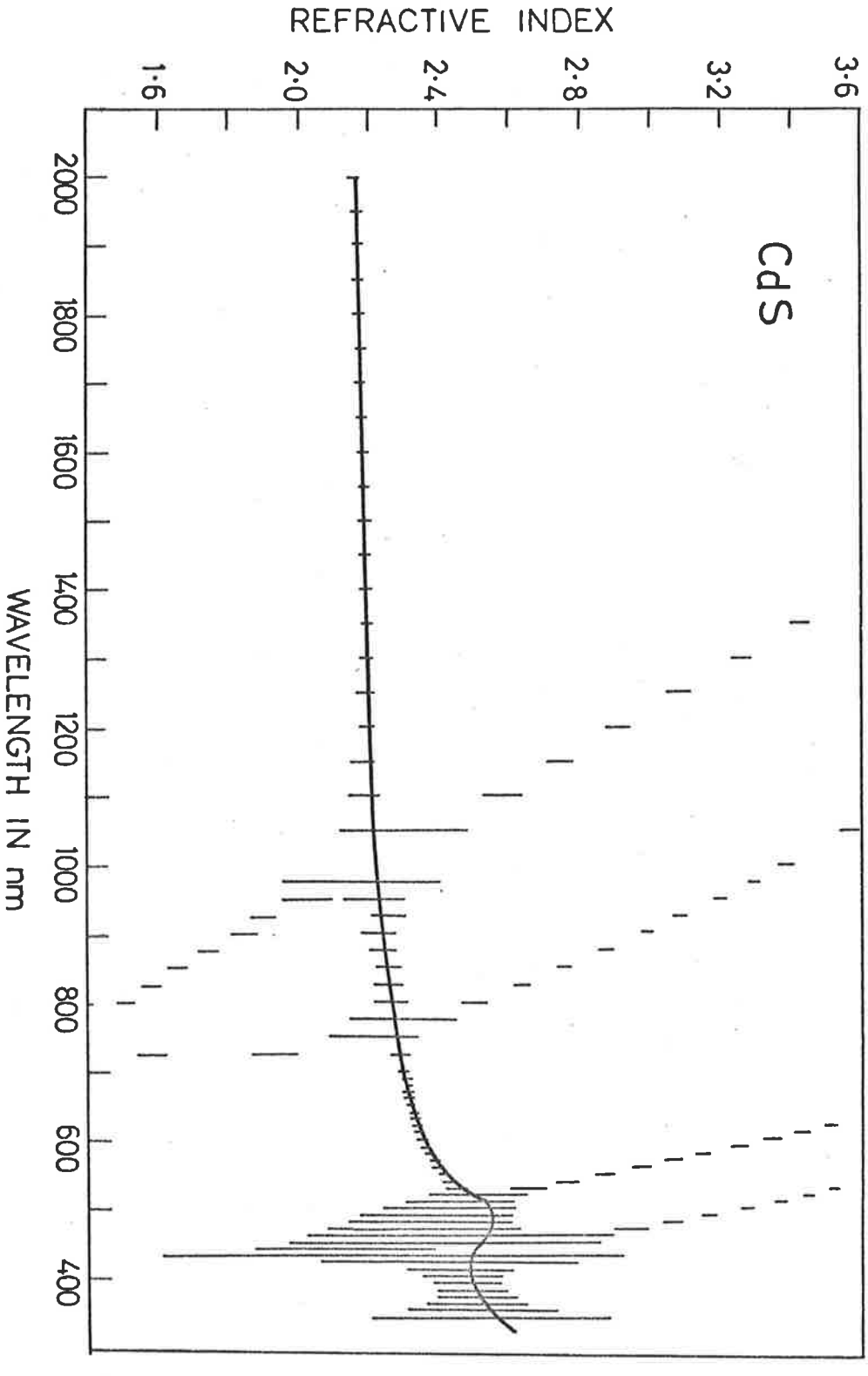
REFRACTIVE INDEX
1·6
2·0
2·4
2·8
3·2
3·6
WAVELENGTH IN nm
2000
1800
1600
1400
1200
1000
800
600
400
CdS

FIGURE 6·6

It may be mentioned that all of the optical results discussed here were obtained by the double layer method outlined above. Figure 6.6 is a typical dispersion curve for a type II film, obtained from the data shown in Figure 6.1 for d_1 = 13 nm and d_2 = 163 nm. It shows the multiple solutions and proper closure of the curve. Where the error bars are large they probably grossly overestimate the error for reasons discussed by Denton et al (1972). Figure 6.7 is the plot of the absorption index versus wavelength for the same film (i.e. type II).

In Figure 6.8, the curves for n and k versus wavelength are plotted for each of the three types of CdS films, as is indicated in the figure. The observed variations in the results for different specimens of a given type of film were less than 1% for n and less than 5% for k.

In Section 6.6.1 it was explained that the Davies reflection-correction method can be applied only in the U.V. region. The n and k values at different wavelengths, obtained by this method are compared with those obtained by the double layer method, in Table I, for a film of each type. The agreement is good for films of type II and III but less good for type I. The double layer method has been preferred since it is valid over the whole wavelength range, and the choice of parameters for the very thin surface layer is not at all critical in its effect on the final values of the optical constants of the film (Denton et al, 1972).

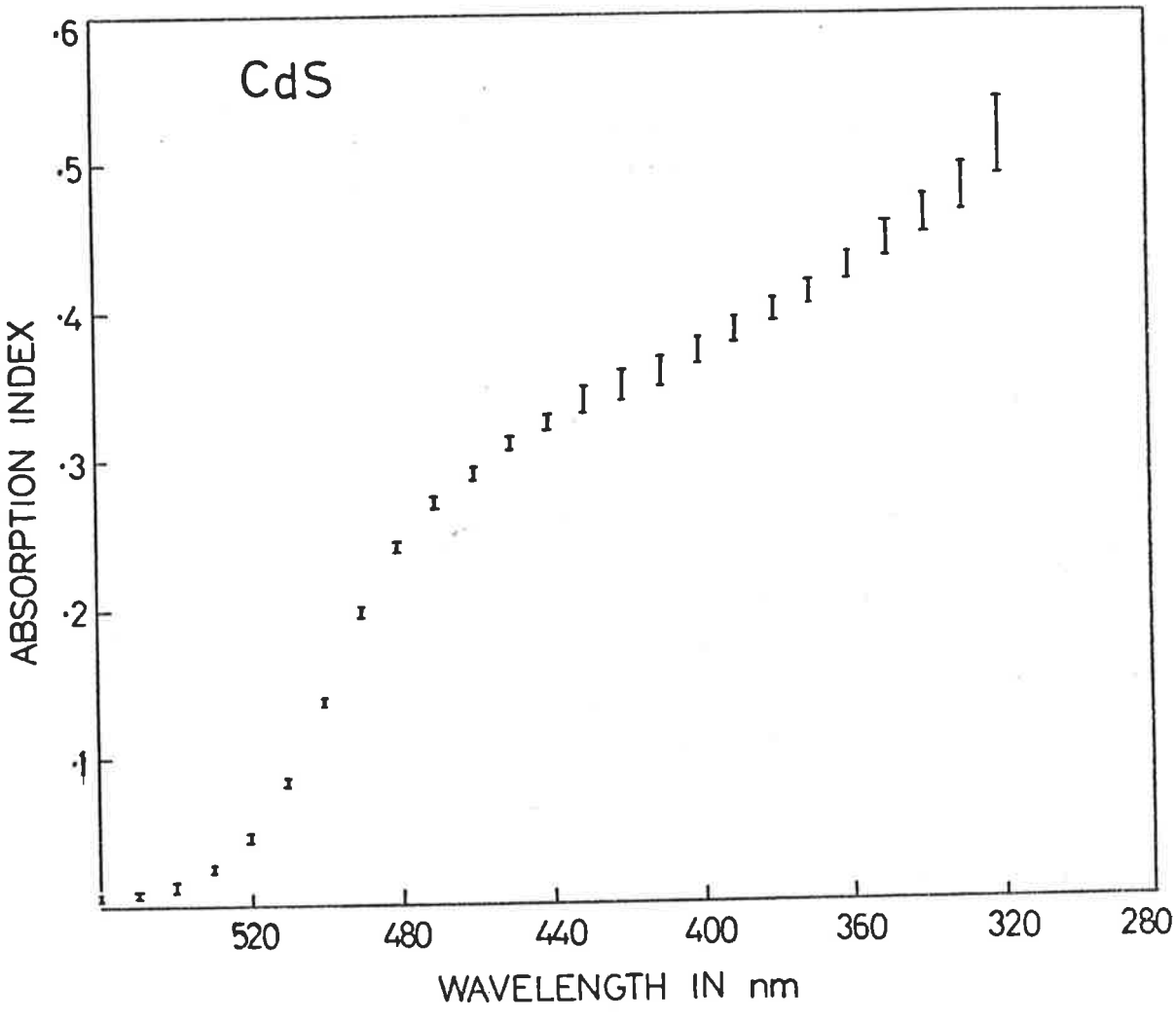
CdS
ABSORPTION INDEX
·6
·5
·4
·3
·2
·1
520
480
440
400
360
320
280
WAVELENGTH IN nm

FIGURE 6·7

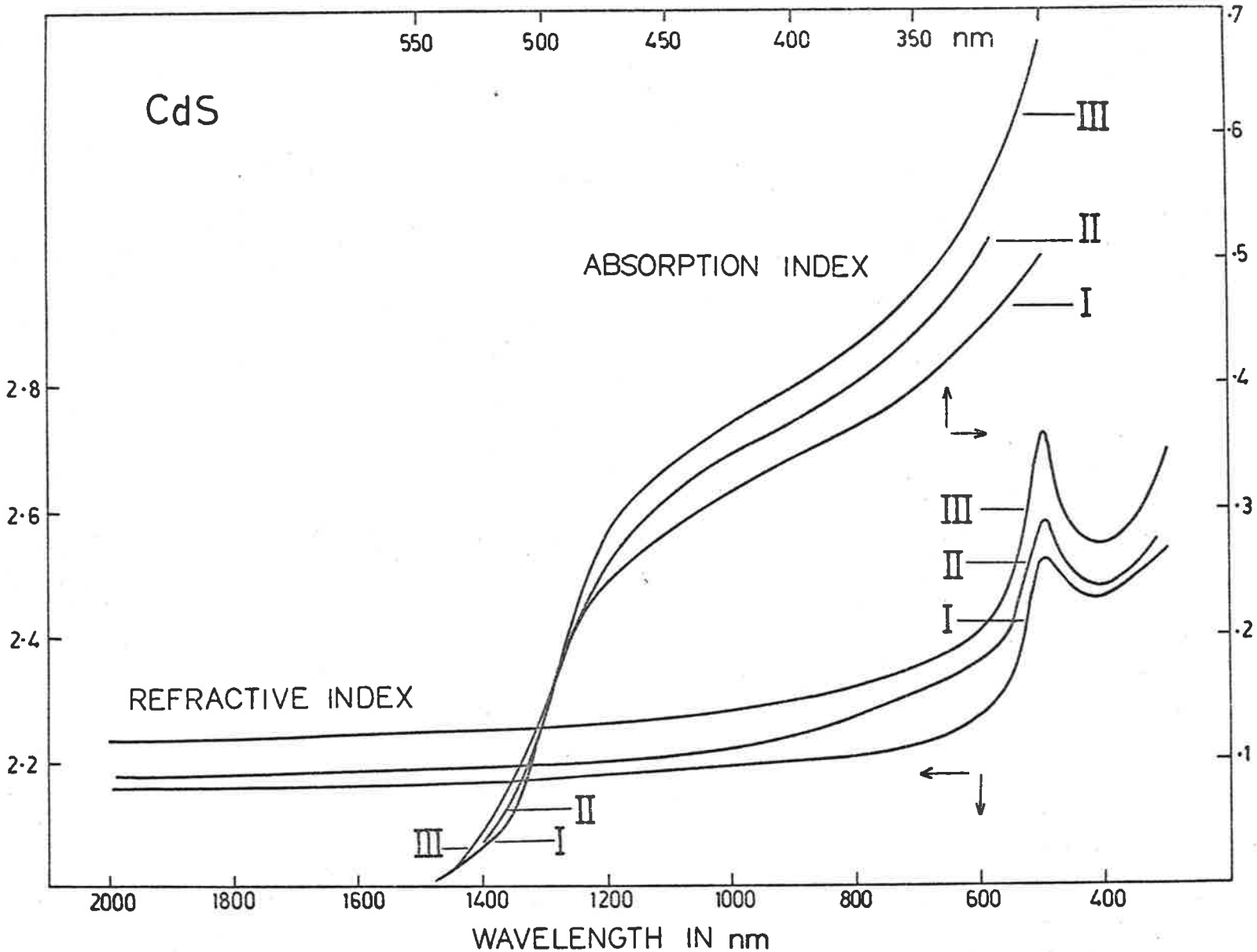
CdS
550
500
450
400
350 nm
ABSORPTION INDEX
III
II
I
REFRACTIVE INDEX
2·8
2·6
2·4
2·2
·7
·6
·5
·4
·3
·2
·1
2000
1800
1600
1400
1200
1000
800
600
400
WAVELENGTH IN nm

FIGURE 6·8

TABLE I

The optical constants of the three types of CdS films obtained by using the two methods of allowing for surface roughness.

FILM TYPE	WAVELENGTH IN nm	DAVIES CORRECTION METHOD		DOUBLE LAYER METHOD	
		n	k	n	k
I	400	2.53	0.316	2.47	0.341
	380	2.51	0.336	2.48	0.361
	360	2.53	0.356	2.49	0.381
	340	2.61	0.383	2.50	0.411
	320	2.85	0.416	2.51	0.452
	300	2.76	0.466	2.53	0.502
II	400	2.49	0.356	2.47	0.370
	380	2.50	0.377	2.49	0.391
	360	2.51	0.405	2.51	0.420
	340	2.55	0.444	2.55	0.460
	320	2.64	0.496	2.62	0.516
III	400	2.55	0.383	2.52	0.397
	380	2.56	0.407	2.56	0.421
	360	2.57	0.440	2.57	0.455
	340	2.59	0.480	2.60	0.496
	320	2.62	0.544	2.63	0.562
	300	2.70	0.653	2.69	0.675

Table II shows the thicknesses of films and surface layers as estimated from the criterion of closure of the dispersion curves. It is seen that the thicknesses of the equivalant surface layers depend on the film thicknesses and on the substrates temperatures. No appreciable dependence on the evaporation rate (ranging from 20 to 60 nm/minute) was observed. It increases with increasing film thickness

for a given type. For a given film thickness it is greater for a type I than for a type II, which in turn is greater than that for a type III film.

TABLE II

Film Type	Film Thickness in nm	Thickness of Surface Layer in nm
CdS Type I	50	4
CdS Type I	70	6
CdS Type I	150	15
CdS Type I	300	18
CdS Type II	150	12
CdS Type II	200	14
CdS Type III	150	10
CdS Type III	200	12
ZnS Type I	40	1
ZnS Type I	150	10
ZnS Type I	200	12
ZnS Type II	150	8
ZnS Type II	200	10

6.8.2 ZINC SULPHIDE

It was found that the dependence, of the optical properties of ZnS films, on the film thicknesses, rates of evaporations and substrates temperatures, was similar to that for CdS films. The ZnS films, studied, may be divided into two groups;

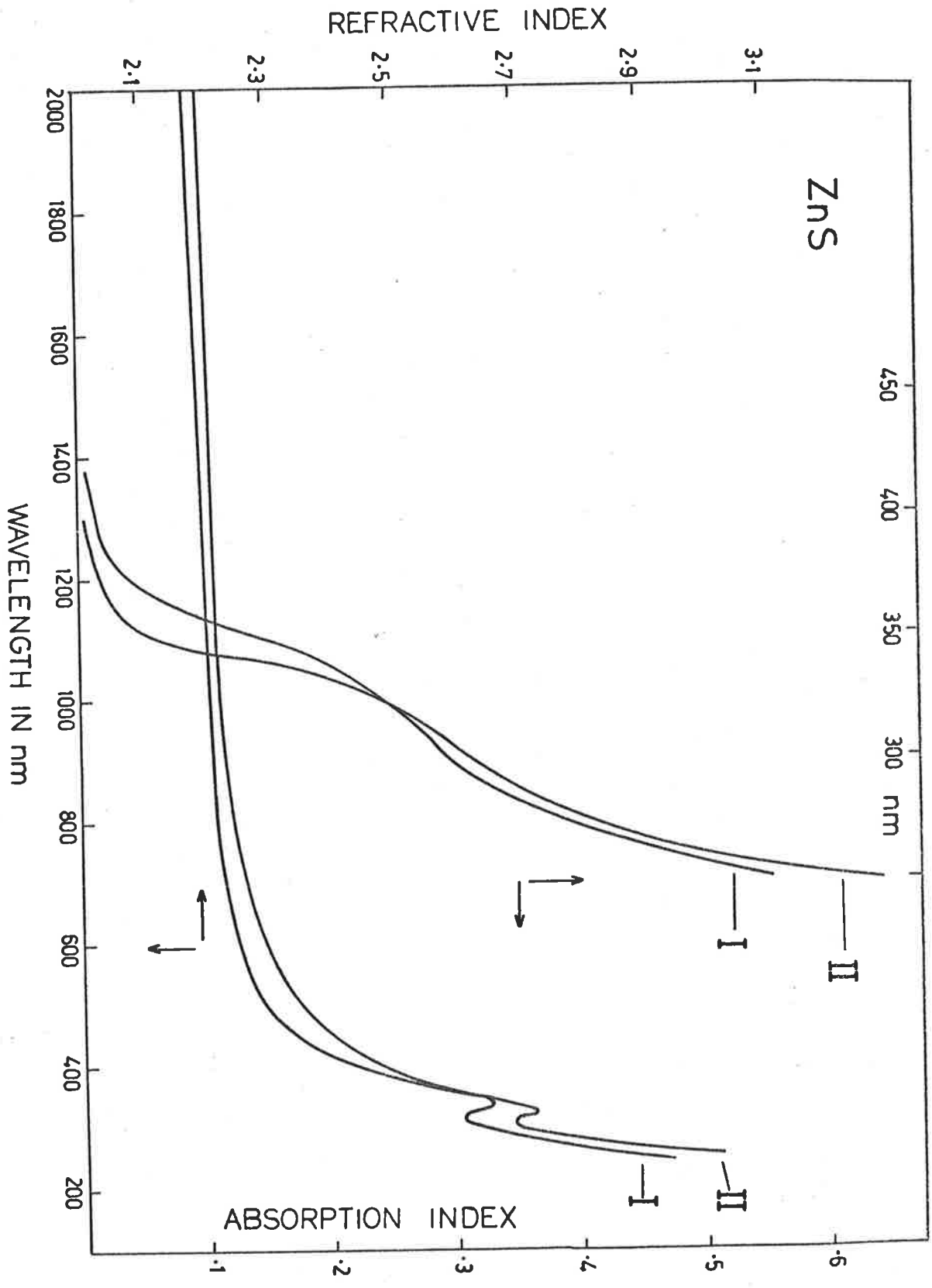
REFRACTIVE INDEX
2·1
2·3
2·5
2·7
2·9
3·1
ZnS
2000
1800
1600
1400
1200
1000
800
600
400
200
WAVELENGTH IN nm
450
400
350
300 nm
I
II
I
II
ABSORPTION INDEX
·1
·2
·3
·4
·5
·6

FIGURE 6·9

type I those deposited on substrates at 25°C.

type II those deposited on substrates at 180°C.

All the results, from different films, were obtained by the use of the double layer method. Figure 6.9 shows the curves for n and k versus wavelength, plotted for each of the two types of ZnS films, as is indicated in the figure. The variations in n and k for different specimens of a given type of film were less than 1% and 5% respectively. The thicknesses of the surface layers for each type of film, estimated from the criterion of closure of the dispersion curves, are shown in Table II.

6.9 STUDY OF STRUCTURE OF THE FILMS BY THE METHOD OF X-RAY POWDER DIFFRACTION

The structures of the films were studied by the x-ray powder diffraction method, for which the films were scraped from the substrates and the material was introduced into thin walled polythene tubes. Exposures were made using Cu Kα radiation.

6.9.1 CdS FILMS

X-ray diffraction patterns (Figure 6.10), thus obtained, show that all the films were predominantly hexagonal. The lines were sharper for films of type III than for films of type I. There is some possibility of cubic structure present in the films for reasons discussed below:

It is found in the ASTM powder diffraction data (Escoffery, 1964), for hexagonal CdS, that the reflection from the plane (101) is the most intense. While, from the patterns for CdS films, shown in Figure 6.10,

(a) CdS type I (Exposure time 2 hours)
(b) CdS type III (Exposure time 2 hours)
(c) CdS type III (Exposure time 8 hours)
(d) ZnS type I (Exposure time 2 hours)
(e) ZnS type II (Exposure time 2 hours)
(a)
(b)
(c)
(d)
(e)

FIGURE 6.10

it is clear that reflection from (002) is the most intense. This difference could be explained by the presence of some cubic phase in the films because the most intense reflection in the cubic structure is due to the plane (111) and the d-value for this is almost equal to that for the hexagonal (002) planes. So the hexagonal (002) reflection observed here may have some contribution from cubic (111) planes. On the other hand reflection from cubic (200) is absent, but this line ought to be weak. Therefore the existance of a small proportion of cubic phase cannot be ruled out. As far as higher order reflections from the cubic phase are concerned, it is found that there are corresponding reflections due to the hexagonal phase with almost the same values of d, and, as is discussed by Escoffery (1964), it is difficult to separate these two structures.

Hence it may be concluded that the CdS films were predominently hexagonal with a possibility of cubic structure in small proportion present in them. It is clear from Figure 6.10 that there was a slight improvement in the crystallinity of the films with the increase of substrate temperature. This is also confirmed by Shallcross (1967).

6.9.2 ZnS FILMS

X-ray diffraction patterns (Figure 6.10) from ZnS films of type I, showed broad diffuse lines (which are clearer in the negatives), which correspond to the cubic structure. Vlasenko (1959) obtained evaporated films of the cubic modification with a poorly ordered lattice on glass substrates at room temperature. Present results seem to be consistent

with those of Vlasenko. But Hall and Ferguson (1955) obtained amorphous films by evaporation on to glass substrates at room temperatures.

The patterns obtained for the type II films were sharper than those of type I. These lines also corresponded to the cubic phase except for a very broad diffuse line appearing adjacent to the (111) line of the cubic phase. This could be attributed to the (100) reflection from hexagonal crystallites. But the higher order reflections for the hexagonal phase could not be detected. This indicated a very small proportion of hexagonal phase present in the samples. It is clear that the crystallinity of the films increased with increasing substrate temperatures.

Use of these results will be made, in the next chapter, to explain the observed variations in the optical constants of the different types of films of ZnS and CdS. Also in the next chapter the dependence of absorption on photon energy, is analysed, to obtain the values of the absorption edges and to explain different electronic transitions that occur in these films.

6.10 COMPARISON OF PRESENT RESULTS WITH THE PUBLISHED WORK

A review of the previous evaluations of the optical constants for evaporated thin films, and bulk forms, of CdS and ZnS is given by Moss (1959).

In Figure 6.11 results obtained by different workers (Moss 1959) for CdS and ZnS films are compared with those of the present work for the type I films of both semiconductors. For CdS, n determined by

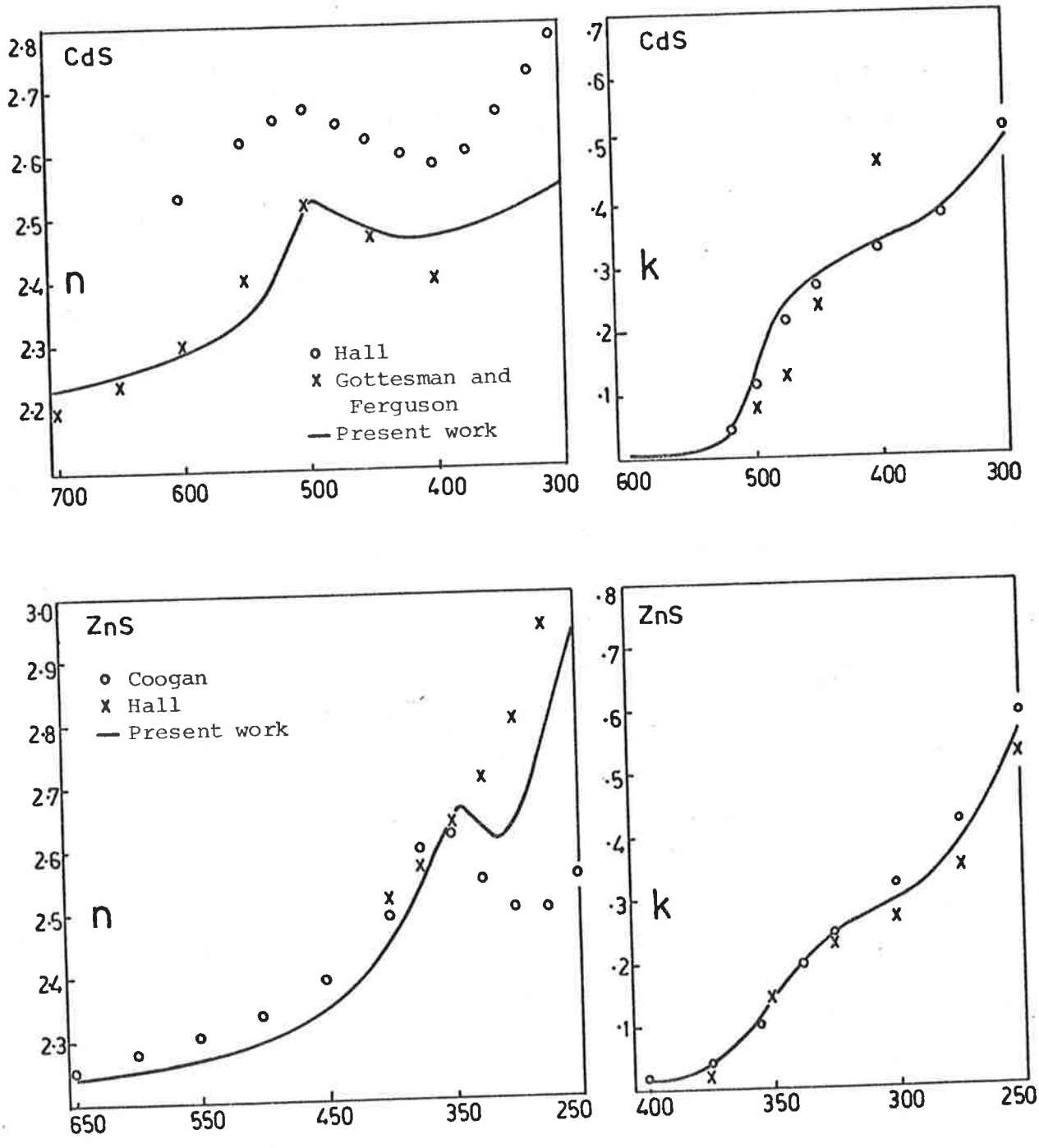
CdS
n
o Hall
x Gottesman and Ferguson
— Present work
2·8
2·7
2·6
2·5
2·4
2·3
2·2
700
600
500
400
300
CdS
k
·7
·6
·5
·4
·3
·2
·1
600
500
400
300
ZnS
n
o Coogan
x Hall
— Present work
3·0
2·9
2·8
2·7
2·6
2·5
2·4
2·3
650
550
450
350
250
ZnS
k
·8
·7
·6
·5
·4
·3
·2
·1
400
350
300
250

FIGURE 6·11

Goltesman and Ferguson (1954) is in agreement but that determined by Hall (1956) is higher than that of the present work. The absorption determined by Hall is in very good agreement with that of present work, while that of Goltesman and Ferguson shows no agreement.

For ZnS, Coogan's (1957) results are in very good agreement with those of the present work, except in the wavelength range below 350 nm where the present n values are slightly higher. This latter difference is a consequence of taking into account the effects of surface roughness, which would be more significant at the shorter wavelengths. Hall's n-values are too large but his absorption is in good agreement with that of the present work. Also the peak in the dispersion curve at a wavelength of 345 nm is missing in Hall's results. Present results show no evidence of a dependence of refractive index on film thickness as suggested by Kuwabara and Isiguro (1952) and in this respect agree with those of Coogan, Hall and Goltesman and Ferguson.

The refractive indices for type III films of CdS and type II films of ZnS, in the transparent regions are about 3 to 4% smaller than those of single crystals of CdS and ZnS, obtained by Czyak et al (1957).

CHAPTER 7

ABSORPTION AND ELECTRONIC TRANSITIONS IN CdS AND ZnS FILMS

7.1 INTRODUCTION

The optical constants of CdS and ZnS films, determined as described in the previous chapter, were analysed in order to determine the band gaps of each of the semiconductors and the nature of the optical transitions taking place due to absorption of photons of energy higher than the band gap. The experimental results for both materials can be explained by the occurance of direct transitions in the energy region just above the band gap, followed by combined direct and indirect transitions beyond this region, assuming the energy bands to be parabolic. The experimental results can also be explained by assuming only direct transitions between non-parabolic bands. It was concluded that direct transitions between non-parabolic bands may occur together with indirect transitions.

7.2 OPTICAL TRANSITIONS

The theory of the absorption process in a crystalline material is treated in detail in a number of books, e.g. Smith (1961), Harbeke (1972) etc. For the allowed direct transitions between parabolic energy bands the absorption coefficient K, follows the relation

$$(EnK_1)^2 = C_1(E-E_{g1}) \qquad 7.2.1$$

and for the allowed indirect transitions between the parabolic energy

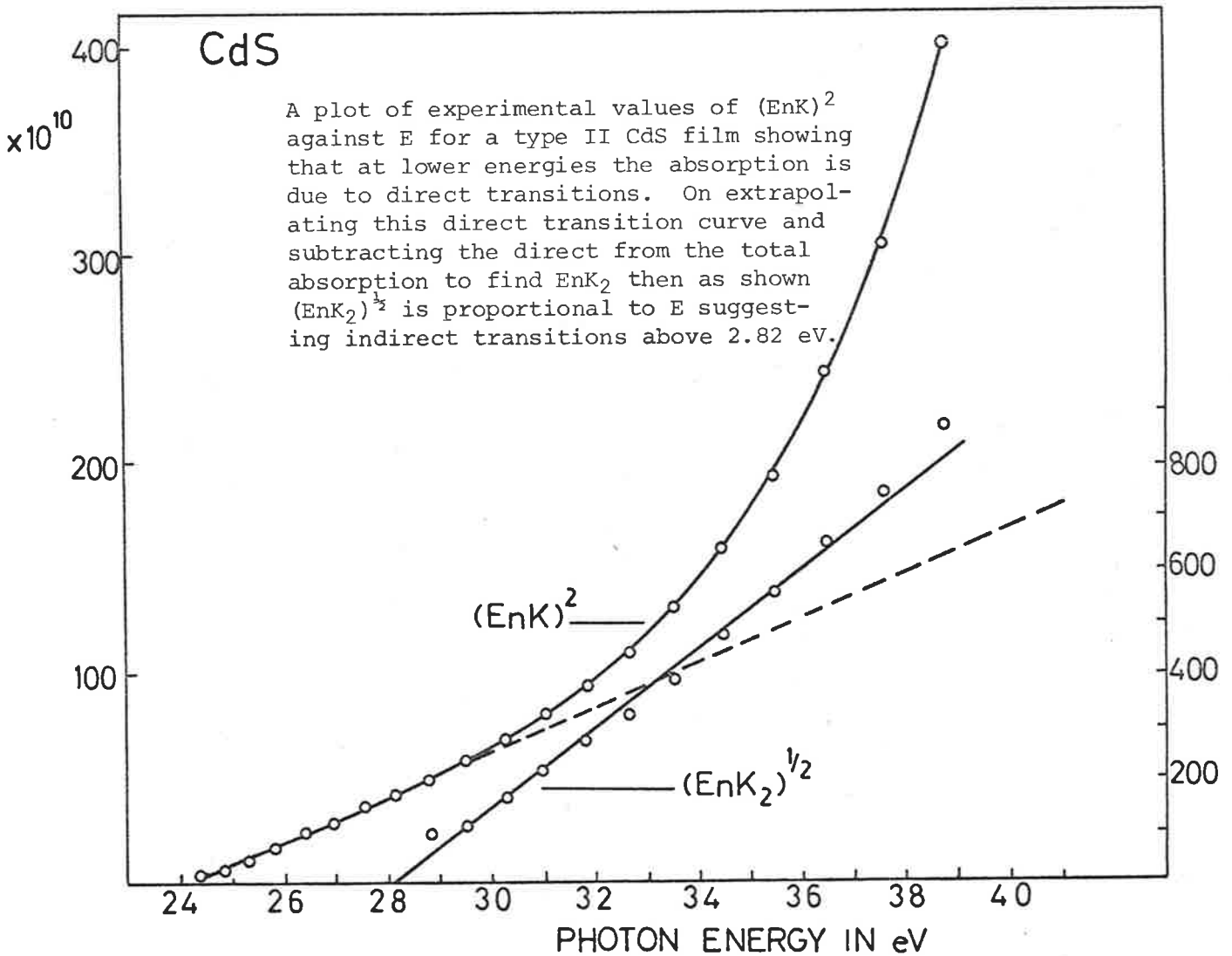
CdS
A plot of experimental values of $(EnK)^2$ against E for a type II CdS film showing that at lower energies the absorption is due to direct transitions. On extrapolating this direct transition curve and subtracting the direct from the total absorption to find EnK_2 then as shown $(EnK_2)^{\frac{1}{2}}$ is proportional to E suggesting indirect transitions above 2.82 eV.
$\times 10^{10}$
400
300
200
100
800
600
400
200
$(EnK)^2$
$(EnK_2)^{1/2}$
24
26
28
30
32
34
36
38
40
PHOTON ENERGY IN eV

FIGURE 7·1

bands the absorption coefficient K_2 follows

$$(EnK_2)^{\frac{1}{2}} = C_2(E-E_{g2}) \qquad 7.2.2$$

where n is the refractive index at photon energy E and E_{g1} and E_{g2} are the band gaps for the allowed direct and indirect transitions, respectively. C_1 and C_2 are constants. In the relation for the indirect transition the phonon energy has been neglected.

7.3 ELECTRONIC TRANSITIONS IN CdS AND ZnS FILMS

The optical constants n and k for different types of films of CdS and ZnS were given in Chapter 6. From these results plots of $(EnK)^2$ against photon energy E are shown in Figure 7.1 for type II CdS film and in Figure 7.2 for type II ZnS film. Figure 7.1 suggests that the absorption follows the law for direct transitions up to an energy of 2.82 eV at which point a second absorption process begins to operate. Similarly it is clear from Figure 7.2 that absorption in ZnS films follows the law for direct transitions up to an energy of 4.1 eV, at which point another absorption process starts.

For energies above 2.82 eV for CdS, and 4.1 eV for ZnS, the absorption coefficient is assumed to be the sum of two parts, K_1 due to the first process, and K_2 due to the second. K_2 was obtained by extrapolating the straight line of Figure 7.1 for CdS (and Figure 7.2 for ZnS) and subtracting the resulting values of K_1 from the total absorption coefficient K. For all the types of CdS and ZnS films this second absorption process appears to be due to indirect transitions as is shown by the plots $(EnK_2)^{\frac{1}{2}}$ against E in Figure 7.1 and Figure 7.2.

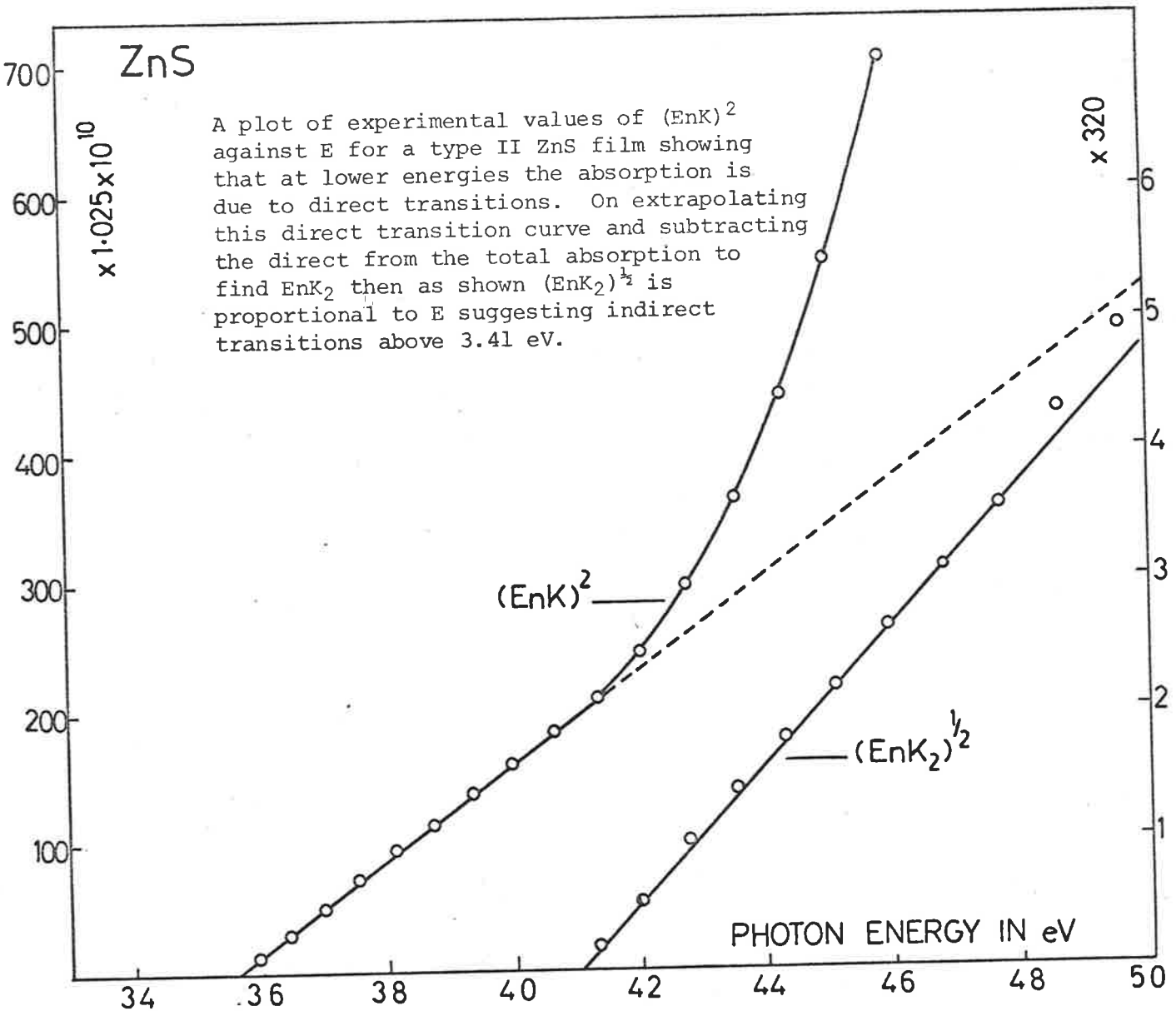
ZnS
A plot of experimental values of $(EnK)^2$ against E for a type II ZnS film showing that at lower energies the absorption is due to direct transitions. On extrapolating this direct transition curve and subtracting the direct from the total absorption to find EnK_2 then as shown $(EnK_2)^{\frac{1}{2}}$ is proportional to E suggesting indirect transitions above 3.41 eV.
x 1·025x10^10
x 320
700
600
500
400
300
200
100
6
5
4
3
2
1
$(EnK)^2$
$(EnK_2)^{1/2}$
PHOTON ENERGY IN eV
34
36
38
40
42
44
46
48
50

FIGURE 7·2

The measured variations in absorption index (k) for a number of samples of each of the three types of CdS are represented by vertical bars in Figure 7.3. The continuous curves shown in the same figure are the results of the calculations based on the theoretical formulae (7.2.1 and 7.2.2) assuming direct transitions from 2.42 to 2.82 eV, and both direct and indirect transitions occuring beyond 2.82 eV, the constants C_1, C_2, Eg_1 and Eg_2 being found from plots like those of Figure 7.1. The band gaps and the other constants for each type of CdS films are given in Table 3. Figure 7.4 shows similar results for the two types of ZnS films and the constants Eg_1, Eg_2, C_1 and C_2 for these are also given in Table 3. The agreement between these theoretical curves and the experimental results for each type of CdS and ZnS films is remarkably good.

TABLE III

FILM	TYPE	Eg_1 in eV	Eg_2 in eV	C_1 in $eV \cdot m^{-2}$	C_2 in $eV^{-\frac{1}{2}} m^{-\frac{1}{2}}$
CdS	I	2.42	2.82	89×10^{14}	7.3×10^{3}
CdS	II	2.42	2.82	107×10^{14}	7.9×10^{3}
CdS	III	2.42	2.82	130×10^{14}	8.5×10^{3}
ZnS	I	3.45	3.98	244×10^{14}	15.1×10^{3}
ZnS	II	3.57	4.10	381×10^{14}	16.9×10^{3}

In Figure 7.5 plots of EnK against E for a type II CdS film are shown. The continuous line is the theoretical curve for direct and indirect transitions between parabolic bands as is discussed above. The open circles

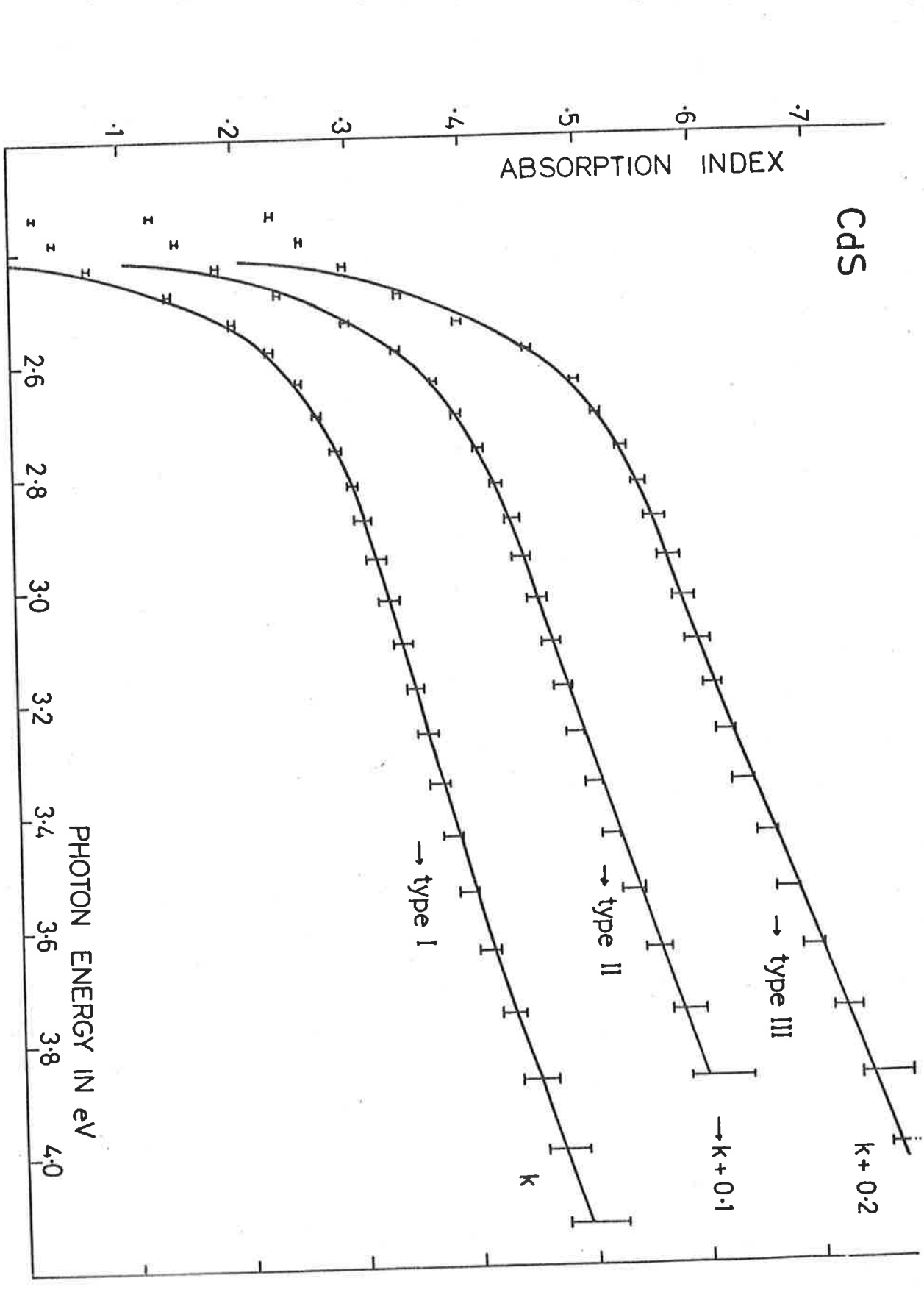
CdS
ABSORPTION INDEX
·1
·2
·3
·4
·5
·6
·7
PHOTON ENERGY IN eV
2·6
2·8
3·0
3·2
3·4
3·6
3·8
4·0
k + 0·2
→ type III
→ k + 0·1
→ type II
k
→ type I

FIGURE 7·3

represent the experimental points. Similar results for a type II ZnS film are shown in Figure 7.6.

From the above it follows that both CdS and ZnS are direct band gap materials which is in agreement with Shionoya (1966) and Segall and Marple (1967). It may be mentioned that the optical properties of these films were measured at room temperature. Therefore the values of band gaps given here are those for room temperature. The value of the band gap for crystalline CdS, quoted by Kittel (1971) is also 2.42 eV and for ZnS 3.6 eV. In the present work the band gap value for type II films of ZnS is 3.57 eV but for type I it is 3.45 eV. This difference in the absorption edges of the two types is probably due to poor crystallinity of type I films (Section 6.9). It was seen in the case of amorphous Ge that the absorption edges shift to lower energies when compared to those in crystalline Ge (Chapter 5).

The indirect transitions beginning at 0.4 eV and 0.53 eV above the band gaps in CdS and ZnS respectively are also consistent with the theoretical band structures which have been calculated for hexagonal CdS and cubic ZnS, for example those of Bergstresser and Cohen (1967), Herman et al (1967), Treusch et al (1967) and Cohen (1967). This is on the assumption that indirect transitions such as $L_3 \rightarrow \Gamma_1$ in cubic crystals, and $A_{56} \rightarrow \Gamma_1$ or $H_3 \rightarrow \Gamma_1$ in hexagonal crystals, can occur.

However, at the higher energy end of the measurements, the magnitude of the indirect absorption is comparable with the direct absorption whereas it might be expected to be an order of magnitude smaller. For this reason the effect of non-parabolic energy bands on the absorption processes have

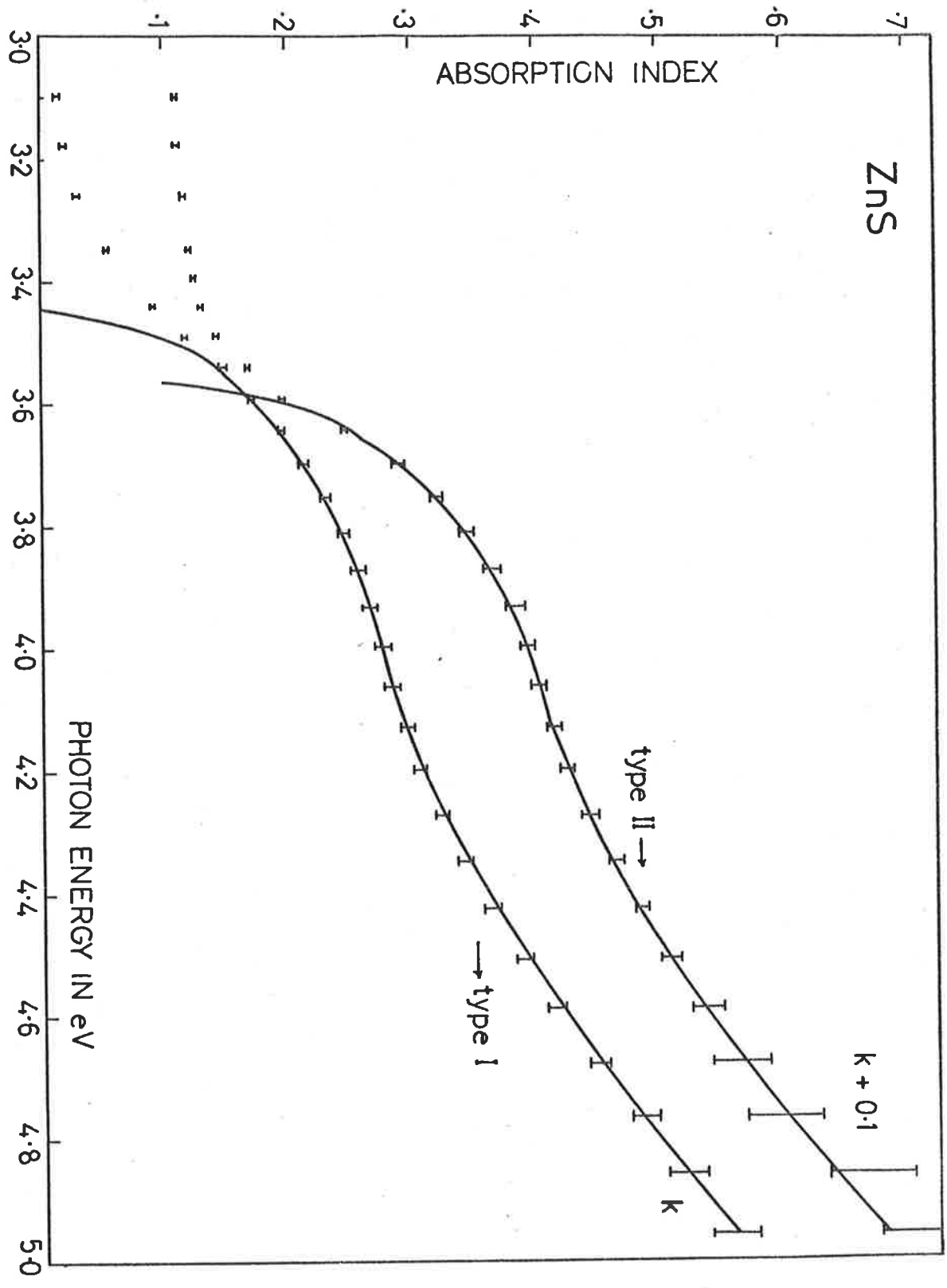
ZnS
ABSORPTION INDEX
·1
·2
·3
·4
·5
·6
·7
3·0
3·2
3·4
3·6
3·8
4·0
4·2
4·4
4·6
4·8
5·0
PHOTON ENERGY IN eV
type II →
→ type I
k + 0·1
k

FIGURE 7·4

been considered, as it is unlikely that a parabolic form could hold over the energy range of the present measurements. An investigation of this possibility, following suggestions made by Dr. Tomlin, is presented in the next section.

7.4 OPTICAL ABSORPTION DUE TO THE DIRECT TRANSITIONS BETWEEN NON-PARABOLIC BANDS

Following Smith (1961, p407), his calculations may be modified by writing the E, κ relation (using κ for the wave vector to avoid confusion with the k used for absorption index) in the form

$$\kappa^3 = (E-E_g)^{3/2} \sum_{n=0} A_n (E-E_g)^{\frac{n}{2}} \qquad 7.4.1$$

instead of $E = E_g + \frac{\hbar^2}{2m_r} \kappa^2$

where $E = h\omega$ is the energy difference between the valence and conduction bands for a given κ, E_g is the direct band gap, m_r is the reduced effective mass of the electron-hole pair given by

$$m_r = \frac{m_e m_h}{m_e + m_h}$$

where m_e and m_h are the effective masses of electron and hole, respectively. A_n are constants. The first term in equation 7.4.1 then gives a quadratic $E-E_g$, κ relation and the remaining terms of the series, or polynomial, express deviation from such behaviour.

On differentiating equation 7.4.1

$$\kappa^2 d\kappa = \frac{1}{3} \hbar \sum_{n=o} \frac{n+3}{2} A_n (E-E_g)^{\frac{n+1}{2}} \qquad 7.4.2$$

The transition probability per second per unit volume $P(\omega)$ is

(Smith, equation 66)

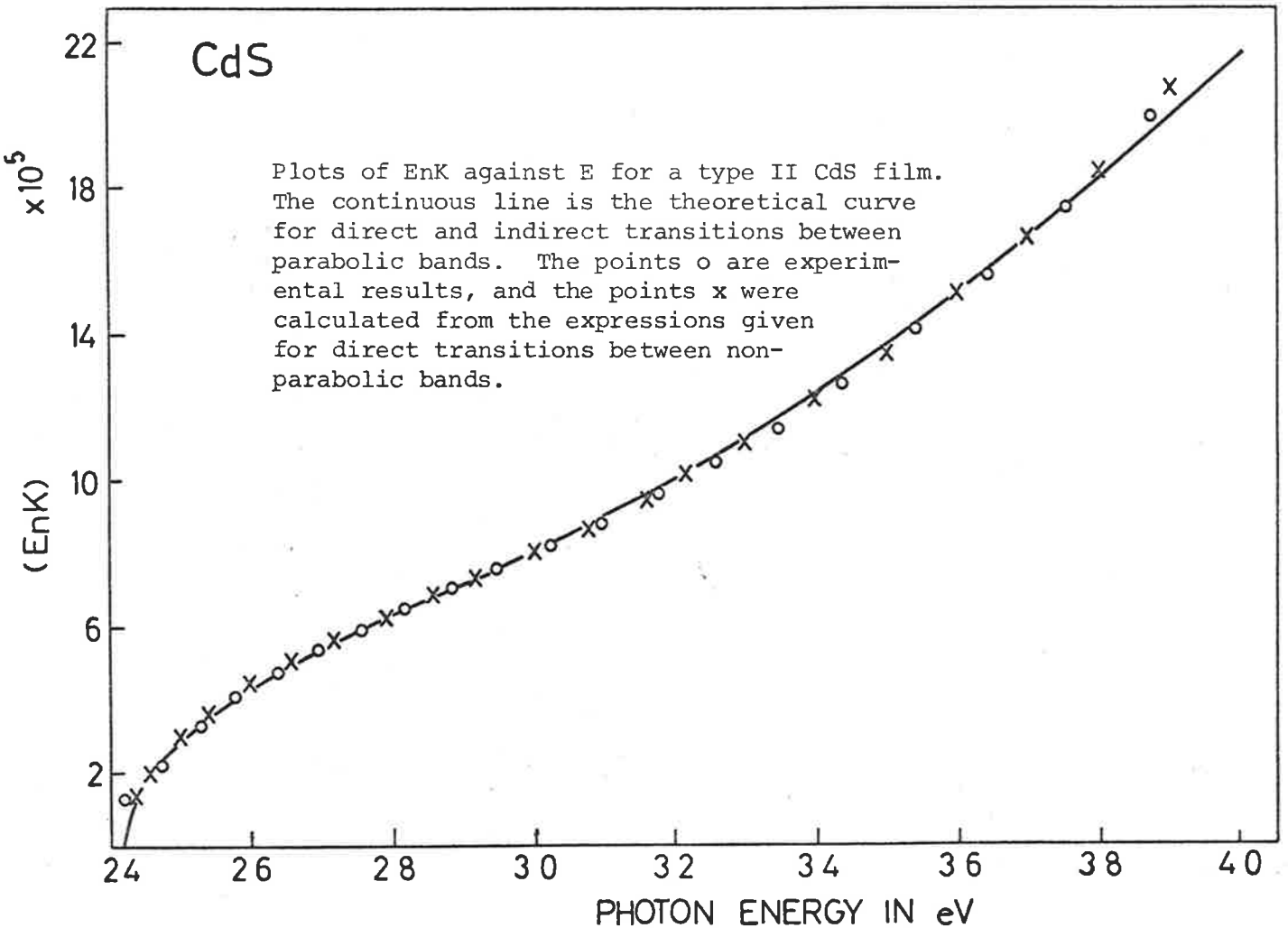
CdS
Plots of EnK against E for a type II CdS film. The continuous line is the theoretical curve for direct and indirect transitions between parabolic bands. The points o are experimental results, and the points x were calculated from the expressions given for direct transitions between non-parabolic bands.
(EnK) x10^5
22
18
14
10
6
2
24
26
28
30
32
34
36
38
40
PHOTON ENERGY IN eV

FIGURE 7.5

$$P(\omega)t = \frac{e^2A^2}{\pi^2m^2\hbar^2} \int \overline{p_{mo}^2} \frac{\sin^2 \frac{1}{2}(\omega_{mo}-\omega)t}{(\omega_{mo}-\omega)^2} \kappa^2 d\kappa \qquad 7.4.3$$

where A is the vector potential of the incident electromagnetic wave, e and m are the charge and mass of a free electron, t is the time and $\overline{p_{mo}^2}$ is the matrix element of the momentum operator.

Putting $\frac{1}{2}(\omega_{mo}-\omega)t = \chi$ and $d\omega_{mo} = \frac{2}{t} d\chi$ in equation 7.4.3

$$P(\omega) = \frac{e^2A^2}{6\pi^2m^2\hbar} \int \overline{p_{mo}^2} \frac{\sin^2\chi}{\chi} \sum_{n=o} \frac{n+3}{2} A_n (E-E_g)^{\frac{n+1}{2}} d\chi \qquad 7.4.4$$

If it is assumed that $\overline{p_{mo}^2}$ is a constant, and since $\frac{\sin\chi}{\chi}$ is significant over a range of ω_{mo} very close to ω the summation may be taken outside the integral to give

$$P(\omega) = \frac{e^2A^2\overline{p_{mo}^2}}{6\pi m^2\hbar} \sum_{n=o} \frac{n+3}{2} A_n (E-E_g)^{\frac{n+1}{2}} \qquad 7.4.5$$

since $\int_{-\infty}^{\infty} \frac{\sin^2\chi}{\chi} d\chi = \pi$

The absorption coefficient K in terms of $P(\omega)$ is (Smith, equation 70)

$$K = \frac{2\hbar P(\omega)}{\omega n A^2 \varepsilon_o c} \qquad 7.4.6$$

Thus from equations 7.4.5 and 7.4.6

$$EnK = A' \sum_{n=o} \frac{n+3}{2} A_n (E-E_g)^{\frac{n+1}{2}} \qquad 7.4.7$$

where $A' = \frac{\hbar^2e^2\overline{p_{mo}^2}}{3\pi\varepsilon_o m^2 c}$

7.4.1 EXPLANATION OF EXPERIMENTAL RESULTS ON THE BASES OF DIRECT TRANSITIONS BETWEEN NON-PARABOLIC BANDS

The theory outlined in the previous section was applied successfully to account for the experimental results for CdS and ZnS films. The points x shown in Figures 7.5 and 7.6 were calculated using the first four terms

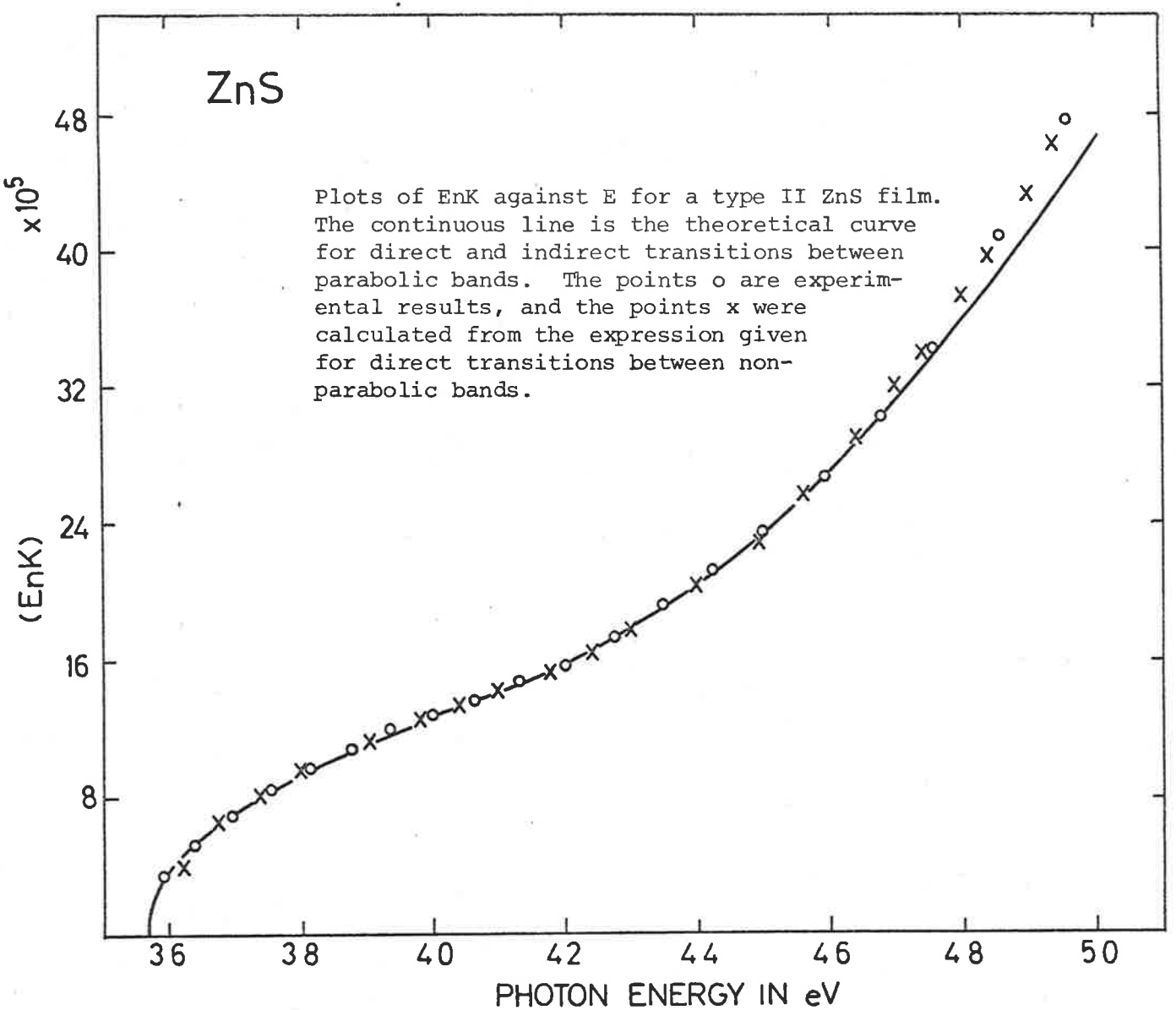
ZnS
Plots of EnK against E for a type II ZnS film. The continuous line is the theoretical curve for direct and indirect transitions between parabolic bands. The points o are experimental results, and the points x were calculated from the expression given for direct transitions between non-parabolic bands.
(EnK) x10^5
48
40
32
24
16
8
36
38
40
42
44
46
48
50
PHOTON ENERGY IN eV

FIGURE 7·6

of equation 7.4.7 and matching the experimental curves at four chosen points to determine the values of the constants $A'A_n$. These figures show also the accuracy with which the experimental data can be fitted with this method. It should be noted that the values of the constants depend significantly on the points chosen, but the resulting curve is little affected (Ralston 1965, p394). A "least squares" method also gave similar accuracy of fit although the constants differed from those obtained by a four point matching procedure.

Thus it is seen that the experimental results can be accounted for equally well by assuming the existance of direct and indirect transitions with parabolic bands, or by assuming only direct transitions between non-parabolic bands.

7.5 $(E-E_g)$ - κ PLOTS FOR NON-PARABOLIC BANDS

The relation between $(E-E_g)$ and κ (wave vector) is given by equation 7.4.1. Using the coefficients $A'A_n$ found by curve fitting, and an arbitrary value of A', the $E-E_g$, κ relation was plotted with an arbitrary κ scale, retaining the first four terms of the relation. Figure 7.7 shows such a plot for a type II CdS film. The curve marked (p) also shown in the same figure is the parabolic curve matched to the first curve at the point marked X (i.e. in equation 7.4.1), all the A_n except A_o were assumed to be zero). It appears that relatively little departure from the quadratic form is needed to account for the form of the experimental absorption curve. The $E-E_g$, κ curves obtained from the results for different types of ZnS films, showed similar behaviour.

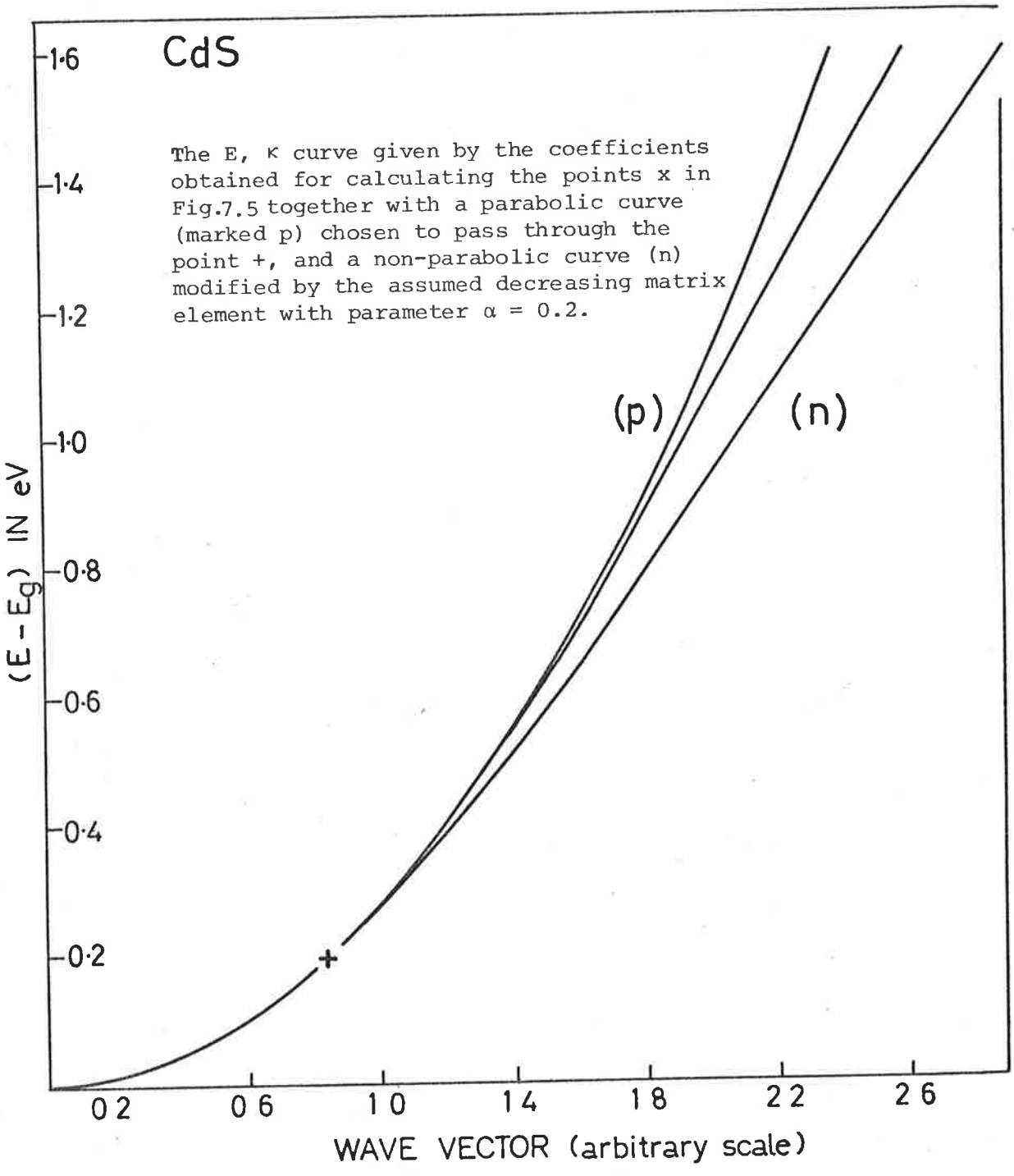
CdS
The E, κ curve given by the coefficients obtained for calculating the points x in Fig.7.5 together with a parabolic curve (marked p) chosen to pass through the point +, and a non-parabolic curve (n) modified by the assumed decreasing matrix element with parameter α = 0.2.
(p)
(n)
(E - Eg) IN eV
1·6
1·4
1·2
1·0
0·8
0·6
0·4
0·2
0 2
0 6
1 0
1 4
1 8
2 2
2 6
WAVE VECTOR (arbitrary scale)

FIGURE 7·7

7.6 NON-CONSTANT MATRIX ELEMENT

In the above discussion it was assumed that the matrix element is a constant. This may not be valid as it is known that in the case of InSb it decreases with increasing $E-E_g$ (Johnson, 1967). To asses, approximately the effect of this it is assumed that the matrix element $\overline{p^2_{mo}}$ could be expressed in terms of a series in powers of $(E-E_g)$ of which only the first two terms may be taken and writing

$$\overline{p^2_{mo}} = P\left[1 - \alpha\,(E-E_g)\right] \qquad 7.6.1$$

then in place of equation 7.4.7, retaining only the first four terms, the following expression can be obtained

$$EnK = A'\left[\frac{3}{2}A_o(E-E_g)^{\frac{1}{2}} + 2A_1(E-E_g) + (\frac{5}{2}A_2-\frac{3}{2}A\alpha)(E-E_g)^{3/2} + (3A_3 - 2A_1\alpha)(E-E_g)^2\right] \qquad 7.6.2$$

and in the expressions for A', $\overline{p^2_{mo}}$ is replaced by P.

The accuracy with which the experimental EnK data for CdS and ZnS can be fitted using the above expression with an arbitrary choice of α was as good as for that obtained using equation 7.4.7 (Figures 7.5 and 7.6). This fitting modifies the values of $A'A_o$, $A'A_1$, $A'A_2$, $A'A_3$ and consequently the shape of the E, κ curve. The curve marked (n) in Figure 7.7, shows the effect for a choice of $\alpha = 0.2$, and a range of $(E-E_g)$ such that $\alpha(E-E_g)$ remains small compared to unity. Such a decreasing matrix element broadens the E, κ curve, making the deviation from the parabolic form more than that for a constant matrix element. However the conclusion still stands that, over the energy range of the present measurements, a relatively small departure from a quadratic $E-E_g$, κ relation is sufficient to explain the form of the absorption curves in terms of direct transitions

only.

7.7 COMBINED EFFECTS OF INDIRECT TRANSITIONS TOGETHER WITH DIRECT TRANSITIONS BETWEEN NON-PARABOLIC BANDS

It was seen (Figures 7.5 and 7.6) that the experimental results can be accounted for by assuming only direct transitions between non-parabolic bands. However, theoretically calculated band structures for CdS (hexagonal form) suggest that direct transitions $\Gamma_6 \rightarrow \Gamma_1$ between non-parabolic bands may occur together with indirect transitions such as $A_{56} \rightarrow \Gamma_1$ or $H_3 \rightarrow \Gamma_1$. Similar results on ZnS (cubic form) suggest that direct transitions $\Gamma_{15} \rightarrow \Gamma_1$ between non-parabolic bands may occur together with indirect transitions $L_3 \rightarrow \Gamma_1$. For a limited range of photon energies above, 2.82 eV for CdS and 4.0 eV for ZnS the indirect absorption would be expected to obey the $EnK_2 \propto (E-E_{g2})^2$ relation, which is for indirect transitions between parabolic bands. But for higher energies this would be modified for non-parabolic bands in a way which is not easily determined. It was found that the experimental results for both the materials can be fitted just as well as in Figures 7.5 and 7.6 by combining direct absorption between non-parabolic bands, as given by equation 7.4.7, with any fraction of the amount of indirect absorption required for strictly parabolic bands. Obviously the larger the amount of indirect absorption included the smaller are the coefficients of the higher terms in equation 7.4.7 and more nearly do the bands become parabolic.

The optical measurements alone are not sufficient to separate the two contributions to the absorption process. It is not possible to assert that the onsets for the indirect transitions at 0.4 eV and 0.53 eV above the

band edges for CdS and ZnS respectively, are precise measurements of the indirect band gaps, although these are consistent with the theoretical band gap calculations.

7.8 ABSORPTION AT THE LOWER ENERGY SIDE OF THE BAND EDGE

It is clear from Figure 7.3 for CdS films and Figure 7.4 for ZnS films that there was some absorption in these films at energies less than the band edges. It was found that these absorption tails obey exponential laws with respect to the photon energy i.e.

$$K \propto \exp(E)$$

The exponential edge was first observed by Urbach (1953) in alkali halides and is often referred to as an Urbach edge. Since then this edge has been observed in various ionic compounds, and amorphous and crystalline semiconductors. There are various interpretations given for these exponential edges for example see Chopra and Bahl (1972), Wood and Tauc (1972), Olley (1973), etc.

The present results show that in all three types of CdS films and type II ZnS films, the strength of absorption in the tails is much weaker than that observed in type I ZnS films. The study of the structure (Section 6.9) of these films, showed that they had a very poor crystallinity. From which it may be concluded that in the present films, the strength of absorption in the tails decreases with the improved crystallinity. This conclusion is in agreement with Olley (1973), according to whom, the exponential absorption edge arises from the broading of excitonic absorption due to the presence of defects. The more numerous the defects the larger would be the absorption.

7.9 DISCUSSION

The n and k curves for all the three types of CdS films are shown in Figure 6.8. There is a variation of about 5% in the values of n for different types, while in the k values it is about 10 to 15%. The variation in n was obvious from the measured reflectivities in the high absorption region. The reflectivity of type I was lower than that of type II, which in turn was lower than that of type III. These veriations in the optical constants may possibly be due either to different stoichiometry or to different crystallinity, or both. No experimental check on stoichiometry of these films was made but it was found that the crystallinity of these films improved with increasing substrate temperatures. Since in all the three types the direct absorption edge was at 2.42 eV and the indirect absorption edge at 2.82 eV, variations in the stoichiometry of different types seems unlikely. Hence it may be concluded that difference in crystallinity was the main cause of the observed variations in the optical constants for the three types of CdS films. It may be mentioned that outgassing of CdS power, prior to deposition of it onto a substrate, was important. When this was not done, the deposited films were dark brown in colour, while the films whose results are discussed here had orange colour. These dark brown films had low reflectivity and showed some absorption in the region where CdS is normally transparent. This absorption may be due to different stoichiometry of these films.

There were some variations in the optical constants of the two types of ZnS films (Figure 6.9). In type I both the absorption edges shift to lower energies by 0.12 eV when compared to those for the type II. There is some possibility of different stoichiometry in the two types but once

again I think it is the difference in crystallinity which is mainly responsible for the shift of the band edges, and also the variations in the optical constants. This is based on the conclusion drawn from the results on amorphous Ge (Chapter 5) that in amorphous Ge the absorption edges shift to the lower energy side when compared with those in crystalline Ge.

7.10 CONCLUSIONS

It was observed that for CdS and ZnS films acceptable dispersion curves could not be obtained by the method of a single film on a substrate. This was because of the rough surfaces of these films. The surface roughness must be accounted for in order to obtain continuous dispersion curves. The method in which the surface of the film was treated as a separate layer, with optical constants different from those of the film itself, and then using the relations for a double layer on a substrate, was successful and reliable values of n and k for a film could be found.

It was found that the absorption increased with improved crystallinity, above the band edges, in both the materials (Table 3). This is consistent with the corresponding results for Ge (Chapter 5).

The analysis of the resulting data on the optical constants for CdS and ZnS allows a precise determination of the direct band gap for the material in thin film form, but the absorption at higher energies cannot be certainly ascribed to the onset of an indirect absorption process because the energy bands may not be precisely parabolic. It seems likely that there is some indirect absorption which may be enhanced by the effect of band shape on the direct transitions. As a result of this the values

given for the indirect band gaps on the assumption of parabolic bands may be uncertain although in agreement with the results of theoretical band calculations.

In the method applied here, the spin-orbital splitting in neither CdS nor ZnS could be determined. These are known to be small (0.065 eV for CdS and 0.07 eV for ZnS, Dimmock 1967), and the accuracy of measurement, and the method of analysing the absorption data does not reveal it. However, it may be remarked that similar studies of CdSe, CdTe, ZnSe and ZnTe carried out by my colleague T.G.K. Murty show the effect clearly and lend to accurate values for the spin orbital splitting of the valence band in these materials, where it is much larger than in the sulphides (Dimmock 1967).

CHAPTER 8

CONCLUSIONS

8.1 ON THE DETERMINATION OF THE OPTICAL CONSTANTS OF SEMICONDUCTORS BY SPECTROPHOTOMETRY AT NORMAL INCIDENCE

For reliable values of band gaps of semiconducting materials and their electronic band structures, it is important that their optical properties be known as accurately as possible. It is clear that spectrophotometry at normal incidence is undoubtedly the most reliable method to determine the optical properties of the materials. The specimens used for measurements are in general of two forms, i.e. in thin films and in bulk forms. Generally, there are some differences between the optical properties of the two forms of the specimens.

The reliability with which these properties for thin films, and also for bulk forms, can be determined, depends on the strength of the absorption in the specimens according to which four different spectral regions are considered below:

REGION I : A region of no absorption.

In this region the constants of semiconductors (i.e. refractive indices) can be determined easily from the reflectance and transmittance measurements of the specimens with almost the same accuracy for both forms. This depends on the accuracy of the measurements and may result in uncertainties of less than 1% in the refractive indices.

REGION II : A low absorption region near the band gap such that the absorption index k is less than, say, 0.01

In this region refractive indices can be determined with the same

accuracy as for region I, for both forms of the specimens. But reliable absorption indices cannot be determined if the measurements are made on thin films. However transmission measurements of the specimens in bulk forms result in reliable absorption data. For example this was the case with Ge (Chapter 5).

REGION III : A moderate absorption region, say, for $0.01 < k < 1.0$.

In this region reliable n and k values could be obtained from measurements on the specimens in the form of thin films; e.g. see Chapter 4 for Ta_2O_5 films and Chapters 6 and 7 for CdS and ZnS films. Though the refractive indices of specimens in the bulk forms could be determined with reasonable accuracy by the use of Tomlin's method in this region, reliable absorption data could not be (Chapter 5). In the lower absorption part of this region, say, for $k < 0.4$, the refractive indices of specimens (such as Ge, with $n > 4$) in bulk forms, could also be obtained from reflectivity measurements alone, when absorption is neglected. This may result in uncertainties less than 2% in the refractive indices, obtained.

The other method applied in this region for specimens in bulk forms is the measurements of transmission and reflection (e.g. Dash and Newman, 1955). In general, for the thicknesses of specimens used, the transmittances of the specimens may be as small as 10^{-6}. Accurate measurements of such a low transmittance is difficult, especially when these measurements are to be made in the I.R. region. Here PbS cells are generally used as detectors and are not nearly as sensitive to the light signal as photomultipliers. Also there may be nonlinearity in the overall detection system (Dash and Newman, 1955). For example, the error

in a measurement of transmittance of order 10^{-6} was estimated by Dash and Newman to be about 20% (Archer, 1958).

REGION IV : A high absorption region, say, for k > 1.0.

In this region, since no multiple interference effect will occur in films of specimens, the measurements will be the same for both forms of specimens. The reliable optical constants could be obtained by the use of Tomlin's method. The application of this, requires a transparent or at least semi-absorbing dielectric material. The use of this method may be limited at higher photon energies because of the lack of suitable dielectrics.

It may be mentioned that a method of analysis of reflectance using Kramers-Kronig theory, which is commonly used, is not brought into the above discussion, because uncertainties in the optical constants determined by this method are far too large. For example see results on crystalline germanium, obtained by this method and the present method (Chapter 5).

It follows from the above discussion that in order to obtain a clear picture of the electronic band structure of a semiconductor it is advantageous to determine the optical properties of both forms of it, especially in case of an indirect band gap semiconductor such as Ge (Chapter 5). It is clear from the literature and also from the present work that the two forms of a material, generally, have different optical properties. This I believe is mainly duc to different degrees of crystallinity. There can be other factors which can contribute to this variation of optical properties, e.g. differences in stoichiometry,

impurities, surface conditions, etc. Though it may be difficult to prepare films with crystalline properties close to those of the parent bulk material, it is not impossible. For example CdS films showed good crystallinity and the value of the absorption edge at room temperature of 2.42 eV is the same as that for bulk CdS (Kittel, 1971). The absorption edge of type I ZnS films was 3.47 eV and that for type II, which had improved crystallinity, was 3.57 eV. The crystallinity of type II ZnS films was not as good as that for CdS films. I believe that if the ZnS were deposited on substrates at higher temperatures (say, > 200^{o}C) their crystallinity would improve and the absorption edge would move closer to that of the bulk material (= 3.6 eV, Kittel 1971).

Thus it is suggested that further work on the optical properties of crystalline Ge might be continued on these lines to study further the dependence of band gap on crystallinity. In the laboratory here work is already being done on the optical properties of Si and the remaining II - VI compounds.

8.2 OPTICAL PROPERTIES OF GERMANIUM

The optical constants for amorphous Ge have been determined successfully in the energy range from 0.62 to 4.13 eV by the use of two methods (Denton et al 1971 and Tomlin 1972). The results are in qualitative agreement with those which appear in the literature. The new analysis of the absorption data presented in this thesis, should remove the existing confusions about the band edge value in amorphous Ge (Adler and Moss 1973).

The optical constants of polycrystalline Ge were determined in the

energy range from 0.70 to 4.13 eV by the use of Tomlin's method. Though the absorption data, near the band gap, could not be obtained by this method. It is suggested that crystalline films of Ge might be prepared and then, from measured reflectances and transmittances, reliable optical constants for these could be determined, in order to form a clear picture of the electronic band structure of Ge. It is clear from the literature that crystalline films of Ge have rough surfaces, but this should not create any problem and can be accounted for as was done in the case for CdS and ZnS films.

8.3 OPTICAL PROPERTIES FOR Ta_2O_5 AND ZrO_2 FILMS

Ta_2O_5 films were amorphous, uniform and had smooth surfaces. The optical constants of these were determined in the energy range from 0.62 to 5 eV. The analysis of the absorption curves showed that the absorption processes followed the law for indirect transitions.

ZrO_2 films were polycrystalline and had rough surfaces. The optical constants of these were obtained by the method which considers a double layer on a substrate, thus accounting for the surface roughnesses. The results obtained were in very good agreement with those of Liddell (1974).

8.4 OPTICAL PROPERTIES FOR CdS AND ZnS FILMS

Both CdS and ZnS films were polycrystalline and had rough surfaces. The optical constants of both were determined by treating the films as double layers on substrates. The absorption data for these films determined by different workers were in good agreement, while the similar

results for the refractive index were in reasonable agreement (Fig. 6.11). This is because the absorption found by our method does not depend critically on the closure of the dispersion curve which is affected by surface roughness of the films.

The analysis of the absorption data led to the conclusion that both these materials have direct band gaps. In both, at energies higher than the band gaps, another absorption process begins which is due to indirect transitions, assuming bands to be parabolic. These results are consistent with the theoretical calculations on band structures. The absorption data can be explained equally well by assuming only direct transitions between non-parabolic bands. It is concluded that these materials both show absorption by direct transitions just beyond the absorption edge and that at higher energies the form of the absorption curve is probably due to the combined effects of indirect transitions together with direct transitions between non-parabolic bands. It has not been possible, on the basis of these optical measurements alone, to separate these two effects.

As far as published experimental work is concerned there has been no doubts about CdS being a direct band gap material but for ZnS there were some doubts until the present project. For example Kittel (1971) in his table for the values and nature of the band gaps for various semiconductors gives Si, Ge, GaP, etc. as indirect gap and InSb, InAs, GaAs, CdS, etc., as direct gap materials but does not specifically mention about the nature of the band gap for ZnS. Segal and Marple (1967) summarising results on the optical absorption of crystalline bulk ZnS, determined by different workers, comment

"Regardless of their origin, the discrepancies among the different studies seem so large that no inferences seem justified concerning the direct or indirect origin of spectra. It appears quite possible that the difference among these results arise from differences in impurity content or crystalline perfection in the ZnS samples".

8.5 GENERAL CONCLUSIONS

In general, the following conclusions may be drawn from the present project.

(1) Shift of band gaps with changes in crystallinity : In the case of ZnS and Ge, it was found that their different band edges shift by a constant energy from lower to higher values as the crystallinity of these materials improve.

(2) Non-direct transitions in amorphous materials : The present results are consistent with the view that the essential features of the band picture for amorphous Ge are basically unaltered from that of crystalline Ge, and the random structure of the amorphous state removes the conditions for the conservation of momentum giving rise to an absorption which then follows the law for indirect (or non-direct) transitions. The absorption data for amorphous Ta_2O_5 films also followed the law for indirect transitions.

(3) Increase in absorption with improved crystallinity : From the present results for CdS, ZnS and Ge, it is clear that except near the absorption edge, the absorption increases with improved crystallinity of the material.

(4) Dependence of surface roughness of a film on its structure : Generally, amorphous films have smooth surfaces, e.g. Ge and Ta_2O_5 and polycrystalline films have rough surfaces e.g. CdS, ZnS and

ZrO_2. This is also confirmed by Grigorovici (1973).

(5) Tomlin's method was applied successfully in the high absorption region in the case of amorphous and polycrystalline Ge thus eliminating the uncertainties in the published results obtained using the Kramers-Kronig analysis of reflectivity data (Chapter 5).

APPENDIX A

DETERMINATION OF REFRACTIVE INDEX OF A TRANSPARENT FILM

The refractive index (n_1) of a transparent film of thickness (d_1) on a transparent substrate of refractive index (n_2) can be determined by measuring its normal incidence transmittance (T). At a wavelength λ, T is given by (Heavens 1955).

$$T = \frac{n_2}{n_o} \frac{(1+g_1)^2 (1+g_2)^2}{1+g_1^2 g_2^2 + 2g_1 g_2 \cos 2\gamma_1}$$

where

$$g_1 = \frac{n_o^2 - n_1^2}{(n_o+n_1)^2}$$

$$g_2 = \frac{n_1^2 - n_2^2}{(n_1+n_2)^2}$$

$$\gamma_1 = \frac{2\pi n_1 d_1}{\lambda}$$

and n_o is the index of refraction of air.

If T is measured at a given wavelength, and d_1 and n_2 are known then in principle n_1 can be determined from the above relation. An expression giving an explicit value of n_1 cannot be obtained. However the equation may be solved by a numerical method similar to that described in Section 3.3.2.

The transparent films may be divided into two types with respect to their refractive indices being greater or smaller than those of substrates on which they rest.

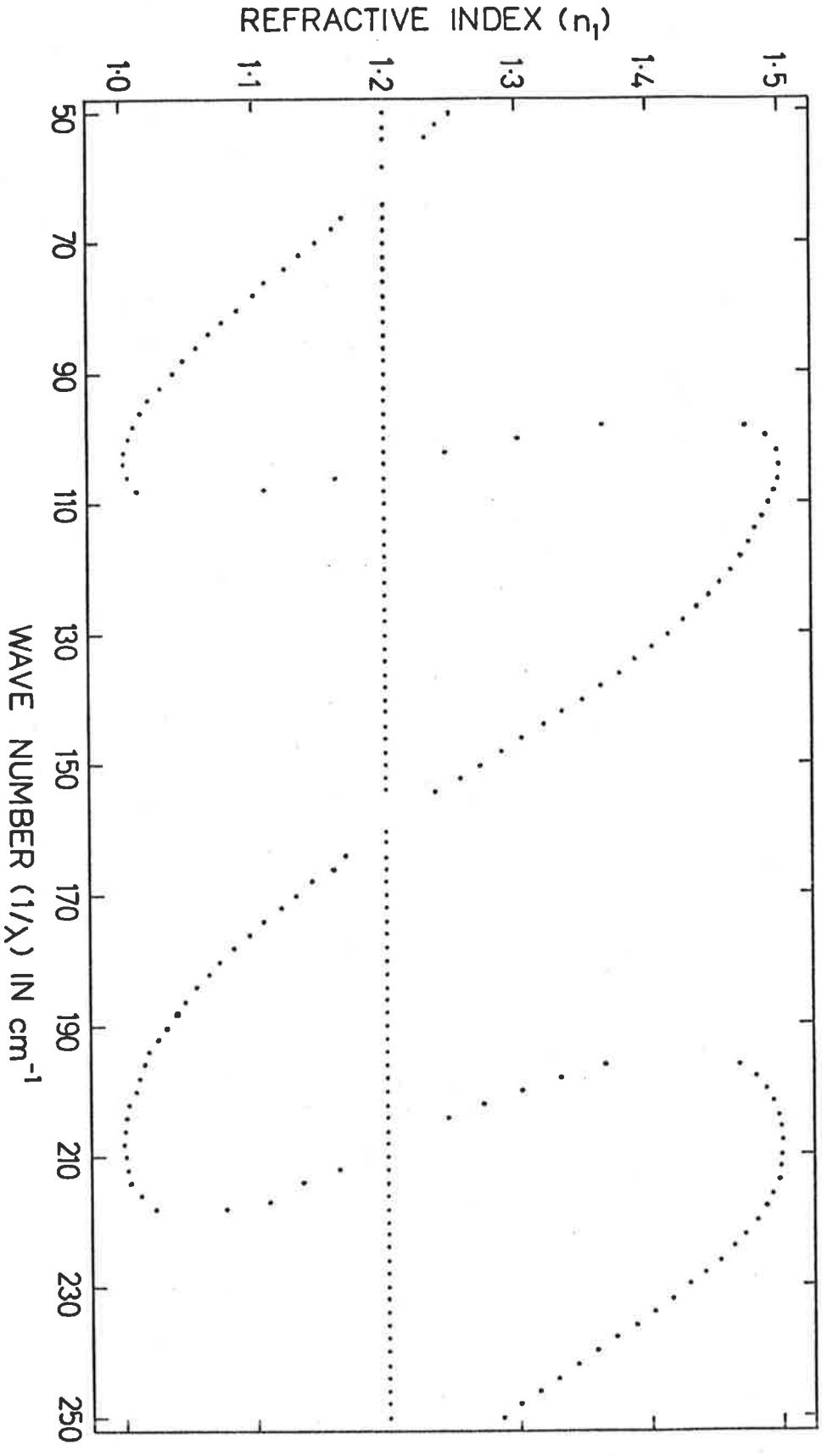
REFRACTIVE INDEX (n_1)
1·0
1·1
1·2
1·3
1·4
1·5
WAVE NUMBER (1/λ) IN cm^{-1}
50
70
90
110
130
150
170
190
210
230
250

FIGURE A1

type I $n_1 > n_2$

type II $n_1 < n_2$

It was seen that the nature of the multiple solutions, arising due to interference effects, in the type I, was similar to that in case of semi-absorbing films such as of CdS, ZnS, Ta_2O_5, etc (where $n_1 > n_2$). Hence type I will not be considered any further.

To illustrate the nature of the solutions in type II, a hypothetical film of refractive index $n_1 = 1.2$ and thickness $d_1 = 400$ nm resting on a substrate of refractive index $n_2 = 1.5$ was considered. Transmittances were calculated for the wave number ranging from 50 to 250 cm^{-1} (λ = 2000 - 400 nm) at an interval of 2 cm^{-1} from the above equation using the values of n_1, n_2 and d_1 stated above. Then these T values were used as data (assuming that n_1 was not known) to calculate n_1 from the above relation. The dispersion curve shown in Figure A1 was obtained. It is clear that the correct solutions form a straight line while the unwanted solutions form a continuous curve with repeated maxima and minima, thus eliminating any doubts about the choice of correct solutions. If in the calculations $d_1 = 380$ nm is used instead of 400 nm then the dispersion curve shown in Figure A2 is obtained. When $d_1 = 420$ nm is used instead of 400 nm then the dispersion curve shown in Figure A3 is obtained. It is clear from Figures A2 and A3 that continuous acceptable dispersion curve cannot be obtained when film thickness is over or underestimated.

An approximate knowledge of the film thickness could be obtained from a plot of transmittance versus wavelength using the relation

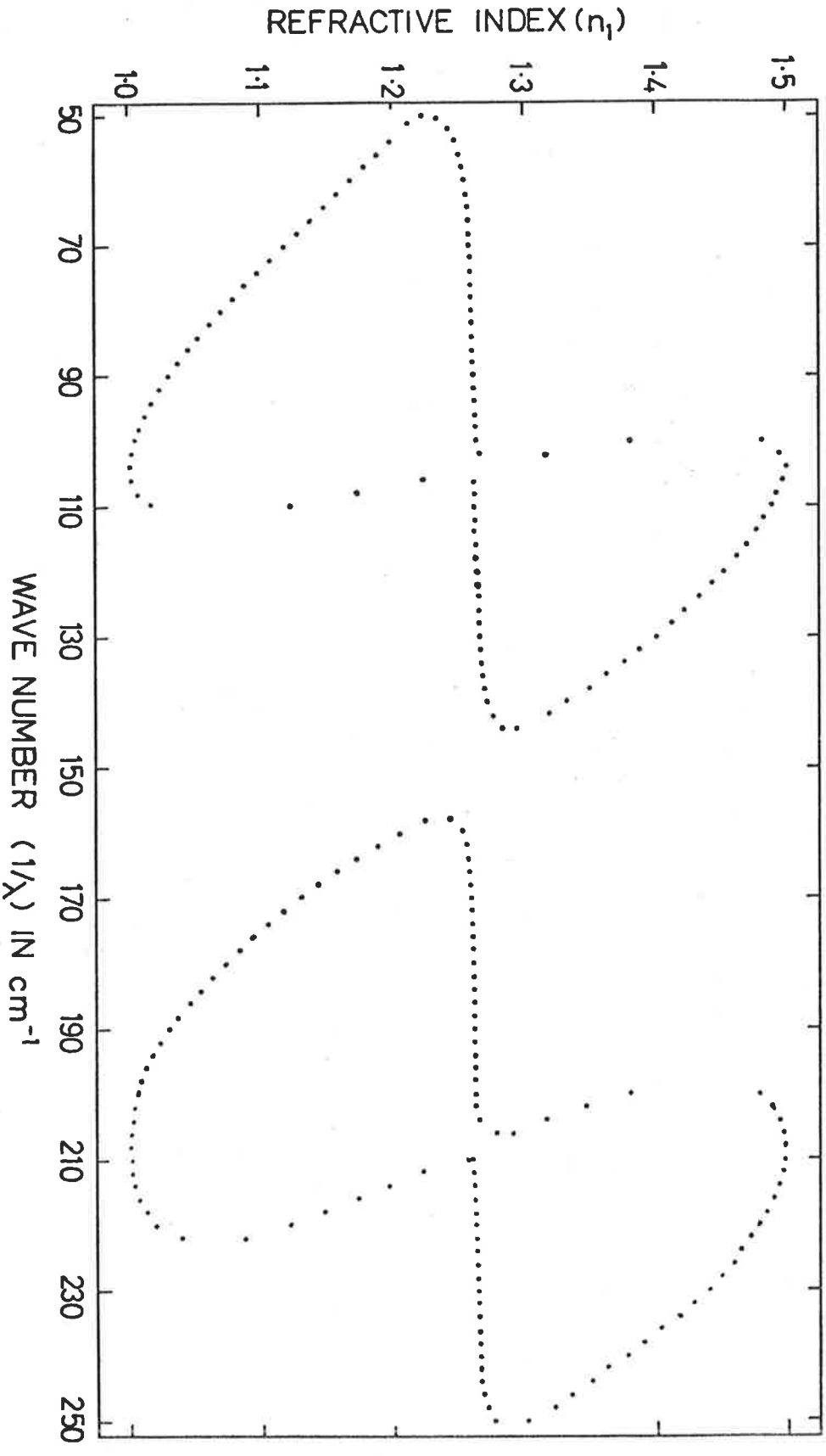
REFRACTIVE INDEX (n_1)
1·0
1·1
1·2
1·3
1·4
1·5
WAVE NUMBER (1/λ) IN cm^{-1}
50
70
90
110
130
150
170
190
210
230
250

FIGURE A2

$$d_1 = \frac{\lambda_1 \lambda_2}{4n_1(\lambda_1 - \lambda_2)}$$

where λ_1 and λ_2 are the wavelengths of consecutive turning points. This is applicable only when approximate value of the refractive index of the film is known. Otherwise separate measurements of thickness could be made. Different methods of determining film thicknesses are discussed by Heavens (1955). These methods may not result in accurate thickness but this could be then obtained by adopting the procedure outlined below.

The approximate knowledge of film thickness could be used to compute a preliminary result. Then for a small change (say 5%) in the initial thickness, the results may be computed once again. If the new dispersion curve shows larger deviation, from the correct dispersion curve (Figure A1), than the first one, then the thickness may be changed in the other way. Thus the thickness could be then adjusted until a continuous dispersion curve resulted. By adopting this criterion the correct optical constant (refractive index) could be obtained together with an accurate value of the thickness of the transparent film.

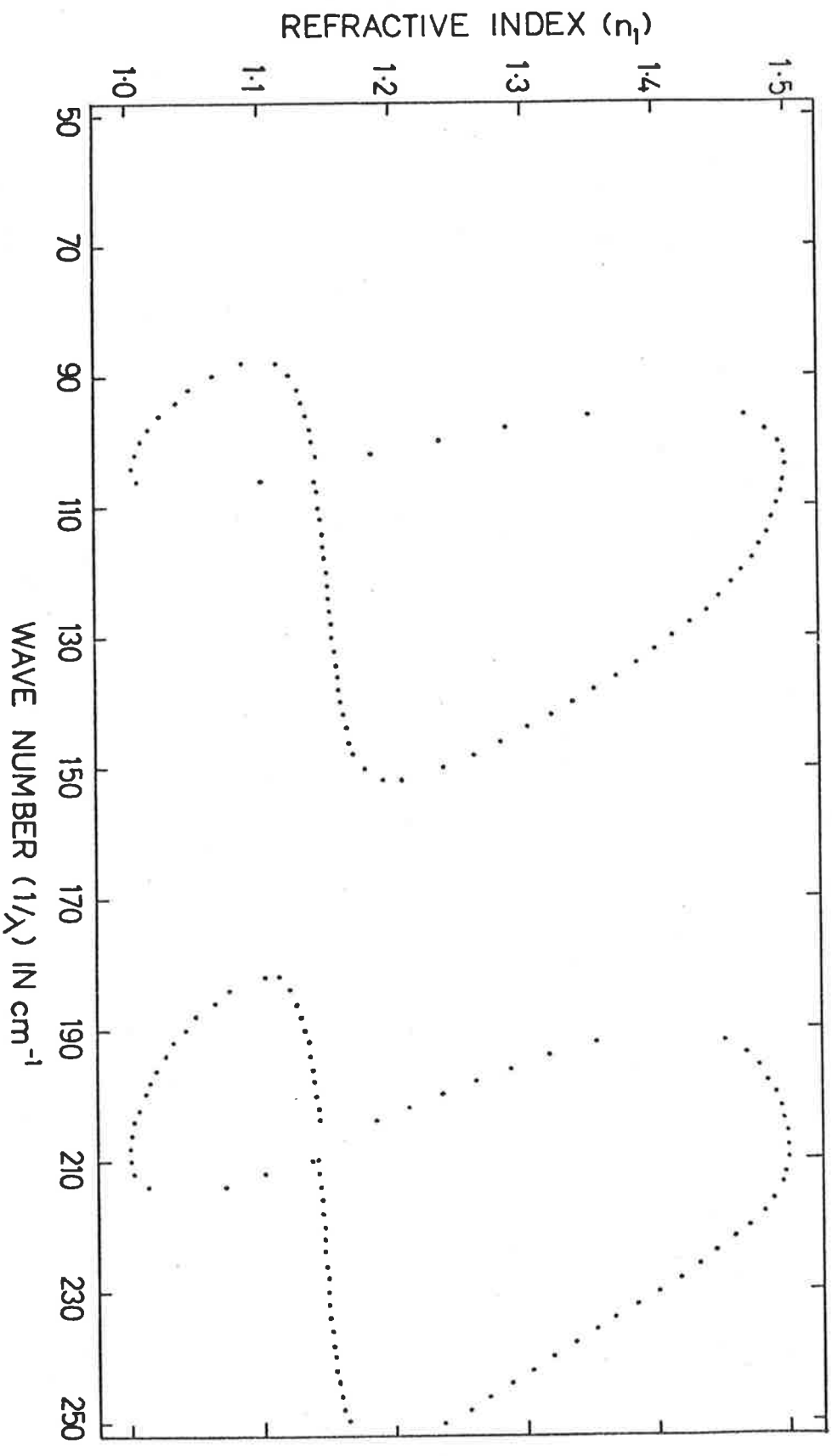
REFRACTIVE INDEX (n_1)
1·0
1·1
1·2
1·3
1·4
1·5
WAVE NUMBER ($1/\lambda$) IN cm^{-1}
50
70
90
110
130
150
170
190
210
230
250

FIGURE A3

APPENDIX B

PARTIAL DERIVATIVES OF R AND $(1+R_1)/(1-R_1)$

$$R = (n_2-n_0)^2 + k_2^2 \;/\; (n_2+n_0)^2 + k_2^2$$

$$\frac{1+R_1}{1-R_1} = \frac{1}{4n_0n_2n_1^2}\Big[(n_0^2+n_1^2)\;(n_1^2+n_2^2+k_2^2)$$

$$+ (n_0^2-n_1^2)\;\{(n_1^2-n_2^2-k_2^2)\cos 2\gamma_1 + 2n_1k_2\sin 2\gamma_1\}\Big]$$

$$\frac{\partial R}{\partial k_2} = 8n_0n_2k_2 \;/\; \{(n_2+n_0)^2 + k_2^2\}^2$$

$$\frac{\partial R}{\partial n_2} = 4n_0\{n_2^2-k_2^2+2n_2(1-n_0) - 1\} \;/\; \{(n_2+n_0)^2+k_2^2\}^2$$

$$\frac{\partial\left(\frac{1+R_1}{1-R_1}\right)}{\partial d_1} = \frac{(n_0^2-n_1^2)\,\pi}{n_0n_2n_1\lambda}\Big[2n_1k_2\cos 2\gamma_1 - (n_1^2-n_2^2-k_2^2)\sin 2\gamma_1\Big]$$

$$\frac{\partial\left(\frac{1+R_1}{1-R_1}\right)}{\partial k_2} = \frac{1}{2n_0n_2n_1^2}\Big[(n_0^2+n_1^2)k_2 + (n_0^2-n_1^2)\;\{n_1\sin 2\gamma_1 - k_2\cos 2\gamma_1\}\Big]$$

$$\frac{\partial\left(\frac{1+R_1}{1-R_1}\right)}{\partial n_2} = \frac{1}{4n_0n_2^2n_1^2}\Big[(n_0^2+n_1^2)\;(n_2^2-n_1^2-k_2^2)$$

$$+ (n_1^2-n_0^2)\;\{(n_1^2+n_2^2-k_2^2)\cos 2\gamma_1 + 2n_1k_2\sin 2\gamma_1\}\Big]$$

$$\frac{\partial\left(\frac{1+R_1}{1-R_1}\right)}{\partial n_1} = \frac{1}{2n_0n_2n_1^3}\Big[(n_1^4-n_0^2n_2^2-n_0^2k_2^2)$$

$$+ \{n_1(n_1+2\gamma_1k_2)(n_0^2-n_1^2) - n_0^2(n_1^2-n_2^2-k_2^2)\}\cos 2\gamma_1$$

$$- \{\gamma_1(n_0^2-n_1^2)(n_1^2-n_2^2-k_2^2) + n_1k_2(n_0^2+n_1^2)\}\sin 2\gamma_1\Big]$$

APPENDIX C

DEPENDENCE OF THE RELATIVE ERROR IN SLOPE ON THE REFRACTIVE INDEX OF THE OVERLYING LAYER

The relative error in slope (Section 3.8) was calculated in case of the hypothetical specimen considered in Section 3.4 for overlying layers of different refractive indices as mentioned below:

(1) $n_1 = 1.3$ and $d_1 = 226.2$ nm

(2) $n_1 = 1.5$ and $d_1 = 196.0$ nm

(3) $n_1 = 2.1$ and $d_1 = 140.0$ nm

The thicknesses used were such that the product $n_1 d_1$ was constant. The results are tabulated with appropriate headings.

λ in nm	γ_1/π in Radians	R	$n_1 = 1.3$		$n_1 = 1.5$		$n_1 = 2.1$	
			R_1	Relative Error In Slope	R_1	Relative Error In Slope	R_1	Relative Error In Slope
300	1.960	.509	.515	.487	.519	.308	.530	.160
310	1.897	.504	.509	.190	.515	.120	.538	.063
320	1.837	.499	.494	.123	.498	.077	.526	.040
330	1.782	.496	.470	.095	.469	.058	.498	.029
340	1.729	.493	.441	.081	.430	.047	.454	.022
350	1.680	.491	.408	.075	.384	.041	.397	.018
360	1.633	.489	.375	.074	.335	.039	.328	.015
370	1.589	.487	.344	.078	.286	.039	.251	.014
380	1.547	.486	.318	.089	.243	.043	.174	.013
390	1.508	.484	.300	.111	.210	.052	.104	.015
400	1.470	.483	.290	.154	.190	.071	.052	.018
410	1.434	.481	.287	.250	.184	.112	.023	.026
420	1.400	.480	.292	.570	.191	.239	.020	.046
430	1.367	.479	.302	10.399	.208	2.684	.040	.120
440	1.336	.478	.316	.663	.231	.412	.074	1.063
450	1.307	.477	.332	.400	.258	.233	.118	.147
460	1.278	.475	.349	.319	.285	.185	.165	.099
470	1.251	.474	.366	.288	.312	.168	.211	.085
480	1.225	.473	.381	.279	.337	.165	.254	.083
490	1.200	.472	.396	.284	.360	.170	.292	.085
500	1.176	.471	.409	.299	.381	.182	.326	.091
510	1.153	.470	.421	.326	.398	.200	.355	.101
520	1.131	.468	.431	.365	.413	.226	.379	.115
530	1.109	.467	.439	.423	.426	.264	.400	.134
540	1.089	.466	.446	.508	.436	.320	.417	.163
550	1.069	.465	.451	.640	.445	.406	.431	.208
560	1.050	.464	.455	.871	.451	.555	.442	.285
570	1.032	.463	.458	1.361	.456	.871	.451	.448
580	1.014	.462	.460	3.065	.459	1.980	.457	1.017
590	.997	.461	.461	13.391	.461	8.015	.462	4.111
600	.980	.459	.461	2.145	.462	1.352	.464	.692
610	.964	.458	.460	1.181	.461	.746	.465	.380
620	.948	.457	.458	.822	.459	.520	.465	.264
630	.933	.456	.456	.636	.457	.401	.463	.202
640	.919	.455	.452	.521	.453	.328	.460	.164
650	.905	.454	.449	.445	.449	.278	.455	.138
660	.891	.453	.445	.389	.444	.243	.450	.120
670	.878	.452	.440	.348	.438	.216	.444	.105
680	.865	.451	.435	.316	.432	.195	.437	.094
690	.852	.450	.430	.290	.425	.178	.429	.085
700	.840	.449	.424	.269	.418	.164	.421	.078

APPENDIX D

NUMERICAL VALUES OF THE OPTICAL CONSTANTS FOR Ta_2O_5 FILMS

The optical constants (n and k) for Ta_2O_5 at different wavelengths are listed below. These are the values, averaged over best curves (for example, continuous curves shown in Figures 4.2.a and 4.2.b) for different Ta_2O_5 films, studied. Variation in n from film to film was very small (only in the third decimal place), while that in k was very small in the long wavelength region but for wavelengths smaller than 260 nm it was slightly larger as shown in Figure 4.2.b. The larger variations for shorter wavelengths resulted, from the inaccuracy in measuring small transmittances in this region. The measured absorption index k of the order of 0.001 - 0.003 in the region 2000 - 315 nm, was neglected for the reasons discussed in Section 4.4.2.

λ (nm)	n	λ (nm)	n	λ (nm)	n	k
2000	2.085	555	2.109	400	2.200	
1900	2.085	550	2.110	395	2.206	
1800	2.086	545	2.111	390	2.213	
1700	2.086	540	2.112	385	2.220	
1600	2.086	535	2.113	380	2.227	
1500	2.087	530	2.114	375	2.235	
1400	2.087	525	2.115	370	2.243	
1300	2.087	520	2.116	365	2.252	
1200	2.088	515	2.117	360	2.260	
1100	2.088	510	2.118	355	2.270	
1000	2.088	505	2.119	350	2.280	
900	2.089	500	2.120	345	2.291	
800	2.089	495	2.122	340	2.303	
700	2.090	490	2.125	335	2.316	
690	2.091	485	2.127	330	2.330	
680	2.092	480	2.130	325	2.345	
670	2.093	475	2.133	320	2.362	
660	2.094	470	2.136	315	2.380	
650	2.095	465	2.139	310	2.401	.003
640	2.096	460	2.143	305	2.426	.004
630	2.097	455	2.146	300	2.452	.006
620	2.098	450	2.150	295	2.481	.010
610	2.099	445	2.154	290	2.520	.018
600	2.100	440	2.158	285	2.560	.030
590	2.102	435	2.162	280	2.610	.053
585	2.103	430	2.167	275	2.670	.089
580	2.104	425	2.172	270	2.730	.136
575	2.104	420	2.177	265	2.790	.203
570	2.106	415	2.182	260	2.850	.288
565	2.107	410	2.188	255	2.900	.397
560	2.108	405	2.194	250	2.920	.541

APPENDIX E

NUMERICAL VALUES OF THE OPTICAL CONSTANTS FOR ZrO_2 FILMS

The optical constants (n and k) for ZrO_2 films at different wavelengths are listed below. The comments made in Appendix D, also apply to these results.

λ (nm)	n	λ (nm)	n	λ (nm)	n	k
2000	1.925	555	1.960	400	2.009	
1900	1.926	550	1.960	395	2.013	
1800	1.928	545	1.961	390	2.016	
1700	1.930	540	1.961	385	2.019	
1600	1.933	535	1.962	380	2.023	
1500	1.935	530	1.962	375	2.027	
1400	1.937	525	1.963	370	2.032	
1300	1.940	520	1.964	365	2.037	
1200	1.942	515	1.965	360	2.042	
1100	1.944	510	1.966	355	2.047	
1000	1.946	505	1.967	350	2.052	
900	1.948	500	1.968	345	2.057	
800	1.950	495	1.969	340	2.063	
700	1.952	490	1.971	335	2.069	
690	1.952	485	1.973	330	2.075	
680	1.953	480	1.975	325	2.082	
670	1.953	475	1.977	320	2.089	
660	1.953	470	1.978	315	2.096	
650	1.954	465	1.980	310	2.103	
640	1.954	460	1.981	305	2.111	
630	1.955	455	1.983	300	2.119	
620	1.955	450	1.984	295	2.129	
610	1.956	445	1.986	290	2.139	
600	1.957	440	1.988	285	2.149	
590	1.957	435	1.990	280	2.160	
585	1.958	430	1.993	275	2.172	
580	1.958	425	1.995	270	2.185	
575	1.958	420	1.997	265	2.199	.005
570	1.959	415	1.999	260	2.215	.006
565	1.959	410	2.002	255	2.233	.007
560	1.959	405	2.005	250	2.255	.010

REFERENCES

ABELES F., Progress in Optics, Vol.2, North Holland Publishing Co., Amsterdam, 1963.

ADLER D., MOSS S.C., Comments on Solid State Physics, 5, 3, 63, 1973.

ARCHER R.J., Phys. Rev., 110, 2, 354, 1958.

AVERY D.G. and CLEGG P.L., Proc. Phys. Soc. (London), B66, 512, 1953.

BARNA A., BARNA P.B., POCZA E.F., CROITORN N., DEVENYI A. and GRIGOROVICI R., Proc. Colloq. Thin Films, Budapest 1965, p.49.

BAUER R.S. and GALEENER F.L., Solid State Commun., 10, 1171, 1972.

BENNETT H.E. and PORTEUS J.O., J. Opt. Soc. Amer., 51, 123, 1961.

BENNETT H.E., J. Opt. Soc. Amer., 53, 1389, 1963.

BENNETT J.M. and BOOTY M.J., Appl. Opt., 5, 41, 1966.

BENNETT H.E., BENNETT J.M., ASHLEY E.J. and GONELLA J., Appl. Opt., 8, 1229, 1969.

BERGSTRESSER T.K. and COHEN M.L., Phys. Rev., 164, 1069, 1967.

BORN M. and WOLF E., Principles of Optics, Peragamon Press, Oxford, 1970.

BOUSQUET P., Ann. Physique, 2, 163, 1957.

BRATTAIN W.H. and BRIGGS H.B., Phys. Rev., 75, 11, 1705, 1949.

BUJATTI M. and MARCELJA F., Thin Solid Films, 11, 249, 1972.

BURGIEL J.C., CHEN Y.S., VRATNY F. and SMOLINSKY G., J. Electrochem. Soc., 115, 729, 1968.

CARDONA M. and HARBEKE G., Phys. Rev., 137, A1467, 1965.

CARDONA M., Semiconductors and semimetals, Vol.3, eds. Willardson R.K. and Beer A.C., Academic Press, New York, 1967.

CHARLESBY A. and POLLING J.J., Proc. Roy. Soc., A277, 434, 1955.

CHOPRA K.L. and BAHL S.K., Thin Solid Films, 11, 377, 1972.

CLARK A.H., Phys. Rev., 154, 3, 750, 1967.

COHEN M.L., II-VI Semiconducting Compounds ed. Thomas D.G., W.A. Benjamin, New York, 1967.

CONNELL G.A.N., TEMKIN R.J. and PAUL W., Advances in Physics, 22, 5, 643, 1973.

COOGAN C.K., Proc. Phys. Soc. London, 70, 845, 1957.

CZYAK S.J., BAKER W.M., CRANE R.C. and HOWE J.B., J. Opt. Soc. Amer., 47, 3, 240, 1957.

CZYAK S.J., CRANE R.C. and BIENIEWSKI T.M., J. Opt. Soc. Amer., 49, 485, 1959.

DASH W.C. and NEWMAN R., Phys. Rev., 99, 1151, 1955.

DAUDE A., SAVARY A. and ROBIN S., J. Opt. Soc. Amer., 62, 1, 1972.

DAVIES H., Proc. Inst. Elec. Eng., 101, 209, 1954.

DENTON R.E., Ph.D. Thesis, University of Adelaide, 1971 (Unpublished).

DENTON R.E. and TOMLIN S.G., Aust. J. Phys., 25, 743, 1972.

DENTON R.E., CAMPBELL R.D. and TOMLIN S.G., J. Phys. D: Appl. Phys., 5, 852, 1972.

DIMMOCK J.O., II-VI Semiconducting Compounds, ed. Thomas D.G., W.A. Benjamin, New York, 1967.

DITCHBURN R.W., "Light", Blackie & Son Ltd., Glasgow, 1963.

DONOVAN T.M. and ASHLEY E.J., J. Opt. Soc. Amer., 54, 9, 1141, 1964.

DONOVAN T.M. and SPICER W.E., Phys. Rev. Lett., 21, 23, 1572, 1968.

DONOVAN T.M., SPICER W.E., BENNETT J.M. and ASHLEY E.J., Phys. Rev. B, 2, 2, 397, 1970.

ESCOFFERY C.A., J. Appl. Phys., 35, 2273, 1964.

GOTTESMAN J. and FERGUSON W.F.C., J. Opt. Soc. Amer., 44, 5, 368, 1954.

GRANT P.M. and PAUL W., J. Appl. Phys., 37, 8, 3110, 1964.

GRIGOROVICI R., Electronics and structural properties of amorphous semiconductors, ed. by LeComber P.G., Academic Press, London and New York, 1973.

HALL J.F. Jr. and FERGUSON W.F.C., J. Opt. Soc. Amer., 45, 9, 714, 1955.

HALL J.F. Jr., J. Opt. Soc. Amer., 46, 1013, 1956.

Handbook of Chemistry and Physics, 49th Ed., Chemical Rubber Co., p.B-265, 1968-69.

HARBEKE G., Optical Properties of Solids, Ed. by Abeles F., North Holland Publishing Co., Amsterdam, 1972.

HEAVENS O.S., Optical Properties of Thin Solid Films, Butterworth, London, 1955.

HEAVENS O.S., Reports on Progress in Physics, XXIII, 1, 1960.

HERMAN F., KORTUM R.L., KUGLIN C.C. and SHAY J.L., II-VI Semiconducting Compounds, ed. Thomas D.G., W.A. Benjamin, New York, 1967.

HERMAN F. and VAN DYKE J.P., Phys. Rev. Lett., 21, 23, 1575, 1968.

HOBDEN M.V., J. Phys. Chem. Solids, 23, 821, 1962.

JAHODA F.C., Phys. Rev., 107, 1261, 1957.

JOHNSON E.J., Semiconductors and semimetals, Vol.3, eds. Willardson R.K. and Beer A.C., Academic Press, New York, 1967.

KITTEL C., Introduction to Solid State Physics, 4th ed., John Wiley & Sons, Inc., New York, 1971.

KUHN H. and WILSON B.A., Proc. Phys. Soc., B63, 745, 1950.

KUWABARA G. and ISIGURO K., J. Phys. Soc. Japan, 7, 72, 1952.

LIDDELL H.M., J. Phys. D: Appl. Phys., 7, 1588, 1974.

LUKES F., Czech. J. Phys., 10, 59, 1960.

MACFARLANE G.G., MCLEAN T.P., QUARRINGTON J.E. and ROBERTS V., Phys. Rev., 108, 6, 1377, 1957.

MCLEAN T.P., Progress in Semiconductors, ed. by Gibson A.F., Vol.5, p.55, Heywood, London, 1960.

MALE D., Thesis, University of Paris, 1952.

MOSS T.S., Optical Properties of Semiconductors, Butterworth, London, 1959.

MURMANN H., Ibid, 80, 161, 1933.

O'BRYAN H.M., J. Opt. Soc. Amer., 26, 122, 1936.

OLLEY J.A., Solid State Comm., 13, 1437, 1973.

PAUL W., CONNELL G.A.N. and TEMKIN R.J., Advances in Physics, 22, 5, 532, 1973.

PHILIPP H.R. and TAFT E.A., Phys. Rev., 113, 4, 1002, 1959.

POTTER R.F., Phys. Rev., 150, 2, 562, 1966.

RALSTON A., A first course in numerical analysis, p.394, McGraw-Hill, New York, 1965.

ROSKOVCOVA L. and PASTRNAK J., Czech. J. Phys., B17, 562, 1967.

ROUARD P. and BOUSQUET P., Progress in Optics, Vol.4, North Holland Publishing Co., Amsterdam, 1965.

SCHOPPER H., Z. Physik, 130, 565, 1951.

SEGALL B. and MARPLE D.T.F., Physics and Chemistry of II-VI compounds, ed. by Aven M. and Prener J.S., North Holland Publishing Co., Amsterdam, 1967.

SERAPHIN B.O. and BENNETT H.E., Semiconductors and semimetals, Vol.3, eds. Willardson R.K. and Beer A.C., Academic Press, New York, 1967.

SHALLCROSS F.V., R.C.A. Review, 28, 569, 1967.

SHIONOYA S., Luminescence of Inorganic Solids, ed. by Goldberg P., Academic Press, New York, 1966.

SIMOV S., Thin Solid Films, 15, 79, 1973.

SMITH R.A., Wave Mechanics of Crystalline Solids, Chapman and Hall, London, 1961.

TAUBER R.N. DUMBRI A.C. and CAFFREY R.E., J. Electrochem. Soc., 118, 747, 1971.

TAUC J., ABRAHAM A., PAJAFOVA L., GRIGOROVICI R. and VANCU A., Proc. Int. Conf. on Physics of Non-Crystalline Solids, Delft, p.606, 1964.

TAUC J., Proc. Int. Conf. Semiconductors., Kyoto., J. Phys. Soc. Japan, Vol.21, Suppl., p.123, 1966.

TAUC J. and ABRAHAM A., Czech. J. Phys., B19, 1246, 1969.

THEYE M.L., Optics Communications, 2, 329, 1970.

THEYE M.L. Mat. Res. Bull., 6, 103, 1971.

TOMLIN S.G., Brit. J. Appl. Phys. (J. Phys. D), 1, 1667, 1968.

TOMLIN S.G., Int. Conf. on Thin Films, Venice, Italy, Thin Solid Films, 13, 265, 1972.

TOMLIN S.G., J. Phys. D: Appl. Phys., 5, 847, (1972a).

TREUSCH J., ECKELT P. and MADELUNG O., II-VI Semiconducting Compounds, ed. Thomas D.G., W.A. Benjamin, New York, 1967.

URBACH F., Phys. Rev. Lett., 92, 1324, 1953.

VERMILYEA D.A., Acta Met., 1, 282, 1953.

VINCENT-GEISSE J., Journal De Physique, 25, 291, 1964.

VINCENT-GEISSE J., NGUGEN TAN TAI and PINAN-LUCARRE J.P., Journal De Physique, 28, 26, 1967.

VLASENKO N.A., Opt. Spectry. (U.S.S.R.) 7, 320, 1959.

WALES J., LOVITT G.J. and HILL R.A., Thin Solid Films, 1, 137, 1967.

WARD J., Private Communication, 1971-1974.

WESTWOOD W.D., BOYNTON R.J. and INGREY S.J., J. Vac. Sci. Technol., 11, 381, 1974.

WILKINS N.J.M., Corrosion Sci., 4, 17, 1964.

WOOD D.L. and TAUC J., Phys. Rev. B, 5, 8, 3144, 1972.

YOUNG L., Anodic Oxide Films, Academic Press, London, p.81, 1961.